MOLECULAR MODELING OF KETENE DIMERIZATION REACTION

by

GIOVANNI MORALES MEDINA

UNIVERSIDAD INDUSTRIAL DE SANTANDER

CHEMICAL ENGINEERING DEPARTMENT

BUCARAMANGA, COLOMBIA

MAY, 2009

MOLECULAR MODELING OF KETENE DIMERIZATION REACTION

by

GIOVANNI MORALES MEDINA

Supervisor

Dr. Ramiro Martínez Rey

A DISSERTATION SUBMITTED IN PARTIAL FULFILLMENT OF THE REQUIREMENTS FOR THE DEGREE OF DOCTOR OF PHILOSOPHY

UNIVERSIDAD INDUSTRIAL DE SANTANDER

CHEMICAL ENGINEERING DEPARTMENT

BUCARAMANGA, COLOMBIA

MAY, 2009

Acknowledgment

To the memory of Juan Carlos Morales

Table of Contents

Chapter 2. The Ketene Dimerization Mechanism: a Tricky Reaction Pathway

Chapter 3. Molecular Modeling: A New Tool in the Analysis of Chemical Engineering Phenomena

List of Tables

List of Figures

List of Graphs

List of Charts

TITULO: MODELAMIENTO MOLECULAR DE LA REACCION DE DIMERIZACION DE CETENAS [*]

AUTOR: GIOVANNI MORALES MEDINA [**]

PALABRAS CLAVES: dimerización, MPW1K, DFT, COSMO, CBS-Q, calor de formación, grupos de contribución, enlace de hidrogeno.

En este trabajo se presenta el primer estudio teórico sobre la dimerización de cetena en solución (en tolueno y acetona) basado en el método de los funcionales de la densidad electrónica y en el modelo COSMO. Los productos de la dimerización considerados fueron dicetena (d-I), 1,3-ciclobutanediona (d-II), 4-dimetilene-1,3-dioxetano y 2-metileneoxetan-3-ona. Las geometrías de estos dímeros fueron optimizadas al nivel PW86x+PBEc/DZP. El calor de dimerización experimental para d-I fue reproducido con el funcional MPW1K (de un total de 58 funcionales estudiados). De acuerdo a los resultados con este funcional, los dímeros d-I y d-II son los únicos productos detectables de la dimerización. Según los resultados con COSMO, la barrera de energía en solución se ve disminuida a la mitad comparada con la barrera en fase gaseosa para d-I y d-II debido a la interacción entre el momento dipolar de los dímeros y las moléculas del solvente. La tendencia de la dimerización cambia con la polaridad del solvente; es decir, d-II presenta la menor barrera energética en fase gaseosa y en tolueno mientras que d-I presenta la menor barrera en acetona.

El análisis de la dimerización finaliza con la obtención de las propiedades termoquímicas y los grupos de contribución (GAVs) para diferentes dímeros sustituidos calculados al nivel CBS-Q. Los resultados muestran que las dicetenas sustituidas son menos estables que sus dímeros homólogos d-II. De acuerdo a lo anterior, la dimerización de alquilcetenas produce el dímero d-II en mayor cantidad debido a un control termodinámico. Los grupos de contribución faltantes para los dímeros fueron obtenidos por medio de regresión lineal sobre un conjunto de 57 compuestos alicíclicos. Diferentes correcciones por interacciones no próximas fueron derivadas para mejorar el desempeño de la regresión. En particular la corrección por puente de hidrogeno es la primera reportada en la literatura.

TITLE: MOLECULAR MODELING OF KETENE DIMERIZATION REACTION [*]

AUTHOR: GIOVANNI MORALES MEDINA [**]

Keywords: dimerization, solvent effects, MPW1K, DFT, COSMO, CBS-Q, heat of formation, Additivity groups, hydrogen bond.

The first theoretical study on ketene dimerization in solution (in toluene and acetone) is presented herein. DFT and COSMO calculations were carried out considering the following dimers: diketene (d-I), 1,3-cyclobutanedione (d-II), 2,4-dimethylene-1,3-dioxetane, and 2-methyleneoxetan-3-one. All structures were optimized at the PW86x+PBEc/DZP level. A total of 58 functionals were used to evaluate the heat of dimerization for d-I in gas phase. The MPW1K functional was found to fit the experimental data best and subsequently used in the final analyses for all energy calculations. It was found that only d-I and d-II are formed during ketene dimerization in gas phase and solution. According to COSMO model, solvation makes dimerization feasible due to a favorable interaction between the dimer dipole moment and solvent molecules. While the dimerization barrier for d-II is lowest for the gas phase and toluene, the barrier for d-I formation becomes lowest for the more polar solvent acetone by 1 kcal/mol as d-I dimerization has the most polar transition state.

Thermodynamic properties of different substituted dimers were analyzed using the CBS-Q method for completion of this research. Calculations were carried out on 20 cyclic structures, such as diketenes, cyclobutane-1,3-diones, cyclobut-2-enones and pyran-4-ones, as well as 57 acyclic base compounds. According to theoretical heat of formation predictions, substituted diketenes had lower stability than substituted cyclobutane-1,3-diones with an increased number of methyl substituents. This suggested that cyclobutane-1,3-diones are the major products because of thermodynamic control of alkylketene dimerization. Missing contribution groups (GAV) for the cyclic structures were calculated through linear regression. Corrections for nonnext neighbor interactions (such as gauche, eclipses and internal hydrogen bond) were needed for obtaining a highly accurate and precise regression model. To the best of our knowledge, the hydrogen bond correction for GAV methodology is the first reported in the literature.

INTRODUCTION

Ketenes are versatile compounds because of their double conjugated bonds, $R_1R_2C=C=O$. These double bonds give to ketenes important chemical properties and allow them to react with both electrophiles and nucleophiles. Ketenes have played a major role not only in synthetic chemistry, e.g. the synthesis of β-lactams leading to penicillins by a [2+2] cycloadditions with imines[1] and the production of ketene heterodimers for the synthesis of proteasome inhibitors[2], but also in the development of chemical theories such as the theory for pericyclic [2+2] cycloadditions of Woodward and Hoffmann[3]. At industrial level, ketene compounds, particularly ketene dimers, have been of major importance in several industries. The highly reactive diketene (parent ketene dimer) is frequently the reagent of choice for acetoacetylations[4]. Methyl acetoacetate and ethyl acetoacetate are the most widely used esters[5]; they are used in the pharmaceutical industries for the production of antibiotics and synthetic sweeteners. High molecular weight alkyl ketene dimers are utilized as constituents of paper sizing agents[6].

Despite their research and industrial importance several topics about the production and the properties of ketene dimers have been vaguely studied. It is well-known that ketene can undergo dimerization in polar solvents within a wide range of temperatures[7,8]. For the parent ketene the main product is diketene, whereas substituted ketenes afford cyclobutane-1,3-diones. The activation enthalpy for ketene dimerization in acetone is determined experimentally to be 10 kcal per mol at room temperature[7]. Ketene dimerization in the gas phase is by contrast a slow process with an activation enthalpy of 31 kcal per mol,[9] and the major product is diketene. It is not

1 Ulrich, H. *Cycloaddition Reactions of Heterocumulenes*; Academic Press: New York and London. 1967.
2 Ma, G.; Nguyen, H.; Romo, D. "Concise Total Synthesis of (±)-Salinosporamide A, (±)-Cinnabaramide A, and Derivatives via a Bis-cyclization Process: Implications for a Biosynthetic Pathway?". *Org. Lett.* 2007, 9, 2143-2146.
3 Woodward, R. B.; Hoffmann, R. "The Conservation of Orbital Symmetry". *Angew. Chem., Int. Ed. Engl.* 1969, 8, 781-932.
4 Clemens, R. J. "Diketene". *Chem. Rev*. 1986, 86(2), p. 241-318.
5 Miller, R.; Abaecherli, C.; Said, A. In *Ullmann's Encyclopedia of Industrial Chemistry*; Elvers, B., Hawkins, S., Schulz, G., Eds.; VCH: New York, 1990; Vol. A1; 69-71. Vol. A15; p. 63-75.
6 Hueter, R. U.S. Patent 2,383,863, 1945
7 Rice, F. O.; Greenberg, J. Ketene II. "Rate of Polymerization". *J. Am. Chem. Soc.* 1934, 56, 2132-2134.
8 (a) Williams, J. W.; Krynitsky, J. A. "Ketene Dimer". *Org. Synth*. 1955, 3, 508. (b) Sturzenegger, A. Preparation of Diketene. U.S. Patent 2,802,872, 1957. (c) Lacey, R. N. Dimerisation of Ketene in Medium of Diketene and Acetic Anhydride. U.S. Patent 2,848,496, 1958. (d) Zima, H. Stabilized Diketene and Method for its Production. U.S. Patent 3,271,420, 1966. (e) Bergmin, R.; Quittmann, W.; Stoffel, J. Process for the Reduction of the Polymer Portion in the Dimerization of Ketene. U.S. Patent 4,999,438, 1990.
9 Chickos, J. S.; Sherwood, D. E., Jr.; Jug, K. "Mechanism of Thermolysis of Diketene in the Gas Phase". *J. Org. Chem.* **1978**, *43*, 1146-1150.

established whether diketene is the major product as a result of kinetic or thermodynamic control or both. It is also not established the class of control for the major product of the dimerization of alkyl substituted ketenes. Design, optimization and control of processes that involve the ketene dimerization require the *prior* knowledge of the kinetics of the reaction and the thermochemical properties of the reactants and products. This knowledge can be achieved by the analysis of the compounds and the processes at molecular level.

The mathematical modeling used by chemical engineers for the analysis of phenomena encompassed in the chemical processes has been hitherto based on the macroscopic principia. Thus, the so-called MESH equations (Mass balance, equilibrium equations, mole fraction summation and enthalpy balance) and the momentum balance equation are widely applied in describing the operational regions into which equipments might operate[10]. The great disadvantage of the continuum macroscopic "tools" is the fact that they are, in their majority, explicitly independent on atomic structure relationship and they can be unable to predict the physical-chemical consequences of new conditions, new compounds or new reactions in the systems thereof. Molecular modeling arises as a new tool for the work of chemical engineers by providing the appropriate laws and equations that describe the systems according to their characteristics of size and time. The molecular modeling laws might describe properly the ketene dimerization reaction.

In fact, there have been several theoretical studies of ketene dimerization in gas phase, starting with the work of Jug et al.[11] A recent investigation by Rode and Dobrowolski[12] finds in opposition to experiments that diketene is more stable than cyclobutane-1,3-dione. It would be adequate to reassess the combustion data for these two compounds in order for clarifying their relative stability. On the other hand, it is surprising that there only are few experimental and no theoretical investigations on ketene dimerization in condensed phase, even though the important industrial production of diketene by dimerization is possible only at ambient temperatures in the

---

10 Grossmann, I. E. and Jackson, J. R. "A disjunctive programming approach for the optimal design of reactive distillation columns", *Com. Chem. Eng*. 25 (2001) 1661–1673.

11 Jug, K.; Dwivedi, C. P. D.; Chickos, J. S. "Reaction Pathways for Various Ketene Dimers". *Theor. Chim. Acta* **1978**, *49*, 249-25

12 Rode, J. R.; Dobrowolski, J. Cz. "Reaction Paths of the [2 + 2] Cycloaddition of X=C=Y Molecules (X, Y = S or O or CH2). Ab Initio Study". *J. Phys. Chem. A* **2006**, *110*, 207-218.

condensed phase[7,9]. The two experimental studies on the dimerization in condensed phase focus on the parent ketene[7] and dimethylketene,[13] respectively. In both investigations the rate of the reaction was second-order in ketene and increased with the polarity of the solvent. Moreover, it was found that the dimerization is an uncatalyzed process[7,9,11]. However, it is remarkable that the formation of the parent ketene dimer in the gas phase has a very high activation energy (31 kcal per mol)[9], whereas the activation energy is reduced to 10 kcal per mol in acetone[7].

We shall in this thesis apply the molecular modeling theories in order to clarify and examine the trends of the ketene dimerization in gas phase and how solvation effects modify the energetics of this reaction as well as the structure of the species involved. Chapter 1 presents a review of the principal features of the ketenes including their properties, reactivities, uses and dilemmas about the ketene dimers. In chapter 2 the readers can see a succinct discussion about ketene dimerization and the application of the available theories and correlations for explaining the character of this reaction in both gas and liquid phase. Chapter 3 introduces the readers to the main theories enclosed into the molecular modeling and some of their applications in the chemical engineering areas. Chapter 4 presents the application of the molecular modeling theories, particularly the density functional theory, in the analysis of the parent ketene dimerization in gas phase. Solvation effects on the ketene dimerization character for the parent ketene are analyzed in Chapter 5 by the use of the COSMO solvation model and the density functional calculations. Chapter 6 completes the analysis on the ketene dimerization reaction by estimating the thermochemical properties for substituted ketene dimers at the CBS-Q multilevel. In this final chapter, several unknown group additivity values are derived for the estimation of thermochemical properties of substituted ketene dimers. Finally, the knowledge generated in this work about the ketene dimerization is summarized in the concluding remarks.

---

[13] Huisgen, R.; Otto, P. "The Mechanism of Dimerization of Dimethylketene". *J. Am. Chem. Soc*. **1968**, *90*, 5342-5343.

Chapter 1

Ketenes and Ketene Dimers: An Overview of Their Distinctive Features

1.1 Introduction

Ketenes are compounds containing the functional group $>C_\beta=C_\alpha=O$ (Figure 1.1) and therefore belong to the family of heterocumulenes which have double bounds adjacent to each other[1]. They have been generally classified as aldoketenes (RCH=C=O) and ketoketenes (RR'C=C=O) exhibiting different reactivity properties.[2] However, we can find a great sort of ketenes reported in the literature[2]; Table 1.1 shows structures for some synthesized and reported ketenes. Theoretical calculations have been helping to understand the properties and reactivity of different class of ketenes (Table 1.1) because their highly reactive nature makes difficult the experimental manipulations and detections.[2,3] Indeed, theoretical calculations on parent ketene structure at different levels of theory are in excellent agreement with microwave structure results which determined the short C=C and C=O bond lengths as 1.3147 and 1.1626 Å, respectively (Figure 1.1)[4a]; Other experimental measurements are similar to these theoretical distances.[4b–d] Such agreement in results, and much other[2], provides confidence for estimating the actual structures and properties of unstudied ketenes and ketene derivatives from theoretical calculations.
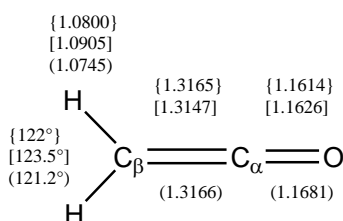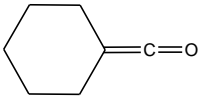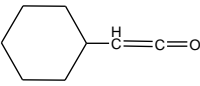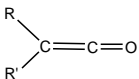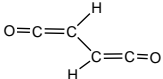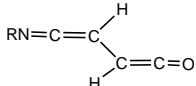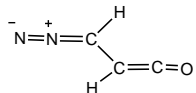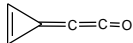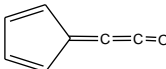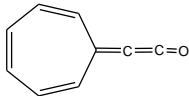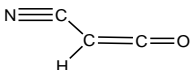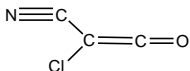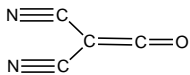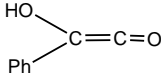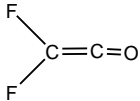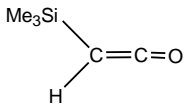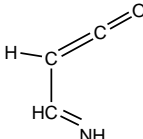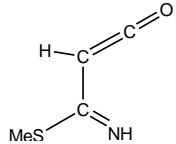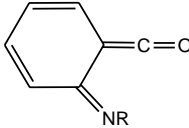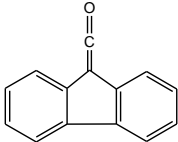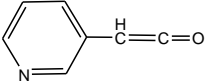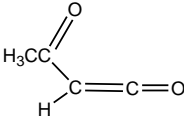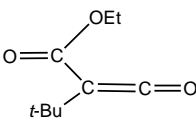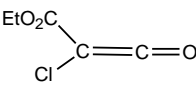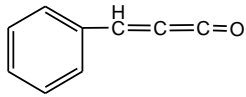
Figure 1.1. Bond distances (Å) and HCH bond angle (deg) of ketene. Experimental data from microwave spectrum Ref. 5a and Ref. 5b in braces and brackets respectively. Theoretical data at the MP3/6-31G(d,p) in parenthesis Ref. 5b.

Table 1.1. Some ketenes synthesized and reported in the literature.[2]

Alkylketenes	Cumulene-substituted ketenes	Fulvenones
Cyclohexylideneketene:	Allenylketenes:	Triafulvenone:
Cyclohexylketene:	Keteniminylketenes:	Pentafulvenone:
Aldoalkylketenes and ketoalkylketenes	Isocyanatoketenes:	Heptafulvenone:
Cyanoketenes	**Substituted ketenes**	**Imidoylketenes**
Cyanoketene:	Phenylhydroxiketene:	Iminoketene:
ChloroCyanoketene:	Difluoroketene:	Imidoylketene:
Dicyanoketene:	(Trimethylsilyl)ketene:	Iminoketene of iminoquinone methide:
Arylketenes	**Acylketenes**	**Cumulenones**
Dibenzofulvenone:	α-Oxoketene:	Carbon suboxide: $O=C=C=C=O$
	Carboethoxyketene:	Methyleneketene: $H_2C=C=C=O$
3-Pyridylketene:	(Carbomethoxy)chloroketene:	(Methylenebenzene)ketene:

Ketenes are much more reactive than simple olefins and they are more likely to enter into combination with reagents from which they are prepared or with the solvents used or into self-condensation to yield dimers or polymers[6]. The high reactivity and regio- and stereoselective properties of ketenes are dictated by their highest occupied molecular orbital, HOMO, and their lowest unoccupied molecular orbital, LUMO, of the CC and CO double bounds (Figure 1.2). These orbitals in both HOMO and LUMO lie in two different planes perpendicular to each other (Figure 1.2).[7] These configurations for the HOMO and LUMO allow for electrophilic attack to occur at C_β from above the ketene plane while nucleophilic attack at C_α is allowed to occur parallel to the ketene plane.[8] Molecular orbital charge densities of ketenes confirm the positive charge on C_α and the negative charge on oxygen and C_β.[9] This fact clearly gives an ambivalent (Figure 1.3) and a very reactive character to ketene compounds.[1]

HOMO   LUMO
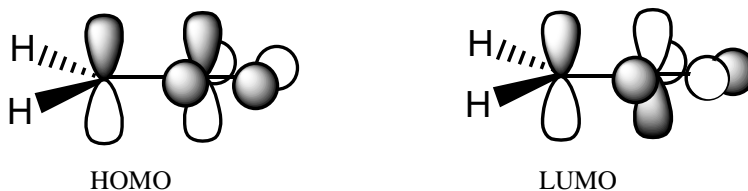
Figure 1.2. Frontier molecular orbitals for both the CC and CO double bounds of the parent ketene.
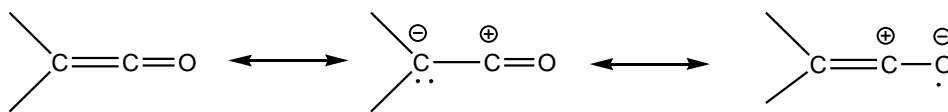
Figure 1.3. Resonance structure of ketene compounds.

Besides the electronic configuration, ketene compounds are geometrically favored for chemical attacks (Table 1.1). The *sp* carbon atom of ketenes is only disubstituted which lowers the steric hindrance and therefore facilitates the nucleophilic attacks. Because of this, ketenes could in principle serve as suitable acylating agents for sterically hindered substrates (r1).[10] On the other hand, the plane shape of ketenes and the occupied C=C orbitals (Figure 1.2) favored the

electrophilic attack to the electron pair on the C_β and therefore ketenes can be able to attach to an electron deficient substrate; for example, the reaction of phenylmercury alkoxide with ketenes may proceed according to r2.[1]

$$(\text{r1})$$

$$(\text{r2})$$
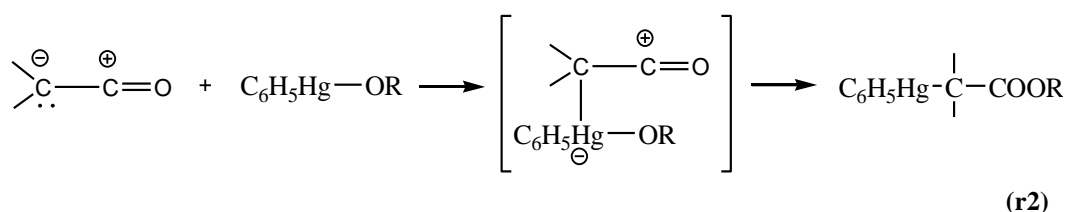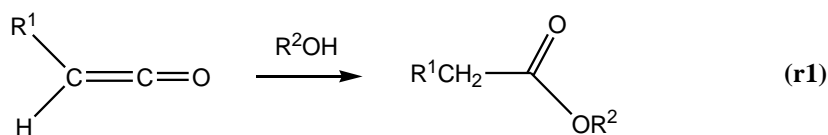
The high reactivity and the low steric hindrance allow ketenes, mainly across the C=C bond[3], to react with unsaturated compounds to give facile cycloadditions. Indeed, ketene cycloaddition of the [2+2] class constitutes one of the few routes to synthetically versatile four-membered rings (r3).[1,2,3,11] In fact, ketenes have been utilized for a high-yield preparation of tropolone, prostaglandins, β-lactams leading to penicillins and synthesis of quinones as well as spirocyclic compounds which are based on the reaction with methylenecycloalkanes.[2,3,11] Another [2+2] cycloaddition is the corresponding to homopolymerization[1] which might occur as an option to leading to a more stable system during the storage of ketenes. However, yet after homopolymerization, the dimers or oligomers formed still have double bonds in their backbone structure which allow these compounds to further transformations. These possibilities to further react make diketene, the prime product of parent ketene dimerization in liquid phase[12,13] (Figure 1.4a), highly valuable as an intermediate to industrial, agronomical and synthetic products.[2,14]

$$(\text{r3})$$

| (a) Diketene | (b) 1,3-Cyclobutanedione |
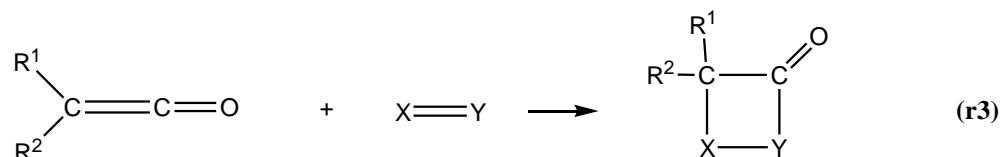
Figure 1.4. Ketene dimer structures.

Diketene type dimer (Figure 1.4a) is very valuable due to its atom oxygen in its heterocyclic arrangement[2,15], but has the characteristic that it is not the prime product of high weight ketenes. The hallmark of high weight ketene dimerization is the generation of cyclobutane-1,3-dione type dimer (Figure 1.4b). It has been widely known the general rule that ketenes, with the exception of parent ketene, undergo dimerization in solution, in the absence of catalysis, to afford the symmetric cyclobutane-1,3-dione type dimer (Figure 1.4b).[1,2] It is very rare that parent ketene can undergo dimerization to the more steric dimer, diketene, without a reported catalyst, even though the rate of dimerization in gas phase is very unfavorable for making the process feasible at moderate time.[13] Indeed, it is undecided whether ketene dimerization is feasible in liquid phase due to solvent effects[2,12,13] or a catalyst, yet unknown, is assisting the liquid-phase reaction. Besides, being an important intermediate, surprisingly ketene dimers do not have their thermochemical properties either experimentally measured or theoretically calculated. These facts make difficult to understand, to simulate and to design equipments and processes in which these compounds are produced and treated. This thesis is devoted to the theoretical study of the parent ketene dimerization in both gas and liquid phase and to the theoretical calculation of thermochemical properties for ketene dimers by the use of proper molecular modeling methods in order for improving the understanding of this fascinating class of versatile compounds.

1.2 Brief history of ketenes and ketene dimers

The history of ketene compounds started in 1905 with the preparation and characterization of diphenylketene (1) by Hermann Staudinger[16]. He prepared the ketene 1 by the dehalogenation of α-chlorodiphenylacetyl chloride with zinc (r4). This sort of reaction was soon utilized in the preparation of other class of ketenes[17].

$$\text{Ph}_2\text{C(Cl)}-\text{C(O)Cl} \xrightarrow{\text{Zn}} \text{Ph}_2\text{C}=\text{C}=\text{O} + \text{ZnCl}_2 \qquad \textbf{(r4)}$$

1
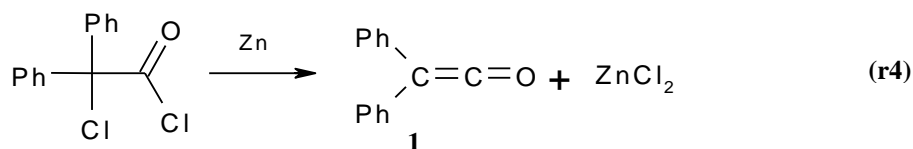
Shortly afterward, the ketene ($H_2C=C=O$) was prepared by N. T. M. Wilsmore[18] by immersing a glowing platinum wire into different reactants like acetic anhydride, ethyl acetate as well as acetone. Wilsmore noticed the tendency of ketene to condense on standing to a brown liquid and also pointed out that the dimerization was rapid and exhothermic in liquid state[18]. On distillation of the dimerization products, the first ketene dimer, named acetylketene by Chick and Wilsmore, was synthesized. The colorless liquid of ketene dimer was characterized to having the formula $CH3–CO–CH=CO$[19]. Although the structure of the ketene was elucidated in those early days, the right structure of the ketene dimer, diketene (Figure 1.4a), required almost half a century to be elucidated[14]. The generation of ketene dimers was found to be characteristically involved in the production of ketenes[20]. In 1908 Staudinger described the preparation of the parent ketene by the dehalogenation of bromoacetyl bromide with zinc[21]. Staudinger summarized the early findings in ketene chemistry in a monograph in 1912[22] and since then, there have been a number of reviews of ketene preparation and ketene chemistry.[7, 17] In 1946, Hanford and Sauer[18] provided an excellent review on the preparation of ketenes and ketene dimers. The most recent and comprehensive book on ketenes is the second edition, year 2006, of the book published by Tidwell[2] in 1995. This book provides a state of the art of all aspects of ketenes, including types of ketenes, reactions, syntheses, spectroscopic, physical properties and theoretical studies.

The chemical and industrial utility of ketenes and ketene dimers was recognized almost immediately to their appearance; the first industrial use of ketene appeared in the 1920's, when large quantities of acetic anhydride were required for the production of cellulose acetate[3]. At the same time, the industrial application of ketene for the production of acetic anhydride by the reaction of ketene and acetic acid took off. In the 1940's the industrial application of ketenes was extended to the paper industry. Higher molecular weight alkyl ketene dimers were utilized as constituents of paper sizing agents[23]. To date, the main industrial application of ketenes and ketene dimers has been in the paper-pulp cellulose industry. Diketene appeared to be an ideal

compound for chemical study; it was found to be inexpensive, readily available, reactive, and highly functionalized. An excellent review of diketene chemistry was made by Clemens[14] in 1986. More recently, ketenes and ketene dimers have received special attention for the synthesis of specialty chemicals as is described in the following section.

A distinctive feature attracted the attention in the earliest period of the ketene chemistry. Substituted ketenes were found to spontaneously dimerize into the cyclobutane-1,3-dione type structure (Figure 1.4b) whereas the unsubstituted ketene spontaneously dimerized into the β-lactone type dimer (Figure 1.4a).[20, 24] Thus, parent ketene dimerization was found as an atypical case for the generation of the β-lactone type dimer. In fact, the β-lactone dimer from dimerization of substituted ketenes could be obtained in most of the cases by a catalytic assistance of the *in-situ*-generated ketene.[20, 25] This procedure for ketenes and ketene dimers generation that comprises the reaction of an acid chloride and a tertiary amine was firstly demonstrated by Staudinger[26] and later patented by Sauer for the production of alkyl ketene dimers[27]. In this prodecure, dehydrohalogenation of the acid halide is assumed to involve the formation of an intermediate ketene monomer which rapidly undergoes self-addition, under the catalytic influence of tertiary amine and tertiary amine hydrohalide.[25] The interesting fact that β-lactone type dimers of substituted ketenes are produced by a non spontaneous way suggests that the parent ketene dimerization is also being affected by an external agent in order to produce this class of dimer.

Due to the special trend of parent ketene, two experimental studies were directed to determine its energetics. The first one[12], in 1934, showed second kinetic law in solution and low activation barrier in acetone. The second one[13], in 1978, obtained a very high activation barrier for the dimerization in gas phase. These results suggested the participation of the solvent as the principal reason for the different behavior of the parent ketene dimerization. Besides, combustion measurements reported that parent ketene dimerization generated β-lactone type dimer due to a kinetic control of the reaction. Since 1978, there have been no additional experimental studies that clarify the tendency of the parent ketene and substituted ketenes in the reaction of dimerization. Alternatively, theoretical studies have been carried out to analyze the dimerization of parent ketene in gas phase[28–33]. Results with high levels of theory[30, 31] validated the high

10

energy barrier obtained in the gas-phase experiment[13]. These calculations have been useful for clarifying some theoretical aspects about the mechanism of the dimerization; however, the clarification of the distinctive feature of the parent ketene dimerization can only be elucidated by the inclusion of solvent effects into these calculations. Extrapolation of the results of gas-phase parent ketene dimerization is also vaguely useful for substituted ketenes due to different steric and electronic effects. Besides, the scarcity of thermodynamic data for substituted ketenes and their dimers makes difficult to known whether the cyclobutane-1,3-dione type dimers are the major dimerization products because of just a kinetic effect. This research enhances the understanding of the ketene dimerization at experimental conditions with the inclusion of the solvent effects into the theoretical calculations and the estimation of thermochemical properties for the different ketene dimers.

1.3 Applications

Ketenes are generally highly reactive and they cannot be shipped over large distances or stored for long times thereof. Most of the industrial applications of ketenes involve a two-step process in which the initial step is the ketene production and the second step, usually carried out *in situ*, is the derivatization of ketenes to more useful and stable industrial commodities. The major industrial applications of ketenes are disclosed in the following.

1.3.1 Production of Acetic Anhydride

Most of the ketene produced worldwide is used in the production of acetic anhydride by the reaction of ketene with acetic acid (r5). This reaction has been known since the 1920's[14, 22] and it has been refined more recently.[20, 23, 26]

$$H_2C=C=O \ + \ CH_3COOH \longrightarrow \qquad \qquad \textbf{(r5)}$$
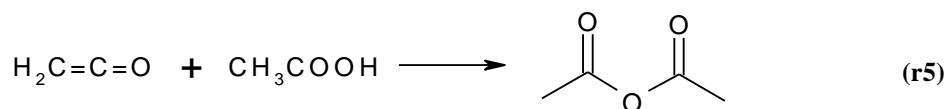
In the 1980's, ketene consumption for this purpose declined significantly when Eastman Chemical Company began producing acetic anhydride via methyl acetate carbonylation. However, other producers like Celanese continue to produce all of their acetic anhydride from

ketene. It is estimated that 22% and 90% of the acetic anhydride in United States and Japan, respectively, are based on the ketene/acetic acid process[34]. As regards world consumption, it was estimated that around 90% of the total amount of ketene produced in 1997 was consumed in the manufacture of the acetic anhydride[35].

Chemical characteristics of acetic anhydride include its ability to acetylate under mild conditions where the action of acetic acid is limited, its resistance to oxidation or cleavage of its methyl groups, its ease of chlorination, and its slow but easily catalyzed hydrolysis to acetic acid[36]. Particularly, its largest single outlet is the acetylation of cellulose to cellulose acetate, used for the manufacture of fibers, plastics, films, filters and coatings. Another important use is as a binding agent for ammonia released in the manufacture of polymethyl acrylimide hard foam. Acetic anhydride is also used in the manufacture of pharmaceuticals like aspirin and paracetamol. Other applications are the clarification of oils and fats, production of ethylenediaminetetracetate (bleaching activator), production of acetylated starch, manufacture of plasticizers such as glycerol triacetate and, in small quantities, for the manufacture of explosives.[24]

1.3.2 Production of Sorbic Acid

The second most important industrial use of ketene is the production of sorbic acid (r6). Reaction of ketenes with crotonaldehyde (3) in the presence of either Lewis acids or manganese (II) salts[37], organic acid zinc salts[38] or tetraalkyl titanates[39] gives, depending on the conditions, either the β-lactone (4) or the polyester (5)[36]. Both intermediate products can be converted to sorbic acid (6) by acid ion exchange[38], saponification[39] or thermal cracking in the presence of acid or alkaline catalysts[39, 40].

(r6)

12
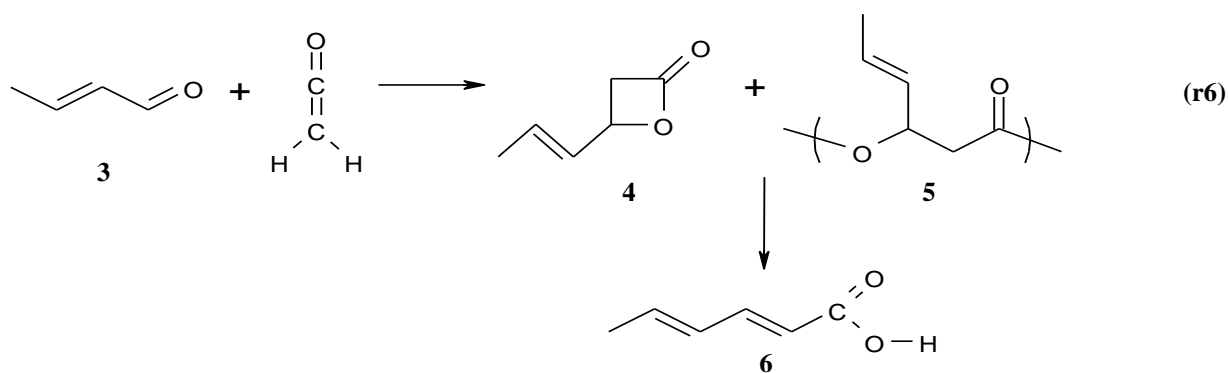
Sorbic acid and its calcium and potassium salts are used as preservatives for foods. The world demand for sorbic acid was estimated about 20,000 tons per year in 1990's[34]. About 5% of the total amount of ketene is consumed in the production of sorbic acid[36].

1.3.3 Production of Diketene and Diketene derivatives

The third major industrial use of ketene, about 4% of the total ketene production[36], is the generation of diketene (Figure 1.4a). Figure 1.5 shows the percentage consumption of ketene and diketene in United States during 1997.[36] The best-known commercial application of diketene is the acetoacetylation of nucleophiles like alcohols and amines in the presence of a catalyst to give the acetoacetate esters and acetoacetamines, respectively. Because it is highly reactive, diketene is frequently the reagent of choice for acetoacetylations on both laboratory and industrial scales[14]. Methyl acetoacetate (MAA) and ethyl acetoacetate (EAA) are the most widely used esters[3]; they are used in the pharmaceutical industries for the production of antibiotics and synthetic sweeteners. In the agricultural industries, MAA is used for the manufacture of insecticides and herbicides. EAA is converted to acetoacetanilide for manufacturing organic pigments[36b]. These two acetoacetate esters account for the 70-80% of the diketene consumption[36a]. Diketene reacts with difunctional amines and ureas to give a variety of heterocyclic compounds[41]. For instance, 6-methyluracil is produced by condensation of diketene with urea. It is used in the production of the feed additive orotic acid and the analgesic meperizole.[24] In spite of the innovative research of the last decades, many aspects of diketene chemistry remain either undeveloped or unexplored. Figure 1.6 illustrates a portion of the derivatives[3] that can be obtained with the assistance of diketene.

1.3.4 Other Industrial Uses

Ketenes are utilized in organic and drug synthesis. For example, ketene undergoes condensation on reaction with chlorine, substituted acyl chloride and acetone to form chloroacetyl chloride, acetoacetyl chlorides and isopropenyl acetate respectively. Chloroacetyl chloride has varied industrial uses, such as the production of alachlor type herbicides and lidocaine type anesthetics[3]. Acetoacetyl chlorides can react with alcohols to give the corresponding haloacetoacetates. Examples of industrial significance are ethyl 4,4,4-trifluoroacetoacetate for the production of herbicides (e.g. Monsanto's Dimension® and Rohm and Haas's Dithiopyr®) and ethyl 4,4,4-

trichloroacetoacetate for the production of pharmaceuticals such as Roche's Mefloquin[®].[36b] Isopropenyl acetate is utilized in the synthesis of acetylacetone which in turn is utilized in the manufacture, among others, of the sulfa drug sulfamethazine[3], production of anti-corrosion preparations and, synthesis of vitamin B6 and vitamin K[42].

(a) Ketene consumption   (b) Diketene consumption
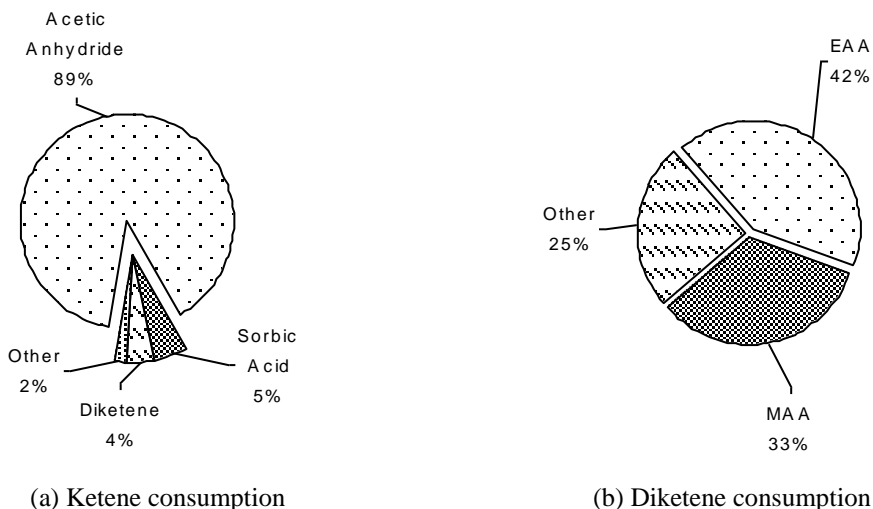
Figure 1.5. Ketene and diketene consumption in US, 1997 (Ref. 36a).

In the paper industry, high molecular weight alkyl ketene dimers, usually referred as AKD, have been utilized as constituents of sizing agents which give the outstanding ability of a paper to resist adsorption of aqueous ink (This topic is explained in some detail in section 1.4.2). These alkylketene dimers (AKD) react with the hydroxyl groups of cellulose and the long-saturated chains, thus added, become the paper surface hydrophobic.[43-44]

1.4 Preparation of Ketenes

Methods of preparation of ketenes are so varied and depend on the particular ketene. In some cases ketene dimers provide a good source of ketenes, most particularly in the case of ketene itself.
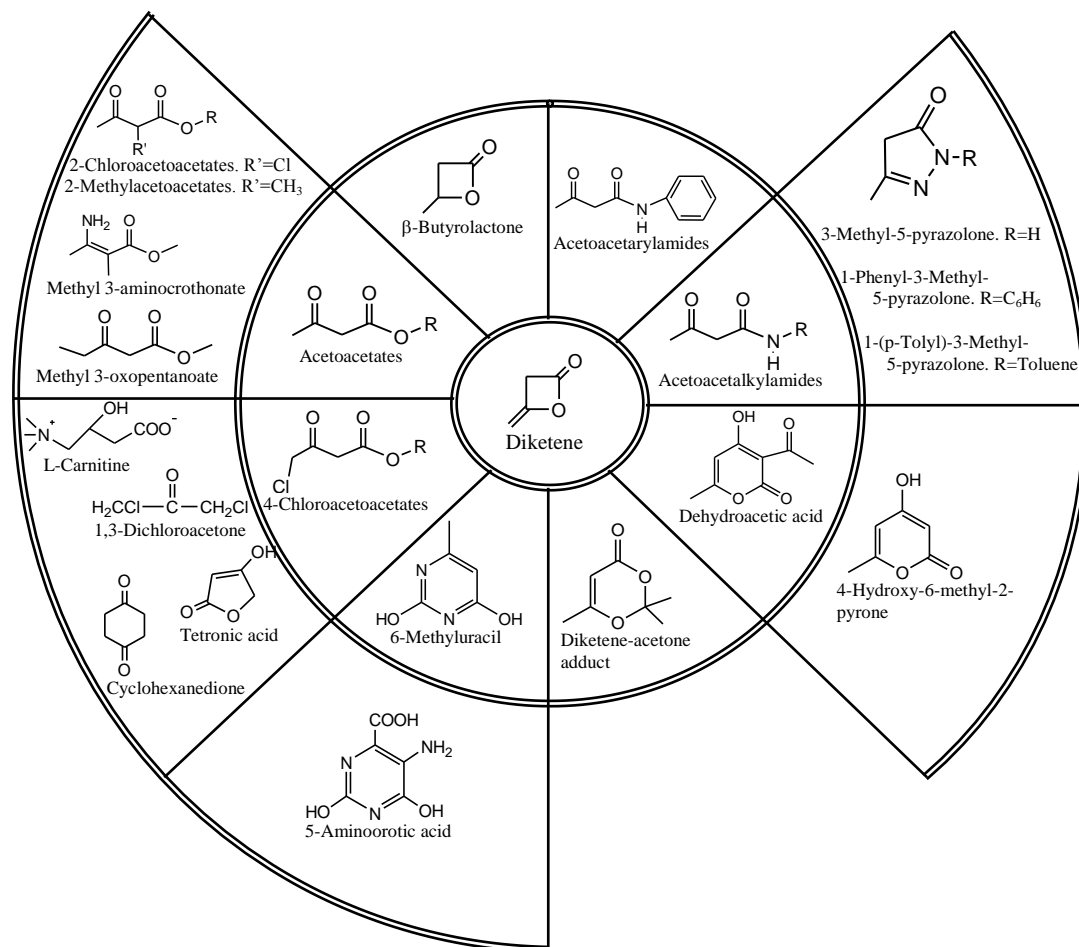
Figure 1.6. Diketene derivatives of the first generation (inner segments) and second generation (outer segments) (Ref. 36b).

1.4.1 Pyrolysis of carboxylic acids

The pyrolysis of acetic anhydride, ethyl acetate, or acetone with a heated metal filament was the first method utilized by Wilsmore for the preparation of ketene.[2] The direct preparation of the parental ketene on an industrial scale is achieved by the pyrolysis of acetic acid (r7). In this process, glacial acetic acid is evaporated and the vapor passed continuously under reduced pressure through a radiant multi-coil reactor at 740-760 °C. The formation of ketene can be accomplished by reaction of the appropriate carboxylic acids over alkali metal-exchanged zeoiltes at 350 °C.[2]

$$CH_3COOH \xrightarrow{750\ °C} H_2C=C=O\ +\ H_2O \qquad \text{(r7)}$$
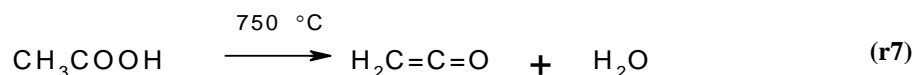
Other reactions occurring under the pyrolysis conditions along with the formation of ketene are the decarboxylation of the acetic acid (r8), the decomposition to produce carbon monoxide and hydrogen (r9), the thermal decomposition of the produced ketene (r10, r11) and acetic anhydride production by the reaction of ketene and the unreacted acetic acid (r12).

$$CH_3COOH \longrightarrow CH_4\ +\ CO_2 \qquad \text{(r8)}$$

$$CH_3COOH \longrightarrow 2CO\ +\ 2H_2 \qquad \text{(r9)}$$

$$2\ H_2C=C=O \longrightarrow CH_4\ +\ C\ +\ 2CO \qquad \text{(r10)}$$

$$2\ H_2C=C=O \longrightarrow C_2H_4\ +\ 2CO \qquad \text{(r11)}$$

$$H_2C=C=O\ +\ CH_3COOH \longrightarrow (CH_3CO)_2O \qquad \text{(r12)}$$
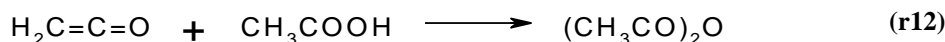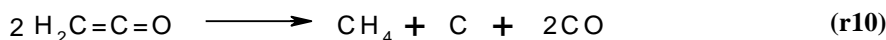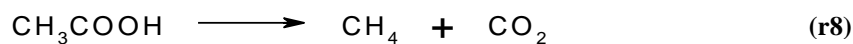
The stream exiting the pyrolysis reactor therefore contains water, acetic acid, acetic anhydride, and a few quantities of other gases (mainly carbon monoxide, carbon dioxide, ethylene, and methane). Finally, the gas mixture is chilled to less than 100 °C to condense and remove water, unconverted acetic acid and the acetic anhydride. The gaseous ketene is immediately treated to form diketene or acetic anhydride.

The pyrolysis of heavier carboxylic acids has not been useful for production of the corresponding heavier ketenes. The decarboxylation reaction is the thermodynamically preferred pathway for this class of acids. Carboxylic acids have also been converted to ketenes by treatment with certain reagents, among them TsCl, cicyclohexylcarbodiimide, and 1-methyl-2-chloropyridinium iodide (Mukaiyama's reagent).[51] Pyrolysis of carboxylic anhydrides, esters, ketones, diazo ketones and cyclobutanones can also generate ketenes.[2]

1.4.2 Dehydrohalogenation of acyl halides

Staudinger[45] demonstrated that the reaction of the acyl chlorides with basic catalysts, such as tertiary amines, correspond to an alternative way to prepare ketenes (r13). The scope of this method is broad, and most acyl halides possessing an α hydrogen give the reaction, but if at least one R is hydrogen, only the ketene dimer, not the ketene, is isolated[46]. This method has been used to prepare different class of ketenes such as methylketene[47], dimethylketene[48], diterbuthylketene[49] and haloketenes[50].

$$RR_1CH-\overset{O}{\underset{Cl}{C}} + Et_3N \longrightarrow RR_1C=C=O + [Et_3NH]^+Cl \qquad \textbf{(r13)}$$
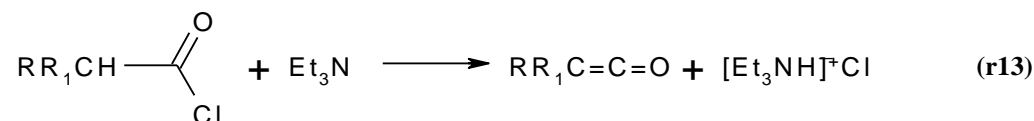
Several important compounds of pharmaceutical and drug discovery uses can be obtained from the ketene generated in situ from this route[25,51], for example, β-lactams from the reaction with imines[52], disubstituted β-lactones from the reaction with ethyl glyoxylate[49] and esters from acylation with alcohols[10]. β-lactams are of clinical relevance in both antibiotic and nonantibiotic uses. β-lactams are the most widely employed family of antimicrobial agents accounting for 50% of the world's antibiotic market[54]. One of the most promising nonantibiotic uses of β-lactams is the inhibition of serine protease enzymes. Several of such enzymes hold potential for the control of human cytomegalovirus[55], prostate and breast cancer[56], thrombotic episodes and, emphysema[57]. Disubstituted β-lactones can be utilized to assess substituted β-aspartates which are an important class of amino acids[53]. β-aspartates have received recent attention as a potential excitatory amino acid transporter (EAAT). EAAT play key roles in the regulation of L-glutamate which participate in fast synaptic communication, synaptic plasticity and learning and memory processes[58]. Ketenes are highly efficient acylating agents capable of forming esters with sterically hindered substrates[10]. Besides, acylation of chiral alcohols with ketenes can produce highly stereoselective compounds[43a]. This highly efficient and stereoselective addition of ketenes was recently utilized in a new method for the synthesis of the neuropeptide Y antagonists which are expected to be therapeutic agents for treating human obesity[43b].

This method of ketene generation has been also used extensively in the chemical industry for the preparation of long chain aldoketenes. These long-chain aldoketenes dimerize in situ to produce, probably under the catalytic influence of tertiary amine hydrohalide, the corresponding β-lactone dimers called alkyl ketene dimers (AKD). AKD, usually synthesized from mixtures of stearic and palmitic acid chlorides in presence of triethylamine, have been used as one of the most efficient sizing agent in alkaline papermaking for many years[43]. Sizing agents, such as AKD, chemically react with cellulosic fibers to render paper surface more water repellent, suitable for printing purposes[15,43,44]. The proposed mechanism of AKD sizing is the electrophilic addition to the free hydroxyl groups to form hydrophobic β-ketoester substituents on the cellulose fibers (r14) [15].

(r14)
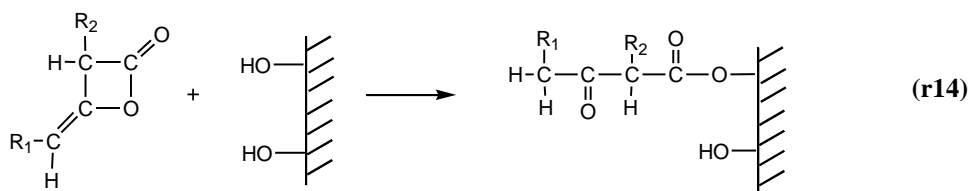
The sizing mechanism occurs during drying of paper sheets and is strongly dependent on different technological parameters like applied raw materials, pH value, time, temperature and method of drying[44].

1.4.3 Dehalogenation of α-halo acyl halides

The dehalogenation of α-bromodiphenylacetyl bromide by zinc was used by Staudinger in the first preparation of a ketene, diphenylketene in 1905, and the procedure has been used widely in the laboratory since. Ketenes can be prepared by dehalogenation of α-halo acyl halides with zinc, triphenylphosphine, and organometallic anions like $Mn(CO)_5^-$ and $Cr(CO)_4NO^{-}$.[2] The reaction generally gives good results when the two R groups are aryl or alkyl, but not when either one is hydrogen[51] (r15).

(r15)

18
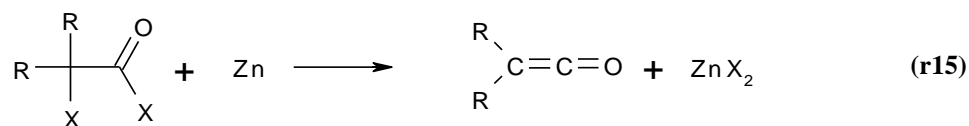
This reaction is carried out in the presence of an anhydrous solvent like ethyl acetate, diethyl ether or THF. The solvent helps to dissolve the zinc halides formed and helps to control the reaction temperature.[18] This process does not have any industrial application because of the limited availability of the starting materials and the complicated route to obtain them.

1.4.4 Other methods

Other non-catalytic ways to prepare ketenes are thermal decomposition of diazo ketones (Wolff rearrangements) and, thermolysis and photolysis of cyclobutanones, cyclobutenones, β-lactones and cyclobutanediones[2]. Ketenes have also been synthesized by catalytic procedures like catalytic partial oxidation of terminal alkynes[59], catalytic dehydration of carboxylic acids on complex silica and silica-boric oxide catalysts[60], reaction of carboxylic acids over alkali metal-exchanged zeolites[61], and catalytic synthesis of ketenes from carboxylic acids over silica[62] and silica monoliths[63].

1.5 Ketene Cycloadditions

Chemical reactions of ketenes are so varied and difficult to classify. However, most of the reviews about it agree that the main reactions are oxidation and reduction of ketenes, thermolysis, radical reactions, polymerization, addition and cycloaddition reactions, and photochemical reactions. The capacity of ketenes to cycloadd with different compounds, including themselves, has been known since the earliest period of ketene chemistry.[2] Cycloaddition is defined as a reaction of unsaturated organic compounds to give a cyclic product by transferring electrons from π bonds to new σ bonds[64]. The first isolated cyclocompounds from ketenes were the unsymmetrical ketene dimer (Figure 1.4a) by Chick and Wilsmore and the symmetrical dimer of dimethylketene (Figure 1.4b) by Staudinger and Klever. Many reviews devoted partially or exclusively to ketene cycloadditions have been published.[1,2,41] Specific topics that have been reviewed include haloketenes, fluoroketenes, cyanoketenes, intramolecular cycloadditions, conjugated ketenes, and β-lactam antibiotics.[1,2,41]

Among the cycloadditions that ketenes can undergo is the category of [2+2] cycloaddition; i.e. the formation of a cycloadduct from 4π electrons.[64] This reaction can produce four, five or even more membered rings.[64,65] The propensity of ketenes in giving facile [2+2] cycloaddition is one of the major important feature of ketene chemistry.[2] In this category of cycloaddition falls the reaction of ketene with alkenes, carbonyl compounds, imines and ketene themselves (i.e. dimerization). All of these reactions give four-membered cycloadducts. Some of these reactions have proven to be very useful in the chemical synthesis of pharmacologically valuable compounds.[66] Cycloaddition with alkenes constitutes one of the few routes to synthetically versatile four-membered rings.[67] Ketenes have general preferences of reacting with olefins through the C=C double bond rather than the carbonyl group and therefore, the preferred products of these reactions are cyclobutanones instead of oxetanones (r16).[68,69] Cycloadditions between ketenes and carbonyl compounds afford β-lactones (2-oxetanones) (r17) which are useful synthetic intermediates in the preparation of alkenes, allenes, carboxylic acid derivatives (including amino acids), and polymers.[70] The formation of β-lactones through this cycloaddition has the character of a nucleophilic attack on C_α and a electrophilic attack on C_β of the ketene (r11 and Figure 1.1).[2] β-Lactams (2-azetidinones) can be produced by the so-called Staudinger reaction between ketenes and imines (r18). β-Lactams are of wide interest because of the presence of this ring system in antibiotics such as penicillin[54] and other biologically important compounds[55-57]. This reaction is often carried out with ketenes generated *in situ*, and therefore, there is a question as to whether a free ketene is the unique participant or whether the reaction involves the raw compounds utilized for the generation of the ketene.[2]

(r16)

(r17)

$$R_1R_2C=C=O \; + \; R_1'R_2'C=N-H \longrightarrow \quad \textbf{(r18)}$$
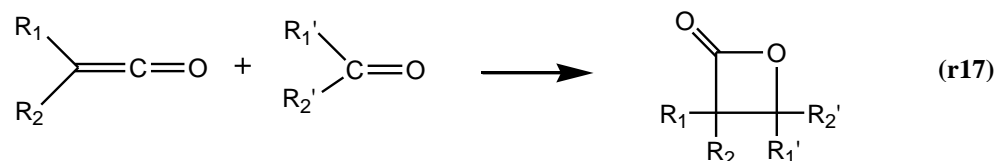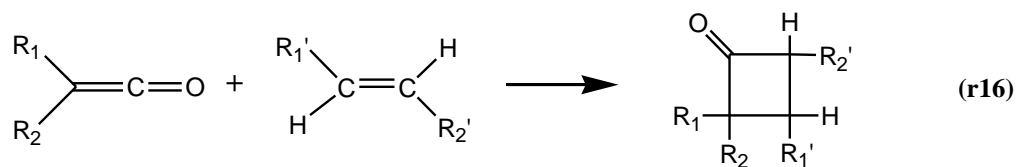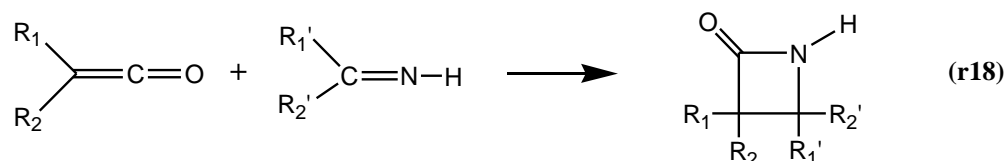
The experimental data for the preceding [2+2] cycloadditions can be explained by either concerted or two-step via zwitterion pathways.[2,71] Surprisingly and in contrast to theses ketene cycloadditions, the parent ketene dimerization has been of less importance for both theoreticians and experimentalists, even though its industrial and synthetic importance since diketene and diketene derivatives production constitutes the third most important application for ketene compounds (section 1.3.3). Extrapolation from these [2+2] ketene cycloadditions cannot be useful for understanding the trends of ketene dimerization in both gas and liquid phase. Ketene dimerization is different from these ketene cycloadditions due to steric and electronic characteristic features of the ketenes. Therefore, ketene dimerization deserves a special treatment that is given in the following.

1.5.1 Ketene dimerization

Another [2+2] cycloaddition of ketenes is the dimerization which corresponds to the main concern of this research. All known ketenes dimerize when heated or when allowed to stand at room temperature or below for a sufficient time. This dimerization is so rapid that ketene does not form β-lactones with alkenes, aldehydes or ketones, except at very low temperatures.[2,72] The driving force of this reaction may be the electronic configuration of the monomer and owing to the ambivalent character of the ketenes (Figure 1.3) two pathways are possible[72]. Addition across both the C=C and the C=O double bonds leads to the asymmetrical dimer (r19), whereas addition across the C=C double bounds affords the symmetrical dimer (r20). Therefore, Dimerization of ketenes can yield cyclobutane-1,3-diones, β-propiolactones or both (Figure 1.4). If the cyclobutanedione has one acidic hydrogen, the enol form generally predominates, and acylation of this enol form can occur[41]. Parent ketene dimerizes exothermically at room temperature or below to yield mostly the β-propiolactone structure for which experiments founded to be the thermodinamically less stable dimer product for this reaction.[13,73] Monosubstituted and disubstituted ketenes generally give cyclobutane-1,3-diones in very high yield.[25,41] Preparation of

asymmetrical, β-propiolactone, type dimer from dimerization of monosubstituted ketenes is a non-spontaneous process.[2,25] The most convenient preparation of aldoketene dimers is that of dehydrohalogenation of acyl halides with tertiary aliphatic amines (section 1.4.2).[2]

(r19)

(r20)
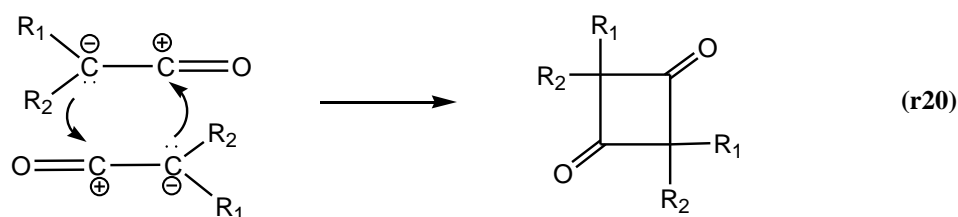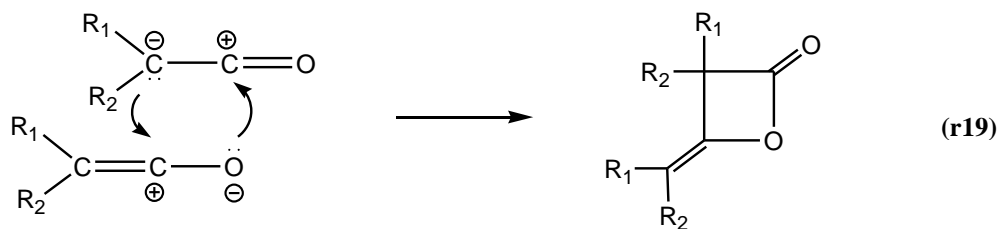
Commercial and research uses of ketene dimers are so varied. Additional to the applications mentioned in the 1.3.3 and 1.3.4 sections are drug discovery and combinatorial chemistry. In drug discovery, 4-Alkylidene-β-lactones (hetero ketene dimers) are useful precursors for total syntheses of the β-lactone-containing proteasome inhibitors salinosporamide, cinnabaramide, and derivatives[74]. Such proteasome inhibitors exhibit valuable therapeutic possibilities in cancer treatment; particularly, salinosporamide is currently in phase I human clinical studies for multiple myeloma.[75] Combinatorial chemistry (CC) is a scientific field that uses a combinatorial process to prepare sets of compounds from sets of building blocks.[76] CC serves as a powerful tool in lead discovery and lead optimization by allowing a rapid generation of potential candidates for screening.[77] Applications of CC are broad and cover from catalyst and materials discovery to sensors design. The development of new methods for the synthesis of heterocyclic compound libraries with molecular diversity is an ever-expanding area in combinatorial chemistry.[77] Recently, combinatorial libraries (i.e. a set of compounds prepared by combinatorial chemistry[76]) of new 1,3-imidazoline-2-thiones and 2-phenylimino-1,3-thiazolines have been developed by using γ-chloroacetoacetanilides. These last compounds were prepared by the sequential reaction of 4-methylene-oxetan-2-one (diketene) with chlorine and various anilines.[78]

Despite the increasing commercial and research importance of diketene and other ketene dimers, the mechanism for their generation is in most of the cases plausible. For the case of ketene (I refer to the parent ketene, $H_2C=C=O$, from this point onward unless otherwise stated), compelling evidences suggest that dimerization proceeds through an asynchronous activated complex, yet along a concerted way; however, explanations for experimental gas and liquid phase findings lead to a dilemma whose solution is the principal concern of this research. It is well known that the major product of the ketene dimerization in solution is the diketene while gas-phase dimerization is not appreciable at room temperature.[19,79,80] Early investigations on parent ketene dimerization obtained this fact when reported that liquid brown deposits produced during the storage of the gaseous ketene were caused by the dimerization in condensed acetone or acetic acid.[17] There have been a few experimental and theoretical studies on ketene dimerization for explaining its facile liquid-phase dimerization.[2] In 1934, Rice and Greenberg[12] carried out liquid-phase experimental dimerization in different solvents covering a wide range of polarity. They found a good agreement of the results with a second order kinetic law and assessed a value of ca. 11 kcal per mol for the energy barrier toward diketene in acetone.[12] Besides, Rice and Greenberg[12] found the ketene dimerization to be independent on the content of oxidants in the reaction mixture and interpreted their results in favor of a concerted process. It is worth mentioning that Rice and Greenberg[12] performed the unique study on the rate of liquid phase dimerization that can be found in the open literature. Rice and Roberts[81] in 1943 studied the pyrolysis of diketene concluding that the reaction does not involve diradical intermediates. In 1968, Månsson et al.[82] assessed a value of -45.8 kcal per mol for the heat of formation of diketene. In 1978, Chickos et al.[13] interpreted the generation of parent ketene from the thermolysis of diketene, in accordance with Woodward and Hoffman rules[3] for pericyclic reactions and in agreement with Rice and Roberts[81], as a concerted process and assessed a value of 31 kcal per mol for the activation energy of the gas-phase dimerization at room temperature.[13] Chickos et al.[13] also measured the heat of combustion and sublimation of cyclobutane-1,3-dione and based on the combustion results of Månsson et al.[82] suggested that the cyclobutane-1,3-dione product was 1 kcal per mol more stable than the diketene product. Additionally, Chickos et al.[13] obtained that cyclobutane-1,3-dione was besides diketene thermodynamically accessible from gas-phase ketene dimerization. Lastly, in 1977, Tenud et al.[83] showed that cyclobutane-1,3-dione

23

was also an accessible compound from liquid-phase ketene dimerization. They reported that a small amount of the symmetrical 1,3-cyclobutanedione dimer was produced in a yield between 4% and 5% in acetone; the principal product was diketene.[83]

Altogether, we can conclude from the analysis of the experimental data (Table 1.2 shows a summary of the principal results) that:

- The high energy barrier makes gas-phase dimerization an unfeasible process.
- The ketene dimerization lowers its activation energy ca. 20 kcal per mol in going from gas phase to acetone solvent.
- Both diketene and 1,3-cyclobutanedione, though this latter in much less proportion, are accessible products from the ketene dimerization.
- It is not clear whether diketene, being the less stable dimer, is the major product because of just a kinetic effect. This due to the reaction toward 1,3-cyclobutanedione has not been studied yet.

Besides, since the common consensus of the literature about concerted [2+2] cycloaddition dictates that they are solvent insensible[41,51,64,84] (Chapter 2 discloses a presentation about the mechanisms for [2+2] cycloadditions) the mechanism for the reaction in liquid phase, yet with the experimental data matching a second-order kinetic law[12], can be only vaguely classified as concerted.

Table 1.2. Experimental data on ketene dimerization.

	Activation barrier, kcal per mol		Heat of reaction gas phase[a], kcal per mol	Experimental facts	
	Gas	Liquid[b]		Gas[c, d]	Liquid[d, e]
Diketene	31[c]	11[d]	-23	Unobserved from the reaction. Geometry from experiments.	Second order kinetic law. No intermediates found.
Cyclobutane-1,3-dione	--	--	-24[c]	Unobserved from the reaction.	Subproduct. 4% - 5% in acetone

[a] Heat of formation for ketene was taken as -11.4 kcal per mol. [b] Acetone. [c] Ref. 13. [d] Ref. 12. [e] Ref. 83.

Mechanistically, gas-phase ketene dimerization has been studied at different levels of theory. In 1991 Seidl and Schaefer[30] studied the ketene dimerization toward diketene and cyclobutane-1,3-dione at the CISDQ/DZP//SCF/DZP level and suggested that the reaction was kinetically controlled towards the less stable product, diketene. The energetic results found at this level were in excellent agreement with experimental values for diketene reaction[13, 82] suggesting that the concerted pathway obtained, yet with asynchronous activated complexes, could explain the ketene dimerization mechanism. The results of Seidl and Schaefer's study[30] were in controversy when the geometry of diketene predicted at SCF/DZP level was found to be in disagreement with the geometry experimentally determined by electron diffraction and X-ray crystallography.[85] This discrepancy meant that the geometry of the activated complexes, yet with the energies in good agreement with experiments (presumably by some error compensation), did not represent the ketene dimerization unequivocally. In 1994, Salzner and Bachrach[31] performed a CCSD(T)/6-31G(d)//MP2/6-31G(d) study yielded activated complex structures fairly similar to that found by Seidl and Schaefer[30]. However, in opposition to experimental results[2, 17, 19, 79, 80], energies obtained by Salzner and Bachrach study[31] were found to favor cyclobutane-1,3-dione over diketene both kinetically and thermodynamically.[31]

In 2004, Kelly et al.[32] performed a Car-Parrinello projector augmented-wave DFT calculation on the ketene dimerization and concluded that diketene was the major product because of a thermodynamic control of the reaction. The energetics found in this work were based on the Gibbs energy and did not calculate the experimental enthalpy data, though. Very recently Rode and Dobrowolski[33] calculated the ketene dimerization at the MP2/aug-cc-pVDZ level and the G3 multilevel. Both levels of theory coincided that the energy for the ketene dimerization reaction toward both diketene and cyclobutane-1,3-dione were so closed to have definitive conclusion. In opposition, these levels of theory found different trends for the heat of the reactions.[33] The MP2/aug-cc-pVDZ level predicted in agreement with experiments that cyclobatane-1,3-dione was more stable than diketene whereas the G3 multilevel predicted the contrary (i.e. in accordance with Kelly et al. results[32], diketene was found to be more stable than cyclobutane-1,3-dione).[33] Altogether, we can conclude that, as Kelly et al.[32] stated, the conflicting predictions on the ketene dimerization trends seem to reside in the quality of the theoretical method used. The utilized methods, until now, have not been able to reproduce the experimental data for the

energy barrier, the heat of reaction toward diketene product and the geometry of this very product. Therefore, the gas-phase ketene dimerization mechanism has not been established unequivocally yet.

Liquid-phase mechanisms for ketene dimerization have only been discussed from theoretical gas-phase results.[2,30] Qualitative concerted and stepwise models have been proposed in order to account for the experimental observations.[2,12,30] However, inclusion of the solvent effects in the theoretical studies is required for a realistic comparison to the experimental situation. The inclusion of solvent effects would clarify some intriguing aspects about the mechanism of the ketene dimerization (*vide supra*). For example, should solvent effects make feasible the reaction, a concerted mechanism may not explain such a lowering in the energy barrier compare to gas phase. In fact, the experimental value for the gas-phase energy barrier towards diketene is very high for the reaction to proceed to any measurable extent (Table 1.2), suggesting that the reaction only is possible at room temperature or below by the assistance of a third agent. This accelerating agent can be either a solvent or an unknown catalyst brought in the stream along with the raw ketene (see section 1.5). As it was stated above, the third agent lowers the energy barrier ca. 21 kcal per mol when the solvent is acetone.[12] It seems improbable that such a lowering in the energy barrier can be achieved by solely solvent effects since the reaction is thought to be concerted.[41,51,64,84] At both experimental and theoretical levels, the role of solvent effects on the feasibility of the cycloadditions, especially in [2+2] reactions, only is generally taken as an ancillary topic of minor importance. Hyatt and Raynolds[41] stated: "Solvent effects, while general, are not always of practical importance, since ketene cycloadditions are generally run without solvent if possible"; March reinforced this conception stating that: "Solvents are not necessary for [2+2] cycloadditions".[51]

Despite the general consensus about the role of solvents in cycloadditions, experiments carried out in the last few decades and the application of powerful theories in the study of chemical reactions in both gas and liquid phase have been reviewing this paradigm. In 1995, Bernardi et al.[86] carried out a theoretical study at the MCSCF/4-31G level with the self-consistent reaction field (SCRF) model for solvent effects suggesting that polar [2+2] cycloadditions can proceed through both a concerted and a non-concerted path. The concerted path possessed greater energy

barrier than the non-concerted one in gas phase and therefore, solvent effects could favor the non-concerted path.[86] This study showed that solvation is favorable for both the concerted and non-concerted process and produce nearly the same quantitative lowering in the energy barrier. However as the non-concerted path has the lower barrier in gas phase it is also the preferred path in liquid phase.[86] Truong[87], in 1998, studied the reaction of ketene with imine at the MP4/cc-pVDZ//MP2/6-31G(d,p) level and inclusion of solvent effects by the generalized (GCOSMO) conductor-like screening model. Truong results suggested that solvent effects change the mechanism in going from gas to liquid phase (aqueous solution) and lower the energy barrier at about 4.5 kcal per mol.[87] This study allowed Truong to state that: "Although direct experimental data for this reaction do not exist, calculated solvent effects on structures and reactivity should be general to other [2+2] polar cycloaddition reactions". The findings of the preceding researches suggest in opposition to experimental results (*vide supra*, Table 1.2) that ketene dimerization may change its mechanism in going from gas to liquid phase in order to make feasible the reaction.

In fact, analysis of the kinetic data collected by Rice and Greenberg[12] in solution shows a tendency of the reactant ketenes to developing charge along the reaction coordinate. This fact and the relative good correlation among the kinetic data and solvent polarity parameters suggest that ketene dimerization proceeds by either an asynchronous concerted or a two-step via zwitterionic intermediate mechanism in liquid phase. Selection of two-step via zwitterionic intermediate mechanism should not be done *a priori* since intermediate have not been detected yet.[12,30] Chapter 2 illustrates the analysis of the kinetic data in solution and comments about the possibility of having the two-step mechanism. The preceding results, yet favoring the solvent effects on [2+2] ketene cycloadditions, may not support the idea of solvent as accelerating agent in ketene dimerization because of the great lowering in energy.[12] Chapter 2 compares the relative lowering in the energy barrier for several cycloadditions and the results suggest that ketene dimerization possesses an anomalous behavior, which we could not found in other [2+2] cycloaddition at theoretical level. The results also shows that the lowering in the energy barrier of ketene dimerization is of comparable magnitude to that achieved in the catalytic acceleration of the cycloaddition of ketene imine with formaldehyde.[88]

The possibility of an unknown catalyst favoring the ketene dimerization in liquid phase is very attractive up to this point. It has been found that certain [2+2] cycloadditions which do not occur thermally can be made to take place by the use of certain catalysts, usually transition-metal compounds.[89] The use of $ZnCl_2$ catalyst enhances the rate of formation of cyclobutanones from the cycloaddition of ketenes and vinyl ethers.[46] The role of the catalyst is not certain and may be different in each cycloaddition case. One possibility is that the presence of the catalyst causes a forbidden reaction to become allowed by a nonconcerted (stepwise) mechanism.[51] Lewis acids are reported to accelerate the dimerization of high weight aldoketenes[2] as well as another [2+2] cycloadditions of ketenes[90,91]. According to experimental analysis in the process of production of ketenes (section 1.5), there is no a Lewis acid involved in the reactions of generation of ketenes, except the ions of metals that may be detached from the wire used in the process. However, there are no reports that show feasible such separation of ions from the wire[63] and therefore a catalytic acceleration may be discarded for explaining the mechanism of the ketene dimerization.

Altogether, the solvent can be proposed as the accelerating agent for the dimerization. This likely accelerating agent may alter the mechanism from concerted in gas phase to stepwise in liquid phase in order to facilitate the [2+2] cycloaddition.[86,92] Thus, ketene dimerization reaction may only be possible if its mechanism switches to a stepwise one in solution. This suggestion may be in opposition to experimental findings on the ketene dimerization[12,30] and conventional assumptions about [2+2] cycloadditions in liquid phase[41,51]. A comprehensive argumentation about the unclear trend of the ketene dimerization in both gas and liquid phase is presented in chapter 2. Elucidation of whether or not the solvent effects become feasible the ketene dimerization is the main concern of this research. For doing this, theoretical quantum mechanics calculations are used to describe the mechanism of the ketene dimerization. Chapter 3 presents a brochure of the principal theories and achievements of the quantum calculations.

1.5.2 A thermochemical approach to ketene dimerization

Reliable thermochemical data of compounds at the conditions of interest are essential to understanding and controlling chemical equilibrium at industrial scale.[91] With this information, different probable reaction mechanisms can be evaluated and compared from kinetic and thermodynamic point of view by considering the energetics of both transition states and

products. For example, when we have a reaction between two molecules (2R) with two possible mechanisms A and B (to products A and B, respectively) and the energetics of them are closed each other, we have either of the following cases (Figure 1.7):

1- Gibbs energy barrier for A is lower than that for B and Gibbs energy of product A is lower than that of product B (Figure 1. 7a): Reaction mechanism that prevails during the reaction corresponds to that for product A due to both kinetic (energy barrier) and thermodynamic (relative energy of the products) control of the process.

2- Gibbs energy barrier for A is greater than that for B and Gibbs energy of product A is lower than that for product B (Figure 1.7b): Reaction mechanism that prevails depends on the measured time for the reaction. Thus, mechanism B prevails at the beginning due to a kinetic control of the reaction and reaction mechanism A prevails at the end of the reaction due to a thermodynamic control.

Accordingly, depending on the relative values for the barriers and the energy of the products, a given reaction with two or more possible mechanisms can be governed by either kinetic or thermodynamic control. For the case in study, thermodynamic control of the mechanism A, which has the lower energy barrier (kinetic control), means that the energetically disfavored product B (Figure 1.7a) is obtained as a sub-product all the time during the process whereas kinetic control of the mechanism B means that the energetically disfavored product B (Figure 1.7b) only is obtained as the major product to some extent at the beginning of the reaction. At engineering level, if the appreciable product B is obtained by kinetic control this implicates a good control scheme for achieving the point of maximal conversion into product B and less conversion into product A while if the appreciable product B is obtained as a consequence of the thermodynamic control it involves long contact times, major consume of raw materials and a scheme of purification from the mixture with the undesirable product A.

The preceding example depicts the case for gas-phase ketene dimerization for which experimental facts suggest to be controlled kinetically towards diketene. [13, 82, 83] These experimental facts are supported by some quantum chemical calculations at low and medium levels of theory.[30,31] Seidl and Schaefer[30] calculated the ketene dimerization at the SCF/STO level and reproduced both the experimental energy barrier for the production of diketene[13] and

the relative less energy of this product[13,82] compare to 1,3-cyclobatenedione. These calculations were partially confirmed by Salzner and Bachrach at the MP2/6-31G(d).[31] These results and the fact that diketene is the major product of the reaction[12,83] classed the ketene dimerization as to be controlled kinetically.[30] However, recent gas-phase calculations at higher levels of theory suggest that ketene dimerization experience thermodynamic control instead of or in addition to kinetic control.[32,33] Calculations at the Car-Parrinello projector augmented-wave DFT level[32] and G3 multilevel[33] found diketene to be more stable than 1,3-cyclobutanedione. Also, the DFT dynamic results[32] found that the energy barrier towards diketene was greater than that towards cyclobutane-1,3-dione whereas results for the energy barrier at the G3 multilevel[33] concluded an unclear tendency in the energy barriers because results were within tolerable error (see discussion in section 1.5.1). These high-level theoretical thermochemical data do not agree with experiments in the value for the energy barrier of ketene dimerization towards diketene and 1,3-cyclobutanedione as well as for the energy of these products (Table 1.2).[13,82,33]

(a) Kinetic and thermodynamic control of A.

(b) Kinetic control of B and thermodynamic control of A.
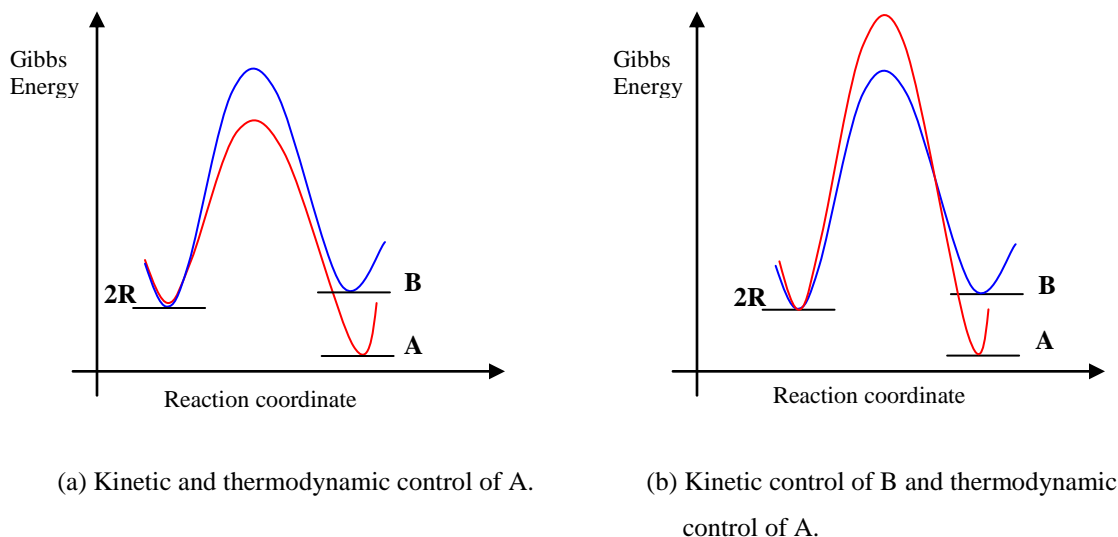
Figure 1.7. Kinetic and thermodynamic control for the system 2R→A and 2R→B.

This class of disagreements between experiments and theoretical calculations seem characteristic for ketenes, though not much is known about the thermochemistry of these compounds. For example, correct values for the heat of formation of methyl- and dimethylketene were originally a subject of dispute until a consensus was reached between experimental and theoretical values.[93] In 2000, Trager[93d] based in threshold photoionization mass spectrometry experiments obtained

the values for the heat of formation of methyl- and dimethylketene that were in good agreement with those calculated by Scott and Radom[93e] at the CBS-APNO level. In 2002, Sumathi and Green[7] using the CBS-Q multilevel reproduced with good agreement the experimental values obtained by Traeger[93d]. With these facts, the persistent disagreement between theoretical and experimental values appeared to arise from an overestimation in the former methods used for assessing the heat of formation due to errors in the experimental detection of methyl- and dimethylketene ions.[93a] In total, theory results could anticipate the right values for these ketene compounds. With this fact, we may not discard *a priori* an experimental error in the measurement of the thermochemistry for diketene and ciclobutane-1,3-dione. Therefore, this suggests that it still is undecided whether diketene is the major product due to kinetic or thermodynamic control of the reaction. Besides, conclusions in gas phase may not represent the experimental conditions for the ketene dimerization as it is found to be feasible only in liquid phase.

High multilevel theoretical calculation, such as CBS-Q, may help to resolve the dilemma about the energetics of diketene and ciclobutane-1,3-dione since it was found to reproduce accurately the experimental values for ketene, mehtylketene and dimethylketene[7]. The goal of this research can be accomplished by studying at the CBS-Q multilevel the heat of formation of these ketene dimers and other high weight ketene dimers. Thermochemistry for high weight ketene dimers can help to clarify the trends for the dimerization of these ketenes since it is unknown whether the formation of cyclobutane-1,3-dione type dimer is the major product due to just a kinetic effect. As it is discussed in chapter 3, CBS-Q method requires so high time machine that it is practically unfeasible in calculations on more-than-nine-heavy-atom molecules with the current computational resources. This hampers the CBS-Q calculations for the thermochemistry of high weight ketene dimers. As an alternative, structure-based methods can be developed for estimating the thermochemistry of these compounds (section 1.6.2). Benson-group-based methods are very suitable for quick preliminary screening of process alternatives due to their success in predicting reliable data at low-computational costs.[94] It is also an objective of this research to estimate the contribution values for unknown groups contained in the ketene dimers in order to ease the calculation of thermochemical properties for high weight ketene dimers and other polymers of ketene.

1.6 Molecular modeling tools

Analysis of different phenomena at wide range of length and time can be performed by the use of proper theories. At nanoscopic and microscopic levels, in which most of the chemical reactions take place, electronic structure methods model the interactions between atoms and molecules. These atomic and molecular interactions influence the tendency of the system not only at nano- and microscopic levels but also at greater levels of length and time (i.e. mesoscale and macroscale). Such influences can be averaged by use of the statistical thermodynamics which bridge the atomic and molecular properties with the bulk properties of the system. In this way, data derived from theoretical calculations can be compared with data measured from experiments in order to validate the theoretical description of the phenomena; e.g. a proper description of the ketene dimerization reaction can be achieved by a level of theory that can match the available experimental data (Table 1.2). The different theories according to the scale of length and time and a brochure of their achievements are disclosed in chapter 3.

Description of the energy along the coordinate of chemical reactions has been particularly a great achievement of electronic structure methods. Potential energy surface characteristics derived from atomic movements within systems (i.e. minima and saddle points) determine the possible mechanisms that chemical reactions can follow from the reactants to the products. Such mechanisms are thus expressed in terms of geometry-energy coordinates that embrace both kinetic and thermodynamic data which can be directly compared to experimental values for the reactions. This research is devoted to analyze the ketene dimerization by use of theoretical electronic structure methods in order to express its mechanism according to the characteristics of its potential energy surface in both gas and liquid phase. In what follows, a brief introduction on the methods for analysis of chemical reactions and prediction of thermochemical properties is presented.

1.6.1 Chemical reaction analysis

As it was stated above, the potential energy surface (PES) dictates the different tendencies of the gas-phase reactions according to the position of the atoms in the reactant molecules. Despite this impressive predictive tool, it is impossible to completely specify the PES for a particular reaction due to the restrictive dimension of the systems and therefore focus are put on particularly

32

interesting points on this surface. These particularly points include minima and saddle points. Physically, minima correspond to molecular stable structures whereas saddle points are lowest energy barrier on a path connecting minima. This path is widely known as reaction coordinate. The preceding concepts are basically the fundamentals of the transition state theory for the description of chemical reaction processes.[95] The minima and saddle points of reactions over the gas-phase PES can be calculated through the use of electronic structure methods. These methods consider the Schrödinger equation of quantum mechanics for describing the movements of nuclei and electrons within the system. Molecular structure and energies for the minima and saddle points can be obtaining by minimizing the molecular energy subject to the position of the atoms. There exist different procedures for solving the Schrödinger equation and therefore different geometrical parameters and energy values describing the interesting point can be obtained. Chapter 3 presents a brochure of the different theoretical procedures for solving the Schrödinger equation.

A proper procedure for describing a coordinate for a given reaction can be discerned with the help of experimental data for the corresponding heat of reaction and energy barrier. The high-level *ab initio* theories and the density functional theory (DFT) are among the most successful procedures for describing the reaction coordinates.[96] The high-level *ab initio* theories, such as configuration interaction (CI) theory, solve the Schrödinger equation including all its terms and therefore, it is waited that the experimental data are reproduced with high reliability; however, the computational resources required for applying these methods make their application in several cases restrictive. The DFT methods do not solve directly the Schrödinger equation and solve the khon-Sham equation based on the electronic density of the system, instead.[97] The DFT methods are faster than the high-level *ab initio* methods and the results with the former methods can be sometimes of the same performance as with the latter.[96, 98] For example, Wiest et al. studied a large number of TS structures for organic electrocyclic reactions and based on comparison to experiment and very high-level *ab intio* calculations, concluded that some DFT calculations, particularly from the B3LYP hybrid functional, are robust for predicting geometries in this area.[99] Likewise, Lynch et al. proved that their DFT method called MPW1K functional leaded to significantly improved performance in the theoretical prediction of experimental energies of activation with respect to other methods.[100] These two hybrid functional, namely

33

B3LYP and MPW1K and some high-level *ab initio* methods have been recently tested for the prediction of activation energy and heat of reaction for cycloadditions and other pericyclic reactions.[101] Main conclusions of this evaluation study were that MPW1K functional performs best for activation barriers whereas the B3LYP functional performs best for reaction enthalpies. These two functionals outperform CBSQ-QB3 multilevel and other high-level *ab initio* methods.[101] Due to their success, the DFT methods were chosen in this research for analyzing the ketene dimerization in gas phase in order to achieve a good level of accuracy at lowest computational cost. It is worth mentioning that there are no reports about the modeling of ketene dimerization using the DFT methods within the static framework. Chapter 3 shows a brief introduction to the *ab initio* and DFT methods for solving the time-independent quantum chemical equation.

Analysis of chemical reactions through the description of the PES and calculation of interesting points, namely minima and saddle points, are more complicate when reactants are surrounded by solvent molecules. As an alternative, gas-phase PES can be utilized for analyzing reactions in liquid phase in a qualitative sense. In fact, the modus operandi of making broad generalization about reactions in condensed phase from accurate gas-phase calculation was much employed well into the 1980s and still sees modest use today.[96] However, gas-phase PES generalizations can be inadequate since liquid phase can affect the reactions drastically in both topology and energetics of the potential surface. This made necessary to research about the inclusion of solvent effects into the calculations. Significant developmental and computational efforts over the last two decades have resulted in the availability of condensed-phase models used to more accurately describe the physical reality of liquid phase experiments.[96] These condensed-phase models were classed as implicit and explicit solvation models according to the way of representing the liquid phase.

The assumption underlying implicit, also named as continuum, solvation models is that the huge amount of molecules constituting the solvent can be removed from the model, as long as the empty space leaving by these molecules is modified to be a continuum medium with properties consistent with those of the solvent itself.[96] For example, when a polar solute is immersed in a polar solvent, the most representative interaction in the solution process consists in the

distribution of charge among the solute and solvent molecules; thus, a continuous averaged electric field can be used in the model for replacing the effects of the solvent molecules. Implicit models can be very efficient, adequate and powerful in situations when the molecular details of the solvent are superfluous to the process occurred in solution.

On the other hand, explicit models consider the solvent molecules as "explicitly" present in a simulation. Thus, the details of the atomic configuration inside the solvent molecules and the number of these molecules intervene during the simulation for correctly representing the course of the process occurred in solution. This class of simulation can consider most of the interactions occurred between the molecules of the solute and the solvent. Although, explicit models clearly represent better the physical reality, practical limitations imposed by explicit representation dictate that it may not be the best choice for simulating all the condensed-phase processes.[96] The degrees of freedom, greatly increased by the solvent molecules required for simulating the condensed phase, may become the system impractical for solving within the confines of present computational resources. Thus, it is one key issue in deciding upon the level of detail in solvent structure (implicit or explicit) that adequately models the influence of the environment on the investigated process.

Particularly for chemical reactions, theoretical investigations on roles of solvents in reaction mechanisms of polar cycloadditions so far have been mostly conducted using continuum solvation models. Results of the application of these models depended on the method itself. Several studies of polar cycloadditions have applied a simple dielectric continuum self-consistent reaction field (SCRF) model. A general conclusion is that polar solvents stabilize the zwitterionic intermediate, consequently altering the mechanism from a concerted process in the gas phase to a stepwise one in solution via a stable zwitterionic intermediate. This is qualitatively in accord with most recent experimental observations. However, quantitatively the magnitude of solvent effects on the free energy of activation was generally overestimated by SCRF models. For example, in the cycloaddition of 1,1-dicyanoethylene and methyl vinyl ether, the solvent effects in going from CCl_4 to CH_3CN were overestimated with respect to observed data by 5 kcal/mol approximately.[102] The Conductor-like Screening Model (COSMO) for solvation proposed by Klamt and Schüürmann[103] has reproduced several energy barriers very close to experimental

data[104]. In COSMO it is assumed that the medium reaches up to the "surface" of the solute molecules. The charge distribution on the surface and the energy of interaction between the solute and the solvent are calculated by considering the permittivity of the solvent and the electric charge of the solvent molecules. This relative easy approach has allowed calculation on large and irregular solvent molecules and therefore, it has attracted people in the field to apply the COSMO model with electronic structure methods such as Hartree-Fock, post Hartree-Fock and DFT.[104] COSMO and its different versions have been applied in different areas such as conformational and tautomeric equilibria, prediction of binary interaction parameters in vapor-liquid equilibria (UNIFAC groups), reaction modeling in the liquid phase, predictions of pKa, polymer simulations, drug development and drug-enzyme interaction studies.[105] Due to its achievements, the COSMO model was selected in this research to analyze the ketene dimerization in condensed phase.

1.6.2 Thermochemical properties

Statistical thermodynamics dictates that the macroscopic properties of the system can be obtained by averaging over the different microscopic configurations that are admissible to the system. Admissible configurations or admissible states of the system are reached when the characteristics of the system are compatible with some set of constraints, such as imposed temperature or imposed energy; the collection of all of these admissible states form the concept of statistical ensemble which is the cornerstone of statistical mechanics. The setting up of the constraints, which depends on the phenomenon on study, frames a determined ensemble and defines the probability density of occurrence of each system microstate in the collection. One of the characteristic ensembles corresponds to the canonical ensemble which entails the imposition of the number of molecules (N), the volume and the temperature of the system. Simulation with these macroscopic conditions can reproduce the phase properties of the systems. The canonical ensemble is referred to as the (N,V,T) ensemble. An important specific aspect of this (N,V,T) ensemble is that the energy of the system fluctuates in order to get the imposed constraints. The analysis of the fluctuations in energy allows us to determine the thermochemical properties of the system by the use of the partition function of the canonical ensemble, Q, as follows:

36

$$U = k_B T^2 \left(\frac{\partial lnQ}{\partial T}\right)_{N,V} \tag{1}$$

$$H = U + PV \tag{2}$$

$$S = k_B lnQ + k_B T \left(\frac{\partial lnQ}{\partial T}\right)_{N,V} \tag{3}$$

$$G = H - TS \tag{4}$$

Where derivatives implies N and V held constant during differentiation with respect to T, U is internal energy, H is enthalpy, P is pressure, S is entropy, and G is Gibbs energy. The partition function, Q, for real systems must be a many-body function involving staggeringly enormous number of energy levels. This extremely complex real partition function can be simplified in order for finding an explicit representation of Q that permits the necessary partial differentiations in Eqs. 1 – 4 to be carried out. From the ideal gas world, we can write the partition function as the product of the partition functions for each class of movement occurred inside the system; i.e. partition functions for translation, rotation, vibration and electronic motions. With this description of the partition function it is possible to apply the well known formulas for obtaining the thermochemical properties of the substances[104].

The thermochemical properties are then expressed in terms of molecular parameters such as geometry, moment of inertia and vibration frequencies. These molecular parameters can be obtained from experimental or theoretical data. Theoretical data have shown to be so close to experimental value of the different microscopic parameters. Several theoretical methods can be used for estimating the molecular properties and among the most successful are the electronic structure methods. Experimentally thermochemical properties have been reproduced with high accuracy by sophisticated quantum mechanical calculations such as *ab initio* multilevel methods which contain empirical corrections depending on the analyzed compound. The CBS-Q multilevel method[106] which includes bond additivity and spin-orbit corrections have been used successfully for ketene compounds (see above and Ref. 7). Despite the excellent performance of *ab initio* multilevel quantum procedures, the time required for calculation makes the application of these methods unfeasible in molecules with several atoms; the CBS-Q method is practically unfeasible in molecules containing more-than-nine atoms.[96]

Another method for estimating the thermochemical properties, yet with less theoretical background than that of the statistical framework, corresponds to the structural methods. Such structural schemes are based on the assumption that the structure (i.e. atoms, bonds and interaction between nonbonded atoms) contributes in a direct additive fashion to the global value of the molecular and bulk properties. This simple additive procedure ease the application of this class of methods.[107] Among the structural models we found the group additivity method of Benson which establishes a set of groups formed by atoms bounded with characteristic valences. These groups are summed according to their appearance in the structure of the compounds in order to estimate the current properties. Benson and others have established the values for the most common molecular groups[94]; however, there are lots of groups for being determined (such as those in most of the ketene and ketene derivative compounds) and, if the compounds have them, the missing groups must be firstly determined before applying the additivity contribution method.

An alternative for obtaining the data needed for assessing the value of the unknown groups is applying quantum mechanical calculations on few-atom molecules containing those missing groups. Quantum mechanical results allow the application of structural schemes on the few-atom-molecule set by taking the theoretical properties as the right values and solving the resulting linear system of equations for getting the values of the missing groups.[7] In this way, the very easy structural methods take advantage of the very exact quantum calculations for allowing a quick estimation of high-weight molecules properties with experimental unknown groups. This procedure is widely used in the literature; more over an important portion of the known contribution groups are based on quantum calculations.[94] It is an objective of this research to obtain the missing groups for ketene dimers in order to allowe the estimation of the thermochemical properties of high-weight ketene dimers.

1.7 Objectives of this Research

Dimerization of ketenes presents a great challenge for the theories of cycloadditions due to their characteristic structure, their special reactivity properties and the difficult experimentation with these highly reactive compounds. Experimental data have exposed that gas-phase parent ketene

dimerization is a very slow process with an activation barrier of 31 kcal per mol[13] and that liquid-phase parent ketene dimerization by contrast is a facile process with an activation barrier of 11 kcal per mol in acetone[12]. Analysis based on the liquid-phase experimental[12] data showed a favorable charge distribution along the reaction coordinate which may comprise a zwitterionic intermediate (section 2.3). However, conclusion of a two-step mechanism for explaining parent ketene dimerization cannot be done *a priori* since intermediates have not been identified yet. Concerted process cannot be assigned *a priori* either due to the dimerization exhibits a large solvation which is uncommon for [2+2] cycloadditions[51]. Likewise, parent ketene is also an atypical case for the production of the asymmetrical β-lactone typer dimer since substitute ketenes, with more steric hindrance than parent ketene, generally yield the symmetrical cyclobutanedione dimer in major proportion[8]. Argumentation of either kinetic o thermodynamic control of the dimerization for explaining this trend is undecided yet because of the scarcity of thermochemical data. The importance of ketene dimers make it priority to clarify the atypical trends of the ketene dimerization in order for allowing major advantages in the production and investigation with this class of compounds. The main goal of this research is to study the parent ketene dimerization reaction by the use of the density functional theory (DFT) and *ab initio* multilevel quantum mechanical methods in order for clarifying both the topology and the energetics of the potential surface for this reaction. The DFT is used for study the trends of the dimerization in gas phase. The Conductor-like Screening Model (COSMO) for solvation is used to implicitly simulate the solvent effects on the quantum calculations. Accuracy of the results in both gas and liquid phase are tested against experimental data. Finally, the CBS-Q multilevel method is utilized for further assessing the thermochemical properties of the dimers and determining the class of control that dominates the yield on the ketene dimerization. CBS-Q results are the base for calculating unknown Benson contribution groups in order for allowing the estimation of thermochemical properties for ketene polymers.

References

(1) Ulrich, H. *"Cycloaddition Reactions of Heterocumulenes"*. Academic Press, New York. 1967.

(2) Tidwell, T. T. *"Ketenes"*. Wiley-Interscience; 2nd edition, 2006.

(3) Miller, R.; Abaecherli, C.; Said, A. In *Ullmann's Encyclopedia of Industrial Chemistry*; Elvers, B., Hawkins, S., Schulz, G., Eds.; VCH: New York, 1990; Vol. A1; 69-71. Vol. A15; p. 63-75.

(4) Brown, R. D.; Godfrey,P. D.; McNaughton, D.; Pierlot, Z. P.; Taylos, W. H. *J. Mol. Spec*. 1990, 140, 340-352.

(5) (a) Duncan, J. L. and Munro, B. *J. Mol. Struct.* 1987, 161, 311 − 319. (b) Brown, R. D. Godfrey, P. D.; McNaughton, D.; Pierlot, A. P.; Taylor, W. H. *J. Mol. Spec.* 1990, 140, 340 − 352.

(6) Hanford, W. E. and Sauer, J. C. "Preparation of Ketenes and Ketene Dimers". *Org. React.* 3, 108, 1946.

(7) Sumathi, R and Green, W. H. "Thermodynamic Properties of Ketenes: Group Additivity Values from Quantum Chemical Calculations". *J. Phys. Chem. A*, 106, 7937 − 7949, 2002.

(8) Tidwell, T. T. "Ketene Chemistry: The Second Golden Age". *Acc. Chem. Res.*, 23, 273-279, 1990.

(9) (a) Del Bene, J. E. *J. Am. Chem. Soc*., 94, 3713-3718, 1972. (b) Dykstra, C. E. and Schaefer, H. F. III. *J. Am. Chem. Soc.,* 98, 2689-2695. (c) Allen, W. D. and Schaefer, H. F. III. *J. Chem. Phys*. 84, 2212-2225, 1986.

(10) Shelkov, R.; Nahmany, M.; Melman, A. "Acylation through Ketene Intermediates". *J. Org. Chem.* 2002, 67, 8975-8982.

(11) Holder, R. W. "Ketene Cycloadditions", *J. Chem. Educ.* 1976, 53, 81.

(12) Rice, F.O. and Greenberg, J. "Ketene II. Rate of Polymerization". *J. Am. Chem. Soc*. 1934, 56, 2132.

(13) Chickos, J. S.; Sherwood, D. E. Jr.; and Jug, K. "Mechanism of Thermolysis of Diketene in the Gas Phase". *J. Org. Chem.* 1978, 43, 1146-1150.

(14) Clemens, R. J. "Diketene". *Chem. Rev*. **1986**, *86(2)*, p. 241-318.

(15) (a) Mohlin, K.; Leijon, H.; Holmberg, K. "Spontaneous Emulsification of Alkyl Ketene Dimer". J. Dispersion Science and Technology, 2001, 22, 569-581. (b) Nolan, T. F. "Process for the Manufacture of Alkyl Ketene Dimer". U.S. Patent 5,484,952. 1996.

(16) Staudinger, H. *Chem. Ber.* 1905, 38, 1735 – 1739.

(17) (a) Staudinger, H.; Klever, H. W. *Chem. Ber.* 1906, 39, 968 – 971. (b) Staudinger, H. *Chem. Ber.* 1906, 39, 3062 – 3067.

(18) Wilsmore, N. T. M. *J. Chem. Soc.* 1907, *91*, p. 1938-1941.

(19) Chick, F and Wilsmore, N. T. M. "Acetylketen: a Polymeride of Keten". *J. Chem. Soc.* 1908, p. 946 – 950.

(20) a) Boese. *Ind . Eng. Chem.*, 32, 16 (1940). B) Hurd, Cashion and Perletz. *J . Org. Chem.*, 1943, 8, 367; 1944, 9, 557. C) Sauer, J. C. "Ketene Dimers from Acid Halides". *J. Am. Chem. Soc.* 1947, 69, 2444 – 2448.

(21) Staudinger, H. and Klever, H. W. *Chem. Ber.* 1908, 41, 594 – 600.

(22) Staudinger, H. *Die Ketene*; Verlag Enke: Stuttgart, 1912.

(23) Hueter, R. U.S. Patent 2,383,863, 1945.

(24) Huisgen, R. and Otto, P. *J. Am. Chem. Soc.* 1968, 90, 5342.

(25) Farnum, J. *J. Am. Chem. Soc.* 1965, 87, 5191.

(26) Staudinger, H. *Chem. Ber.* 1911, 44, 1619 – 1623.

(27) Sauer, J. C. U. S. Patent 2,369,919.

(28) Jug, K.; Dwivedi, C. P. D.; Chickos, J. S. *Theoret. Chim. Acta (Berl.).* 1978, 49, 249.

(29) Fu, X. Y.; Decai, F.; Yanbo, D. *J. Mol. Structure (THEOCHEM).* 1988, 167, 349.

(30) Seidl, E. T. and Schaefer, H. F. III. *J. Am. Chem. Soc.* 1991, 113, 5195.

(31) Salzner, U. and Bachrach, M. S. *J. Am. Chem. Soc.* 1994, 116, 6850.

(32) Kelly, E.; Seth, M.; Ziegler, T. "Calculation of Free Energy Profiles for Elementary Bimolecular Reactions by ab Initio Molecular Dynamics: Sampling Methods and Thermostat Considerations". *J. Phys. Chem. A*, 2004, 108, 2167.

(33) Rode, J. R. and Dobrowolski, J. Cz. *J. Phys. Chem. A* 2006, 110, 207.

(34) Weissermel, K.; Arpe, H. J. "*Industrial Organic Chemistry*". 3rd ed.; VCH Publishers: New York, 1997.

(35) Johnson, W.; Fink, U.; Sakuma, Y.; *Ketene/Diketene, http://ceh.sric.sri.com/Public/Reports/669.5000/.* 1999.

(36) (a) Mcketta, J. J. and Cunningham, W. A. *"Encyclopedia of Chemical Processing and Design. Marcel Dekker"*, Inc: USA, 1976; p. 258-271. (b) Abaecherli, C.; Miller, R.J. In *Kirk-Othmer Encyclopedia of Chemical Technology*; John Wiley & Sons: New York, 1991; p. 954-978.

(37) Takasu, I.; Higuchi, M.; Hijioka, Y. U.S. Patent 3,574,728, 1971.

(38) Nakajima, M. "Process for producing sorbic acid". U. S. Patent 5,200,559, 1993.

(39) Kunstle, G. "Process for Continuously Producing Sorbic Acid by Converting Ketene with Crotonaldehyde". U.S. Patent 3,759,988, 1973.

(40) Mollenkopf, C. "Process for the preparation of sorbic acid". U. S. Patent 6,794,540, 2004.

(41) Hyatt, J. A. and Raynolds, P. W. "Ketene Cycloadditions". *Organic Reactions*, Vol. 45, John Wiley & Sons, Inc. USA. 1994.

(42) http://www.chemicworld.com/show/showcoop1.asp?id=18&menu=3.

(43) (a) Yoshida, Y.; Yanagisawa, M.; Isogai, A.; Suguri, N.; Sumikawa, N. "Preparation of polymer brush-type cellulose b-ketoesters using LiCl/1,3-dimethyl-2-imidazolidinone as a solvent". *Polymer* 46 (2005) 2548–2557. (b) Wieland, H. A.; Hamilton, B. S.; Krist, B.; Doods, H. N. *Exp. Opin. Invest. Drugs* 2000, 9, 1327-1346.

(44) Zule, J. and Dolenc, J. "Determination of AKD Sizing Agents in Papermaking Systems by Gas Chromatography". *Acta Chim. Slov.* 2003, 50, 115−122.

(45) Staudinger, H. *Chem. Ber.* 1911, 44, 1619-1623.

(46) Aben, R. W. and Scheeren, H. W. *J. Chem. Soc., Perkin Trans. I*, 1979, 3132 – 3138.

(47) Calter, M. A.; Orr, R. K.; Song, W. "Catalytic, Asymmetric Preparation of Ketene Dimers from Acid Chlorides". *Org. Lett.* 2003, 5, 4745 – 4748.

(48) Brady, W. T. and Scherubel, G. A. *J. Am. Chem. Soc.* 1973, 95, 7447-7449.

(49) Newman, M. S.; Arkell, A.; Fukunaga, T. *J. Am. Chem. Soc.* 1960, 82, 2498- 2501.

(50) (a) Brady, W. T. and Ting, P. L. *J. Org. Chem.* 1976, 41, 2336-2339. (b) Brady, W. T. and Lloyd, R. M. *J. Org. Chem.* 1980, 45, 2025-2028.

(51) Smith, M. B. and March, J. *"March's Advanced Organic Chemistry. Reactions, Mechanisms, and Structures"*. Wiley-interscience. John Wiley & Sons, Inc. Sixth Edition. USA. 2007.

(52) Jiao, L.; Liang, Y.; Xu, J. "Origin of the Relative Stereoselectivity of the β-Lactam Formation in the Staudinger Reaction". *J. Am. Chem. Soc.* 2006, 128, 6060-6069.

(53) Armstrong, A.; Geldart, S. P.; Jenner, C. R.; Scutt, J. N. "Organocatalytic Synthesis of β-Alkylaspartates via β-Lactone Ring Opening". *J. Org. Chem.* 2007, 72, 8091-8094.

(54) Alcaide, B.; Almendros, P. "4-Oxoazetidine-2-carbaldehydes as useful building blocks in stereocontrolled synthesis". *Chem. Soc. Rev.* 2001, 30, 226-240.

(55) Ogilvie, W. W.; Yoakim, C.; Do, F.; Hache, B.; Lagace, L.; Naud, J.; O'Meara, J. A.; Deziel, R. "Synthesis and antiviral activity of monobactams inhibiting the human cytomegalovirus protease". *Bioorg. Med. Chem.* 1999, 7, 1521-1531.

(56) Adlington, R. M.; Baldwin, J. E.; Chen, B.; Cooper, S. L.; McCoull, W.; Pritchard, G. J.; Howe, T. J. "Design and synthesis of novel monocyclic β-lactam inhibitors of prostate specific antigen". *Bioorg. Med. Chem. Lett.* 1997, 7, 1689-1694.

(57) Han, W. T.; Trehan, A. K.; Wright, J. J.; Federici, M. E.; Seiler, S. M.; Meanwell, N. A. "Azetidin-2-one Derivatives as Inhibitors of Thrombin". *Bioorg. Med. Chem.* 1995, 3, 1123-1143.

(58) Esslinger, C. S.; Agarwal, S.; Gerdes, J.; Wilson, P. A.; Davis, E. S.; Awes, A. N.; O'Brien, E.; Mavencamp, T.; Koch, H. P.; Poulsen, D. J.; Rhoderick, J. F.; Chamberlin; A. R.; Kavanaugh, M. P.; Bridges, R. J. "The substituted aspartate analogue L-β-threo-benzyl-aspartate preferentially inhibits the neuronal excitatory amino acid transporter EAAT3". *Neuropharmacology*, 2005, 49, 850 – 861.

(59) (a) Ciochetti, J. E. U.S. Patent 3,161,683, 1964. (b) Ciochetti, J. E. U.S. Patent 3,193,512, 1965.

(60) Maeda, C.; Mishima, C.; Mishima, G.; Osaka, F.; Mauro, K. S. U.S. Patent 3,366,689, 1968.

(61) Parker, L. M.; Bibby, D. M.; Miller, I. J. *J. Catal.* 1991, *129*, 438-446.

(62) (a) Libby, M. C.; Watson, P. C.; Barteau, M. A. *Ind. Eng. Chem. Res*. 1994, *33*, 2904-2912. (b) Watson, P. C.; Libby, M. C; Barteau, M. A. U.S. Patent 5,475,144, 1995.

(63) Martínez, R.; Huff, M. C.; Barteau, M. A.; Poggoda, U. U.S. Patent 6,232,504, 2001.

(64) Lowry, T. H. and Richardson, K. S. *"Mechanism and Theory in Organic Chemistry"*. Harper & Row, Publishers, New York, third edition, 1987.

(65) Singh, P.; Bhargava, G.; Mahajan, M. P. "Tandem [2D2] cycloaddition and Cope rearrangement in reactions of cross-conjugated azatrienes with conjugated ketenes: a facile single step synthesis of novel azocinone derivatives". *Tetrahedron* 2006, 62, 11267–11273.

(66) Pommier, A.; Pons, J.-M. *Synthesis* 1995, 729.

(67) Holder, R. W. "Ketene Cycloadditions". *J. Chem. Ed.* 53, 81-85, 1976.

(68) Bernardi, F.; Bottoni, A.; Robb, M. A.; Venturini, A. "MCSCF Study of the Cycloaddition Reaction between Ketene and Ethylene". *J. Am. Chem. Soc.* 1990, 112, 2106-2114.

(69) (a) Ketene + alkene: [1] Machiguchi, T.; Okamoto, J.; Morita, Y.; Hasegawa, T; Yamabe, S.; Minato, T. "Challenge To Detect 1,4-Zwitterions Spectroscopically in a Ketene-Alkene Reaction". *J. Am. Chem. Soc*. 2006, 128, 44-45. [2]

(70) Lecea, B.; Adeta, A.; Rea, G.; Ugalde, J. M.; Cossío, F. P. "Catalytic and Solvent Effects on the Cycloaddition Reaction between Ketenes and Carbonyl Compounds To Form 2-Oxetanones". *J. Am. Chem. Soc.* 1994, 116, 9613-9619.

(71) Chemouri, H. and Mekelleche, S.M. "Elucidation of the substitutent effects on the reaction pathway of the cycloaddition of 1,3-diazabuta-1,3-dienes with ketenes using DFT-based reactivity indexes". *J. Mol. Structure: THEOCHEM,* 2007, 813, 67–72.

(72) Ulrich, H. *"Cycloaddition Reactions of Heterocumulenes".* Academic Press, USA. 1967.

(73) Seidl, E. T. and Schaefer, H. F. III. *J. Am. Chem. Soc.* 1990, 112, 1493-1499.

(74) Ma, G.; Nguyen, H.; Romo, D. "Concise Total Synthesis of ($\pm$)-Salinosporamide A, ($\pm$)-Cinnabaramide A, and Derivatives via a Bis-cyclization Process: Implications for a Biosynthetic Pathway?". *Org. Lett.* 2007, 9, 2143 – 2146.

(75) (a) Voorhees, P. M.; Dees, E. C.; O'Neil, B.; Orlowski, R. Z. Clin. *Cancer Res.* 2003, 9, 6316. (b) Rajkumar, S. V.; Richardson, P. G.; Hideshima, T.; Anderson, K. C. *J. Clin. Oncol.* 2005, 23, 630. (c) Joazeiro, C. A. P.; Anderson, K. C.; Hunter, T. *Cancer Res.* 2006, 66, 7840.

(76) Maclean, D.; Baldwin, J. J.; Ivanov, V. T.; Kato, Y.; Shaw, A.; Schneider, P.; Gordon, E. M. "Glossary of Terms Used in Combinatorial Chemistry". *J. Comb. Chem.* 2000, 2, 562-578.

(77) Franzen, R. G. *J. Comb. Chem.* 2000, 2, 195-214.

(78) Bae, S.; Hahn, H. G.; Nam, K. D. "Syntheses of 1,3-Imidazoline-2-thione and 2-Phenylimino-1,3-thiazoline Combinatorial Libraries through Different Sequences of the Same Components". *J. Comb. Chem.* 2005, 7, 826-836.

(79) Rice, F.O. and Greenberg, J. *J. Am. Chem. Soc*. 1934, 56, 2132.

(80) Chickos, J. S.; Sherwood, D. E. Jr.; and Jug, K. *J. Org. Chem*. 1978, 43, 1146.

(81) Rice, F. O. and Roberts, R. "The Structure of Diketene". *J. Am. Chem. Soc.* 1943, 65, 1677.

(82) Mansson, M.; Nakasi, Y.; Sunner, S. *Acta Chem. Scand.,* 1968, 22, 171.

(83) Tenud, L.; Weilenmann, M.; Dallwigk, E. "1,3-Cyclobutanodionderivate aus Keten". *Helv. Chim. Acta* 1977, 60, 975-977.

(84) Pross, A. *"Theoretical and Physical Principles of Organic Reactivity"*. John Wiley & Sons, USA, 1995.

(85) Seidl, E. T. and Schaefer, H. F. III. "Molecular structure of diketene: a discrepancy between theory and experiments?". *J. Phys. Chem.* 1992, 96, 657-661.

(86) Bernardi, F; Pappalardo, R. R.; Robb, M. A.; Venturini, A. "An ab initio MC-SCF study of the solvent effects in polar and non-polar [2+2] cycloadditions". *J. Mol. Structure: THEOCHEM*, 1995, 357, 33-36.

(87) Truong, T. N. "Solvent Effects on Structure and Reaction Mechanism: A Theoretical Study of [2 + 2] Polar Cycloaddition between Ketene and Imine". *J. Phys. Chem. B* 1998, 102, 7877-7881.

(88) Fang, D-C and Fu, X-Y. "Ab initio studies on the mechanism of the cycloaddition reactions between ketene imine and formaldehyde – catalytic and solvent effects". *Chem. Phys. Lett.* 1996, 259, 265 – 270.

(89) Masters, A. P. and Sorensen, T. S. *Tetrahedron Lett.,* 30, 5869-5872, 1989.

(90) West, R. and kwitowski, P. T. "Reactions of hexabromocyclpentadiene and the synthesis of octabromofulvalene". *J. Am. Chem. Soc.*, 90, 4697, 1968.

(91) Orr, R. K. and Calter, M. A. "Asymmetric synthesis using ketenes". *Tetrahedron*, 2003, 59, 3545–3565.

(92) Huisgen, R. "Tetracyanoethylene and Enol Ethers. A Model for 2 + 2 Cycloadditions via Zwitterionic Intermediates". *Acc. Chem. Res.* 1977, 10, 117-124.

(93) (a) Nguyen, M. T.; Nguyen, H. M. T. "On the Heats of Formation of Methylketene, Dimethylketene and related ions". *Chem. Phys. Lett.* 1999, 300, 346. (b) Aubry, C.; Holmes, J. L.; Terlouw, J. K. *J. Phys. Chem. A* 1997, 101, 5958. (c) Bouchoux, G.; Salpin, J. K. *J. Phys. Chem. A* 1996, 100, 16555. (d) Traeger, J. C. *Int. J. Mass Spectrom.* 2000, 194, 261. (e) Scott, A. P.; Radom, L. *Int. J. Mass Spectrometry and Ion Processes* 1997, 160, 73.

(94) Benson, S. W. *"Thermochemical Kinetics. Methods for the Estimation of Thermochemical Data and Rate Parameters"*. John Wiley & Sons. USA 1976.

(95) Glesston, S.; Laidler, K.; Eyring, H. *"The Theory of Rate Processes"*. McGraw-Hill Book Comp. N. Y. 1941.

(96) Cramer, C. J. *"Essentials of Computational Chemistry. Theories and Models"*. John Wiley & Sons, LTD. Second edition. 2002.

(97) (a) Hohenberg and Kohn, "Inhomogeneous Electron Gas", *Phys. Rev.* 136, B864 - B871, 1964. (b) Kohn, W. and Sham, L. "Self-Consistent Equations Including Exchange and Correlation Effects", *J. Phys. Rev.*, 140, A1133-A1138, 1965. (c) Koch, W. and Holthausen, M. C. *"A Chemist's Guide to Density Functional Theory"*. Second edition. Wiley-VCH Verlaf GmgH. 2001.

(98) (a) Parthiban, S.; Oliveira, G. de; Martin, J. L. M. "Benchmark ab Initio Energy Profiles for the Gas-Phase SN2 Reactions Y- + CH3X →CH3Y + X- (X,Y = F,Cl,Br). Validation of Hybrid DFT Methods". *J. Phys. Chem. A*, 105 (5), 895 -904, 2001. (b) Zhang, Q.; Bell, R.; Truong, T. N. "Ab Initio and Density Functional Theory Studies of Proton Transfer Reactions in Multiple Hydrogen Bond Systems". *J. Phys. Chem.* 1995, 99, 895-904. (c) Somnitz, H. and Zellner, R. "Theoretical studies of unimolecular reactions of C2–C5 alkoxy radicals. Part I. Ab initio molecular orbital calculations". *Phys. Chem. Chem. Phys.*, 2000, **2**, 1899 – 1905. (d) Jursic, B. S. "Properties, Dynamics, and Electronic Structure of Atoms and Molecules. Complete basis set ab initio and hybrid density functional theory exploration of the potential energy surface in the reaction between an amino radical and nitrogen oxide". *Int. J. Quant. Chem.* 1998, 66, 409-414. (e) Bento, P. A.; Sola, M.; Bickelhaupt, F. M. "E2 and SN2 Reactions of X^- + CH3CH2X (X = F, Cl); an ab Initio and DFT Benchmark Study". *J. Chem. Theory Comput.*, 4, 929–940, 2008. (f) Quintal, M. M.; Karton, A.; Iron, M. A.; Boese, A. D.; Martin, J. M. L. "Benchmark Study of DFT Functionals for Late-Transition-Metal Reactions". *J. Phys. Chem. A.*; 2006; 110(2); 709-716.

(99) Wiest, O.; Montiel, D. C.; Houk, K. N. *J. Phys. Chem. A.* 1997, 101, 8378.

(100) Lynch, B. J.; Fast, P. L.; Harris, M.; Truhlar, D. G. *J. Phys. Chem. A.* 2000, 104, 4811.

(101) Ess, D. H. and Houk, K. N. "Activation Energies of Pericyclic Reactions: Performance of DFT, MP2, and CBS-QB3 Methods for the Prediction of Activation Barriers and Reaction Energetics of 1,3-Dipolar Cycloadditions, and Revised Activation Enthalpies for a Standard Set of Hydrocarbon Pericyclic Reactions". *J. Phys. Chem. A*, 2005, 109, 9542 - 9553.

(102) Lim, D; Jorgensen, W. L. *J. Phys. Chem.* 1996, 100, 17490-17500.

(103) Klamt, A. and Schüürmann, G. *J. Chem. Soc., Perkin trans. 2*, 1993, 799.

(104) McQuarrie, D. A. *"Statistical Mechanics"*, Harper and Collins, New York, 1976.

(105) Klamt, A. *"COSMO-RS: From quantum chemistry to fluid phase thermodynamics & drug design"*. Elsevier Science, USA, 2005.

(106) (a) Petersson, G. A.; Tensfeldt, T. G.; Montgomery Jr., J. A. *J. Chem. Phys.* 94, 6091, 1991. (b) Montgomery Jr., J. A.; Frisch, M. J.; Ochterski, J. W.; Petersson, G. A. *J. Chem. Phys.* 112, 6532, 2000. (c) Petersson, G.; Malick, D.; Wilson, G.; Ochterski, J.; Montgomery, J. and Frisch, M. *J. Chem. Phys.* 1998, 109, 10570.

(107) Carpenter, B. K. *"Determination of Organic Reaction Mechanisms"*. John Wiley & Sons, USA 1984.

Chapter 2

The Ketene Dimerization Mechanism: a Tricky Reaction Pathway

Chapter 1 exposed a global panorama of the cumbersome situation presented when we try to analyze the ketene dimerization. Experiments classed ketene dimerization as concerted in gas and liquid phase. However, acceleration found by comparing gas and liquid phase experiments indicates an anomalous situation that may involve either susceptibility to solvent effects or an unknown catalyst. For helping to thorough analyze and setup the challenges faced with the ketene dimerization, this chapter is devoted to resolve the following doubts: How many mechanisms are possible in a [2+2] cycloaddition? May ketene dimerization follow all of these mechanisms in both gas and liquid phase? Are the trends of the dimerization the same in both gas and liquid phase? Can the kinetic available data for ketene dimerization help us to understand its mechanism? Can we wait a great lowering in the energy barrier for a concerted [2+2] cycloaddition in going from gas to liquid phase? To answer these doubts and to clarify some other aspects about [2+2] cycloadditions we shall look for theoretical explanation and experimental findings about the mechanisms for this class of reactions.

2.1 Mechanisms for [2+2] Cycloadditions

A reaction mechanism is the description of the atomic movements and electronic changes that occur between reactants in a chemical reaction. The description of a mechanism involves, among others, the following knowledge: which bonds are broken, in what order, how many elementary steps are required, the relative energies and rates of the steps, and what possible pathways can the reaction follow from the reactants to the final products.[1] For stating a mechanism completely, we should specify the positions of all atoms, including those in solvent molecules, and the energy of the system, at every point in the process in order to fit or prove all the experimental and theoretical facts available. The usual course of a mechanistic description of a reaction is that the gross features of a mechanism are the first to be known and then increasing attention is paid to finer details.[1]

There have been developed different theories for explaining and predicting the mechanisms of a given reaction.[1,2] In the case of cycloadditions, the Woodward and Hoffmann rules[3] (W&H rules) and the theory of interaction between the frontier orbitals (highest occupied molecular orbital, HOMO, and lowest unoccupied molecular orbital, LUMO)[2] can help to identify the most probable mechanisms for a particular pericyclic process (Figure 2.1 depicts the frontier orbitals for the ketene). Pericyclic processes are reactions in which more than one bond is being made or broken in a concerted and synchronous manner and therefore they exhibit a cyclic and aromatic transition state[4]; a pericyclic reaction is illustrated by mechanism *a*. By this concerted and synchronous way, a reaction may be conduced in an "efficiently" manner with low energy barrier due to the rupture of the bonds capitalizes the energy released from the formation of the new bonds along the reaction coordinate. Besides, the aromatic character of the activated complexes due to the presence of delocalized π electrons allows an extra stability in systems that match the Hückel's rule of *(4n+2)* for the number of delocalized π electrons.[5]

For the case of [2+2] cycloadditions, as the number of delocalized π electrons in the transition state does not match the Hückel's rule (*4n+2=4*; i.e. *n* is not an entire number), these concerted reactions are thermally forbidden via a supra-supra transition state but thermally allowed via a supra-antara transition state[3] (Figure 2.2 depicts both of the [2+2] pathways for the case of ketene dimerization). Thus, for a [2+2] cycloaddition to happen it is required that one of the reactant molecules approaches in an antarafacial fashion whereas the other reactant molecule approaches in a suprafacial fashion in order to preserve the orbital symmetry and the synchronism of the reaction (Figure 2.2b). This symmetry-allowed supra-antara process is named [$_\pi 2_s + _\pi 2_a$] cycloaddition.[3] Particularly for ketene [2+2] cycloadditions, the low steric demand in the carbonyl carbon side of the ketene rises the readiness of the reaction to proceed by this symmetry-allowed supra-antara way. However, theoretical calculations at HF/DZP[6], MP2/6-31G(d)[7], and MP2/aug-cc-pVDZ[8] levels on the ketene dimerization suggest that the symmetry of the transition state is different to the supra-antara approach and therefore ketene dimerization does not proceed through the [$_\pi 2_s + _\pi 2_a$] mechanism predicted by the W&H rules.

HOMO

LUMO
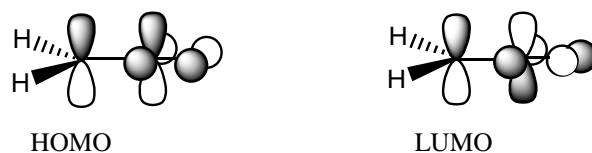
Figure 2.1. Frontier molecular orbitals for the parent ketene.

πCO

π^*CC
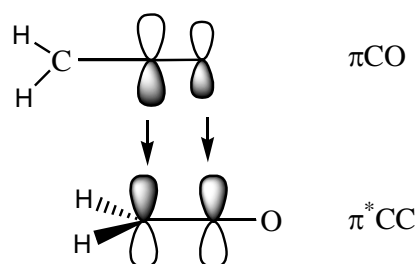
(a) $[_\pi 2_s + _\pi 2_s]$ rule achieved by the occupied orbitals on the CO group of one ketene monomer and the virtual orbitals of the CC double bound of the other ketene monomer.

π^*CO

πCC
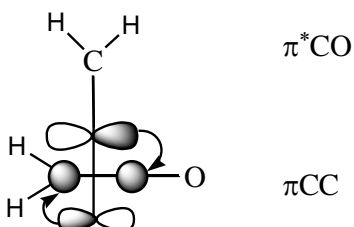
(b) $[_\pi 2_s + _\pi 2_a]$ rule achieved by the occupied orbitals on the CC double bond of one ketene monomer and the virtual orbitals of the CO group of the other ketene monomer.

Figure 2.2. Topological alternatives for the activated complex for [2+2] cycloadditions according to the Woodward and Hoffmann selection rules[3].

(a)

50
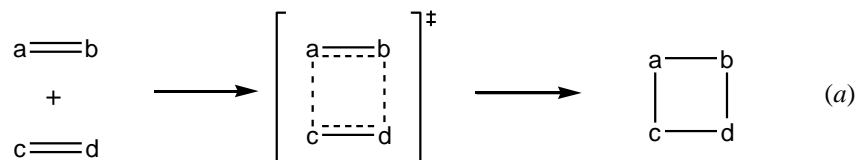
There is another mechanism by which two unsaturated compounds can undergo pericyclic [2+2] cycloaddition; the $[_\pi 2_s +_\pi 2_s +_\pi 2_s]$ mechanism was theoretically analyzed for the cycloaddition between ketene and ethylene and latter proposed for explaining the ketene dimerization (Figure 2.3).[6,9] This mechanism was proposed for ketene dimerization in gas phase because the two perpendicular π systems of the ketenes (Figure 2.1) can conduce to a symmetric distortion and a charge distribution in the activated complex[6,10] (Figure 2.3). Although this asymmetric transition state has been obtained by different theoretical calculations at HF/DZP[6], MP2/6-31G(d)[7], and MP2/aug-cc-pVDZ[8] levels, the orbital connection characteristic of pericyclic mechanisms has not been proved yet.
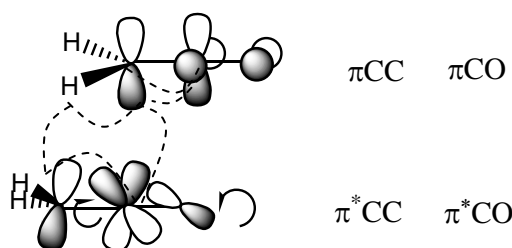
Figure 2.3. Concerted asynchronous $[_\pi 2_s +_\pi 2_s +_\pi 2_s]$ pericyclic pathway for ketene dimerization. Doted lines describe the orbital interaction in this mechanism.

All the preceding mechanisms (i.e. $[_\pi 2_s +_\pi 2_s]$, $[_\pi 2_s +_\pi 2_a]$ and $[_\pi 2_s +_\pi 2_s +_\pi 2_s]$) have the particular property that preserves the orbital symmetry connection. Thus, W&H rules predicts that [2+2] cycloadditions proceed by a concerted and highly stereospecific[*] mechanism (*a*). The following up of the predicted W&H mechanisms depend on the nature of the reactant molecules which may influence the orbital connection. Many [2+2] cycloadditions that are expected to need high temperatures to overcome the energy barrier of an orbital connection proceed in a good yield independently to the paradigms imposed by W&H rules[+]. These [2+2] cycloadditions can follow

---

[*] A reaction is stereoespecific when the reactants and intermediates, if apply, must adopt a properly spatial configuration in order to generate the products.

[+] For example cyclobutane cannot be prepared in a preparative scale by dimerization of ethylene due to the high activation energy of 44 kcal per mol which is the inheritance of a steric-demanded-supra-antara-allowed pathway. However, polyhaloolefines are able to dimerize by the biradical route (mechanism b) because destabilization of the π bond and stabilization of the terminal centers of the biradical intermediate by the halogen substituents[11].

a stepwise mechanism as an alternative to avoid the high barrier of the pericyclic pathway.[4,10] They can proceed through stepwise mechanisms due to a favorable charge distribution that occurs along the reaction path.[4] According to the polarity of the reactant molecules, the [2+2] cycloadditions can be classified into two classes, namely, nonpolar and polar cycloadditions, having rather different stepwise mechanisms. Stereochemical and kinetic data indicate that nonpolar cycloadditions can be feasible to proceed via a two-step biradical mechanism (*b*) with less activation energy than for the case of a pericyclic route, yet with rather large activation energy.[12] On the contrary, polar cycloadditions have much lower activation energies and were suggested to have a two-step mechanism with a diionic or zwitterionic intermediate (*c*).[11,13,14] This zwitterionic intermediate is highly probable to exist mainly in liquid phase because of solvent effects. Differences in energy profile between the diradical and diionic mechanisms are due to the class of rupture accounted for the bonds[*].[4]
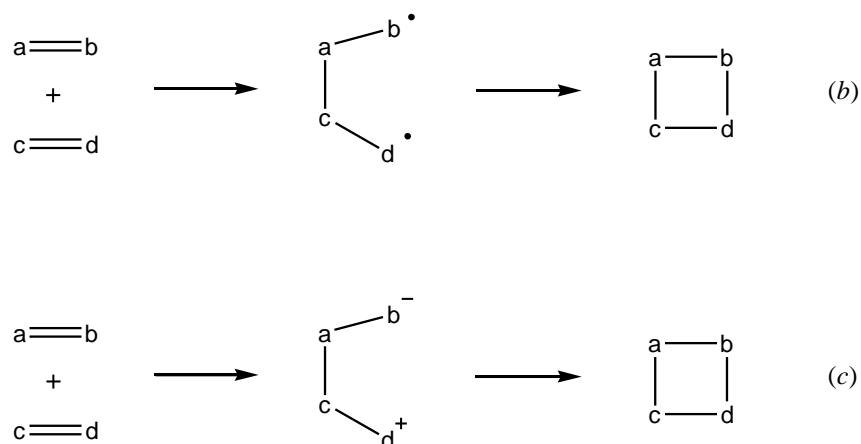
Conventionally, literature reports the preceding three mechanisms for explaining thermal [2+2] cycloadditions.[1,2, 15,16] As regarding for these, mechanism *a* is a concerted pericyclic process, and mechanisms *b* and *c* are two-step reactions involving, respectively, a diradical and a diion intermediates. Mechanism *c* is expected to be sensitive to changes in solvent polarity, while the

---

[*] Homolytical-ruptured bonds, occurred in diradical pathway, generally need higher energies than heterolytical-ruptured bonds occurred in diionic pathway.

other mechanisms are found to be generally insensitive[1,2,15,16]; rates of reactions proceeding through pericyclic transition states are normally insensitive to solvent polarity because there is little separation of charge.[1,2] Mechanisms *a* and *b* are happen in most non-polar cycloadditions, whereas mechanism *c* is appeared in most polar cycloaddition. For the case of ketene compounds, mechanism *c* is proposed for explaining most of the ketene [2+2] cycloadditions due to the polarity of the ketene, although mechanism *a* (presumably by an asynchronous transition state as occur in the $[_\pi 2_s +_\pi 2_s +_\pi 2_s]$ mechanism, Figure 2.3) can also be used to explain these reactions.[17,18] It is suggested that mechanisms *a* and *c* may compete, depending on the nature of the compound reacting with the ketene and the external conditions.[1,17]

At this point it is reasonable to think that ketene dimerization is either pericyclic proceeding by the $[_\pi 2_s +_\pi 2_s +_\pi 2_s]$ mechanism or involves zwitterionic intermediates. However, orbital connection has only been proposed[6] but not probed for the ketene dimerization and it is undecided whether or not the $[_\pi 2_s +_\pi 2_s +_\pi 2_s]$ pathway can explain this cycloaddition thereof. Likewise for the case of two-step mechanism, even though ketenes are polar compound, the polarity in the transition state may not be enough for creating a zwitterion; charge separation also depends on the nature of the compound reacting with the ketene. Comparing these two mechanisms with experimental facts, it is found that the $[_\pi 2_s +_\pi 2_s +_\pi 2_s]$ pathway may explain the route found in gas phase from the thermolysis of diketene due to the concertedness of the reaction. Nonetheless, as it was stated above, this mechanism may not represent the reaction in liquid phase due to it is waited that solvents have negligible effects on the rate of pericyclic reactions;[2] this negligible effect is not the case of the ketene dimerization whose activation barrier is lowered ca. 21 kcal per mol when the solvent is acetone[19]. On the contrary, solvents affect decisively the rate of reaction of several two-step mechanisms with zwitterionic intermediates.[1,2,16] However, neither identification nor isolation of a probable zwitterionic intermediate has been achieved for the ketene dimerization in both gas and liquid phase so far; it is also worthwhile to mention that ketene dimerization had not been studied at theoretical level with inclusion of solvent effects.[17] Therefore, as these mechanisms are only proposed but neither mechanistically nor experimentally validated, it seems like there is no a unified mechanism that can satisfactorily explain the ketene dimerization in both gas and liquid phase.

Nonetheless, these two mechanisms are not the unique alternatives for the [2+2] cycloadditions to proceed. There is another concerted mechanism that this class of cycloaddition can follow regardless the W&H rules. This mechanism is called pseudopericyclic and has been recently reported for explaining some ketene cycloadditions.[8,20] Consideration of the existence of the pseudopericyclic mechanism (*d*) was procrastinated by almost 20 years. The pioneer work of Ross et al[21] showed that some classes of pericyclic reactions exhibit orbital disconnection in the transition state and named these reactions as pseudopericyclic. This pathway can be visualized as an intermediate route among pericyclic and two-step mechanism. Opposite to pericyclic, pseudopericyclic mechanism involves a non-overlapped-orbital and highly asynchronous activated complex with a great charge distribution. This charge distribution is not high enough to stabilize a zwitterionic intermediate species, though. This fact can make pseudopericyclic reactions to have activated complexes with strong newly formed bond ahead of these at the disconnection center, resembling to a product-like transition state (Figure 2.4), and therefore a low energy barrier, yet in a concerted pathway, may be expected.[22]
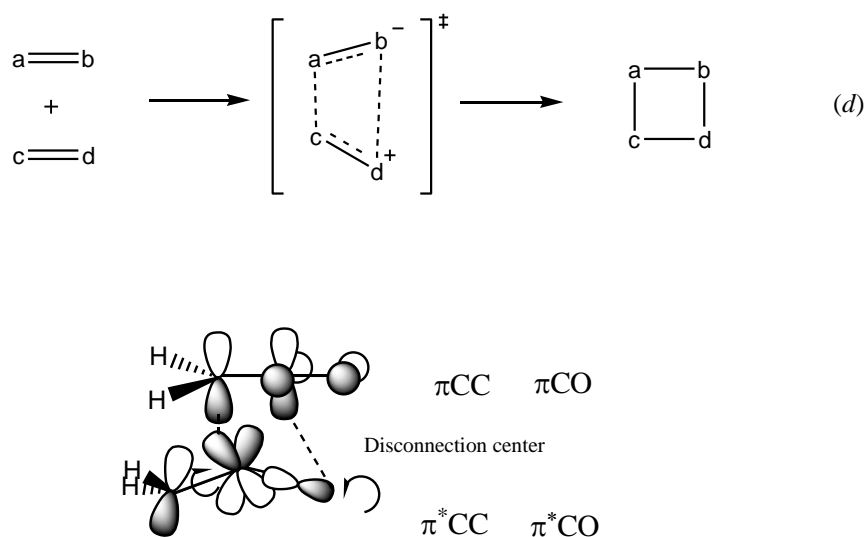
Figure 2.4. Proposed concerted asynchronous pseudopericylic pathway for ketene dimerization.

Pseudopericyclic reactions are highly probable in polar [2+2] cycloadditions. The electronic array showed in polar molecules, such as ketenes, can allow for either one or two orbital disconnections. Orbital disconnections occur in regions where orthogonal sets of orbitals meet

but do not overlap at the activated complex associated with their cyclization. Such a disconnection in the cyclic array of overlapping orbitals can be caused by the presence of non-bonding orthogonal orbital systems (Figure 2.1) that exert perturbations by either nonbonding electrons or electron-deficient centers[21]. As a result, the $[_\pi 2_s + _\pi 2_s + _\pi 2_s]$ pathway can not be an alternative for this class of molecules. This situation characterizes the pseudopericyclic reactions as a new subset of pericyclic reactions with nonaromatic transition states.[23,24] All pseudopericyclic reactions are orbital symmetry allowed because no electrons are exchanged between the in-plane and out-plane orbitals from the reactants, through the activated complex, to the product[22]. Such non-exchange is afforded via a pathway that maintains the orbital disconnections, regardless of the number of electrons involved.[22]

Pseudopericyclic reactions may have planar symmetry in the activated complex unless crowding of atoms lead to distortion from planarity, as in ketene dimerization (Figure 2.4).[22] Due to the theoretical foundations for pseudopericyclic reactions were established very recently by the work of Birney[25] and others[26], several aspects related to this class of reactions remain to be discovered and enunciated. Definition of the grade of distortion that can show a pseudopericyclic reaction, for example, is one aspect that remains to be clarified. Some authors[20] assumed planar pseudopericyclic reactions when the activated complex shows distortion from planarity up to $\pm 30°$ and others[8] up to $\pm 45°$. Theoretical studies obtained that the activated complex for the ketene dimerization have a distortion greater than $40°$ which suggests that this reaction is nonplanar pseudopericyclic. The nonplanarity may influence the activated complex exhibiting especial properties such as increasing the number of disconnection centers, increasing the strength of the newly formed bond and thus generating very low activation energy and, presumably increasing sensitiveness to solvent effects.

As a final remark of this section, ketene dimerization may follow either pericyclic or pseudopericyclic or two-step via zwitterion mechanisms. Experimental and theoretical differentiation between these possible mechanisms is our next concern. As the behavior of the ketene dimerization varies markedly with solvent effects, the different mechanisms are discerned in gas phase and liquid phase separately. Also, the changes in the topology of the reaction in going from gas to liquid phase have to be disclosed.

2.2 Differentiation between pericyclic and pseudopericyclic mechanisms for ketene dimerization in gas phase

Additional to the differences described in the preceding section, pseudopericyclic type of reactions can be differenced from pericyclic reactions by the use of the following approaches: the natural bond analysis (NBO)[21,22,27], the anisotropy of the current induced density (ACID) analysis[28], electron localization functions (ELF)[29], the ellipticity of atoms-in-molecules (AIM)[30] and the nucleus independent chemical Shift (NICS)[20]. These approaches try to differentiate the mechanisms of the reactions based on the assumed fact that the orbital disconnection in a pseudopericyclic reaction prevents its transition state of being aromatic.[20,28,30]

With respect to the topic of this research, it is possible to use the preceding methodologies for discarding between pericyclic and pseudopericyclic mechanisms for the ketene dimerization in gas phase. Indeed, Rode and Dobrowolski[8] very recently applied the AIM methodology[30] to the optimized transition states for the ketene dimerization; geometry calculations were done at the MP2/aug-cc-pVDZ level. Rode and Dobrowolski[8] found the presence of one new bond critical point (BCP) and the absence of ring critical points (RCP) in the transition state for the production of both diketene and 1,3-cyclobutanedione. The presence of only one BCP and the absence of RCP indicate, respectively, one orbital overlap and no cyclic transition states. Figure 2.5 clearly shows the formation, in the activate complex, of one bond ahead of the other yet not formed and thus generating a disconnection center. These facts suggest a pseudopericyclic type of reaction rather than a pericyclic one. Besides, distortion from planarity of these transition states suggest that the reactions are not ordinary pseudopericyclic. According to these results, Rode and Dobrowolski[8] discarded both the $[_\pi 2_s +_\pi 2_a]$ and $[_\pi 2_s +_\pi 2_s +_\pi 2_s]$ mechanisms of pericyclic reactions for representing the ketene dimerization toward diketene and 1,3-cyclobutanedione and classified these reactions as nonplanar pseudopericyclic instead.

The geometrical parameters found by the research of Rode and Dobrowolski[8] for the activated complexes of diketene (Figure 2.4) and 1,3-cyclobutanedione agree with previous theoretical static works at the SCF/DZP[6] and MP2/6-31G(d)[7] levels and, a dynamic work at DFT level[31]. Therefore, it seems that the conclusions of Rode and Dobrowolski[8] can explain the topology of the ketene dimerization in gas phase so far (section 1.5.1). However, their result for the

activation energy barrier appears to reproduce improperly the experimental value obtained from the thermolysis of diketene (section 1.5.1)[32]; i.e. Rode and Dobrowolski[8] expressed that their calculated activation barrier of 30.1 kcal per mol for the production of diketene is in agreement with the experimental value[32] of 31 kcal per mol, although in Chart 1 and in the supporting information, they showed this energetic value of 30.1 kcal per mol as the corresponding for the Gibbs energy barrier. Errors in predicting the energy barrier usually mean that the geometries were improperly determined as well and therefore, the transition state structures, yet with the agreements to other studies, may have been miscalculated.[33] This controversial disagreement in the energy barrier suggests that ketene dimerization mechanism still remains to be clarified and classified in gas phase.

(a) Reaction towards diketene   (b) Reaction towards 1,3-cyclobutanedione
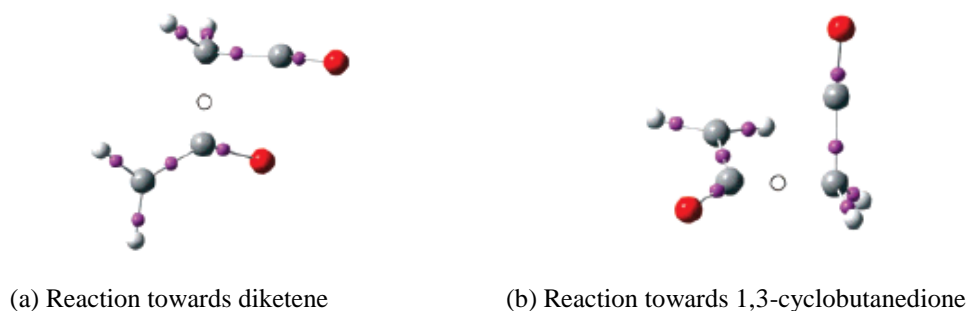
Figure 2.5. AIM analysis for the transition states structures of ketene dimerization calculated at the MP2/aug-cc-pVDZ level. Bond critical points are shown as small balls for the ordinary bonds and as open circles for newly formed bonds (Taken from ref. 8).

2.3 Differentiation between pericyclic, pseudopericyclic and two-step mechanisms for ketene dimerization in liquid phase

As it was stated in section 2.1, mechanism for the cycloadditions in gas phase can be different in solution. Independently to the facts found in the ketene dimerization in gas phase, the solvent effects[15] may alter both the kinetic and the topology of the reaction. Changes in reaction rates that can occur with changes in the polarity of the liquid phase can be characteristic of a determined sort of mechanism. In fact, the preceding disclosed mechanisms for [2+2]

cycloadditions can be qualitatively and quantitatively differentiated by analyzing the reaction rates in different solvents.

2.3.1 Qualitative differentiation

The different mechanisms (i.e. *a*, *b*, *c* and *d*) can be qualitatively differentiated by considering the ratio of the kinetic constants between the reaction carried out in a polar and a dipolar solvent. According to the magnitude of the ratio of kinetic constants (rkc) observed in the different mechanisms it has been suggested a particular tendency that can help to identify the different pathways; e.g. the rates of reactions proceeding through pericyclic activated complex are normally insensitive to solvent polarity because of the little separation of charge.[1, 2, 13, 15, 16, 34] In the case for asynchronous concerted reactions, which involves an activated complex with different polarity than the reactants, an increase in solvent polarity should have a greater enhance in rkc.[15] This class of reaction can be associated in several cases to planar and nonplanar pseudopericyclic reactions. In the case for two-step cycloadditions via diradical and zwitterionic intermediates it was found that these are respectively insensitive and sensitive to solvent effects.[2,13,15,34] For the case of two-step mechanism via zwitterionic intermediate, the magnitude of the solvent effects on the reaction rate depend on the relative size of the barriers. The rate of this two-step mechanism is accelerated with increasing solvent polarity when the formation of the zwitterionic intermediate is reversible or when the formation of the zwitterionic intermediate is irreversible and the first barrier is higher than the second barrier.[35] In many cases the raising in the reaction rates of two-step mechanisms via zwitterion can raise the magnitude of the ratio of kinetic constants to several hundreds or thousands. [2,13,15]

Altogether, it is found that both asynchronous concerted and two-step via zwitterionic intermediate may experiment rate acceleration with increasing solvent polarity. The distinction between them can be made only when the solvent effects are large.[15,34,36] Table 2.1 illustrates the ratio of kinetic constants for different [2+2] cycloadditions. From this Table it is clear that very high values for rkc mean two-step mechanisms with zwitterionic intermediates while very low values are particularly characteristic for synchronous concerted and diradical two-step mechanisms. It is also noticeable that mean values for rkc can be characteristic of both

asynchronous concerted and zwitterionic two-step mechanism and therefore such interval can not help to make definitive conclusions.

For the case of ketene dimerization, kinetic studies in different solvents[89] found it to be solvent-polarity dependent and to follow second-order kinetic law, which may be proof of a two-step process. Rice and Greenberg[19] calculated the rate constant (k_2) for the ketene dimerization in different nonpolar and polar aprotic solvents; Table 2.2 shows these results. According to the Rice and Greenberg[19] results, the ratio of kinetic constant for ketene dimerization is 445 when the polar solvent is glycol diacetate and the dipolar solvent is carbon tetrachloride. This value can be considered as intermediate according to the scale shows in Table 2.1 and therefore we can qualitatively classify the ketene dimerization as either concerted or two-step via zwitterionic intermediate without concluding a definitive mechanism.

Table 2.1. Ratio of kinetic constants for several [2+2] cycloadditions.

Reac.	Ref.	$\dfrac{k_{acetonitrile}}{k_{cyclohexane}}$	Class[a]	Reac.	Ref.	$\dfrac{k_{acetonitrile}}{k_{cyclohexane}}$	Class[a]
(r1)	37	63000	Two-step Z	(r8)	42	163	Concerted, asynchronous
(r2)	38	18800	Two-step Z	(r9)	13	37	Concerted, asynchronous
(r3)	13	4900	Two-step Z	(r10)	41	31 [d] 2 [e]	Concerted [4+2] cycloaddition
(r4)	39	2160 [b]	Two-step Z	(r11)	44	29 [b]	Two-step Z or Concerted asynchronous?
(r5)	40	1700 [c]	Two-step Z	(r12)	35	2 [f]	Two-step Z
(r6)	41	740 [d] 12 [e]	Concerted [4+2] cycloaddition	(r13)	45	2 [g]	Two-step R
(r7)	13	407	Two-step Z	(r14)	46	1.2 [h]	Concerted, synchronous

[a] "Two-step Z" stands for a two-step mechanism with zwitterion generation. "Two-step R" stands for a two-step mechanism with diradical generation. [b] CH_3CN/CCl_4. [c] dichloromethane/hexane. [d] water/isooctane. [e] methanol/isooctane. [f] $C_6H_5NO_2/CCl_4$. [g] DMSO/Cyclohexane. [h] $C_6H_5Br/HCON(CH_3)_2$.

p-CH₃OC₆H₄-CH=CH₂ + (NC)₂C=C(CN)₂ ⟶ (r1)

$p\text{-}CH_3OC_6H_4\text{-}CH=CH_2$ + $(NC)_2C=C(CN)_2$ ⟶ (r1)

$ClO_2S-N=C=O$ + $H_2C=C(C_2H_5)(C_4H_9)$ ⟶ (r2)

$(CH_3)_2C=CH-OC_2H_5$ + $(NC)_2C=C(CN)_2$ ⟶ (r3)

$CH_2=CH-S-C(CH_3)$ + $(F_3C)(NC)C=C(CN)(CF_3)$ ⟶ (r4)

$H_2C=CH-OC_4H_9$ + $(NC)_2C=C(CN)_2$ ⟶ (r5)

$O=C(CH_3)-CH=CH_2$ + (cyclopentadiene) ⟶ (r6)

$(CH_3)_2C=C=O$ + (pyrrolidine)N-C=C(CH_3)_2 ⟶ (r7)

60

$CH_2=CH-O-n-C_4H_9$ + $(C_6H_5)_2C=C=O$ $\longrightarrow$ (r8)

$(CH_3)_2C=C=O$ + [pyrrolidine]$N-C=C(CH_3)_2$ $\longrightarrow$ (r9)

$HC=CH_2$ / NC + [cyclopentadiene] $\longrightarrow$ (r10)

$(CH_3)_2C=C=O$ + $(CH_3)_2C=C=O$ $\longrightarrow$ (r11)

[oxazolone with C_6H_5, CH_3, N, O, CF_3] + $H_3C-N=C(H)-C_6H_5$ $\longrightarrow$ (r12)

$(CH_3)_2C=C=CH_2$ + $CH_2=CH-CN$ $\longrightarrow$ (r13)

$(C_6H_5)_2C=C=O$ + $H_2C=C(H)C_6H_5$ $\longrightarrow$ (r14)

61

2.3.1 Quantitative differentiation

There exist more elaborate methodologies for helping us determining the most probable mechanism for a reaction between neutral-dipolar molecules according to the trend of the reaction in different solvents.[13,15] One group of these methodologies establishes a relationship between the phenomenon, in this case the reaction rates, and a physical macroscopic solvent parameter that represent the solvent effects (such as dielectric constant, dipole moment, or refraction index). Kirkwood developed a theoretical expression that relates the standard Gibbs energy of transfer of a spherical molecule of radius r and dipole moment μ from the gas phase to a continuous medium of dielectric constant ε_r according to[13]

$$\Delta G^0_{solv} = -\frac{N_A}{4\pi\varepsilon_0}\frac{\mu^2}{r^3}\left(\frac{\varepsilon_r - 1}{2\varepsilon_r + 1}\right) \tag{1}$$

where ε_0 is the permittivity of vacuum and N_A is the Avogadro constant. Applying the transition state theory of Laidler and Eyring[48] to the dipolar reaction A+B, it is found that the rate constant in solution k can be expressed in terms of the dielectric constant of the solvent ε_r as follows

$$\ln(k) = \ln(k_0) - \frac{N_A}{4\pi\varepsilon_0 RT}\left(\frac{\varepsilon_r - 1}{2\varepsilon_r + 1}\right)\left(\frac{\mu_A^2}{r_A^3} + \frac{\mu_B^2}{r_B^3} - \frac{\mu_{\neq}^2}{r_{\neq}^3}\right) \tag{2}$$

where k_o refers to the rate constant in vacuum and subscript $\neq$ refers to the activated complex species. This equation holds the hypothesis that the electrostatic solute/solvent interaction such as dipole-dipole forces should above all determine the reaction rates in a manner as described by Hughes-Ingold theory.[2,15,16] This equation also predicts that if the activated complex is more dipolar that the reactants, as it is waited for ketene dimerization case, the rate of reaction increases with the relative permittivity of the medium; thus, there would be a linear correlation between $ln(k)$ and the Kirkwood function, $(\varepsilon_r-1)/(2\varepsilon_r+1)$. This linear correlation is due to a medium with high ε_r value favors the production of a diionic species and therefore increasing the rate of reaction. This equation reflects that the optimal solvation is probably not achieved in the transition state, but in the zwitterion.

Table 2.2. Kinetic measurements for the ketene dimerization in different solvents at 0°C[19].

Solvent	[Ketene], mol per l	$k_2 \pm 10\%$	$k_2 / k_2^{CCl_4}$	ε_r	E_T,[a] kcal per mol
Carbon tetrachloride	0.711	0.00005	1	2.24	32.5
Xylene	0.756	0.00038	9	2.4	33.1
Bromobenzene	0.770	0.00047	12	5.4	36.6
Chlorobenzene	0.802	0.00056	15	5.6	36.8
Toluene	0.910	0.00064	23	2.38	33.9
1,2-Dichloroethylene	0.742	0.00075	18	4.6	---
Tetrachloroethylene	0.511	0.00099	11	2.5	32.1
Heptane	0.309	0.00153	6	1.92	31.1
Carbon disulfide	0.468	0.00177	16	2.64	41.3
Ethyl trichloroacetate	0.640	0.00190	33	7.8	38.7
Benzyl chloride	0.861	0.00225	71	6.4	---
Benzene (24°C)	0.502	0.00280	30	2.27	34.3
Acetone (-23°C)	0.686	0.00400	80	---	---
1,2-Dichloroethane	0.774	0.00425	108	10.36	41.3
Ethyl Benzoote	0.812	0.00552	155	6	38.1
Chloroform	0.786	0.00401	105	4.89	39.1
Ethyl acetate	0.705	0.00465	98	6.02	38.1
1,1,2,2-Tetrachloroethane	0.876	0.00939	307	8.50	39.4
Benzyl ether	0.745	0.01800	425	4.22	36.3
Glycol diacetate	0.706	0.02100	**445**	---	---
Nitrobenzene (24°C)	0.368	0.07300	421	34.78	41.2
Acetone (O2 absent)	0.524	0.01480	173	1.0159	42.2
Acetone (O2 present)	0.498	0.01460	154	1.0159	42.2
Acetone (20°C)	0.498	0.06020	703	20.56	42.2

(a)   The Dimroth-Reichardt parameter[36, 47].

It may be inadequate to describe quantitatively the solvent effects by single physical macroscopic solvent parameter, as the Kirkwood function, due to the multiple microscopic solvent/solute interactions. For covering the lack of comprehensive theoretical expressions for the calculations of solvent effects at microscopic level, another group of methodologies, the so-called empirical parameters of solvent polarity[*], establishes that a particular, carefully selected, well understood and strongly solvent dependent chemical reaction or spectral absorption may serve as suitable reference for describing another resembling process[47]; various scales of solvent polarity have been developed in this way. The most comprehensive empirical solvent scales of

---

[*] Solvent polarity is defined as the overall solvation power of solvents arising from the action of all possible, specific and non-specific, intermolecular interactions between solute and solvent molecules, excluding, however, those interactions leading to chemical alterations of the molecules such as protonation, oxidation, reduction, chemical complex formation, etc.[49]

one parameter for determining the solvent effects in a given reaction are those derived from spectroscopic reference processes[47]. These spectroscopic empirical scales consider the changes in the absorption spectra in different solvents[36,47] and thus derivate a linear Gibbs energy relationship approach. Absorption spectra of chromophore compounds[+] are greatly dependent of the properties of the medium in which the chromophores are dissolved in. The spectral changes (i.e. positions, intensities and shapes of the absorption bands) occurred in the solvated chromophore (solvatochromism process) arise from the physical intermolecular solute/solvent interaction forces; such interaction forces tend to alter the energy gap between ground and excited state of the absorbing species[50, 51] and therefore, solvent effects on absorption spectra can be used to provide information about microscopic solute/solvent interactions. Kosower[52] in 1958 was the first to setup a comprehensive solvent scale from solvent-sensitive standard compounds absorbing radiation in UV/Vis spectra. Solvatochromic dyes were used as indicators of solvent polarity. Lots of solvent-dependent absorption spectra of a great variety of compounds have been used since then for establishing empirical scales of solvent polarity (see ref. 47). In developing these scales, it is assumed that a particular solvent-influenced UV/vis/near-IR absorption is a suitable and representative model for a large class of other solvent-dependent processes such as chemical reactions.

The Dimroth-Reichardt parameter $E_T(30)$ based on the solvatochromism of the pyridinium N-phenolate betaine dye (PPBD) can be used as an empirical scale for the quantitative and qualitative influence of solvent polarity[47] in a particular phenomenon. This $E_T(30)$ parameter is easily measurable and its value mainly reflects the electrophilicity (i.e. the hydrogen-bond donor activity) of the solvent. It is defined as the molar electronic transition energies (E_T) of disolved PPBD, measured in kcal per mol at room temperature and normal pressure according to

$$E_T(30) = \frac{28591}{\lambda_{max}} \tag{3}$$

[+] A chromophore is generally regarded as any grouping of an organic molecule which is responsible for the light absorption under consideration.[47]

Where λ_{max} is the wavelength of the maximum of the longest wavelength, intramolecular charge-transfer $\pi \rightarrow \pi^*$ absorption band of PPBD in the solvent in turn.[53] Thus, the parameter $E_T(30)$ constitutes the excitation energy of PPBD at the long-wave absorption maximum. This scale has found wide applications in various fields of solvent effects such as in empirical measurements of the polarity of all kind of liquid media[120] (solvents, binary solvent mixtures, electrolyte solutions, microheterogeneous solution, supercritical fluid solvents), characterization of polarity of polymers[54] as well as chromatographic materials[55]. This $E_T(30)$ parameter can also be used for discerning the influence of the solvents on a particular reaction. It is found that if *log k_2* entertains relations of tolerable increasing linearity with the empirical parameter $E_T(30)$, formation of zwitterionic species is highly probable with relatively small values of the ratio of kinetic constants[13,47]; this affirmation is based on the supposition of parallelism between the reaction coordinate of the studied process in liquid phase and the solvent-mediated stabilization of the highly dipolar zwitterionic ground state of PPBD. According to this fact, a poor linear relationship entertained between *log k_2* and $E_T(30)$ suggests either a concerted reaction proceeding in liquid phase or a change of solvent polarity scale[13,47].

In several cases single-parameter empirical scales can achieve satisfactory description of the processes.[36,47,56] However, in many cases reactions in solution do not exhibit a clear trend due to the lacks in describing the multitude of microscopic solute/solvent interactions. An alternative for better analyzing the solvent influence, from empirical point of view, is to apply multiparameter equations which can, in principle, take into account several of the multiple solvent effects. The multiparameter equations proposed by Koppel and Palm (KoP)[15] and by Kamlet and Taft (KaT)[15,57] are among the most generally applicable and elaborate equations for determining the solvent effects both qualitatively and quantitatively. Both equations consider non-specific and specific solute/solvent interactions separately; non-specific interactions include *electrostatic forces* arising from the Coulomb interactions between charged ions and dipolar molecules (i.e. ion/ion, ion/dipole, dipole/dipole) and *polarization forces* that arise from dipole moments induced in molecules nearby ions or dipole molecules (i.e. ion/nonpolar molecule, dipole/nondipole molecule, two nonpolar molecules). The main difference between the KoP and the KaT correlations is in the term for these non-specific interactions. In the KoP equation the polarity and the polarizability interactions are considered separately whereas in the KaT equation

both interactions are grouped into *one only term*. On the other hand, the term for specific interactions is divided, in both equations, into *solvent Lewis-acidity interactions* (electrophilic solvating power) and *solvent Lewis-basicity interactions* (nucleophilic solvating power). Table 2.3 describe explicitly the terms for the KoP and KaT correlations.

Table 2.3. Multiparameter Koppel-Palm (KoP)[15] and Kamlet-Taft (KaT)[57] empirical equations.

Correlation	Non-specific interactions		Specific interactions	
	Polarity	Polarizability	Electrophilicity	Nucleophilicity
KoP[a]	$Y = \dfrac{\varepsilon - 1}{\varepsilon + 2}$	$P = \dfrac{n^2 - 1}{n^2 + 2}$	$E = E_T(30) - 25.57$ $- 14.39\,Y - 9.08\,P$	$B = \tilde{v}^{\,0}_{CH_3OD} - \tilde{v}_{CH_3OD \cdots B}$
KaT[b]	π^*		α	β

(a) $ln(\,k\,) = ln(\,k_o\,) + yY + pP + eE + bB$. (b) $ln(\,k\,) = ln(\,k_o\,) + s\pi^* + a\alpha + b\beta$

The parameters for the KoP equation are easily obtained from physical measurements of both macroscopic and microscopic properties of the solvents. Thus, the polarity and polarizability interactions are in function of the dielectric constant and the refraction index, respectively (Table 2.3) whereas the specific interactions where correlated to empirical scales based on absorption spectra. The electrophilic term, E, was correlated to the $E_T(30)$, Y and, P parameters whereas the nucleophilic term, B, was correlated to the wave number of the IR stretching frequency of deuteriomethanol in the gaseous phase and in the given solvent (Table 2.3).[13,56]

In the KaT multiparameter equation, π^* is an index of solvent polarity-polarizability, and α and β are the indexes selected for the specific interactions. The π^* scale, which measures the ability of the solvent to stabilize a charge or a dipole in virtue of its dielectric field, was selected to run from 0 for cyclohexane to 1 for dimethyl sulfoxide and its value are derived from electronic transitions occurring on a molecular-microscopic level in solute-organized cybotactic regions (i.e. within the solvation shell of the solute).[57] The α is a measure of the solvent hiydrogen-bond donor acidity and therefore it describes the ability of a solvent to donate a proton in a solvent-to-solute hydrogen bond. The α -scale was selected to extend from zero for cyclohexane to about 1

for methanol. The β scale measures the solvent hydrogen-bond acceptor basicity and therefore describes the solvent's ability to accept a proton (or to donate an electron pair) in a solute-to-solvent hydrogen bond. The β-scale was selected to extend from zero for cyclohexane to about 1 for hexamethylphosphoric acid triamide.[57] The solvent coefficients for the KoP and the KaT correlations measure the relative susceptibilities of the solvent-dependent solute rate velocity for the indicated solvent parameters.[47]

The physical model of Kirkwood, the $E_T(30)$ parameter and the multiparameter approaches of KoP and KaT, *vide supra*, were applied to analyze the kinetic data[19] collected for the ketene dimerization in liquid phase (Table 2.2). Graph 2.1a and 2.1b show the correlation found between the dimerization and the Kirkwood function and the Dimroth-Reichardt parameter[47]. According to these graphs, ketene dimierization data in liquid phase are reproduced by neither the physical model of Kirkwood nor the $E_T(30)$ parameter; linear correlation is better for the single-parameter empirical method. It can also be seen in these Graphs that there exists a plausible trend in raising the rate of reaction with the increasing of the value of the solvent polarity scale, especially with the $E_T(30)$ parameter. This fact may indicate either an asynchronous concerted or a two-step mechanism with zwitterion formation. However, the poor linear correlations ($R^2=0.109$ for the Kirkwood model and $R^2=0.476$ for the $E_T(30)$ scale) cannot favor the two-step mechanism over the concerted one for representing the ketene dimerization. Notwithstanding, these results are in contradiction with stepwise mechanisms[17,58,59] involving diradical intermediates due to the rough dependence between the rate of reaction and a single-parameter solvent scale. This is in agreement with the qualitative results obtained from the intermediate value for the ratio of kinetic constant (Table 2.2).

It is important to recall that these two possible behaviors for the dimerization in liquid phase, i.e. concerted and two-step via zwitterion, explain acceptably the reaction due to both an activated complex with a high degree of charge distribution and a zwitterionic intermediate can be stabilized by the solvent effects[15]. According to the results with one parameter equations, the lack of correlation between the reaction rate and the Kirkwood function and the $E_T(30)$ parameter means that the multitude of solvent/solute interactions occurred along the ketene dimerization cannot be accounted by a single macroscopic parameter of the solvent in all the

reactions. Therefore, analysis of experimental data with single-parameter scales does not help for classify conclusively the ketene dimerization as either concerted or two-step process. The study on these scales also reveals that if the reaction is concerted the transition state have to be highly asynchronous due to the roughly influence of the solvent polarity[*].

As an alternative for better understanding the ketene dimerization mechanism, the kinetic data were analyzed by the use of both the KoP and KaT multiparameter correlations. Tables 4 and 5 show the available solvent parameters for the KoP and KaT correlations and Tables 6 and 7 show the linear regression coefficients obtained by the least square method. As it can be noticed, the correlation coefficient for the adjusting processes indicates that the kinetic data of the ketene dimerization correlates much better with the KoP equation than with the KaT equation (Tables 6 and 7); indeed, an independent principal component analysis on the inter-relationship between the diverse solvent scales and the mechanisms by which chemical structure determines the solvent properties reports that the KoP correlation parameters are among the essentially independent solvent scales that can describe the solvent effects.[60] Despite the relative good performance of the KoP correlation, correlation coefficients are not high enough for making definitive conclusions about the mechanism, though. The multiparameter equations are one of the most elaborate and successful empirical methodologies for studying solvent effects in a given process, however, the total of the intermolecular specific solute/solvent interactions on several processes, such the ketene dimerization reaction, are of too highly complicated nature to be accounted for only a few of linear parameters.[60]

Normalization of the KoP equation (Table 2.8) shows that the main factors that account for a great portion of the solute/solvent interactions, according to percentage-wise analysis, are the polarization parameter *Y* and the electrophilic solvating power *E*. Indeed, the polarizability parameter *P* and the nucleophilic solvating power *B* can in many cases be neglected (Table 2.8). This is also supported by the large uncertainties at 95% of confidence for the *P* and *B* parameters which are larger, in a lesser degree for *B*, than the corresponding regression coefficients (Table 2.6).

---

[*] The unequal bond formation goes along with partial charges may somewhat increase the dipole moment of the activated complex[13] and thus the sensibility to solvent effects.

$$y = 5.13799x + 2.36437$$
$$R^2 = 0.10948$$
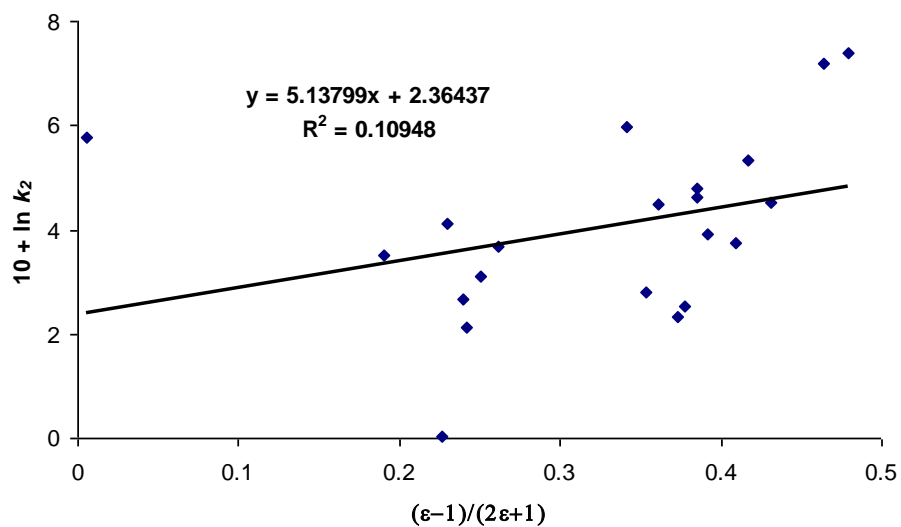
(a) Kirkwood function

$$y = 0.15238x - 3.23563$$
$$R^2 = 0.47586$$
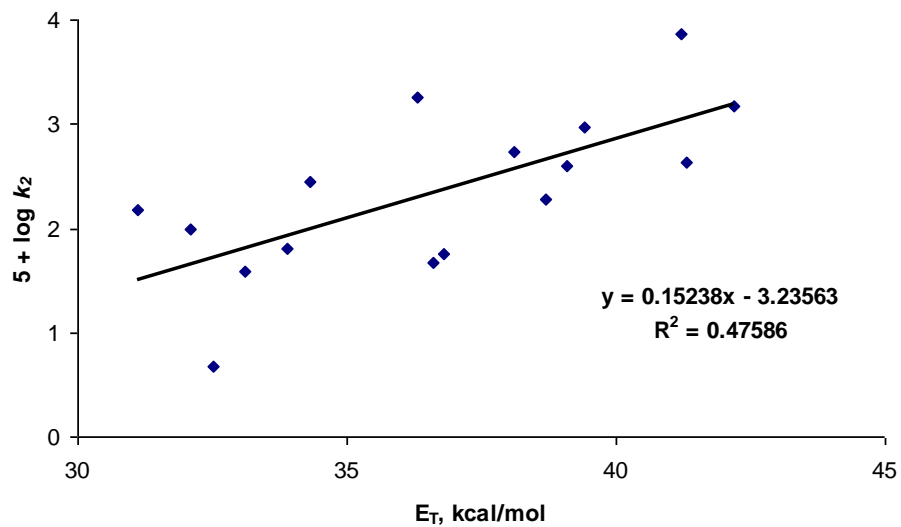
(b) $E_T(30)$ parameter

Graph 2.1. Relationship between the single-parameter solvent polarity scales and the rate constant of the ketene dimerization.

The fact that the parameter E is one of the most important factors shows that one of the role of the aprotic solvents in the ketene dimerization reaction is being a Lewis acid; i.e. solute appears to be a good hydrogen-bond acceptor whereas solvents act as good hydrogen-bond donors. In

fact, ketene has the group $>C=C=O$ with a central carbon atom charged strongly positively due to boundary *sp2* carbon atom and on the oxygen atom; the negative charge on the oxygen can therefore be taken and stabilized by solvents of large polarity thus affecting the topology and energy of the reaction coordinate.

On the other hand, normalization of the KaT equation (Table 2.9) shows that the main factor influencing the correlation is the parameter π^*. In fact, neither the parameter α nor the parameter β can be neglected *a priori* since their percentage-wise influences total ca. 20%. However, the study of the KaT correlation parameters can give only meagerly qualitative conclusions due to its poor correlation; this may be a consequence of inappropriate nonspecific and specific solvent scales for describing the ketene dimerization phenomenon. The KoP equation stands much better correlation with the ketene dimerization data than that achieved by single-parameter equations because the combined use of a function of the dielectric constant of the medium and the Dimroth-Reichardt parameter. Thus, the ketene dimerization reaction is affected by several interactions which should be studied together. This can be better visualized with a single-parameter form of the multiparameter correlation (Graph 2.2). Comparing with the very poor results of linearity achieved by the use of the Kirkwood function, a much better single-parameter correlation between a function of the dielectric constant and the reaction rate is achieved by the use of the electrophilic and nucleophilic parameters[*] of the KoP equation (Graph 2.2a). The solvent polarity parameters of the KaT equation improve little the correlation (Graph 2.2b).

The combined use of the nonspecific and specific interactions for describing the ketene dimerization reaction, according to the corresponding KoP parameters, permits to suggest that both interactions are favoring the bond-making process by enhancing the charge separation and that a very large solvation is taking place along the reaction coordinate presumably forming an activated complex with a high degree of zwitterionic character. Formation of a zwitterionic intermediate in the ketene dimerization in liquid phase can not be certainly concluded.

---

[*] Nucleophilic parameter affects in much lesser degree the correlation with $(\varepsilon\text{-}1)/(\varepsilon\text{-}2)$ than the electrophilic parameter does. A correlation coefficient of 0.715 is achieved by withdrawing the parameter *B*.

Table 2.4. Solvent parameters for the KoP correlation[a][b].

Solvent	log(k_2)	Y	P	E	B
Carbon tetrachloride	-4.33255	0.292453	0.273992	0.43242	31
Xylene	-3.41341	0.318182	0.291822	0.479612	68
Bromobenzene	-3.32514	0.594595	0.321823	0	51
Chlorobenzene	-3.24949	0.605263	0.306361	0	50
Toluene	-3.19111	0.315068	0.292571	1.318626	54
1,2-Dichloroethane	-2.37161	0.757282	0.266046	2.410565	54
Chloroform	-2.39686	0.564586	0.266616	3.06469	35
Ethyl acetate	-2.33255	0.625935	0.227497	1.529423	91
Acetone (O2 absent)	-1.82974	0.005272	0.219982	14.91213	116

[a] Ref. 15. [b] T=0°C.

Table 2.5. Solvent parameters for the KaT correlation[a][b].

Solvent	ln(k_2)	α	β	π^*
Carbon tetrachloride	-9.97606	0	0.1	0.28
Xylene	-7.85967	0	0.12	0.43
Chlorobenzene	-7.48223	0	0.07	0.68
Toluene	-7.34781	0	0.11	0.54
1,2-Dichloroethylene	-7.19544	0	0	0.44
Heptane	-6.48249	0	0	-0.08
Carbon disulfide	-6.33678	0	0.07	0.51
1,2-Dichloroethane	-5.46084	0	0.1	0.81
Chloroform	-5.51896	0.2	0.1	0.58
Ethyl acetate	-5.37089	0	0.45	0.55
1,1,2,2-Tetrachloroethane	-4.66811	0	0	0.95
Acetone (O2 absent)	-4.21313	0.08	0.48	0.71

[a] Ref. 58a. [b] T=0°C.

Table 2.6. Linear regression model for the KoP correlation[a][b].

	Ln(k_o)	y	p	e	b	r^2
Coefficient	-4.348 ± 5.74	2.490 ± 2.155	-2.166 ± 16.96	0.144 ± 0.154	0.008 ± 0.0218	0.874

[a] $ln(k) = ln(k_o)+ yY + pP + eE + bB$. [b] Uncertainties at 95% of confidence.

Table 2.7. Linear regression model for the KaT correlation[a][b].

	Ln(k_o)	a	b	s	r^2
Coefficient	-8.411 ± 2.25	6.522 ± 16.81	2.592 ± 6.35	2.662 ± 3.84	0.425

[a] $ln(k) = ln(k_o)+ s\pi^* + a\alpha + b\beta$. [b] Uncertainties at 95% of confidence.

Table 2.8. Influence of the parameters in the normalized KoP correlation[a].

	Y	P	E	B
Coefficient	42.75	4.15	40.32	12.78

[a] In percentage.

Table 2.9. Influence of the parameters in the normalized KaT correlation[a].

	α	β	π^*
Coefficient	24.65	23.52	51.82

[a] In percentage.

$y = 2.86976x + 1.34468$
$R^2 = 0.75697$

x-axis: $(\varepsilon-1)/(\varepsilon+2)$

y-axis: log k_2 + 6.715 - 0.155E - 0.014B

(a) Koppel-Palm equation

$y = 3.42137x + 0.41778$
$R^2 = 0.30715$

x-axis: $(\varepsilon-1)/(\varepsilon+2)$

y-axis: ln k_2 + 8.813 - 4.574β
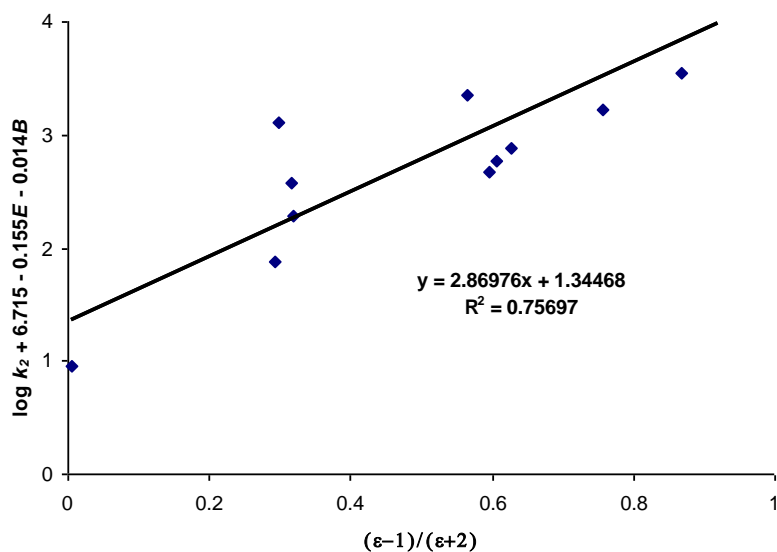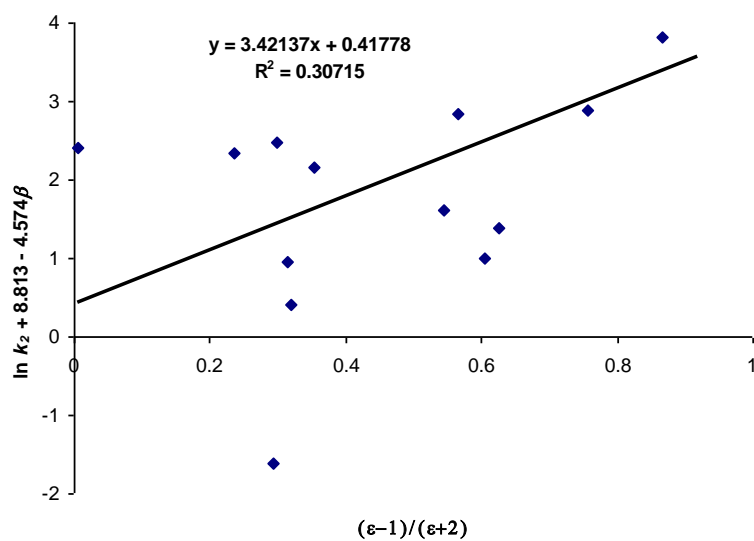
(a) Kamlet-Taft equation

Graph 2.2. Correlation for the multiparameter equation and the dielectric constant.

The preceding suggestions are consistent with large negative entropy (e.g. -38.0 cal per mol per K for the transition state in acetone[19]) which is a consequence of the dipole alignment undergone by the molecules of the aprotic solvents.[61] Owing to the fact that there can be a close resemblance in structure and dipolarity between the activated complex of one-step mechanism and the first activated complex of two-step mechanism[15, 26], we can not classify the ketene dimerization reaction *a priori*; indeed, the reaction can present simultaneously both of the mechanisms according to the solvent in turn. Multiparameter correlation results with the KoP equation also suggest that the nucleophilic power of the aprotic solvents does not play an important role in the solvation of the ketene dimerization reaction.

In spite of the preceding considerations, the qualitative conclusions based on empirical correlations may have little sense since the KoP correlation is not good enough to reproduce the kinetic data quantitatively (Table 2.6). The principal reason of the KoP equation for not to reproduce the kinetic data is that it does not consider the dependency between the nonspecific and specific interactions; the correlation assumes that these interactions work independently of each other and in a linear manner.[15,60,61,63] This can lead to conclusions of little interpretative value about the influence of each parameter on the mechanism of the reaction.[63] According to this fact, we should seek for more appropriate scales and correlations for interpreting the ketene dimerization. In fact, it is probable that more appropriate scales for mechanistically interpreting the ketene dimerization based on homolog processes have been studied and published elsewhere[*]; nevertheless, yet found the appropriate scale, the application of most of them is restricted by the fact that their parameters are known only for a few number of solvents.[47,60,61] In addition, considerable mechanistic information (such as the manner of the reactant attack, the distortion in the activated complex geometry and, the temperature trend of the reaction) is uncovered from a set of simple kinetic measurements.[64]

As an alternative to models based on physical solvent macroscopic properties and empirical microscopic parameters of solvent polarity, quantum-chemical methods can be used for describing and understanding the complex phenomena accounted in the solvation of reactants, activated complex, and products. The results obtained from these theoretical analyses, yet with

---

[*] In Ref. 60, authors study at about 40 solvent scales grouped in six classes of interactions.

their limitations and flaws, are very impressive.[92] Prediction of different mechanisms and influence of the environment on reaction coordinate from quantum chemical calculations have been widely reported.[2,17, 33] Due to these facts, the quantum chemical methods were chosen in this research for studying the ketene dimerization in both gas and liquid phase.

We can conclude from the empirical methodologies used to analyze the kinetic data in liquid phase that neither physical single models nor single-parameter models nor multiparameter models (reviewed in this research) describe quantitatively properly the ketene dimerization reaction. However, it is possible to qualitatively describe the mechanism of the ketene dimerization as a partial-charge-increasing pathway which makes the rate of reaction to increase with the increase of solvent polarity. This conclusion is in agreement with the Hughes-Ingold rules that state that an increase in solvent polarity results in an increase in solvation of those reactions in which the activated complex have greater charge density than in the initial reactant molecules[15]. However, as it was already stated, this qualitative agreement may not be used for providing a convincing classification of the ketene dimerization as either asynchronous concerted or two-step via zwitterionic intermediate.

2.4 Changing the mechanism in going from gas to liquid phase: is it the ketene dimerization case?

The differences in the trends of a chemical reaction in gas phase and in solution are dictated mainly by the solvent effects. Properties such as acidity and basicity of organic compounds are expected to be different in the gas phase and in solution. Whereas in gas phase acidity and basicity are intrinsic properties of the molecules, in solution these properties are a result of the interactions between solute and solvent molecules.[15] Due to the solvent is in major proportion than the solute, the behavior of solute molecules is dictated mainly by the solvent and only to a lesser extent by their intrinsic properties. Quantitatively, the principal reason for the differences in behavior between molecules in gas phase and in solution corresponds to the molecular energy alteration due to the Gibbs energy of solvation.

The overall problem of solvent effects is very complex, and much of it still needs to be unraveled.[64] One special component in the phenomenon of solvation is the development of charge or partial charge along the reaction coordinate. In fact, bond fission in solution is generally heterolytic due to the electron-par-donating and electron-par-accepting properties of the solvents.[15] This fact is a consequence of an important feature of the process of solvation, solvation energies of charged species are substantially larger than solvation energies of neutral species.[64] Due to this fact, solvation of ionic species must be considered as an important contributor to the energy profile of reactions in which there are developments of charge dispersal. Solvation of charged species affects not only the energy but also the topology of the potential surface and the extent of the charge dispersal.

Nucleophilic substitutions are especially susceptible to effects of the solvents due to the presence and development of charge. Reactions 15 and 16 show two nucleophilic reactions greatly affected by the process of solvation.

$$Cl^- \quad + \quad H_3C{-}Cl \quad \longrightarrow \quad Cl{-}CH_3 \quad + \quad Cl^- \qquad (r15)$$

$$H_3N \quad + \quad H_3C{-}Br \quad \longrightarrow \quad H_3N{-}CH_3 \quad + \quad Br^- \qquad (r16)$$

In the first reaction (r15), called the identity change reaction, the barrier height in gas phase, after formation of an ion-molecule complex [Cl----CH$_3$Cl]$^-$, is only 2.5 kcal per mol. In solution, the tendency of the reaction change strikingly due to the reaction barrier is increased with respect to that in gas phase by 8 and 10 times in DMF and in aqueous solution, respectively[65]; besides, a no well-defined intermediate is formed along the reaction pathway in aqueous solution. The barrier height difference of ca. 24 kcal per mol means that reactivity in the gas phase is almost 18 orders of magnitude greater than in aqueous solution. In the second reaction (r16), the so-called Mensshutkin reaction, the effect of the solvent on the barrier height is reverse; the gas phase barrier is extremely high, while the solution reaction is facile.[64] According to these examples, it is clearly seen that the solvent effects on reactivity can be very substantial; in some cases solvent effects on chemical reactions can be visualized as catalytic intervention.[61] Recalling the ketene dimerization, the substantial lowering of the free energy barrier in solvent indicates a substantial development of charge along the reaction coordinate. Considering this fact among the different

75

mechanims, we can propone an asynchronous concerted process (presumably a pseudopericyclic process) and a two-step with zwitterionic intermediate process as the most probable mechanisms for representing the ketene dimerization.

Altogether, the following question would be if both of the mechanisms proposed for the ketene dimerization can achieve such a lowering in the Gibbs energy barrier in going from gas to liquid phase. Indeed, ketene dimerization in gas phase is an unfeasible process with an experimental activation barrier of 31 kcal per mol whereas ketene dimerization in solution is a feasible reaction with experimental Gibbs energy barriers of 22.15 and 21.17 kcal per mol in toluene and acetone,[19] respectively. Although [2+2] cycloadditions are conventionally thought not to require solvent for generating the reaction[1,2,64], many examples in the literature, besides the ketene dimerization, illustrate that some [2+2] cycloadditions[12,15,66,67] may need of solvent effects for being feasible.

Due to the lack of a theory for predicting the changes that reactions can undergo in going from gas to liquid phase, qualitative description can be taken as a way for classifying the behavior of the reactions. Many [2+2] cycloadditions show different potential energy surface (PES) topology when going from gas to liquid phase; e.g. the topology of the PES for the polar [2+2] cycloaddition between ketene and imine is changed from concerted to two-step profile in going from gas to aqueous solution.[12] This change in topology may also mean a change in kinetic and therefore the reaction may show different rates in gas and liquid phase. Studies comparing reactivity of organic reactions in gas and liquid phase have been doing mainly using theoretical approach instead of experimental analysis due to the difficult in working in gas phase.[33] The different theoretical results regarding the effects on the PES topology of the [2+2] cycloadditions in the pass from gas to liquid phase can be grouped in two general classes:

a) Insensitive [2+2] cycloaddition. There exist some reactions which show insignificant differences between the PES topology of the reaction in gas phase and that in solution. In this group of reactions, the solvent effects are not able to stabilize further the charge distribution and therefore the asynchrony of the activated complex and the zwitterionic intermediate remains undeveloped. Solvent effects can either modify or not the rate of the

reaction. To this group belongs the reaction between methyleneketene and 5-methylene-1,3-dioxan-4,6-dione[68], the cycloaddition of allene ($CH_2=C=CH_2$) to isocyanic acid[69] and, the cycloaddition of ethylene to Isocyanatomethane[70].

b) Sensitive [2+2] cycloaddition. In this class, solvent effects are able to stabilize further the asynchronous character of the activated complexes and the charge distribution thus obtained generates the zwitterionic intermediate. Examples of this sensitive cycloadditions are the reaction between ketene imine and formaldehyde[71], the reaction of 1,1-dicyanoethylene and methyl vinyl ether[67], cycloaddition of ketene to vinylimine[69] and, cycloaddition of vinyl alcohol to chlorosulfonyl isocyanate[70].

The energetic data reported for each class of these cycloadditions (i.e. insensitive and sensitive reactions) were analyzed in order to find a qualitative tendency that helps to classify the ketene dimerization reaction in the pass from gas to liquid phase. Table 2.10 shows the energetics for the different insensitive and sensitive [2+2] cycloadditions studied at different theoretical levels. According to the classification, there exist a tendency to have low energy of solvation (assumed to be the difference between the activation energy barriers in gas and liquid phase, $E_a^G - E_a^S$) for these cycloadditions termed as insensitive, while "sensitive" reactions generally tends to have appreciable values of solvation. Graph 2.3 clearly shows the values for the energy of solvation and the classification of the mechanisms of reaction. The value taken as the limit point for describing a cycloaddition as either sensitive or insensitive was the corresponding to the cycloaddition between 1,1-dicyanoethylene and methyl vinyl ether (r21) analyzed at the MP2/6-31G*//HF/6-31G* level and solvation effects included by the SCRF model.[65] According to the calculations of Lim and Jorsense[65], this cycloaddition presents both of the tendencies; i.e. it is concerted in gas phase and apolar solvents, such as CCl_4 ($\varepsilon=2.23$), whereas it is two-step via zwitterion in polar solvents, such as acetonitrile ($\varepsilon=35.94$). Since this reaction changes its mechanism with the polarity of the solvent, the difference between the energy barriers in CCl_4 and acetonitrile gives an idea of how much solvation is required for changing the mechanism of a cycloaddition.

Results in Graph 2.3 also show the tendency in raising the energy of solvation with the increasing of the dielectric constant in those reactions termed as sensitive. Ketene dimerization results in gas and liquid phase were included in this graphics in order to qualitatively classify this cycloaddition. For doing this, the energy of solvation, taken as $E_a^G - E_a^S$ for the other cycloadditions, was modified for the corresponding calculation in toluene solvent. Due to there is only one reporting value for ketene dimerization in toluene, the value of energy of solvation was taken as the difference of the corresponding Gibbs energy barrier for the activated complex in gas and in toluene. The value for the Gibbs energy barrier in gas phase was assumed to be the energy of activation plus eight (8) kcal per mol, which is roughly the value for the entropic contribution of the transition states to the barrier in cycloadditions.[2, 33] According to the results on the energy of solvation and the classification of the cycloaddition mechanisms as insensitive and sensitive, the ketene dimerization reaction can be classified as a sensitive cycloaddition in the pass from gas to liquid phase. Results also suggest that the mechanism of the ketene dimerization is low dependent on the dielectric constant of the solvent due to the low increase in the assumed energy of solvation. These results agree with the results obtained in the previous section.
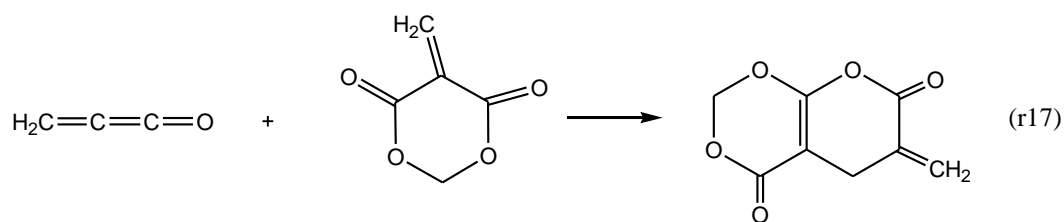
Analyzing the results obtained by the classification of the cycloadditions (Table 2.10 and Graph 2.3), it is found that the existing reports on the large acceleration achieved by [2+2] cycloadditions in going from gas to liquid phase concern a change in the mechanism from concerted to two-step one. According to this fact, ketene dimerization should be considered as a concerted one in gas phase and as a two-step reaction in liquid phase. However, it is worthwhile to mention that the large characteristic acceleration achieved by the ketene dimerization in going from gas to liquid phase, even in an apolar solvent as toluene, is anomalous among the studied [2+2] cycloadditions. Such acceleration is very rare and we could only find two cycloadditions with the same order of magnitude: the polar solvent accelerated cycloaddition between 1,1-dicyanoethylene with methyl vinyl ether[65] and the catalytically assisted [2+2] cycloadditions of ketene imine and formaldehyde[69].
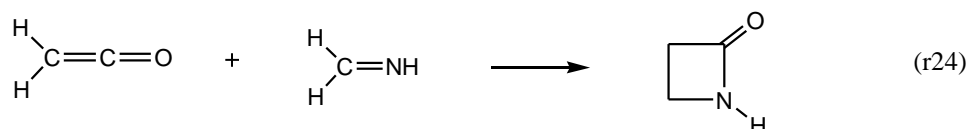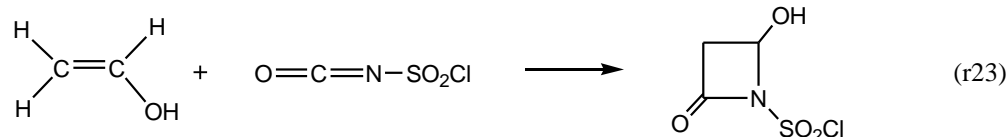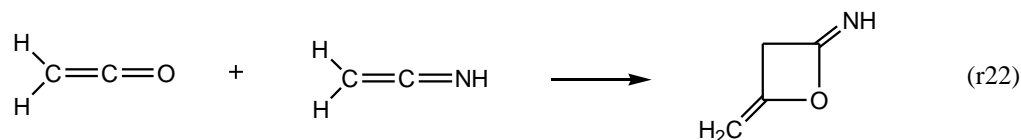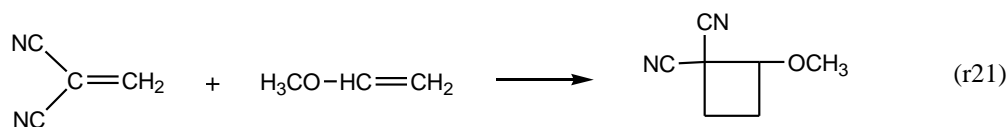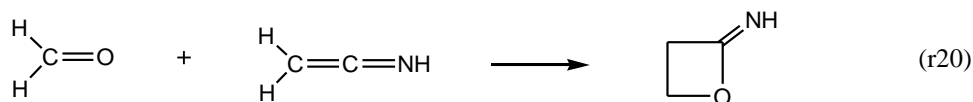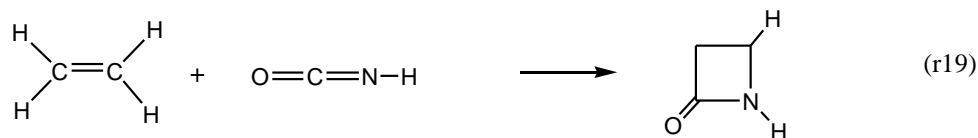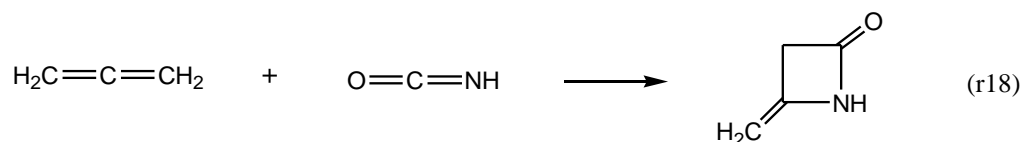
Table 2.10. Energy barriers for insensitive and sensitive [2+2] cycloadditions in the pass from gas to liquid phase[a].

Reaction	Ref.	E_a^G, kcal per mol	$E_a^{S,\,[b]}$, kcal per mol	$E_a^G - E_a^S$, kcal per mol	ε, solvent	Classification
r17[e]: Methyleneketene + 5-methylene-1,3-dioxan-4,6-dione B3LYP/6-31G*. SCRF	66	0.25	1.05	-0.80	9.08	Insensitive, Asynchronous
r18: $CH_2=C=CH_2$ + Isocyanic acid MP3/aug-cc-pVDZ. IEF-PCM	67	39.84	40.21 39.94	-0.37 -0.10	2.38 36.64	Insensitive, Asynchronous Pericyclic
r19: Ethylene + Isocyanatomethane MP2/6-31G*//HF/6-31G*. SCRF	68	42.20	46.60	-4.40	9.08	Insensitive, $[_\pi 2_s +_\pi 2_s +_\pi 2_s]$
r20: Ketene imine + Formaldehyde MP2/6-31G*//HF/6-31G*. SCRF	69	34.83	37.02	-2.25	9.08	Sensitive, asynchronous
r21: 1,1-dicyanoethylene + Methyl vinyl ether MP2/6-31G*//HF/6-31G*. SCRF	65	24.98	20.30 7.02	4.68 17.96	2.23 35.94	Insensitive in 2.23 Sensitive in 35.94, asynchronous
r22: Ketene + Vinylimine MP3/aug-cc-pVDZ. IEF-PCM	67	19.65	12.11 8.12	7.54 11.53	2.38 36.64	Sensitive, NP-pseudopericyclic
r23: Vinyl alcohol + Chlorosulfonyl isocyanate MP2/6-31G*//HF/6-31G*. SCRF	68	6.20	4.00	2.20	9.08	Sensitive, asynchronous
r24: Ketene + Imine MP4/cc-pVDZ//MP2/6-31G**. GCOSMO	12	37.79[c]	25.07[c]	12.72[c]	78.40	Sensitive, asynchronous
Ketene dimerization	19 32	31 40[d]	10 22.15[c]	21 17.85[c]	20.56 2.38	**?** asynchronous

[a] E_a^G stands for activation energy in the gas phase. E_a^G stands for activation energy in solvent with the corresponding ε value. [b] Values for sensitive reactions correspond to the greatest barrier in stepwise mechanisms. [c] These data correspond to the Gibbs energy barriers. It is assumed that $\Delta G_{\neq}^G - \Delta G_{\neq}^S$ is roughly equal to $E_a^G - E_a^S$. [d] Gibbs energy barrier for the reaction in gas phase is assumed to be $E_a^G + 8.0$ kcal per mol. [e] [4+2] cycloaddition.

$$H_2C=C=C=O \quad + \quad \text{[5-methylene-1,3-dioxan-4,6-dione]} \quad \longrightarrow \quad \text{[product]} \qquad (r17)$$

$$H_2C{=}C{=}CH_2 \quad + \quad O{=}C{=}NH \quad \longrightarrow \qquad \text{(r18)}$$

$$\text{H}_2\text{C}{=}\text{CH}_2 \quad + \quad O{=}C{=}N{-}H \quad \longrightarrow \qquad \text{(r19)}$$

$$\text{H}_2\text{C}{=}\text{O} \quad + \quad \text{H}_2\text{C}{=}C{=}NH \quad \longrightarrow \qquad \text{(r20)}$$

$$\substack{NC\\NC}\text{C}{=}CH_2 \quad + \quad H_3CO{-}HC{=}CH_2 \quad \longrightarrow \qquad \text{(r21)}$$

$$\text{H}_2\text{C}{=}C{=}O \quad + \quad \text{H}_2\text{C}{=}C{=}NH \quad \longrightarrow \qquad \text{(r22)}$$

$$\text{H}_2\text{C}{=}\text{CH}{-}OH \quad + \quad O{=}C{=}N{-}SO_2Cl \quad \longrightarrow \qquad \text{(r23)}$$

$$\text{H}_2\text{C}{=}C{=}O \quad + \quad \text{H}_2\text{C}{=}NH \quad \longrightarrow \qquad \text{(r24)}$$

Calculations on the former reaction, which corresponds to that taken as the limiting point between sensitive and insensitive cycloadditions, suggested that the zwitterionic character of the transition state entailed a two-step mechanism in polar solvents.[65] Solvations of the transitions states and the formed intermediate in acetonitrile ($\varepsilon{=}35.94$) achieved a lowering in the energy barrier of ca. 18 kcal per mol compare to gas phase. According to experimental values[19], this magnitude of the lowering in the energy barrier for the cycloaddition between 1,1-dicyanoethylene with methyl vinyl ether[65] in polar solvents is also achieved by the ketene dimerization but in apolar solvents instead (Table 2.10). For the catalytically assisted reaction of

ketene imine and formaldehyde[69], the calculated barrier of the reaction in dichloromethane (ε=9.08) is lowered from 37.02 kcal per mol (r20) to 13.81 kcal per mol by use of a Lewis acid[69] such as BH_3 (r25). This means that the use of BH_3 in dichloromethane lowers the energy barrier ca. 21 kcal per mol compare to gas phase[*]. This magnitude of the lowering in the energy barrier is also achieved by the ketene dimerization but in a more polar solvent, such as acetone (ε=20.56).[19] This coincidence in the values for the energy barrier suggest that ketene dimerization is accelerated by an unknown catalyst. However, a catalytic acceleration for the ketene dimerization should be discharged due to there is neither a Lewis-acid species nor a nucleophilic catalyst identified in the reaction system yet.[71]

According to the foregoing arguments, the anomalous values for the lowering in the energy barrier underwent by ketene dimerization in going from gas to liquid phase may be attributed to two principal explanations: firstly, to a special unexplored behavior of the ketene dimerization and secondly, to experimental errors due to the lacks of instrumental analysis by the year when the data were taken (i.e. 1934. See Ref. 19). Nonetheless the causes for these anomalous values, the ketene dimerization, as Lim and Jorgensen stated for [2+2] cycloadditions[65], emerge as an unusually challenging reaction for experimental and computational study.

Altogether, it is unclear whether ketene dimerization is able to be feasible due to only solvent effects because there are no reports about such a lowering in the energy barrier of no catalytic [2+2] cycloadditions. If solvent effects are responsible for the rate acceleration, the possibility of a change in mechanism from concerted to two-step via zwitterionic intermediate seams to be the most prominent for explaining the tendency of ketene dimerization in going from gas to liquid phase.

Summary and Conclusions

Experimental and theoretical facts allow ketene dimerization mechanism to be classified as either pericyclic or pseudopericyclic or two-step via a zwitterion. Differentiation among these possible mechanisms was done separately in gas and liquid phase. Both experimental and theoretical

---

[*] Another example for catalytic [2+2] ketene cycloadditions, yet without energy values for comparison, is the production of β-lactone type dimer[17,70] from the dimerization of high weight ketenes assisted by catalysts like $ZnCl_2$ and $Et_3NH^+Cl^-$ (*vide* chapter 1, section 1.5).

81

studies in gas phase suggested that ketene dimerization was concerted with an asynchronous transition state. According to an independent AIM study[8], this transition state has one disconnection point between the orbitals at the unformed C-O bond (Figure 2.5a) and therefore ketene dimerization should be classified as nonplanar pseudopericyclic reaction instead of pericyclic. Despite the geometrical parameters for the activated complex of diketene obtained in that study were found to be in good agreements with previous theoretical studies, the theoretical energy barrier for ketene dimerization in gas phase predicted in that study[8] appeared to be in disagreement with the experimental results obtained from the thermolysis of diketene[32]. This suggests that ketene dimerization still remains to be clarified in gas phase.
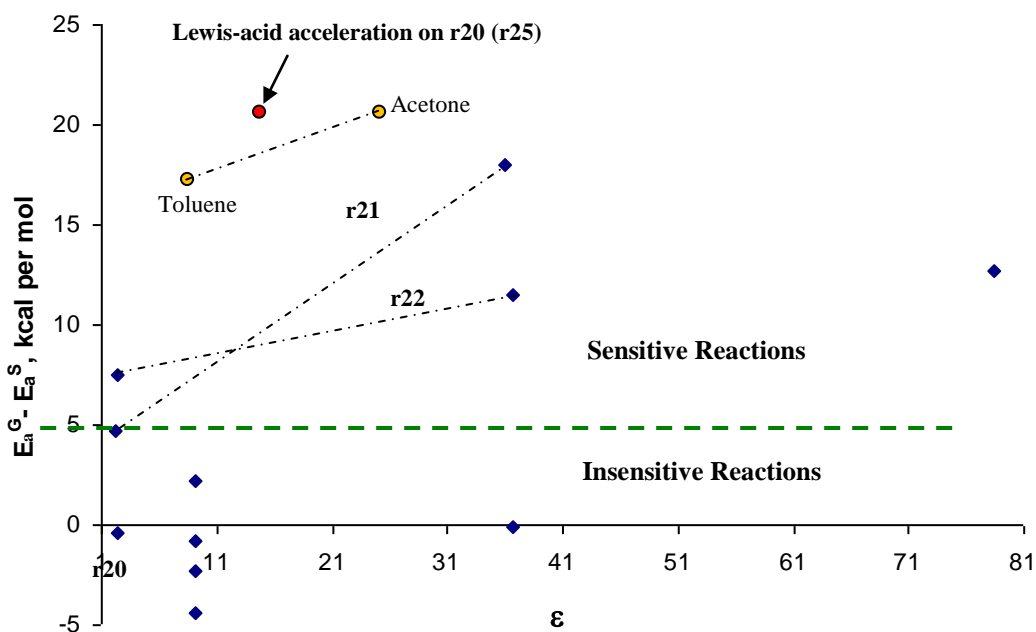
Graph 2.3. Energy of solvation achieved in different solvents for insensitive and sensitive [2+2] cycloadditions. Orange circles correspond to the values for ketene dimerization. Red circle corresponds to the r25 reaction.

(r25)
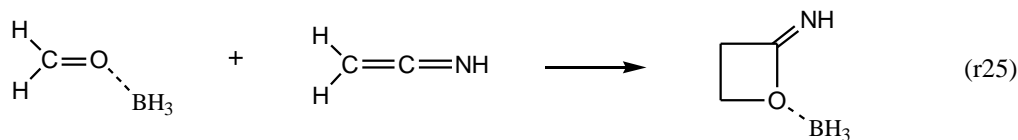
Empirical analysis of experimental data for ketene dimerization in liquid phase appeared to favor both stepwise and nonsychronous concerted mechanisms (presumably a pseudopericyclic mechanism) and the selection of either of both mechanisms cannot be done *a priori* due to the different topology of the potential energy surface, the medium value of the ratio of kinetic constants (Table 2.2) and, the not-high-enough correlation between the kinetic constant and the multiparameters for solvent scale. Qualitative interpretation of the Koppel and Palm correlation parameters suggested that one of the principal roles of the solvents in the ketene dimerization was as hydrogen-bond donators (i.e. Lewis acids). It also suggested that both nonspecific and specific solute/solvent interactions collaborated for the process of solvation of the ketene dimerization reaction. Development of charge along of reaction coordinate was a distinctive characteristic of the ketene dimerization in liquid phase.

Qualitative comparison between ketene dimerization in gas and ketene dimerization liquid phase showed an anomalous tendency of this reaction. A great energy of solvation was achieved by the ketene dimerization in a wide range of solvent polarity. The reduction in the energy barrier achieved in liquid phase compared to gas phase made the ketene dimerization feasible in solution, even in low polar solvents as toluene. The magnitude in the energy barrier reduction presumably due to solvation was comparable to that achieved by the catalytically assisted reaction of ketene imine and formaldehyde in dichloromethane[69]. According to the classification of the reaction, ketene dimerization should be considered as a sensible [2+2] cycloaddition and therefore its mechanism may change from concerted in gas phase to two-step via zwitterion in liquid phase.

Altogether, we can conclude that the tendency of ketene dimerization is clearer in gas phase than in liquid phase. Several aspects of the reaction in both phases appear anomalous and so challenging, although. Quantitative agreement for the energy barrier between experimental and theoretical calculations in gas phase seems not to be achieved yet. Also, it is undecided whether or not the solvent effects are able to further stabilize the activated complex in order to generate a zwitterion and if solvent effects are entirely responsible for the great acceleration achieved by the ketene dimerization in going from gas to liquid phase.

References

(1) Smith, M. B. and March, J. "*March's Advanced Organic Chemistry. Reactions, Mechanisms, and Structures*". Wiley-interscience. John Wiley & Sons, Inc. Sixth Edition. USA. 2007.

(2) Lowry, T. H. and Richardson, K. S. "*Mechanism and Theory in Organic Chemistry*". Harper & Row, Publishers, New York, third edition, 1987.

(3) Woodward, R. B. and Hoffmann, R. "The Conservation of Orbital Symmetry", *Ang. Chem. Int. Ed. Eng.*, 1969, 8, 781.

(4) Rauk, A. "*Orbital Interaction Theory of Organic Chemistry*". Wiley Interscience. Second edition, USA, 2001.

(5) Levine, I. N. "*Química Cuántica*". Prentice Hall. Traducción de la quinta edición en inglés. España 2001.

(6) Seidl, E. T. and Schaefer, H. F. III. *J. Am. Chem. Soc*. 1991, 113, 5195.

(7) Salzner, U. and Bachrach, M. S. *J. Am. Chem. Soc*. 1994, 116, 6850.

(8) Rode, J. R. and Dobrowolski, J. Cz. *J. Phys. Chem. A* 2006, 110, 207.

(9) Zimmerman, H. E. "*Pericyclic Reactions*". Marchand, A. P., Lehr, R. E., Eds.; Academic Press; Vol. I, New York, 1977.

(10) (a) Epiotis, N. D. and Shaik, S. *J. Am. Chem. Soc*. 1978, 100, 9. (b) Reinhoudt, D. N.; Geevers, J.; Trompenaars, W. P. "Solvent Effects in Thermal [2+2] Cycloaddition Reactions. Intramolecular Capture of 1,4-Dipolar Intermediates vs. [2+2] Cycloaddition in Reactions of 3-(1-Pyrrolidiny)thiophenes with Electron-Deficient Acetylenes". *J. Org. Chem*. 1981, 46, 424-434.

(11) Huisgen, R. *Acc. Chem. Res*. 1977, 10, 117-124.

(12) Truong, T. N. "Solvent Effects on Structure and Reaction Mechanism: A Theoretical Study of [2 + 2] Polar Cycloaddition between Ketene and Imine". *J. Phys. Chem. B* 1998, 102, 7877-7881.

(13) Huisgen, R. "Cycloaddition Mechanism and the Solvent Dependence of Rate". *Pure Appl. Chem.* 1980, 52, 2283.

(14) Gilchrist, T. L.; Storr, R. C. "*Organic Reactions and Orbital Symmetry*", 2nd ed.; Cambridge University Press: New York, 1979.

(15) Reichardt, Christian. "*Solvents and Solvent Effects in Organic Chemistry*". Wiley-VCH. Third edition, Germany 2003.

(16) Pross, A. "*Theoretical and Physical Principles of Organic Reactivity*". John Wiley & Sons, USA, 1995.

(17) Tidwell, T. T. "*Ketenes*". Wiley-Interscience; 2nd edition, 2006.

(18) Moore, H. W. and Wilbur, D. S. "Cyanoketenes. Mechanism of tert-butylcyanoketena cycloaddition to methyl- and dimethylketene". *J. Am. Chem. Soc.*, 100, 6523, 1978.

(19) Rice, F.O. and Greenberg, J. *J. Am. Chem. Soc.* 1934, 56, 2132.

(20) Cabaleiro-Lago, E. M.; Rodríguez-Otero, J.; González-López, I.; Peña-Gallego, A.; Hermida-Ramón, J. M. "A DFT Study of the Pericyclic/Pseudopericyclic Character of Cycloaddition Reactions of Ethylene and Formaldehyde to Buta-1,3-dien-1-one and Derivatives". *J. Phys. Chem. A* 2005, 109, 5636-5644

(21) (a) Ross, J. A.; Seiders, R. P.; Lemal, D. M. "An Extraordinary Facile Sufoxide Automerization". *J. Am. Cem. Soc.,* 1976, 98, 4325 – 4327. (b) Chamorro, E.; Notario, R.; Santos, J. C.; Pérez, P. "A Theoretical Scales for Pericyclic and Pseudopericyclic Reactions". *Chem. Phys. Letters* 2007, 443, 136-140.

(22) Birney, D. M.; Ham, S.; Unruh, G. R. "Pericyclic and Pseudopericyclic Thermal Cheletropic Decarbonylations: When Can a Pericyclic Reaction Have a Planar, Pseudopericyclic Transition State?". *J. Am. Chem. Soc.* 1997, 119, 4509-4517.

(23) de Lera, A. R.; Alvarez, R.; Lecea, B.; Torrado, A.; Cossío, F. P. "On the Aromatic Character of Electrocyclic and Pseudopericyclic Reactions: Thermal Cyclization of (2Z)-Hexa-2,4-5-trienals and Their Schiff Bases". *Angew. Chem. Int. Ed.* 2001, 40, 557-561.

(24) Herges, R.; Jiao, H.; Schleyer, P. v. R. *Angew. Chem., Int. Ed. Engl.* 1994, 33, 1376.

(25) (a) Birney, D. M. *J. Org. Chem.* 1996, 61, 243. (b) Birney, D. M.; Ham, S.; Unruh, G. *J. Am. Chem. Soc.* 1997,119, 4509. (c) Birney, D. M.; Xu, X.; Ham, S.; Huang, X. *J. Org. Chem.* 1997, 62, 7114. (d) Birney, D. M.; Xu, X.; Ham, S. *Angew. Chem., Int. Ed. Engl.* 1999, 38, 189. (e) Birney, D. M. *J. Am. Chem. Soc.* 2000, 122, 10917. (f) Shumway, W. W.; Dalley, N. K.; Birney, D. M. *J. Org. Chem.* 2001, 66, 5832. (g) Zhou, C.; Birney, D. M. *J. Am. Chem. Soc.* 2002, 124, 5231.

(26) (a) Luo, L.; Bartberger, M. D.; Dolbier, W. R., Jr. *J. Am. Chem. Soc.* 1997, 119, 12366. (b) Liu, R. C. Y.; Lusztyk, J.; McAllister, M. A.; Tidwell, T. T.; Wagner, B. D. *J. Am. Chem.*

Soc. 1998, 120, 6247. (c) Fabian, W. M. F.; Bakulev, V. A.; Kappe, C. O. *J. Org. Chem.* 1998, 63, 5801. (d) Fabian, W. M. F.; Bakulev, V. A.; Kappe, C. O. *J. Org. Chem.* 2000, 65, 47.

(27) Birney, D. M.; Xu, X.; Ham, S. "[1,3], [3,3], and [3,5] Sigmatropic Rearrangements of Esters Are Pseudopericyclic". *Angew. Chem. Int. Ed. Engl.* 1999, 38, 189 – 193.

(28) Schleyer, P. v. R.; Maerker, C.; Dransfeld, A.; Jiao, H.; Hommes, N. J. R. v. E. *J. Am. Chem. Soc.* 1996, 118, 6317.

(29) (a) Chamorro, E. "The nature of bonding in pericyclic and pseudopericyclic transition states: Thermal chelotropic decarbonylations". *J. Chem. Phys.* 2003,118, 8687-8698.

(30) (b) Silva López, C.; Nieto Faza, O.; Cossio, F. P. York, D. M.; de Lera, A. R. "Ellipticity: A convenient Tool To Cheracterize Electrocyclic Reactions". *Chem. Eur. J.* 2005, 11, 1734-1738.

(31) Kelly, E.; Seth, M.; Ziegler, T. "Calculation of Free Energy Profiles for Elementary Bimolecular Reactions by ab Initio Molecular Dynamics: Sampling Methods and Thermostat Considerations". *J. Phys. Chem. A* 2004, 108, 2167-2180.

(32) Chickos, J. S.; Sherwood, D. E. Jr.; and Jug, K. *J. Org. Chem.* 1978, 43, 1146-1150.

(33) Cramer, C. J. C. J. *"Essentials of Computational Chemistry. Theories and Models"*. John Wiley & Sons, LTD. Second edition. 2002.

(34) Gompper, R. "Cycloadditions with Polar Intermediates". *Angew. Chem., Int. Ed. Engl.* 1969, 8, 312-327.

(35) (a) Wagner, H. U. and Gompper, R. *Tetrahedron Lett.* 1970, 2819-2822. (b) Yamabe, S.; Minato, T.; Osamura, Y. *J. Chem. Soc., chem. Commun.* 1993, 450.

(36) Huisgen, R. "Tetracyanoethylene and Enol Ethers. A Model for 2 + 2 Cycloadditions via Zwitterionic Intermediates". *Acc. Chem. Res.* 1977, 10, 117-124.

(37) Williams, J. K.; Wiley, D. W.; McKusick, B. C. "Cyanocarbon Chemistry. XIX. Tetracyanocyclobutanes from Tetracyanoethylene and Electron-rich Alkenes" *J. Amer. Chem. Soc.* 1962, 84, 2210-2215.

(38) (a) K. Clauß, *Liebigs Ann. Chem.* 1969, 722, 110. (b) Bestian, H. *Pure Appl. Chem.* 1971, 27, 611.

(39) (a) Proskow, S.; Simmons, H. E.; Cairns, T. L. "Stereochemistry of the Cycloaddition Reaction of 1,2-Bis(trifluoromethyl)-1,2-dicyanoethylene and Electron-Rich Alkenes". *J.*

Am. Chem. Soc. 1966; 88; 5254-5266. (b) Rasmussen, J. K. and Hassner, A. "Recent Developments in the Synthetic Use of Chlorosulfonyl Isocyanates", *Chem. Rev.* 1976, 76, 389.

(40) Huisgen, R. and Plumet, J. *Tetrahedron Lett.,* 1978, 3975.

(41) Rideout, D. C. and Breslow, R. "Hydrophobic Acceleration of Diels-Alder Reactions". *J. Am. Chem. Soc.* 1980, 102, 7816-7817.

(42) Huisgen, R.; Feiler, L. A.; Otto, P. *Tetrahedron Letters* 1968, 4485.

(43) Huisgen, R. and Otto, P. *J. Am. Chem. Soc.* 90, 5342 (1968).

(44) Kiefer, E. and Okamura, M. Y. "Evidence for a concerted mechanism for allene cycloaddition", *J. Amer. Chem. Soc.* 1968, 90, 4187-4189.

(45) Baldwin, J. E. and Kapecki, J. A. *J. Am. Chem. Soc.* 92, 4868 (1970).

(46) Reichard, C. "Solvatochromic Dyes as Solvent Polarity Indicators". *Chem. Rev*. 1594, 94, 2319-2358.

(47) Glesston, S.; Laidler, K.; Eyring, H. *"The Theory of Rate Processes"*. McGraw-Hill Book Comp. N. Y. 1941.

(48) Müller, P. "Glossary of Terms Used in Physical Organic Chemistry - IUPAC Recommendations 1994". *Pure Appl. Chem.* 1994, 66, 1077-1184.

(49) Sheppard, S. E. *Rev. Mod. Phys.* 1942, 14, 303-340.

(50) Hantzsch, A. *Ber. Dtsch. Chem. Ges.* 1922, 55, 953-979.

(51) (a) Kosower, E. M. *J. Am. Chem. Soc.* 1958, 80, 3253-3260; 3261-3267; 3267-3270. (b) Kosower, E. M.; Skorcz, J. A.; Schwarz, W. M.; Patton, J. W. *J. Am. Chem. Soc.* 1960, 82, 2188-2191. (c) Kosower, E. M. "*An Introduction to Physical Organic Chemistry*"; Wiley: New York, 1968.

(52) Dimroth, K.; Reichardt, C.; Siepmann, T.; Bohlmann, F. *Liebigs Ann. Chem.* 1963, 661, 1-37.

(53) (a) Paley, M. S.; McGill, R. A.; Howard, S. C.; Wallace, S. E.; Harris, J. M. *Macromolecules* 1990, 23, 4557-4564. (b) Spange, S.; Keutel, D.; Simon, F. *J. Chem. Phys.* 1992, 89, 1615-1622.

(54) (a) Carr, P. W. *Microchem. J.* 1993, 48, 4-28. (b) Johnson, B. P.; Gabrielsen, B.; Matulenko, M.; Dorsey, J. G.; Reichardt, C. *Anal. Lett.* 1986, 19, 939-962. (c) Abbott, T. P.; Kleiman, R. *J. Chromatogr.* 1991, 538, 109-118.

(55) Amis, E. S. and Hinton, J. F. "*Solvent Effects on Chemical Phenomena*". Academic Press, New York, 1973.

(56) (a) Kamlet, J. M.; Abboud, J.-L. M.; Abraham, H. M.; Taft, R. W. "Linear Solvation Energy Relationships. 23. A Comprehensive Collection of the Solvatochromic Parameters, π*, α, and β, and some Methods for Simplifying the Generalized Solvatochromic Equation". *J. Org. Chem.* 1983, 48, 2877. (b) Kamlet, J. M.; Doherty, R. M.; Abboud, J.-L. M.; Abraham, H. M.; Taft, R. W. *CHEMTECH* 1986, 566. (c) Kamlet, J. M.; Taft, R. W. *Acta Chem. Scand.*, B 1985, 39, 611.

(57) R. N. Lacey in "*The Chemistry of Alkenes*", S. Patai, Ed., Interscience, New York, N.Y., 1964. pp 1182-97.

(58) Huisgen, R. and Otto, P. *J. Am. Chem. Soc.*, 1968, 90, 5342.

(59) Katritzky, A. R.; Tamm, T.; Wang, Y.; Karelson, M. "A Unified Treatment of Solvent Properties". *J. Chem. Inf. Comput. Sci.* 1999, 39, 692-698.

(60) Arcoria, A.; Librando, V.; Maccarone, E.; Musumarra, G.; Tomaselli, A. G. "Studies of Solvent Effects by the Approach of Multiparameter Empirical Correlations". *Tetrahedron*, 1977, 33, 105-111.

(61) Sustmann, R.; Ansmann, A.; Vahrenholt, F.; "Analysis of ketene cycloadditions by self-consistent perturbation theory". *J. Am. Chem. Soc.*, 94, 8099, 1972.

(62) Wells, P. R. *"Linear Free Energy Relationship"*. Academic Press inc. Ltd. London, 1968.

(63) Chandrasekhar, J. and Jorgensen, W. L. *J. Am. Chem. Soc.* 1985, 107, 2974.

(64) Bernardi, F.; Bottoni, A.; Olivucci, M.; Robb, M. A.; Schlegel, H. B.; Tonachini, G. "Do Supra-Antara Paths Really Exist for 2 + 2 Cycloaddition Reactions? Analytical Computation of the MC-SCF Hessians for Transition States of C2H4 with C2H4, Singlet 02, and Ketene". *J. Am. Chem. Soc.* 1988, 110, 5993-5995.

(65) Lim, D; Jorgensen, W. L. *J. Phys. Chem.* 1996, 100, 17490-17500.

(66) Sheng, Y-H.; Fang, D-C.; Wu, Y-D.; Fu, X-Y; Jiang, Y. *THEOCHEM*, 1999, 488, 187-194.

(67) Rode, J. E. and Dobrowolski, J. Cz. "An ab initio Study on the Allene-Isocyanic Acid and Ketene-Vinylimine [2+2] Cycloaddition Reaction Paths". *J. Phys. Chem. A* 2006, 110, 3723-3737.

(68) Cossío, F. P.; Roa, G.; Lecea, B.; Ugalde, J. M. "Substituent and Solvent Effects in the [2+2] Cycloaddition Reaction between Olefins and Isocyanates". *J. Am. Chem. Soc.* 1995, 117, 12306-12313.

(69) Fang, D-C and Fu, X-Y. "Ab initio studies on the mechanism of the cycloaddition reactions between ketene imine and formaldehyde – catalytic and solvent effects". *Chem. Phys. Lett.* 1996, 259, 265 – 270.

(70) Farnum, D. G. Johnson, J. R.; Hess, R. E.; Marshall, T. B.; Webster, B. "Aldoketene dimers and trimers from acid chlorides. A synthesis of substituted 3-Hydroxycyclobutenones". *J. Am. Chem. Soc.* 87, 5191, 1965.

(71) Martínez, R. "Catalytic synthesis of ketenes on silica monoliths at short contact times". Ph. D. Thesis, Department of Chemical Engineering, University of Delaware, 2001.

Chapter 3

Molecular Modeling: A New Tool in the Analysis of Chemical Engineering Phenomena

We called molecular modeling to the application of suitable laws in the analysis of phenomena at the scales less than those at macroscopic level. Such scales can be classified according to their size-time magnitudes as nanoscale, atomistic scale and mesoscale. From an ambitious view, such different scales and the macroscale can link and integrate in order to improve predictions of complex phenomena. Lots of chemical engineering phenomena are so complex due to the interrelation among different scales of size and time. Molecular modeling rises as an alternative for an outstanding mathematical and conceptual representation of such complex phenomena. This adequate representation of complex phenomena might help us to understand, to optimize and to design chemical and petrochemical processes from a low scale point of view. Herein we present a brief introduction of the molecular methods. Opportunities for applying the different scales of modeling to the analysis of complex phenomena are commented and analyzed. The fundamental mathematical machinery of the molecular modeling methods is presented in order to motivate the study of this new engineering tool.

3.1 Introduction

It is a great challenge to model real world because of its complexity. Phenomena at different scales of size and time are often involved within systems meanwhile these are treated and processed in chemical and petrochemical plants. These size and time scales concern different approaches for the movement and interaction of bodies and therefore, different mathematical structures must be coupled in a global describing algorithm. The complicated model that might appear has to be resolved by using computers. In this way, advances in computer science make possible the understanding and solution of different models related to the interaction within the systems.

90

According to described above, different body interactions encountered throughout the different scales of time and size must be heeded for understanding and developing systematic procedures for the design and optimal operation of chemical plants. Conventionally, process engineering ranges its tools in the macro-scale. However, necessities such as new characteristics of the products and new environmental restrictions have motivated chemical engineers to think in the body interactions at low scales. With the use of the different scales of the body interactions, molecular-based models can appear into the equations for describing a process. These molecular-based models can incorporate multilevel information from quantum chemical calculations to macroscale balances into a mathematical representation of a process. The molecular-based models can also serve as a common fundamental link for both process and chemistry research and development[1]. The study of the interaction between the different scales and the inclusion of molecular-based models can provide companies with new "tools" to design and operate chemical processes effectively in such a way they can be outstanding in today's competitive commerce. Grossman and Westerberg[2] have identified the study of the different scales and the inclusion of molecular-based models squared in the area of Process Systems Engineering (PSE). PSE assists industry to meet its needs by tying science to engineering in a multi-scale integration that improves decision-making processes for the creation and operation of the chemical supply chain.

Chemical and process engineering are entering a new era, characterized by unprecedented control over chemical reactions, as well as product molecular architecture, conformations and morphology[1]. They are entering a "molecular" era in which low scale manufacturing and complex miniature processes are beginning to be designed and commercialized for a number of applications. Experiments and processes are being interpreted and predicted through a multi-scale coupling represented in molecular-based models (e.g. see Ref. 3). The purpose of this chapter is to present some applicative examples of molecular modeling in engineering phenomenon analysis as well as to provide engineers with key concepts about the different scales of modeling for welcoming the new entering "molecular" era.

3.2 Analysis of Engineering Phenomena

Conceptual representation of a real process (e.g., chemical process) cannot completely encompass all the details of the process in spite of modern computational techniques and

methods of mathematical analysis. As an alternative to the global representation, the conceptual model of the process can be broken down into distinguishable subsystems which, when assembled into a whole, can simulate the process. Using this splitting of the process, we attempt to obtain a reasonable faithful representation of each subsystem or scales based on fairly simple, well-known principles. These subsystems are classified according to different body interactions which depend on scales of time and size. Such classification originates nanoscale, atomistic scale, mesoscale and macroscale.

Scale that covers ranges of time less than nanoseconds and ranges of sizes less than 10 nm[4,5] is called nanoscale and it is utilized for predicting molecular properties (e.g. polarizability, hydrogen bond, dipole moment and electrostatic potential) for which electronic distribution definitely plays the major role. As electronic structure is the main concern, quantum mechanical theory rules the behavior within this subsystem or scale. Atomistic subsystem is enclosed in scales of size and time greater than those in the nanoscale (i.e., $1nm - 0.1\mu m$ and $1ps - 1ns$). Central issue in this scale corresponds to evaluate interactions among large number of atoms and molecules and how such interactions influence the macroscopic properties of the subsystem. This scale uses empirical or quantum-mechanical derived force fields, together with statistical mechanics to determine thermodynamics and transport properties of the subsystem. Therefore, the explicit influence of the electronic structure of atoms and molecules is lost in atomistic simulations. In the next scale, namely mesoscale or mesoscopic scale, the atomistic details are lost to generate groups of atoms or molecules ("blobs of matter") which are treated as individual entities interacting through effective potentials[5]. This scale covers range of size between $0.1\mu m$ and $100\mu m$ and range of time between 1ns to 1s approximately. Simulation of phenomena encountered in systems constituted for several homogeneous matters, such as that encountered in polymer blends, are the main concern in this scale.

Both the atomistic scale and the mesoscale consider classical mechanics for modeling interactions between atoms ("blobs of atoms" for mesoscale case) and can simulate their movements in two different approaches, stochastic and deterministic. The molecular simulation that is done in a stochastic manner receives the name of Monte Carlo simulation and it is based on a probabilistic approach for the relative position of the atoms in the subsystem. On the other

hand, molecular simulation that describes the movement of atoms in a deterministic fashion is called molecular dynamics and it is based on Newton's laws of motion for predicting the future position of atoms. Methods and theories involved in the three first scales of modeling (i.e., nanoscale, atomistic scale and mesoescale) are grouped in the so-called molecular modeling theories.

Macroscale is the following level in the time-size scale. This scale treats matter as continuous and the properties of the system as field quantities and therefore can efficiently handle phenomena at sizes greater than those treated in the preceding scales. As a consequence, electronic details and atomistic details as well as "blob" details are not explicitly included into the calculations. Phenomenological laws and balance equations represented in both algebraic and differential equations rule the macroscale.
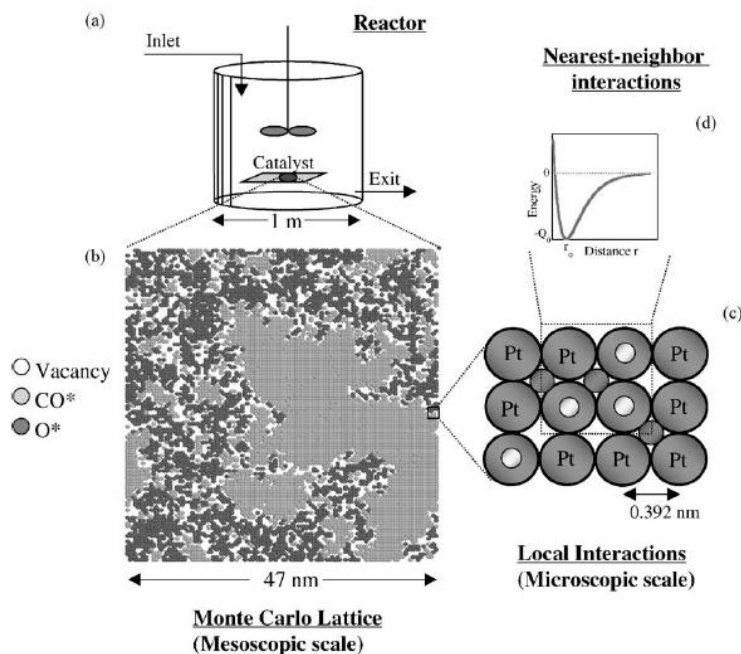
Figure 3.1. Size scales involved in the oxidation of CO on a platinum(1 0 0) surface embedded in a CSTR at atmospheric pressure (a); snapshot form a MC simulation, illustrating the distribution of adsorbates (b); schematic of atomic species (O^*) adsorbed on hollow sites and the molecular species (CO^*) adsorbed on-top sites (c); schematic of interactions in the BOC framework which are described using a Morse potential (d) (Ref. 6).
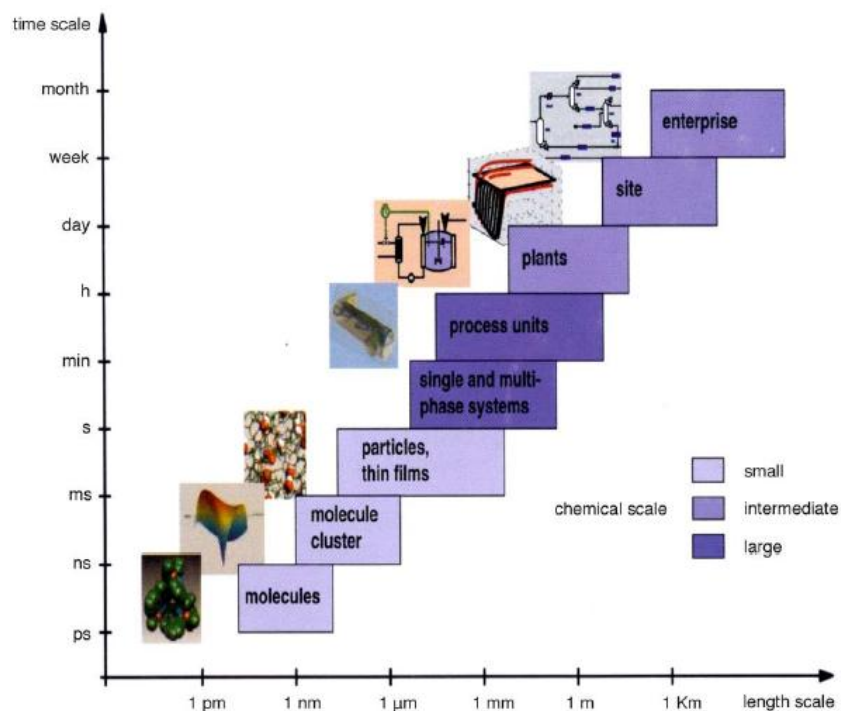
Figure 3.2. Chemical supply chain (Ref. 2).

Influence of the different scales in a real process can be studied in a hierarchy that starts at the nanoworld, follows at the atomistic scales, pass through mesoscale and directly impact on the macroscale (*vide infra* in Figure 3.1, in which scale influence is seen from macroscopic level to nanoscopic scale, and in Figure 3.2 which presents the scale influence in the chemical supply chain). Accordingly, if we consider the chemical supply chain (Figure 3.2), the feasibility of the process and the desired properties of final products, after this supply chain, are greatly determined at low scales of time and size. Role of macroscale can be squared in to control product quality and planning and scheduling of the production. As we can see, the successful of a supply chain is defined in a great part at the primary levels of the body interactions.

The mathematical modeling used by chemical engineers for the analysis of phenomena encompassed in the chemical processes has been hitherto based on the macroscopic principia. Thus, the so-called MESH equations (Mass balance, equilibrium equations, mole fraction summation and enthalpy balance) and the momentum balance equation are widely applied in

describing the operational regions into which equipments might operate[7]. The process of optimization of operational conditions in behalf of profitability can be guided using the MESH equations as restrictions. These laws and equations have been quite useful for the work of chemical engineers. The great disadvantage of the continuum macroscopic "tools" is the fact that they are, in their majority, explicitly independent on atomic structure relationship and they may be unable to predict the physical-chemical consequences of new conditions, new compounds or new reactions in the systems thereof (*vide supra*). This disadvantage would further complicate if some experimental-depended equations will be used to predict in regions of extrapolation.

For a deep (real) control and simulation of the chemical supply chain, chemical engineering community must widely apply the benefits in considering nanoscale, atomistic scale and mesoscale and therefore, to include molecular modeling as an important "tool" for the development and maintaining of the chemical supply chain. There are some areas for which the molecular modeling is visualized to be a common and strong "tool" for process engineering:

- *Design*: there is an emphasis on reducing the development time and cost by omitting some phases of the activity that have traditionally been considered vital in the conceptual design of chemical processes (e.g., omitting the pilot plant[8]). Molecular modeling can contribute to improve procedures for process development by probing the feasibility of some steps in the design. One of the key initial steps at each level in the design procedure is to decide quickly what's feasible and what's not. Molecular modeling has an important role to play in support the different design activities by providing estimates of critical pieces of data that are missing in the early stages of process development, and new models that are uniquely suited to providing information that classical models have failed to provide.

- *Planning and operation:* Molecular modeling can help in the conception of manipulating chemical plants. Globally, a chemical plant must close mass and heat balance in order to model production. At this level, economical and environmental restrictions must be achieved in order to make chemical plants economically feasible. Decisions taken at planning-based level serve as targets for the process engineers to operate their plants.

Different operational conditions must be considered and evaluated for achieving the target goals. However, as molecules are the common foundation for feedstock composition, different interactions inside streams may be presented as operational conditions are tested. As a result of these interactions, molecules may behave in a completely different way and the process can generate streams with different properties than the target properties thereof. According to this feature, the hierarchy of decisions would have to be altered to consider the different possibilities of body interactions at the different scales of time and size into the planning model by using molecular-based models.

- *Simulation*: Process that lead to microstructured products may include reaction and/or separation steps and besides, structure-forming steps (e.g., producing crystals). The shape of a crystal produced by a process often has a major impact on product quality as well as processability. Estimating the shape of crystal during the discovery and conceptual design phases of product and process development is of major value in many cases. Models that predict crystal morphology and shape have as a main drawback the inability to account for effects of solvent, impurities and other process conditions. On the other hand, models based on kinetic theory generate results that are in good agreement with experiment, but these models recognize the significance of interfacial phenomena in crystal shape modeling. Molecular modeling may conduce to the estimation of interfacial free energy prediction in order to improve the predictions of kinetic theory based models[8].

Another example in which molecular modeling may help is the attainable region which is defined as a domain in the concentration space that can be achieved by using any system of steady-flow chemical reactors[9]. For isothermal consecutive reactions A→B→C, the attainable region depends on the value of the rate constants k_1 and k_2 respectively. According to the values of these constants it may be impossible to get high selectivities at conversions above $25 - 30\%$ in any kind of reactor configuration. This implies that the process is doomed to operate at low conversions and high recycle flow rates. To estimate the attainable region and the selectivity we need an estimate of the relative rates, i.e. k_1/k_2. The molecular modeling can estimate the relative rates of the reaction whether in

gas or liquid phase with a good accuracy (*vide* relative rates prediction in ketene dimerization in Ref. 10).

- *Control*: In systems such as nanobiological devices, micromachines, nanoelectronic devices, and protein microarrays and chips, the control of events at nanoscale and atomistic scale is the major importance for desired final properties and product quality[11,12]. Simplified models or trial-and-error experimentation are used to design many of these devices. A multiscale model in which details from nanoscale to atomistic scale can be utilized to design and control these sorts of processes. Recently, Braatz and coworkers[12] illustrated how to use molecular modeling methods in order for achieving control in these processes.

- *Estimation of properties*: When one or more of the chemicals in a process are dangerous or extremely expensive then physical properties are difficult to measure and are usually missing. Molecular modeling provides a means of estimating missing properties including phase equilibrium properties. Moreover, molecular modeling can help to complement and resolve experimental measurements and discrepancies with respect to right molecular and bulk properties (see Refs. 4, 13, 14).

- *Experiment design:* Molecular modeling can be useful in early steps of experiment design. Results from molecular modeling can help to put limits and shorten intervals of the independent variables by obtaining unfeasible regions in which experiments may fail. Molecular modeling also may help to interpret laboratory results in order to guide additional clarifying experiments.

- *Researching*: New developments in different areas such as materials[4], catalysis[15], polymers[16], corrosion[17], electronics[11] and drug design[18] can be guided by molecular modeling "tools". Developments in these areas can be firstly tested by using computational experimentation to obtain probes of feasibleness. These probes can justify lab experimentation in order to synthesize the new compound with the corresponding modifications.

Chemical engineering community has already started to use frequently the "tools" of the molecular modeling to investigate in some of these areas. There is no doubt that molecular modeling is playing an increasingly important role in future chemical and process engineering research and practice[19]. Efforts of the community have been concentrated by the AICHE organization in a series of international conferences called Foundations of Molecular Modeling and Simulation (FOMMS) in which applications and contributions are collected to motivate the industrial application of the molecular modeling.

3.3 Molecular Modeling Methods

Molecular Modeling[*] can be defined as the development and application of physical and chemical theories in the description of a phenomenon whose model, exclusively solved by computer, predicts the behavior of the phenomenon from a molecular point of view. This definition involves two principal issues in molecular modeling, the theories and the computer calculations. Development of these issues improves the quality of the predictions of the phenomenon. New theories like e.g. Density Functional Theory or the *ab initio* molecular dynamics have been applied successfully with large contribution to the progress in this area. However, it was not possible without the developments of computational techniques which have revolutionized molecular modeling to the extent that most calculations could not be performed without the use of a computer[20].

Molecular modeling relies on different approximations, both analytical and numerical, for the theories about the body interactions. All of the phenomena appeared in the microworld can be described using quantum mechanics only. However, actual computational resources would make the program code and the solution of the model an impossible goal. Fortunately, some phenomena do not need calculation of electronic distribution (and properties derived) especially those phenomena accounted at atomistic and mesoscopic scales. Many successful chemical

---

[*] Molecular modeling includes investigations on the branches of theoretical chemistry and computational chemistry. Former branch considers application of quantum mechanics to develop theories and rules about atoms and molecules, whereas the latter encompasses not only quantum mechanics but also molecular mechanics and computer-based methods for predicting the behavior of the system.

models exist that do not necessarily have obvious connections with quantum mechanics. Typically, these models were developed based on intuitive concepts, i.e. their forms were determined inductively[21]. One of these models is classical models which fall under the heading of molecular mechanics. Molecular mechanics can computationally power the modeling at atomistic and mesocopic scales allowing calculation of body interactions in a simple way. Simulations of the movement in these scales may be modeled in stochastic (Monte Carlo methods) and deterministic (dynamic simulation) manner and so originating the so-called molecular simulation methods.

3.3.1 Quantum Mechanical Description of Molecular Systems.

Quantum mechanics explicitly represents the electrons in a calculation, and so it is possible to derive properties that depend upon the electronic distribution and in particular to investigate chemical reactions in which bonds are broken and formed. Postulates and theorems of quantum mechanics assert that microscopic systems are described by wave functions that completely characterize all of the physical properties of the system. In particular, there are quantum mechanical operators corresponding to each physical observable that, when applied to the wave function, allow us to predict the probability of finding the system to exhibit a particular value or range of values for that observable[21].

The typical form of the Hamiltonian operator (without considering amongst others the presence of an external electric or magnetic fields, the spin-orbit coupling in heavy elements and, the relativistic effects) takes into account five contributions to the total energy of a molecular system: the kinetic energy of the α nuclei and i electrons, the attraction of the electrons to the nuclei with atomic number Z, and the internuclear and interelectronic repulsions[22] (1),

$$\hat{H} = -\frac{\hbar^2}{2} \sum_{\alpha} \frac{\nabla_{\alpha}^2}{m_{\alpha}} - \frac{\hbar^2}{2m_e} \sum_{i} \nabla_i^2 - \sum_{\alpha} \sum_{i} \frac{Z_{\alpha} e'^2}{r_{i\alpha}} + \sum_{\alpha} \sum_{\beta > \alpha} \frac{Z_{\alpha} Z_{\beta} e'^2}{r_{\alpha\beta}} + \sum_{i} \sum_{j > i} \frac{e'^2}{r_{ij}} \qquad (1)$$

Then, the Schrödinger equation can be written in an operator manner according to

$$\hat{H} \, \Psi_n\left(\vec{r}\right) = E_n \Psi_n\left(\vec{r}\right) \qquad (2)$$

The term Ψ is the wavefunction that depends on spatial coordinates $\vec{r}$ and on the n state of the system. E_n corresponds to the energy of the system in the n state. Exact solution of the Schrödinger equation is a very difficult task mainly owing to the internuclear and interelectronic repulsion which have independent variables included into denominator (1). First repulsion term can be handled using the approximation of Born-Oppenheimer that allows treating nuclei and electrons in a separate way. The electrons move faster than nuclei due to the difference in their masses and therefore, nuclei can be considered as static meanwhile electrons move around them[22]. According to this, an electronic Hamiltonian for the system can be derived and written as,

$$\hat{H}_{el} = -\frac{\hbar^2}{2m_e}\sum_i \nabla_i^2 - \sum_\alpha \sum_i \frac{Z_\alpha e'^2}{r_{i\alpha}} + \sum_i \sum_{j>i} \frac{e'^2}{r_{ij}} \tag{3}$$

Second repulsion term (i.e. interelectronic repulsion), yet included into the electronic Hamiltonian, can be treated from different approaches such as semiempirical and *ab initio* methods. Alternatively, density functional theory (DFT) can treat the electronic system by solving the electronic density equation of Kohn-Sham instead of solving the electronic Schrödinger equation. The principal features of the methods for solving the electronic equation are discussed in the following.

3.3.1.1 Semi-empirical Molecular Orbital Methods.

Semi-empirical (SE) methods are computationally attractive alternative for *ab initio* methods, especially when medium and large molecules are subject of study. For treating the electron Hamiltonian easily, we can consider two kinds of approximations: in first place, Coulomb integrals are set to be zero in long distance interactions and in the second place, interchange integrals are often replaced by analytical expressions with parameters, which are either experimentally or theoretically determined[22]. Different semi-empirical methods are largely characterized by their different parameter sets. Another distinctive approximation in SE methodologies is to take into account only valence electrons. Formerly, SE methods considered only part of the valence electrons of conjugated molecules. Thus, only π-electrons were treated explicitly into the electron Hamiltonian; the effects of σ electrons and the nuclei were

incorporated in a type of effective electron Hamiltonian[23]. Currently, SE methods consider all of the valence electron not only in conjugated molecules but also in organometalic and in a great variety of organic compounds.

It is possible to classify the SE methods into two general categories: SE theories that use a Hamiltonian composed by the sum of one-electronic contributions and those that consider both one-electronic terms and two electron repulsion terms[22]. The most important one-electron SE method for non-planar molecules is the extended Hückel theory (EH). The method was further developed and widely applied by Hoffman[22]. It was found that the EH method gave appropriate value for bond length of soft polar molecules, but failed in the prediction for strong polar molecules[21]. The EH method is also unable to predict appropriate values for dipolar moments, internal rotation barriers and molecular conformations[22]. Owing to these drawbacks, the results of the EH method should be used in a qualitative way. The SE theories that consider both one-electron term and two-electron term approximate the overlap integrals in different way. However, most of them apply the approximation of zero differential overlap (ZDO). According to that, the integral overlap is approximated as the Kronecker delta[21]. Among the methods that apply the ZDO approximation are CNDO, INDO, PNDO, MINDO, MNDO, AM1 y PM3.

Semi-empirical methods are more expensive than the molecular mechanics method, but they allow breaking of bonds and take electronic effects explicitly into account, which molecular mechanics cannot. Semi-empirical methods are appropriate, among others, for very large systems for which they are only computationally practical quantum mechanical methods, for a first step in a study of large and complex systems (see Ref. 24 for application in catalysis) and, for obtaining qualitative information about molecular properties (such as molecular orbitals, atomic charges and vibrational normal modes)[25]. Important shortcomings of semi-empirical methods are low reliability (particularly for transition states and hydrogen bonding) and lack of reliable parameters for transition metals which are concerned in most homogeneous and heterogeneous catalytic phenomena[4,25].

3.3.1.2 Hartree Fock and *ab initio* methods

We can describe a molecular system by treating the all possible pairwise interelectronic repulsions in an average way and so obtain the Hartree-Fock Hamiltonian (eq. 4).

$$H = \sum h_i, \qquad h_i = -\frac{1}{2}\nabla_i^2 - \sum \frac{Z_k}{r_{ik}} + V_i^{HF} \tag{4}$$

The term V_i^{HF} represents an interaction potential of the *i* electron with all of the other electrons occupying orbitals {j}. This interaction potential may be computed as:

$$V_i^{HF}\{j\} = \sum_j 2\left[J_{ij} - \frac{1}{2}K_{ij} \right], \qquad \psi_j = \Phi_k, \tag{5}$$

$$\Phi_k = (N!)^{-1/2}\begin{vmatrix} \phi_1(1)\alpha(1) & \phi_1(1)\beta(1) & \phi_2(1)\alpha(1) & \dots & \phi_N(1)\beta(1) \\ \phi_1(2)\alpha(2) & \phi_1(2)\beta(2) & \phi_2(2)\alpha(2) & \dots & \phi_N(2)\beta(2) \\ . & . & . & \dots & . \\ \phi_1(N)\alpha(N) & \phi_1(N)\beta(N) & \phi_2(N)\alpha(N) & \dots & \phi_N(N)\beta(N) \end{vmatrix} \tag{6}$$

$$\phi_r = \sum C_{ir}\chi_r \tag{7}$$

Where J_{ij} is the Coulomb operator which gives the potential energy appeared by the interaction between the *i* electron and the electronic density *j*; K_{ij} corresponds to the interchange operator which is related to antisimmetric wavefunctions[*] and ψ_j corresponds to the wave function which is usually expressed as a Slater determinant Φ_k. A Slater determinant yields an antisymmetric[*] wave function by permutations of spin-orbit monomials which are constituted by the product of a molecular orbital ϕ_r and a spin function α or β; in turn, molecular orbitals ϕ_r are taken as linear combinations of finite basis functions χ_r [29,30]. In this way, electrons are considered as wavefunctions with their charge spread out.

---

[*] Antisymmetry states that the sign of the wave function is changed under the exchange of the coordinates of any pair of electrons. The symmetry properties of the electron wave functions generate the Pauli Exclusion Principle.

The HF equation (4) is solved for each electron of the system in an iterative method called self-consistent field (SCF). In the first step of the SCF procedure, a guess of the wave function ψ in terms of Slater determinant, for all the occupied molecular orbitals, is used to construct the necessary one-electron operators. Solution of each differential equation provides a new set of coefficients for the orbitals. So the one-electron Hamiltonian are formed anew using the new set of coefficients, and the process is repeated many times until obtaining a difference between a newly determined set and the immediately preceding set that falls bellow some threshold criterion. In this point, the final set of coefficients determines the converged SCF orbitals[21].

The energy of the molecular system is given by the sum of all of the eigenvalues associated to the HF equations corrected by the double counting of the electron-electron repulsion. The energies and properties predicted with the HF theory may not be accurate enough for chemical applications due to the neglect of "electron correlation"[*]. However, the HF method allows for tremendous progress to be made in carrying out practical molecular orbital calculations. In fact, the HF method is a very attractive computational alternative for solving the Schrödinger equation compare to the perturbational and variational approaches. Thus, HF theory, in spite of its poorly significant fundamental assumption provides a very well defined stepping stone on the way to more sophisticated theories called *ab initio* theories (Latin for 'from the beginning').

The *ab initio* methods include the "electron correlation" by using a linear combination of Slater determinants Φ_k. The simplest form of the total wave function is a single Slater determinant, which is used by the Hartree-Fock approximation. The Configuration Interaction method (CI) is probably from conceptual point of view the simplest method to improve HF results[25,29]. CI includes excited states in the description of an electronic state. For this method, the many electron wave functions are written as a linear combination of Slater determinants with coefficients determined to minimize the expectation value of the electronic energy. In order to generate a suitable set of trial functions, it is possible to consider all possible combinations of the molecular orbitals. This full combination generates all possible excitations and the full-CI wavefuntion is obtained thereof. Inherently, the resulting number of Slater determinants

---

[*] Electron correlation allows for the change of instantaneous position of an electron by the presence of a neighboring electron. Neglecting electron correlation can lead to some clearly anomalous results, especially in dissociation processes (Ref. 28).

becomes too enormous to be computationally evaluated. So, in practical terms, the possible excitations are truncated to a small fraction of excitations such as single and double, and then forming the CIS (configuration interaction single) and the CISD (configuration interaction single double).

An improving of the CI method results when not only the coefficients of the determinants vary but also the coefficients of the basis functions. This approach is known as the multiconfiguration self-consistent field method (MCSSCF)[28]. One MCSSCF that has attracted considerable attention is the complete active-space SCF method (CASSCF) which enables very large number of configurations to be included into the calculation by considering all possible arrangement of the active electrons among the unoccupied orbitals (active orbitals).

The excitations (electron correlation) can also be incorporated by applying the Coupled Cluster theory (CC). The central tenet of the CC theory is that the full-CI wave functions (i.e., the exact one within the basis set approximation) can be described as $\psi = \exp(T)\psi_{HF}$, where ψ_{HF} corresponds to the Hartree-Fock wavefunction and T is the cluster operator that generates all possible excitations[21]. The cluster operator is expressed in terms of a Taylor series expansion. When the full Taylor series is taken, the CC method coincides with the full-CI method. As happen in the CI method, the sequence of the Taylor series must be truncated to be computationally feasible. A frequently used truncation, referred as the CCSD case, considers only one-particle and two-particle excitation operators. The CC method incorporates higher order excitations than the CI method. Figure 3.3 presents a hierarchy of the *ab initio* methods according to the approaches taking for both the "basis set" and the "total wave function".

When heavy atoms are treated in the *ab initio* methods, the effective core potential (ECP) or pseudo-potential approximation has been proved to be very useful[31]. In this approximation, core electrons are replaced by an effective potential. Thus, the number of electrons in the quantum mechanics is reduced and so requiring fewer basis functions and making the calculation less expensive. Most important, the effective core potential generates very little loss of reliability. Actually the recent success of quantum mechanical calculations for catalysis, an important use of molecular modeling in industry, owes very significantly to the availability of ECP[4].
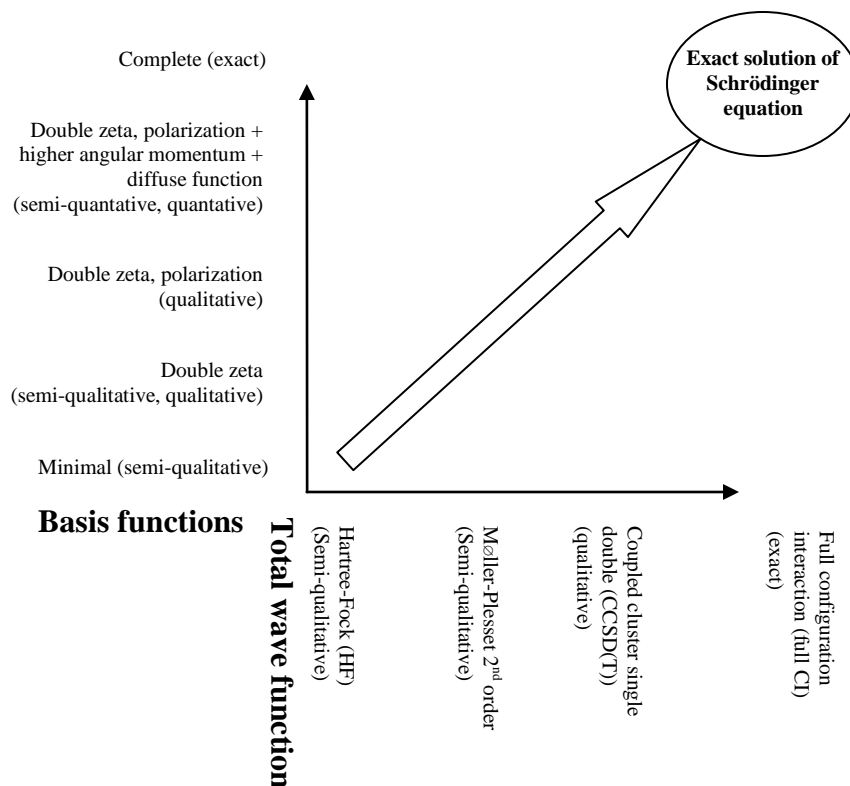
Figure 3.3. Hierarchy of methods and basis functions to approach a full, exact solution to the Schrödinger equation (Ref. 4).

Prediction of energy in the *ab initio* methods can be further improved by utilizing multilevel methods. The multilevel methods assume that errors in correlation energy prediction could be accounted for in some additive fashion. For instance, the quantum mechanical energies for glucose conformers can be improved by the following multiple calculations[21]:

$$
\begin{aligned}
E = {} & E(MP2/cc-pVTZ \;//\; MP2/cc-pVDZ) \\
& + \{E(CCSD/6-31G(d) // MP2/6-31G(d)) - E(MP2/6-31G(d))\} \\
& + \{E(HF/cc-p^{T}VQZ // MP2/cc-pVDZ) - E(HF/cc-pVTZ // MP2/cc-pVDZ\}
\end{aligned}
\tag{8}
$$

Thus, MP2 energies at MP2 geometries (line 1 on the r.h.s. of eq. 8) are augmented with a correction for doubles contributions (line 2 on the r.h.s. of eq. 8) and a correction for basis set[*]

---

[*] VTZ, VDZ.

size increase beyond *VTZ* (line 3 on the r.h.s. of eq. 8). Several of the systematic approaches for improving energies, and thus thermochemistry, have been grouped in the multilevel methods. The first of such multilevel methods that appeared was the so-called G1 theory of Pople and coworkers, which was followed rapidly by an improved modification called G2 theory, so that the former may be considered to be obsolete[32]. In general, the Gn multilevel methods assume basis-set incompleteness effects to be completely accounted for by additive corrections[21].

Alternatively, complete basis set (CBS) multilevel methods of Petersson and coworkers define a composite energy by extrapolating to the complete-basis-set limit from results for different levels of theory. Four well-defined CBS models exist, CBS-4, CBS-q, CBS-Q, and CBS-APNO, these being in order of increasing accuracy and, naturally, cost[21]. CBS models typically include a Hartree-Fock calculation with very large basis set, an MP2 calculation with a medium-sized basis set, one or more higher-level calculations with a medium-to-modest basis set, and most of the CBS methods also include an empirical correction for spin contamination in open-shell species (Table 3.1 illustrates this sequence of calculation for CBS-4 and CBS-Q multilevel methods). Multilevel methods, because most of them include empirically derived parameters, outperform single-level calculations at an equivalent expensive level of theory. However, the creation and the performance of a multilevel method depend on the existing of sufficient data for the particular system of interest. One should be disposed to use expensive multilevel methods, which improve the *absolute* energy prediction, instead of less expensive, and therefore less accurate, single-level method. Yet, many chemical studies are undertaken in order to better understand *relative* energy differences, for which single-level models are more tractable due to cancellation of errors and less computational time.

The traditional *ab initio* approaches as explained in this section, provide us a variety of techniques to obtain almost all the molecular properties to any desired accuracy. For small molecules, the accuracy that can be achieved in both excited states and ground estates is outstanding[20]. The *ab initio* have been and will be used in industrial applications when the accuracy is needed or when less expensive alternative methods, such as semiempirical methods or DFT, do not perform well[4].

Table 3.1. Sequence of calculation for CBS-4 and CBS-Q multilevel methods[25].

Energy Component	CBS-4	CBS-Q
Optimized geometry	HF/3-21G(d)	MP2/6-31G(d)
ZPE {scale factor}	HF/3-21G(d) {0.91671}	HF/6-31G† {0.91844}
CSF energy	HF/6-311+G(3d2f,2df,p)	HF/6-311+G(3d2f,2df,2p)
2nd order correlation	MP2/6-31G†	HF/6-311+G(3d2f,2df,2p)
CBS extrapolation	≥ 5 configurations	≥ 10 configurations
Higher order correlation	MP4(SDQ)/6-31G	MP4(SDQ)/6-31+G(d(f),d,f) QCISD(T)/6-31+G†
Additional empirical corrections	1 and 2-electron higher order corrections (size-consistent), spin contamination	1 and 2-electron higher order corrections (size-consistent), spin contamination, core correlation for sodium

3.3.1.3 DFT methods

Density functional theory (DFT) is a method that offers a useful tool to overcome the limitations of the computational demands of most of the *ab initio* methods. Based on the famous Hohenberg and Kohn theorems, DFT offers in principle an exact treatment of the electronic quantum problem[20] and a sound basis for the development of computational strategies for obtaining information about the energetics, structures, and properties of atoms and molecules at much lower costs than traditional *ab initio* wave function techniques. The basic variable of this theory is the one-electron density instead of the wavefunction.

The first Hohenberg and Kohn's theorem[32] showed that all the ground-states properties and therefore, the wave function were uniquely determined by the charge or electron density. The Second Hohenberg and Kohn's theorem provided a variational procedure for obtaining ρ: search for the ρ(r) minimizing the total electronic energy, E. Thus, the total electronic energy, due to the preceding affirmations, can be written as a function of the electron density ρ (i.e. the energy is a functional of ρ):

$$\rho(r) = N \int \psi^*(q_1, q_2, ... q_N) \psi(q_1, q_2, ... q_N) d\tau \tag{9}$$

$$E[\rho] = \min_{\rho} (T[\rho] + E_{ee}[\rho] + E_{Ne}[\rho]) \tag{10}$$

T[ρ] is the kinetic energy of the system, *E_ee[ρ]* is the electron-electron attraction, and *E_Ne[ρ]* corresponds to the nuclei-electron attraction. With the DFT theorems, the problem of many-electron is stated as a three dimensional one-body density problem. Although the power behind the preceding theorems, it was only by the introduction of the Kohn-Sham equation[33] that DFT started to be computationally workable. Kohn and Sham realized that the real system can be reduced to a non-interacting reference system with the same density as the former interacting one[34]. With this analogy, Kohn and Sham accounted for describing the unknown functionals (i.e., *T* and *E_ee*) by introducing the following separation,

$$E[\rho] = E_{KE}[\rho] + E_C[\rho] + E_H[\rho] + E_{XC}[\rho] \tag{11}$$

Where *E_KE[ρ]* is the kinetic energy of the non-interacting reference system. *E_C[ρ]* accounts for the electron-nucleus interaction term and *E_H[ρ]* for the electron-electron Coulomb energy, and *E_XC[ρ]* contains the exchange and correlation contributions that correct the behavior of the non-interacting system. Last two right terms in eq. 11 contain the electron interactions. For the first three right contributions in eq. 11 standard expressions in function of ρ can be used as follows[4,28,32]:

$$E[\rho] = \sum_i \int \phi_i \left(-\frac{\nabla^2}{2} \right) \phi_i dr + \sum_A \int \frac{Z_A}{|R_A - r|} \rho(r) dr + \frac{1}{2} \iint \frac{\rho(r)\rho(r')}{|r - r'|} dr d r' + E_{XC}[\rho] \tag{12}$$

The Kohn-Sham orbitals ϕ_i link the original system to the non-interacting reference system. With the help of the ϕ_i orbitals the kinetic energy functional can be computed up to a small correction term that is taken up into the *E_xc* functional according to the Kohn-Sham equation[33]:

$$\left[-\frac{\nabla^2}{2} + \sum_A \frac{Z_A}{|R_A - r|} + \int \frac{\rho(r)}{|r - r'|} dr' + \frac{\delta E_{XC}}{\delta \rho} \right] \phi_i = \varepsilon_i \phi_i \tag{13}$$

A brief mathematical description of the theorems of DFT is presented in Figure 3.4. The fundamental problem in a DFT calculation is that the correct form of the *E_xc* functional is

unknown. Various approximate exchange and correlation functionals have been proposed. The simplest are the local density based functionals (LDA), in which functionals depend only on ρ. The LDA approximation assumes that, like in a uniform electron gas, the charge density varies slowly throughout a molecule. According to this, the $E_{XC}[\rho]$ for the system can be obtained by integrating the $\varepsilon_{XC}[\rho]$ of a uniform electron gas over all space[28]:

$$E_{XC}[\rho] \approx \int \rho(r) \varepsilon_{XC}[\rho] dr \qquad (14)$$

Several analytical representations for the exchange and correlation energies for the uniform electron gas can be found in literature[34]. The LDA approximation is not accurate enough for chemists for molecular modeling though. Then, the dependence on gradient of ρ was also introduced into the x-c functionals[34]. This made the calculated results acceptably enough at the chemistry level in order to give reliable properties, such as NMR chemical shifts, vibrational frequencies and intensities, electrostatic potential and electron density. Some examples of the gradient-corrected functionals are Becke88-LYP and Becke88-Perdue86 as well as hybrid functionals, such as B3LYP, which mix the "exact HF" exchange with DFT in a somewhat empirical fraction in order for improving the energies further[4].

The practical implementation of DFT reduces to the self-consistent solution of a set of coupled differential eigenvalue equations for the ϕ_i orbitals. The HF (eq. 4) and DFT equations (eq. 13) are solved in quite resemble computational procedures; the basic principles of the two approaches are basically different, although. Both schemes are solved self-consistently in configuration space by introducing a basis set to expand the molecular orbitals or the ϕ_i orbitals. As it was stated above, the accuracy of the results depends on the choice of the exchange correlation energy functional. If the correlation effects are included in the appropriate functional, the solution can go beyond the HF results in a very attractive computational way. When using well-known functionals derived from the generalized gradient approximations, one can achieve an accuracy that is comparable to the MP2 or MP4 level of theory[20]. Additional to the Hohenberg and Kohn theorems that apply only for ground states, many new developments are

taking place for excited states, and the time-dependent perturbation method (TD-DFT) seems to be emerging as a method of choice[4].

DENSITY FUNCTIONAL THEORY

Hohenberg and Kohn Theorems

1st   2nd

ρ determines nuclei-electron potential

$$V(\rho) = \int \rho(r) v(r) dr$$

ρ determines number of electrons of the system

$$N = \int \rho(r) dr$$

ρ determines electronic Hamiltonian operator

$$\hat{H}_{el} = -\frac{\hbar^2}{2m_e} \sum_i \nabla_i^2 - \sum_\alpha \sum_i \frac{Z_\alpha e'^2}{r_{i\alpha}} + \sum_i \sum_{j>i} \frac{e'^2}{r_{ij}}$$

ρ determines energy of the system and the energy is a functional thereof

$$E = E[\rho]$$

ρ is determined by minimizing E subject to N constant

$$Min \quad L = E - \mu\rho$$

Applying optimality conditions

$$\frac{\delta E}{\delta \rho} = \mu$$

E can be split into nuclei-electron interaction (v) and the Hohengerg-Kohn functional (F_{HK}).

$$\frac{\delta F_{HK}}{\delta \rho} + v(r) = \mu$$

Kohn-Sham Equation

The F_{HK} is taken and corrected from a non-interacting reference system

$$F_{HK} = -\frac{1}{2} \sum \langle \psi_i | \nabla^2 | \psi_i \rangle + \iint \frac{\rho(r)\rho(r')}{|r - r'|} drdr' + E_{xc}$$

According to the 2nd HK theorem, an effective potential is derived

$$v_{eff}(r) + \frac{\delta Ts}{\delta \rho} = \mu$$

$$v_{eff}(r) = v(r) + \int \frac{\rho(r)}{|r - r'|} dr' + \frac{\delta E_{xc}}{\delta \rho}$$

Kohn-Sham equation integrates this effective potential.

$$\left(-\frac{1}{2} \nabla^2 + v_{eff} \right) \psi_i = \varepsilon_i \psi_i$$

Figure 3.4. Fundamentals of DFT theory.

3.3.2 Classical Description of Molecular Systems: Molecular Mechanics

The molecular mechanics method was developed by Westheimer, Hendrickson, Wiberg, Allinger, Warshel and others[35] and it is applicable to organic and organometallic compounds as well as coordinative compounds of transition metals. Principal supposition of molecular mechanics (MM) withdraws the explicit influence of electrons and relies on considering that the energy of the system can be obtained by different interaction of punctual particles doted of mass and charge (atoms). These punctual particles are joined by springs to allow representing molecules. Therefore, contributions to potential energy due to bounded atoms are obtained by bond stretching, angle bending and torsion contributions.

MM models also permit non-bonded punctual particles to interact by considering electrostatic interactions and van der Waals interactions. By the sum of bounded and non-bonded interactions, the energy of a molecular system can be expressed as,

$$V = \sum_{bonds} \frac{k_i}{2}(l_i - l_{i,0})^2 + \sum_{angles} \frac{k_i}{2}(\theta_i - \theta_{i,0})^2 + \sum_{torsions} C_n \cos(\omega)^n \tag{15}$$

$$+ \sum_{i} \sum_{j=i+1} \underbrace{\left(4\varepsilon_{ij} \left[\left(\frac{\sigma_{ij}}{r_{ij}}\right)^{12} - \left(\frac{\sigma_{ij}}{r_{ij}}\right)^{6} \right] \right)}_{van\ der\ Waals} + \sum_{i} \sum_{j=i+1} \underbrace{\left(\frac{q_i q_j}{4\pi\varepsilon_0 r_{ij}} \right)}_{electrosta\ tic}$$

Where k_i corresponds to force constant (bond stretching or angle bending). $l_{i,0}$ and $\theta_{i,0}$ are the equilibrium values for bonds and angles respectively. ω is the torsion angle. This form for the potential energy (also called strain energy) depends only on the positions of the atoms. The set of terms for each of the energy contributions and parameter values in the potential energy equation is called force field. The relative simple expression for the potential energy surface allows treating systems of thousands of atoms. Sophisticated force fields may have additional terms, but invariably contain the components of eq. 15. The force fields classify atoms according to their hybridization and to the other atoms they are bonded to. Typically, a force field contains from 50 to 75 sorts of atoms[22].

The general procedure to obtain the values of the parameters in a force field consists in taking a training set of molecules. The training set posses a collection of known molecular information (such as molecular structures, vibrational frequencies, internal rotation barriers, dipole moments and molecular interactions) from either experiments or theoretical *ab initio* calculations. The values of the parameters are varied in order to minimize the gap among predicted information and known information for the training set[28]. Transferability is a key attribute of a force field, for it enables a set of parameters developed and tested on a relatively small number of cases to be applied to a much wider range of problems, including from simple molecules to polymers[35].

MM methods are very fast and have proven their success to handle systems such as polypeptides or proteins with a huge number of atoms and stable conformations[36]. The difference among potential energies calculated by MM methods can be utilized for calculating conformers of the same molecules, stereoisomers among different molecules (such as *cis* and *trans* conformers), studying the geometry in the same molecule and even, hydrogen bridge. The difference between the potential energies of the equilibrium structures of two species with the same number of atoms and the same class of bonds gives an estimation of the electronic energy difference among these molecules[22]. In some cases force fields can provide answers that are as accurate as even the highest level quantum mechanical calculations, in a fraction of computer time. Principal drawbacks of MM methods are related to poorness of general applicability due to their empirical input. MM methods are additionally not suited to study bond-breaking and bond-forming reactions in which electronic distribution changes drastically along the nuclear path. Examples of force fields available in literature are AMBER94[37] and CHARMM[38] for biomolecules, MM2 and MM3 for organic molecules and proteins[39], MM4 for hydrocarbons[40], SHAPES for transition metal compounds[41] and PEF95SAC for carbohydrates[42].

3.3.3 Simulation at Grand Scales: Molecular Simulation Methods.

A molecular simulation (i.e. Monte Carlo simulation or Molecular Dynamic simulation) generally consists of a computer realization of a system in which actual molecular configurations are used to extract structural, thermodynamic and dynamic information[43]. The term "configuration" denotes a set of cartesian coordinates (and momentum in the case of dynamic simulation) for all the atoms or molecules that constitute a system. The quality of this

information depends strongly on the number of uncorrelated configurations available for subsequent analysis. Molecular simulation counts with two methods to generate these configurations as a direct consequence of the ergodic[*] hypothesis. In molecular dynamics method, the system is described by integrating its Newton's equations of motion and therefore the parameters obtaining are time-averaged. On the other hand, in Monte Carlo methods, spatial samples are generated under the restriction of a probability distribution function dictated by statistical mechanics and therefore parameters obtained are ensemble-averaged. On the basis of these configurations, appropriate statistical averages are performed to derive fluid properties that can be compared with experimental measurements[28].

Properties that can be obtained from molecular simulations include thermodynamic properties (such as equations of state, phase equilibrium, and critical constants), mechanical properties (such as stress-stretch relationships and elastic moduli), transport properties (such as viscosity, diffusion and thermal conductivity), and morphological information (such as location and shape of binding sites on a biomolecule and crystal structure). It is worth to say that this list continues to grow as algorithm and computer hardware advances make it possible to access more properties. In this way, we can predict the properties of a macroscopic sample of the systems based on statistical averaging over the possible microscopic states of the system as it evolves under the rules of classical mechanics. Thus, the building blocks are molecules, the dynamics are described by classical mechanics, and the key concept is statistical averaging.

Molecular dynamics (MD) simulation have greatly contributed to the understanding of equilibrium and non-equilibrium properties of molecular systems. Classical-mechanical trajectories of the system are generated by solving a set of Newtonian equations of motion for each of the consisting atoms:

$$F_i = m_i a_i, \quad F_i = \nabla V \tag{16}$$

---

[*] Ergodic hypothesis states that temporal average of a process parameter is equal to spatial average over the statistical ensemble.

In these equations m_i is the mass of the atom i while F_i stands for the force on the atom i. The equations of motion are coupled since the potential energy V, of the molecular system depends on all atomic coordinates. In classical MD techniques the potential is modeled as a sum of interatomic potentials with a simple analytical form and determined by parameters adjusted to experimental data (this is molecular mechanics technique, eq. 15). Initial positions for integration are chosen in a somewhat arbitrary manner due to the simulation time is long enough for the equilibration of the system; on the other hand, initial velocities are established using the Maxwell Boltzmann distribution at the temperature of interest. Numerical integration of the equations of motion along with the boundary conditions and any constraints on the systems is done with the Verlet algorithm and its variants[44,45]. An appropriate statistical ensemble[*] of the system is generated if enough trajectories are computed on the equilibrated system.

The solution of equation of motion simulates the microcanonical or *NVE* ensemble and therefore the energy (i.e. the sum of kinetic and potential energy) remains constant at any point over the phase-space trajectories. In order to perform a molecular dynamics calculation at imposed temperature (i.e. *NVT* ensemble), a thermostat method must be used to change the total energy of the system during the simulation, so that the Boltzman distribution of energies is respected. In a thermostat method, the energy is changed by altering particle velocities at regular intervals[47,48]. Simulations at both imposed temperature and pressure (i.e. *NPT* ensemble) can be achieved by the pressostat or barostat methods[48] which allow for volume variations. MD is especially suitable for studying the evolution of an equilibrium structure or the dynamics of transport phenomena. From results of MD, it is possible to calculate diffusion coefficients, thermal conductivity and viscosity.

In Monte Carlo (MC) methods, movement of the molecules are generated in a random fashion according to an algorithm that accepts or rejects by calculating the probability of having such generated configuration (canonic ensemble have a probability which is proportional to exp(-$\Delta E/KT$), where *K* and *T* are the Boltzman constant and the temperature respectively).

[*] An ensemble consists in a collection of all possible states of a system compatible with some set of constraints, such as imposed temperature or imposed number of molecules (Ref. 46). Different average properties can be calculated on the base of such collection; e.g. with canonical ensemble (i.e. imposed *NVT* values) phase properties can be calculated.

Equilibrium properties are averaged over the different generated configurations. Sorts of movements in a MC simulation depend on the analyzed system. For instance, the Gibbs Ensemble Monte Carlo method (GEMC) for the simulation of liquid vapor equilibrium treats two separate microscopic regions (one for each phase) and performs cycles with the following random movements[49,50]: displacements, volume changes, particle transfers and particle exchange. The goal in the GEMC is to calculate the densities, compositions and pressures of the two coexisting phases at equilibrium without including the analysis of phenomena in their common interface. The GEMC method is illustrated in Figure 3.5.

The key step in the GEMC method is the particle transfer which becomes as cumbersome as the increasing in length of chain of the treated molecules. This produce prohibitively low acceptance of transfer attempts. Particle transfer in GEMC can be improved by configurational-bias sampling techniques which are based on segment-by-segment insertions or removals of a multisegment molecule[41,51]. Several trial directions are attempted for every segment insertion, and a favorable growth direction is preferentially selected for the segment addition. Each segment growth or removal step generates a correction factor that is incorporated into the overall acceptance criterion in order to correct for the bias introduced by the non-random growth along preferential directions[52]. The main drawback is that GEMC fails at high densities. Furthermore, near the critical point, the simulation boxes may switch identity several times due to large fluctuations in their densities in the course of the simulation.

All methods of molecular simulation have the common lack of appropriate intermolecular potential functions which is often quoted as the most important barrier to overpass for widely application to problems of industrial interest (see for example Ref. 4). It is required the development of major number of force fields for chemical process conditions for properly representing the phase and reaction equilibria; currently, chemical engineering community count on useful force fields for a limited range of systems, including alkanes, alkenes, perfluoroalkanes, CO_2, H_2O and other low molecular weight species[53].

Phenomena with size and time scales larger than those treated in normal molecular simulations can be studied with mesoscale or coarse-graining methods. This is typically the case when

115

surface diffusion is fast and diffusion-reaction instabilities occur. Monte-Carlo-based methods are widely used in analyzing phenomena at mesoescale. In general, simulations at this scale can be classified in continuum and discrete mesoscale theories. Mesoscale methods have been applied in different areas such as chemical reactions[54], biomolecules[55], crystallization and mechanical stability of particle gels[56] and polymers[16].
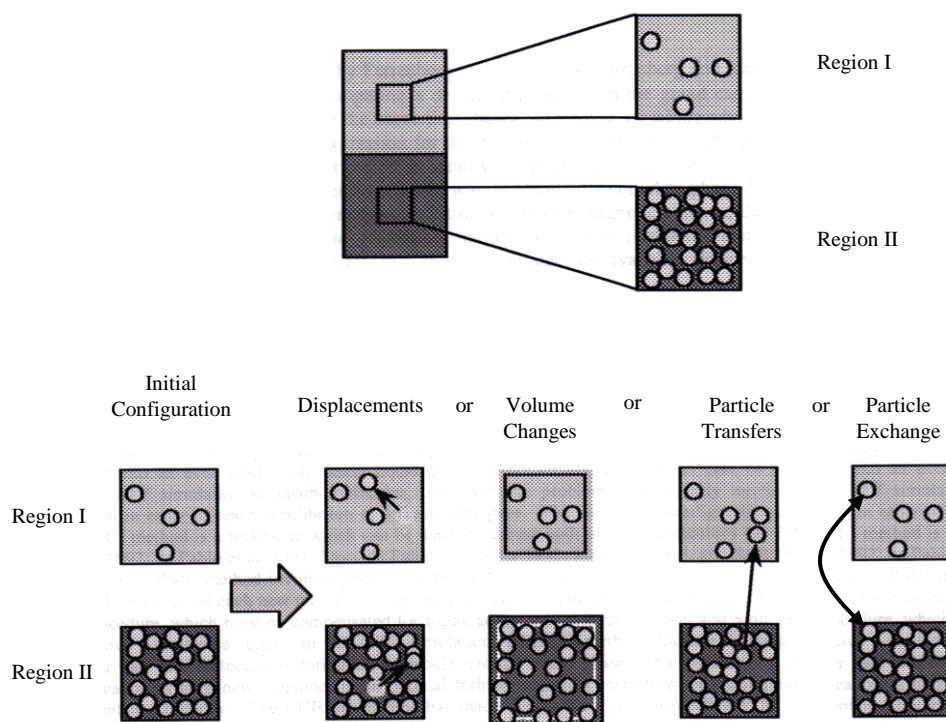
Figure 3.5. Schematic Gibbs Ensemble Monte Carlo Simulation (Refs. 49 and 50).

3.3.4 Hybrid Methods of Low-scale

Hybrid methods combine the best features of various levels and approaches in order to analyze accurately the complex systems. We called low-scale hybrid methods those that integrate in the same iteration cycle quantum mechanical methods and classical atomic scale methods (*vide* preceding section). Accordingly, we can count three classes of low-scale hybrid methods: temporal hybrid, spatial hybrid and spatiotemporal hybrid. To the first class belong methods that are hybrid in a temporal sense, mixing electronic structure calculations (i.e., quantum mechanical calculations) with molecular simulation methods. With this hybrid, the system is simulated at a

finite temperature with an electronic structure method rather than an empirical force field. Accordingly, finite temperature effects on systems where electronic distribution plays a central role, such as chemical reactions, can be taken into account in a realistic manner. An example of this hybrid is the Car-Parrinello molecular dynamic method[57], in which the atoms undergo motion described by classical dynamics in response to forces computed on the fly at each time step by one of the DFT theory; thus, Car-Parrinello is concerned with the problem of performing quantum simulations involving both the electronic and the nuclear motions. This method and its various modifications have been very successful and popular for material modeling and for calculations for heterogeneous and homogeneous catalysts in industrial applications[4]. The DACAPO, VASP and CAMP-Atami methods also belong to this class of hybrid.

The second class of hybrids is related to the spatial division of the complex system. In this sort, different methods are applied in different physical regions of molecules or realms. Basically, the second class of hybrids combines a more accurate (more expensive) method for the principal part of the system and a less accurate (less expensive) method for the rest of the system. This hybrid allows analyzing systems in a rather accurate fashion that otherwise a high level quantum mechanical calculation over a stripped down model would fail by oversimplifying the system. Among this class of hybrid, the so-called QM/MM method[58] compound quantum mechanical and molecular mechanics by dividing the Hamiltonian into the form[59]:

$$H = H_{QM} + H_{MM} + H_{QM-MM}$$ (17)

Where H_{QM} and H_{MM} are the quantum mechanical and molecular mechanic Hamiltonians respectively. H_{QM-MM} corresponds to the correction of the Hamiltonian by the interaction between the QM and the MM parts. This method allows bond breaking and forming processes of extended systems to be simulated in computationally tractable times[15]. The QM part is the region that necessitates a quantum mechanical description to be properly studied. The remainder part, which acts only as a perturbation to the QM region, is approximated adequately in a classical mechanical fashion. One of the first and main application areas has been the study of solvation and reactivity of small molecules in condensed phases, but other application areas include studies of surface reactivity, zeolites, crystal formation and study of reactivity in enzymes[59]. Figure 3.3

illustrates the QM/MM method in two different systems, in a solvent reaction and in a catalytic reaction. There are many limitations to the QM/MM method related to the interaction between the QM and the MM parts. Such interaction is only approximated and the results should be validated and examined carefully before conclusions.

A third class of hybrid method, called spatiotemporal hybrid, can be formed when spatial and temporal hybrids are combined[15,60]. Thus, when the motion of the system is analyzed by molecular simulation and the spatial realm of the system is treated by coupling two different molecular structural methods. Such hybrid can be applied productively to modeling solvent molecules explicitly and to the chemistry of the catalysis. Most chemical measurements and experiments are performed in solution, and there is a great need to evaluate the effects of solvents on properties and reactivities of molecules.

As the systems to be analyzed become more complex and the accuracy required become higher, hybrid methods are expected to become more and more popular, in both academic and industrial applications, as the method codes become more readily available[4] and the number of specialized people increases.

Final Remarks

Modeling and simulation of chemical engineering phenomena based on different body interaction theories have started to contribute for understanding and improving the different steps that form the chemical supply chain. The coupling among different scales of modeling arises as a useful tool for developing molecular-based models which can represent detailed conditions of systems that different isolated models cannot take into account. Future developments in theories, hardware and software can become multiscale modeling widely applicable and the molecular modeling a common tool in the analysis of chemical engineering phenomena. Theories that underlie the applicability of molecular modeling involve new concepts for traditional chemical engineering community. Such concepts should be incorporated into the chemical engineering curriculum due to the needs for applying multiscale modeling in the analysis of chemical engineering phenomena.

118

References

(1) de Pablo, J. J. "Molecular and Multiscale Modeling in Chemical Engineering – Current View and Future Perspectives". *AIChe journal*, 51, 2372, 2005

(2) Grossmann, I. E. and Westerberg, A. E. "Research challenges in Process Systems Engineering". *AIChe Journal*, 46 (9), 1700–1703, 2000.

(3) Sengupta, D. "Does the Ring Compound [(CH3)2GaNH2] Form during MOVPE of Gallium Nitride? Investigations via Density Functional and Reaction Rate Theories". *J. Phys. Chem. B*, 107, 291-297, 2003.

(4) Westmoreland, Phillip R.; Kollman, Peter A; Chaka, Anne M; Cummings, Peter T; Morokuma, Keiji; Neurock, Matthew; Stechel, Ellen B; Vashishta, Priya. "*WTEC panel Report on Applications of Molecular and Materials Modeling. International Technology Research Institute. World Technology (WTEC) Division*". January 2002.

(5) Hung, F. R.; Franzen, S.; Gubbins, K. E. "A Graduate Course on Multi-scale Modleing of Soft Matter", *Chem. Eng. Ed.* 38 (4), 242-249, 2004.

(6) Raimondeau, S. and Vlachos, D. G. "Recent developments on multiscale, hierarchical modeling of chemical reactors", *Chem. Eng. Journal,* 90, 3–23, 2002.

(7) Grossmann, I. E. and Jackson, J. R. "A disjunctive programming approach for the optimal design of reactive distillation columns", *Comp. Chem. Eng.* 25, 1661–1673, 2001.

(8) Doherty, M. F. "Conceptual design of chemical processes: Opportunities for molecular modeling". *Foundations of Molecular Modeling and Simulation*. AIChe Symposium Series 325, 97, 120-126, 2001.

(9) Glasser, D.; D. Hildebrant, and C. Crowe. "A geometric approach to steady flow reactors: the attainable region and optimization in concentration space", *Ind. Eng. Chem. Res.*, 26, 1803-1810, 1987.

(10) Morales, G.; Martínez, R; Ziegler, T. "Theoretical Comparison of Ketene Dimerization in the Gas and Liquid Phase". *J. Phys. Chem. A*, 112, 3192-3200, 2008.

(11) Lidorikis, E. ; Bachlechner, M. E. ; Kalia, R. K. ; Nakano, A. ; Vashishta, P. "Coupling Length Scales for Multiscale Atomistics-Continuum Simulations: Atomistically Induced Stress Distributions in Si/Si3N4 Nanopixels", *Phys. Rev. Lett.* 87, 86104, 2001.

(12) Braatz, R. D.; Alkire, R. C.; Seebauer, E.; Rusli, E.; Gunawan, R.; Drews, T. O.; Li, X.; He, Y. "Perspectives on the design and control of multiscale systems". *Journal of Process Control*, 16, 193–204, 2006.

(13) Traeger, J. C. "Neutral and Cationic heats of formation for ketene, methylketene, and dimethylketene". *Int. J. Mass Spectrom.* 2000, 194, 261.

(14) Sumathi, R. and Green, W. H. Jr. "Thermodynamic Properties of Ketenes: Group Additivity Values from Quantum Chemical Calculations". *J. Phys. Chem. A*, 106, 7937, 2002.

(15) Woo, T. K.; Margl, P. M.; Deng, L.; Cavallo, L.; Ziegler, T. "Towards more realistic computational modeling of homogenous catalysis by density functional theory: Combine QM/MM and ab initio molecular dynamics". *Catalysis Today*, 50, 479-500, 1999.

(16) Cagin, T.; Wang, G.; Martin, R.; Zamanakos, G.; Vaidehi, N.; Mainz, D. T.; Goddard III, W. A. "Multiscale modeling and simulation methods with application to dendritic polymers", *Comp. Theor. Pol. Science* 11, 345-356, 2001.

(17) Gómez, B.; Likhanova, N. V.; Domínguez, M. A.; Olivares, O.; Hallen, J. M.; Martínez-Magadán, J. M. "Theoretical Study of a New Group of Corrosion Inhibitors", *J. Phys. Chem. A*, 109, 8950-8957, 2005.

(18) Drummond, M. L. and Sumpter, B. G. "Use of Drug Discovery Tools in Rational Organometallic Catalyst Design", *Inorg. Chem.*, 46, 8613-8624, 2007.

(19) Charpentier, J.C. "The triplet 'molecular processes-product-process' engineering: the future of chemical engineering?". *Chem. Eng. Science*, 57, 4667-4690, 2002.

(20) Van Speybrook, V. "Ab Initio Static and Dynamic Molecular Methods: a Useful Tool in the Study of Chemical Reactions". Doctoral dissertation. Universiteit Gent. 2001-2002.

(21) Cramer, C. J. *"Essentials of Computational Chemistry: Theories and Models"*. John Wiley & Sons, Ltd.: London, 2002.

(22) Levine, I. N. *"Química Cuántica"*. Segunda edición en Español. Prentice Hall, 2001.

(23) Parr, R. G. *"Quantum Theory of Molecular Electronic Structure"*, ed. By Benjamin, New York 1963, Pages 41-45, 211-218.

(24) Klein, M. T.; Hou, G.; Bertolacini, R. J.; Broadbelt, L. J.; Kumar, A. *"Molecular Modeling in Heavy Hydrocarbon Conversions"*. CRC Press. Taylor & Francis Group. USA 2006.

(25) Foresman, J. B. and Frisch, Æ. *"Exploring Chemistry with Electronic Structure Methods"*. 2nd edition, Gaussian, Inc. 1996.

(26) Roothan, C. C. J. "New developments in molecular orbital theory", *Rev. Mod. Phys.*, 23, 69-89, 1951.

(27) Zerner, M. C. "New developments in molecular orbital theory", *Theor. Chem. Acc.*, 103, 217, 2000.

(28) Leach, A. "*Molecular Modeling: Principles and Applications*". Longman, 1996.

(29) Foresman, J. B.; Head-Gordon, M.; Pople, J. A.; Frisch, M. J. "Toward a systematic molecular orbital theory for excited states", *J. Phys. Chem.*, 96, 135, 1992.

(30) Hay, P. J. and Wadt, W. R. "*Ab initio* effective core potentials for molecular calculations. Potentials for K to Au including the outermost core orbitals", *J. Chem. Phys.* 82, 299-310, 1985.

(31) Curtiss, L. A.; Raghavachari, K.; Trucks, G. W.; Pople, J. A. "Gaussian-2 theory for molecular energies of first- and second-row compounds", *J. Chem. Phys.*, 94, 7221-7230, 1991.

(32) Hohenberg and Kohn, "Inhomogeneous Electron Gas", *Phys. Rev.* 136, B864 - B871, 1964.

(33) Kohn, W. and Sham, L. "Self-Consistent Equations Including Exchange and Correlation Effects", *J. Phys. Rev.*, 140, A1133-A1138, 1965.

(34) Koch, W. and Holthausen, M. C. "*A Chemist's Guide to Density Functional Theory*". Second edition. Wiley-VCH Verlaf GmgH. 2001.

(35) Burkert, U. and Allinger, N. L. "*Molecular Mechanics*". ACS monograph No. 177, American Chemical Society, Washington, D.C. 1982.

(36) McCammon, J. A. and Harvey, S. C. *Dynamics of Proteins and Nucleic Acids*. Cambridge University Press, New York, 1987.

(37) Cornell, W. D. "A Second Generation Force Field for the Simulation of Proteins, Nucleic Acids, and Organic Molecules", *J. Am. Chem. Soc.*, 117, 5179, 1995.

(38) MacKerell, A. D., Jr.; Bashford, D.; Bellott, R. L.; Dunbrack, R. L., Jr.; Evanseck, J. D.; Field, M. J.; Fischer, S.; Gao, J.; Guo, H.; Ha, S.; Joseph-McCarthy, D.; Kuchnir, L.; Kuczera, K.; Lau, F. T. K.; Mattos, C.; Michnick, S.; Ngo, T.; Nguyen, D. T.; Prodhom, B.; Reiher, W. E., III; Roux, B.; Schlenkrich, M.; Smith, J. C.; Stote, R.; Straub, J.; Watanabe, M.; Wiorkiewicz-Kuczera, J.; Yin, D.; Karplus, M. "All-Atom Empirical Potential for Molecular Modeling and Dynamics Studies of Proteins", *J. Phys. Chem. B*, 102, 3586-3616, 1998.

(39) Allinger, N. L. and Yan, L. "Molecular mechanics (MM3). Calculations of furan, vinyl ethers, and related compounds", *J. Am. Chem. Soc.*, 115, 11918, 1993.

(40) Allinger, N. L.;Chen, K.; Lii, J.-H. "An Improved Force Field (MM4) for Saturated Hydrocarbons", *J. Comput. Chem.*, 17, 642, 1996.

(41) Allured, V. S.; Kelly, C.; Landis, C. R. "SHAPES empirical force field: new treatment of angular potentials and its application to square-planar transition-metal complexes", *J. Am. Chem. Soc.*, 113, 1, 1991.

(42) Fabricius, J.; Engelsen, S. B.; Rasmussen, K. "The Consistent Force Field. 5. PEF95SAC: Optimized potential energy function for alcohols and carbohydrates", *J. Carbohydr. Chem.*, 16, 751-772, 1997.

(43) Frenkel, D. and Smit, B. "*Understanding Molecular Simulation: From Algorithms to Applications*". San Diego: Academic Press. 1996.

(44) Verlet, L. "Computer Experiments on Classical Fluids. I. Thermodynamical Properties of Lennard-Jones Molecules", *Physical Review*, 159, 98-103, 1967.

(45) Allen, M.P. and Tildesley, D.J. "*Computer simulation of liquids*" Oxford Science Publications: New York, 1987.

(46) McQuarrie, D. A. "*Statistical Mechanics*", Harper and Collins, New York, 1976.

(47) Nosé, S. "A unified formulation of the constant temperature molecular dynamics methods", *J. Chem. Phys.*, 81, 511, 1984.

(48) Hoover, W. G. "Canonical dynamics: equilibrium phase-space distributions", *Phys. Rev. A*, 31, 1695, 1985.

(49) (a) Panagiotopoulos, A. Z. "Adsorption and capillary condensation of fluids in cylindrical pores by Monte Carlo simulation in the Gibbs ensemble", *Mol. Phys.*, 62, 701, 1987. (b) Panagiotopoulos, A. Z. "Exact calculations of fluid-phase equilibria by Monte Carlo simulation in a new statistical ensemble". Int. J. Thermophysics, 10, 447, 1989.

(50) Panagiotopoulos, A. Z. and Stapleton, M. R. "The Gibbs Method for Molecular-based Computer Simulation of Phase Equilibria", *Fluid Phase Equilibria*, 53, 133-141, 1989.

(51) de Pablo, J. J.; Laso, M.; Siepmann, J. I.; Suter, U. W. "Continuum-configurational-bias Monte-Carlo simulations of long-chain alkanes". *Mol. Phys.*, 80 (1), 55-63, 1993.

(52) Panagiotopoulos, A. Z. "Force-Field Development for Simulation of Condensed Phases". *Foundations of Molecular Modeling and Simulation*. AIChe Symposium Series 325, Vol. 97, 61-70, 2001.

(53) Thompson, T. B. "Chemical industry of the future: technology roadmap for computational chemistry", available from http://www.ccrhq.org/vision/index/roadmaps/complete.html.

(54) Chatterjee, A.; Snyder, M. A.; Vlachos, D. G. "Mesoscopic modeling of chemical reactivity", *Chem. Eng. Science,* 59, 5559-5567, 2004.

(55) Huber, G. A. "Multiscale modeling of large biomolecules", *Foundations of Molecular Modeling and Simulation*. AIChe Symposium Series 325, Vol. 97, 54-60, 2001.

(56) Irfachsyad, D. and Tildesley, D. "Simulation study of crystallization and mechanical stability of particle gels", *Foundations of Molecular Modeling and Simulation*. AIChe Symposium Series 325, Vol. 97, 234-238, 2001.

(57) Car, R. and Parrinello, M. "Unified Approach for Molecular Dynamics and Density-Functional Theory", *Phys. Rev. Lett.* 55, 2471–2474, 1985.

(58) Warshel, A. and Karplus, M. "Calculation of ground and excited state potential surfaces of conjugated molecules. I. Formulation" *J. Am. chem. Soc.*, 94, 5612–5625, 1972.

(59) Monard, G. and Merz, K. Jr. "Molecular Mechanical Methodologies Applied to Biomolecular Systems". *Acc. Chem. Res.*, 32, 904-911, 1999.

(60) Gao, J. "Absolute Free Energy of Solvation from Monte Carlo Simulations Using Combined Quantum and Molecular Mechanical Potentials". *J. Phys. Chem.* 96, 537-540, 1992.

Chapter 4

Parent Ketene Dimerization in Gas Phase: an extensive DFT Study

An extensive DFT study on gas-phase ketene dimerization is presented. Calculations on the ketene dimerization were carried out considering the following product dimers: diketene (d-I), cyclobutane-1,3-dione (d-II), 2,4-dimethylene-1,3-dioxetane (d-III) and 2-methyleneoxetan-3-one (d-IV). Single point calculations with different meta and hybrid functionals (58 in total) were applied on the optimized structure at PW86x+PBEc/DZP level to fix experimental values for the energy barrier and heat of reaction of the diketene product. Between the functionals applied in this study, the MPW1K functional had the lowest absolute deviation related to the experimental values. The results at the MPW1K level suggested that the diketene is the major product in gas phase because of a thermodynamic control of the reaction and that the d-III and d-IV dimers are unfeasible products from the dimerization in gas phase. Extended transition state (ETS) analysis demonstrated the transition state for the d-II dimer is favored over the corresponding transition state for the d-I dimer by the major orbital interaction[54] between its fragments.

4.1 Introduction

Ketenes are of major importance as starting materials in organic synthesis, for example, in the formation of β-lactams leading to penicillins by a [2+2] cycloadditions with imines,[1,2a-c] the formation of prostaglandin precursors,[2c-d] the syntheses of benzoquinones,[2e] the enantioselective synthesis of allenes,[2f] the synthesis of R-amino acid derivatives,[2g] and the production of ketene heterodimers for the synthesis of proteasome inhibitors.[2h] The reaction of the ketene (we refer to the parent ketene, $H_2C=C=O$, from this point onward unless otherwise stated) with itself was described almost simultaneously in 1908 by Chick and Wilsmore in England, and by Staudinger and Klever in Germany[3]. Among the products that may be formed during the ketene dimerization are diketene (d-I), cyclobutane-1,3-dione (d-II), 2,4-dimethylene-1,3-dioxetane (d-III) and 2-methyleneoxetan-3-one (d-IV). The structures of these products are shown in Figure 4.1. The highly reactive diketene, which is prepared on a multimillion pound per year scale by the pyrolysis of acetic acid, is an industrially important raw material used in the preparation of acetoacetates and acetoacetamides[3]. The diketene is also used for introducing functionalized C2, C3, and C4 units into organic compounds[2] as well as a potent bactericide useful for disinfecting

large areas[4]. The cyclobutane-1,3-dione can be used for the production of squaric acid which is an intermediate product for the production of pharmaceutical agents, dyes and herbicides[5]. The cyclobutane-1,3-dione ring was recently incorporated into a novel copolymer prepared by cycloaddition polymerization of the bisketene derived from 1,4-cyclohexanedicarbonyl chloride[6]. Polymers that contain the 1,3-dioxetane can be used as constituents of electrophotographic photoreceptor[7] and oil-based inks[8] in the photographic and lithographic industries, respectively. The oxetan-3-one structure has been found in numerous steroids whose biological activities include antiinflammatory activity and antiglucocorticoid activity, while some of them act as oral diuretics[9].

| d-I | d-II | d-III | d-IV |
| Diketene | cyclobutane-1,3-dione | 2,4-dimethylene-1,3-Dioxetane | 2-methyleneoxetan-3-one |
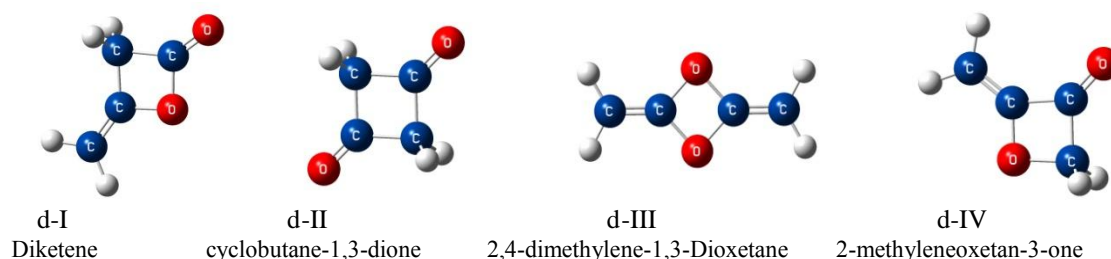
Figure 4.1. The structure of the ketene dimers studied in this work.

It is well known that the major product of the dimerization of the ketene is the diketene (d-I) while high weight ketenes dimerize to their corresponding cyclobutanedione structure (d-II)[2, 10]. Despite the industrial importance of diketene, there only are one experimental study and a few theoretical studies for explaining the trend of the dimerization for the lowest weight ketene (Chapter 1). In 1978, Jug et al.[11] studied experimentally the mechanism of the thermolysis of diketene in gas phase. They found both d-I and d-II dimers accessible from the ketene dimerization and assessed a very high activation energy[11] of 31 kcal per mol for the dimerization toward d-I. This fact could indicate the intervention of an external agent on the reaction in the liquid phase since it was found an activation energy barrier of only 11 kcal per mol in acetone[10]. Jug et al.[11] also assessed the heat of combustion of d-II dimer and found the d-II dimer to be 1 kcal per mol more stable than the d-I dimer. With this less stability for the d-I dimer its production could be due to a kinetic control of the reaction. Yet, this can not be conclusive since

ketene dimerization is carried out in liquid phase. Ketene in gas phase does not dimerize appreciably at room temperature or below[10, 11, 12, 13].

Several previous theoretical studies in gas phase have attempted to explain the predilection of the ketene to dimerize toward the d-I dimer instead of the d-II dimer using different levels of theory. In 1978, Jug and coworkers[14] investigated the thermolysis of diketene with a semiempirical SINDO method. They concluded that the energy barrier toward the d-I and d-II dimers were of the same magnitude and that the preference for the d-I dimer was based on the shape of the potential energy curve. In 1988, Fu and coworkers[15] studied the ketene dimerization using ab initio methods and they found that the d-I dimer is disfavored both kinetically and thermodynamically at the MP4/6-31G level. In 1991, Seidl and Shaefer[16] analyzed the reaction applying, among others, energy calculations at the CISD+Q/DZP level on the geometries optimized at the SCF/DZP level. Their conclusion was that the energy barrier toward the d-I dimer was lower than the energy barrier toward the d-II dimer and that the former was the observed product because of a kinetic control of reaction. In 1994, Salzner and Bachrach[17] obtained for the d-I dimer a higher energy barrier than for the d-II dimer at the MP2/6-31G*, MP4/6-31G* and CCSD(T)/6-31G* levels. In 2006, Rode and Dobrowolski[18] obtained the same tendency as in Salzner and Bachrach study at the MP2/aug-cc-pVDZ and in contrast with combustion data[11], the d-I dimer was found to be more stable than d-II dimer with the G3 multilevel method. A dynamic DFT study of Kelly and coworkers[19] suggested that the d-I dimer was the major product because of a thermodynamic control of the reaction. The preceding contradictions between the experimental and theoretical results suggest a reevaluation of the energy profile for the ketene dimerization in gas phase before attempting to calculate the reaction including a solvation model.

4.2 Computational details

Geometry optimizations and frequency calculations were applied using the exchange functional of Perdew-Wang (PW86x)[20] and the correlation functional of Perdew-Burke-Ernzerhof (PBEc)[21]. The standard double-ζ STO bases with one set of polarization functions were applied. The 1s electrons of C and O were treated within the frozen core approximation[22]. An auxiliary basis set

of s, p, d, f and g STOs was utilized to fit the molecular densities to represent the Coulomb and exchange potentials in each SCF cycle[23]. Gas phase electronic enthalpies were calculated from Kohn-Sham energies and standard expressions[24] were used to calculate the remaining gas phase enthalpic and entropic contributions at nonzero temperature, including zero point energy (ZPE) contribution. Linear transit search were carried out to localize transition states for each kind of dimer. The intrinsic reaction coordinate (IRC)[25] calculation was applied to verify the TS structures for each dimer. Single point calculations using different functionals (58 in total) were applied on the optimized structures. The calculations were carried out using the Amsterdam Density Functional (ADF) program package[26] version 2004.02.

4.3 Results and Discussion

4.3.1 Geometries

Some geometric results for the dimers and their corresponding transition state structures in gas phase are shown in Figures 2 and 3 respectively. Stationary points for the different structures were characterized by frequency calculations. The complete list of all geometries, moments of inertia, dipolar moments and frequencies for the dimers and their corresponding transition state structures are given in the annexes. The molecular parameters for the d-I dimer found in this work are in good agreement with theoretical predictions at different levels of theory[17, 18, 27]. We obtained the same tendency that in the other theoretical works[17, 18, 27] for the C–C and C–O bonds; thus, the longitude for the C–C bond adjacent to methylene group was found to be shorter than the longitude for the C–C bond adjacent to the carbonyl group. Similarly, the longitude for the C–O bond adjacent to the carbonyl group was found to be shorter than the longitude of the C–O bond adjacent to the methylene group (Figure 4.2). Such tendencies are in disagreement with the experimental molecular parameters obtained from electron diffraction[28] and X-ray crystallography[29]. The electron diffraction data predicted the same longitude for both the C–C bonds and the C–O bonds, whereas the X-ray crystallographic data predicted larger longitudes for both the C–C bond adjacent to the methylene group and for the C-O bond adjacent to the carbonyl group than those predicted by the theoretical procedures (Figure 4.2). Further

comments about the disagreements between theory and the experimental molecular structures can be found in Seidl and Schaefer's work[27].

The discrepancies among the different available molecular structures for the d-I dimer can be solved by comparing the corresponding values for the predicted rotational constants with those obtained from microwave spectrum[30]. The rotational constants for the d-I dimer are compared in Table 4.1 for the theoretical and experimental molecular structures. As it can be seen, the values predicted in this work at the PW86x+PBEc/DZP level show an absolute deviation of 56 MHz related to the experimental values from the microwave spectrum. This absolute deviation is the smallest value among the calculated deviation for the theoretical and the experimental molecular structures for the d-I dimer. This suggests that the geometric parameters predicted at the PW86x+PBEc/DZP level of theory are the appropriate parameters for the molecular structure for the d-I dimer. For the other dimers, there are no experimental geometric data available in the literature. However, the results obtained in this work are in good agreement with previous predictions at MP2/6-31G(d) level[17] and at MP2/aug-cc-pVDZ level[18] of theory (Figure 4.2). According to the facts presented in this section it is expected that the geometric parameters for the ketene dimers and for their transition states are well predicted by using the PW86x exchange functional[20], the PBEc correlation functional[21] and the DZP basis set.

The linear transit searches for the d-I dimer and for the d-II dimer (Graph 4.1) show that rearrangement between these dimers need only a rotation around the new formed 1C–4C bond in the transition state structures (TS). Such an isomerization was observed experimentally for the d-I type dimer of p-methoxyphenylketene by the reaction with potassium hydroxide in aqueous dioxane[31a] and for the d-II type dimer of the dimethylketene when heated with a trace of aluminum chloride[31b]. The TS structures for each dimer were found using the highest point of the corresponding linear transit search (Graphs 1, 2 and 3).

Previous TS structures for the d-I dimer (TS d-I) and the d-II dimer (TS d-II) calculated by Salzner and Bachrach[17] at the MP2/6-31G(d) level and by Rode and Dobrowolski[18] at the MP2/aug-cc-pVDZ level are in relative agreement with these found in this work (Figure 4.3). The major differences among the results correspond to the distances for the new 1C–4C and 3O–

2C bonds in the TS d-I and for the new 1C–4C and 5C–2C bonds in the TS d-II. The distances predicted by Salzner and Bachrach[17] for the formed 1C–4C bond and the quasi-formed 3O–2C bond of TS d-I are in good agreement with the distances predicted in this work. However, these authors predicted a large distance for the formed 1C–4C bond in the TS d-II. With respect to the results of Rode and Dobrowolski[18] for both the TS d-I structure and the TS d-II structure, their calculated distances for the formed and the quasi-formed bonds were found to be shorter and larger, respectively, than our predictions.
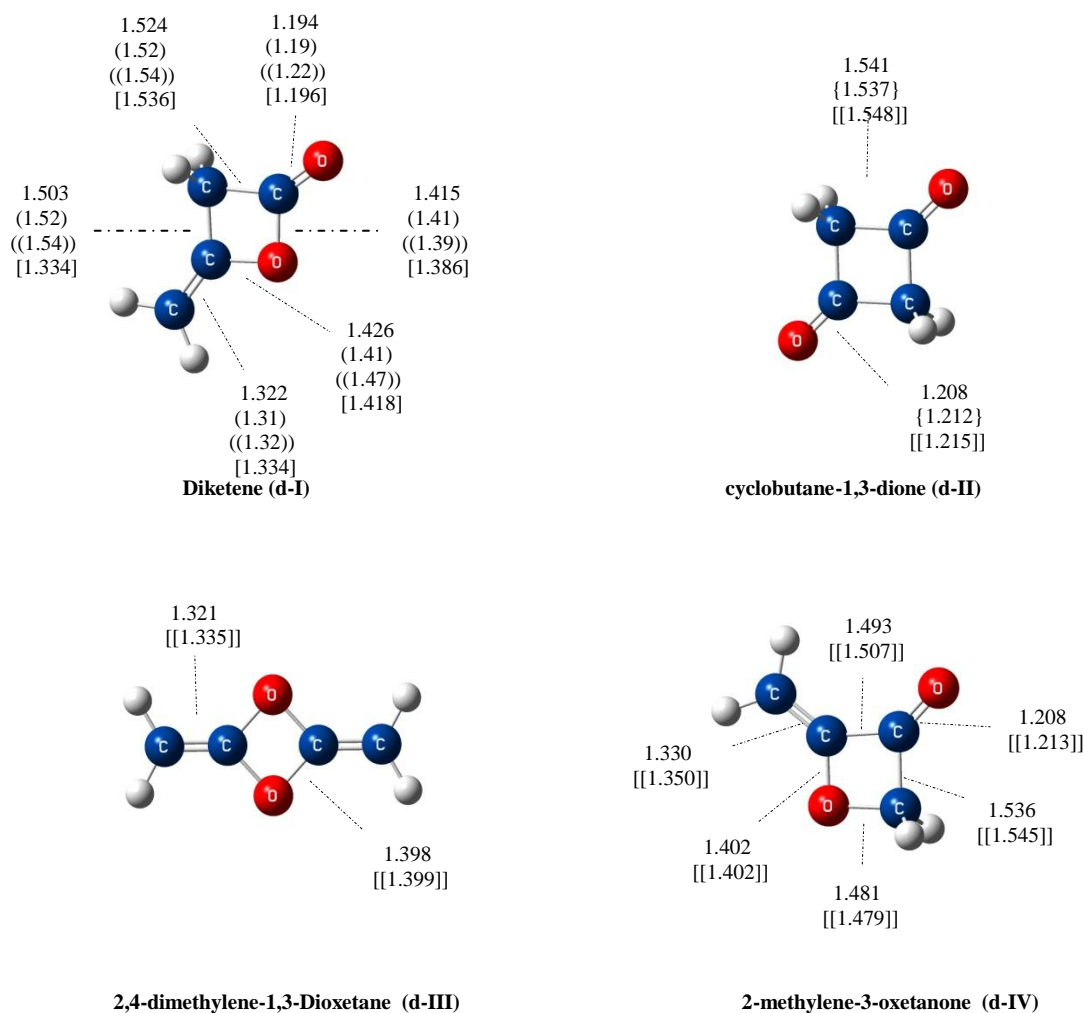
Figure 4.2. Some bond lengths for ketene dimers in gas phase in Å. Electron diffraction in parenthesis Ref. 28. X-ray spectrum in double parenthesis Ref. 29. Theoretical prediction of Seidl and Schaefer in brackets Ref. 27. Theoretical prediction at the MP2/6-31G(d) level in braces Ref. 17. Theoretical prediction at the MP2/aug-cc-pVDZ level in double brackets Ref. 18.

129

Table 4.1. Rotational constants for the d-I dimer in MHz*.

Method	A	B	C	Absolute
Microwave spectrum[30]	12141.36 ± 0.04	2781.27 ± 0.01	2296.59 ± 0.01	-----
Electron diffraction[28]	11711 (-430)	2846 (65)	2323 (26)	521
X-ray crystallography[29]	11757 (-387)	2736 (-45)	2250 (-47)	479
MP2/aug-cc-pVDZ[18]	12053 (-88)	2716 (-65)	2249 (-47)	200
CISD/DZd[27]	12289 (148)	2798 (17)	2313 (16)	181
CCSD/DZd[27]	12051 (-90)	2747 (-34)	2270 (-27)	151
MP2/6-31G(d)[17]	12044 (-97)	2777 (-4)	2290 (-6)	107
PW86x+PBEc/DZP	*12139 (2)*	*2749 (32)*	*2274 (22)*	*56*

* Numbers in parenthesis indicate the deviation from experimental microwave results. Rotational constants for the electron diffraction and X-ray structures were taken from ref. 27.
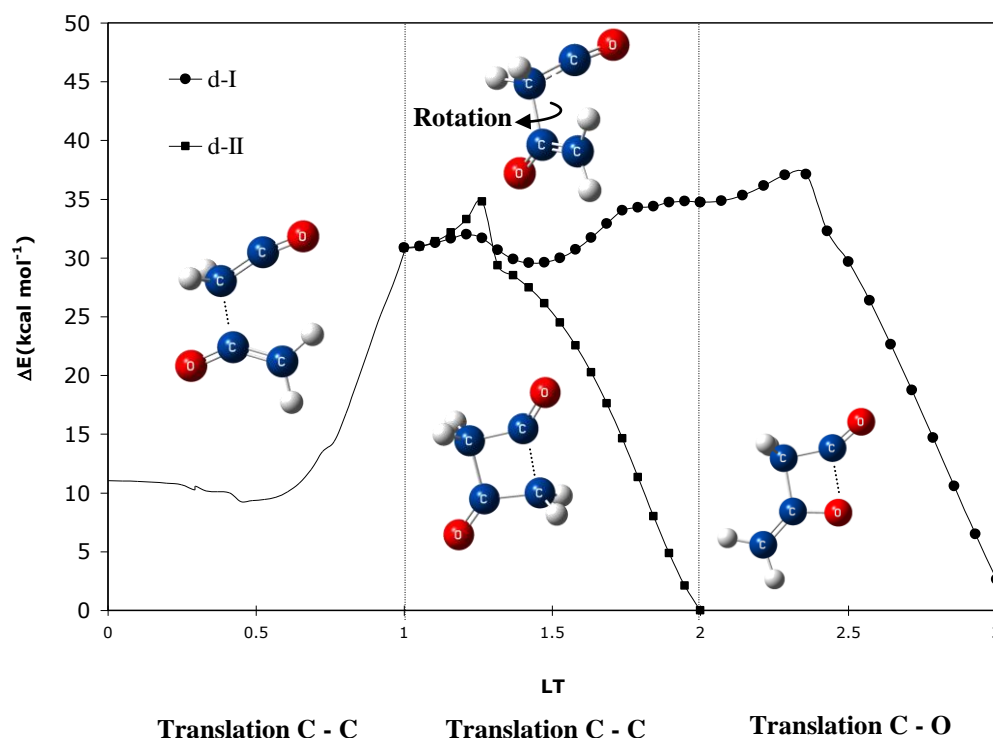
Graph 4.1. Linear transit search profiles at the PW86x+PBEc/DZP level in reduced coordinates for the ketene dimerization toward the diketene and toward the cyclobutane-1,3-dione in gas phase.
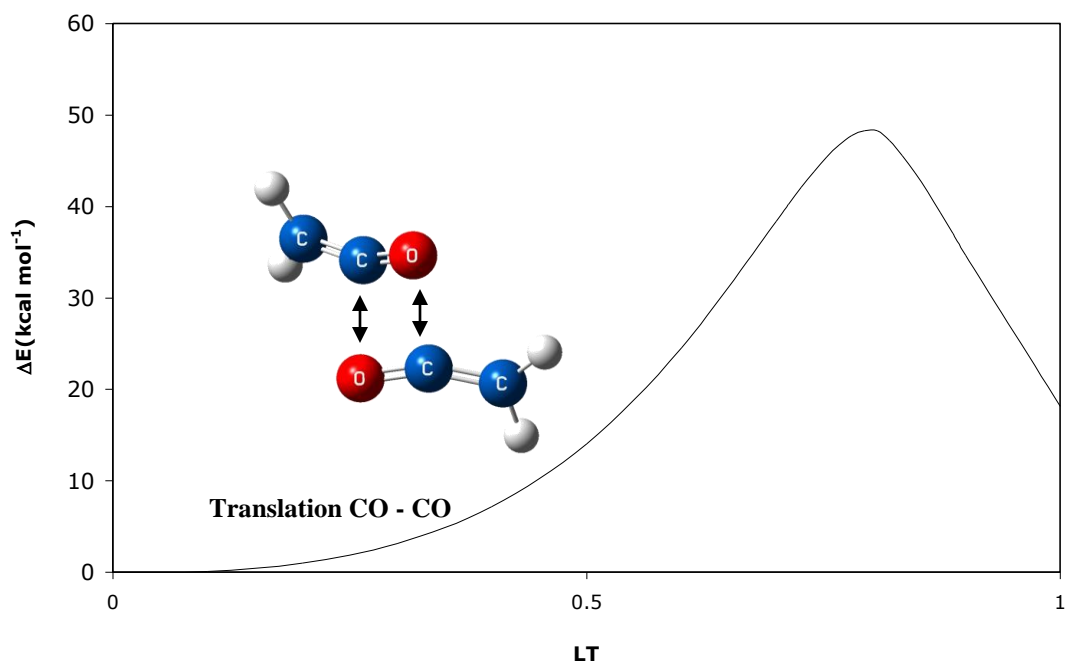
Graph 4.2. Linear transit search profile at the PW86x+PBEc/DZP level in reduced coordinate for the ketene dimerization toward the d-III dimer in gas phase.
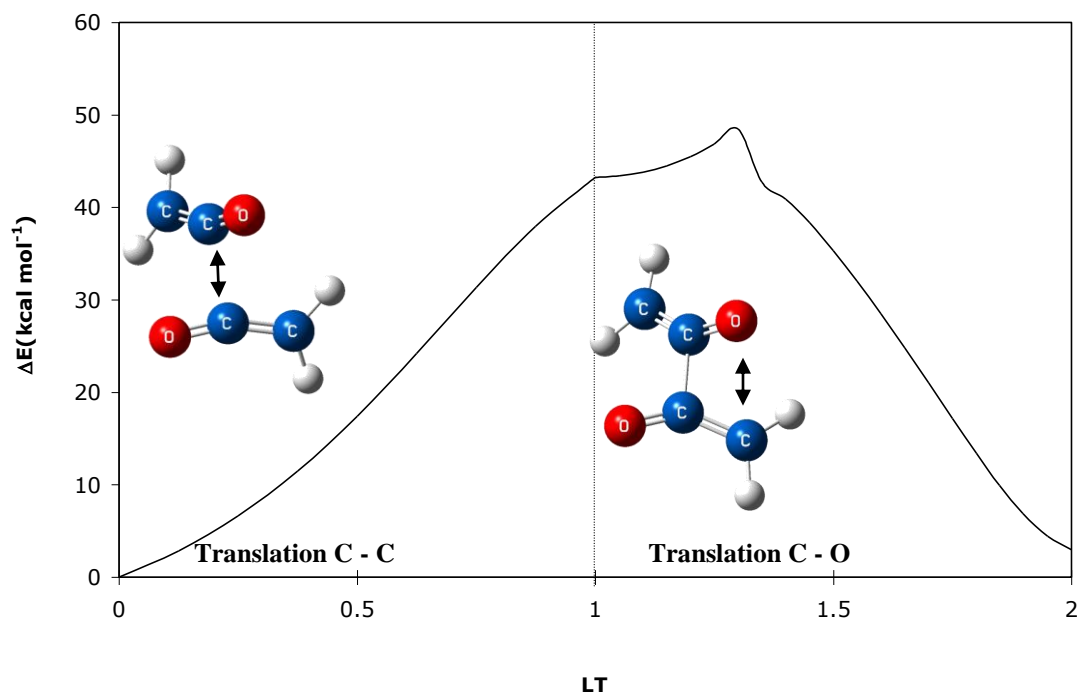
Graph 4.3. Linear transit search profile at the PW86x+PBEc/DZP level in reduced coordinate for the ketene dimerization toward the d-IV dimer in gas phase.

Thus, according to the preceding facts we can remark that our estimated geometry for the TS d-II corresponds to an intermediate geometry, approximately, between the calculated by Salzner and Bachrach and by Rode and Dobrowolski. As the difference in the results between these authors corresponds to the basis set, it is also worth to say that for the MP2 level, the 6-31G(d) basis set favors the prediction of the geometry for TS d-I, whereas the geometries predicted with the aug-cc-pVDZ basis set for both the TS d-I and the TS d-II have approximately the same error in the length of the new formed bonds. The errors in the prediction of the geometry for TS d-II with each of those basis sets have the same order of magnitude and the differences between the estimations using those basis set are compensated with the distances between the formed 1C–4C bond and the quasi-formed 5C–2C bonds. According to this, the 6-31G(d) basis set predicts much better the molecular structure of the transition state for the dimers than the aug-cc-pVDZ basis set. This relative good performance of medium-size gaussian basis sets over the aug-cc-pVDZ basis set in the prediction of the geometry for small organic compounds has been reported elsewhere[32].

The TS structures obtained in this work are in agreement with the conclusion[18] that the dimerization reactions toward the d-I dimer and toward the d-II dimer proceed by neither $[_\pi 2_s +_\pi 2_a]$ nor $[_\pi 2_s +_\pi 2_s +_\pi 2_s]$ mechanisms of Woodward-Hoffmann[33] for pericyclic reactions (see Figure 4.3 and Chart 4.3). In the dimerization of two ketenes, each monomer makes use of a set of (π_{CC}/π^*_{CC}) orbitals (Chart 4.1) on the C=C double bond and a (π_{CO}/π^*_{CO}) set of orbitals (Chart 4.2) on the CO group. The two sets are perpendicular to each other and therefore concede special characteristics to the reaction. A synchronous and coplanar approach in TS d-I and TS d-II would have resulted in a $[_\pi 2_s +_\pi 2_a]$ symmetry forbidden cycloaddition.[33] By adopting instead a nonplanar asynchronous approach the initial part of the dimerization process, leading to the formation of the 1C-4C bond, can be viewed as an allowed nucleophilic attack of 4C, using the occupied π_{CC} orbital, Chart 4.3. In TS d-I, the subsequent attack of 3O (with π_{CO}) on 2C (with the virtual π^*_{CC}) leading to the 3O-2C bond can take place without any further rearrangement as $\omega(2,4,1,3)$ tends to zero.
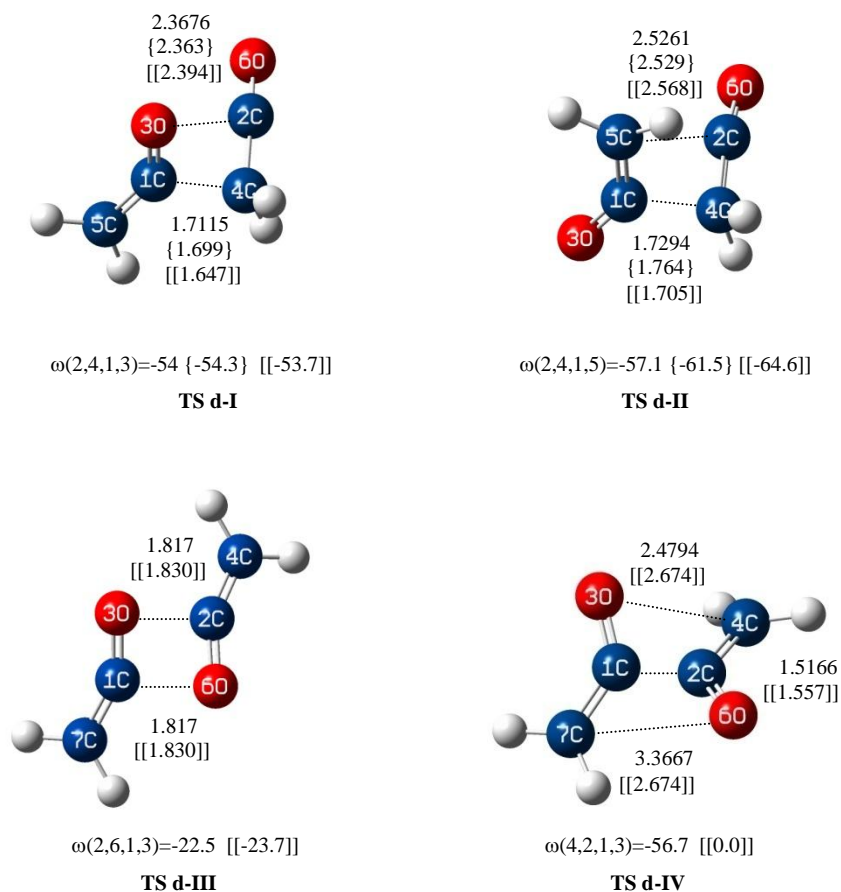
Figure 4.3. Some geometric measurements for transition state of ketene dimers in gas phase (bond lengths in Å). Prediction at the MP2/6-31G(d) level in braces Ref. 17. Prediction at the MP2/aug-cc-pVDZ level in double brackets Ref. 18.

In TS d-II, the second 5C-2C bond-making step must be accompanied by the rotation of the methylene group around the former 4C=2C double bound. It follows from Graph 4.4 and Graph 4.5, where we depict the IRC to the two dimerization processes leading to d-I and d-II, that the second rearrangement step involving 3O-2C or 5C-2C bond formation takes place without a second energy barrier. Thus, once TS d-I and TS d-II has been reached, the energy decreases all the way down to the product. The two-step cycloaddition mechanism discussed here has also been analyzed in ketene addition to $CH_2=CH_2$, $CH_2=O$ and $CpO_2Re=O$ by Deubel[34]. It is referred to as a nonplanar pseudopericyclic reaction.[18]
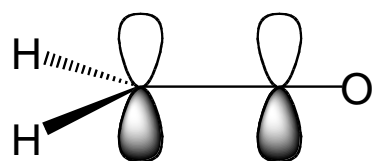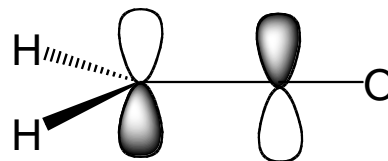
Chart 4.1. Occupied and virtual orbitals on the C=C double bond of ketene monomer.
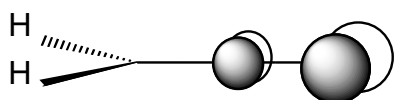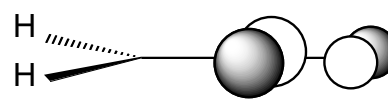
Chart 4.2. Occupied and virtual orbitals on the CO group of ketene monomer.
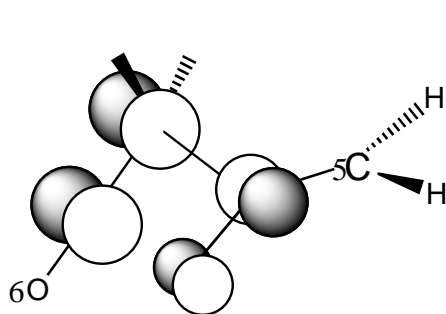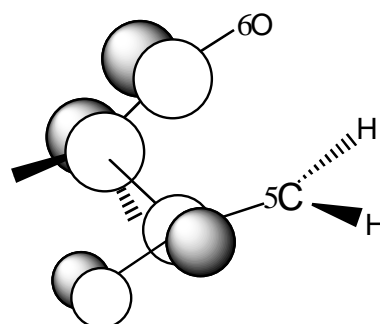
Chart 4.3. Virtual and occupied orbitals involved in the formation of TS d-I and TS d-II.

134

Table 4.2. Bond order for the transition states based on the Mayer methodology[35].

Structure	Bond	Bond Order	Structure	Bond	Bond Order
TS d-I	1C-4C	0.680	TS d-III	1C-6O	0.455
	3O-2C	0.203		3O-2C	0.456
TS d-II	1C-4C	0.665	TS d-IV	1C-2C	0.873
	5C-2C	0.255		3O-4C	0.345
				7C-6O	0.103
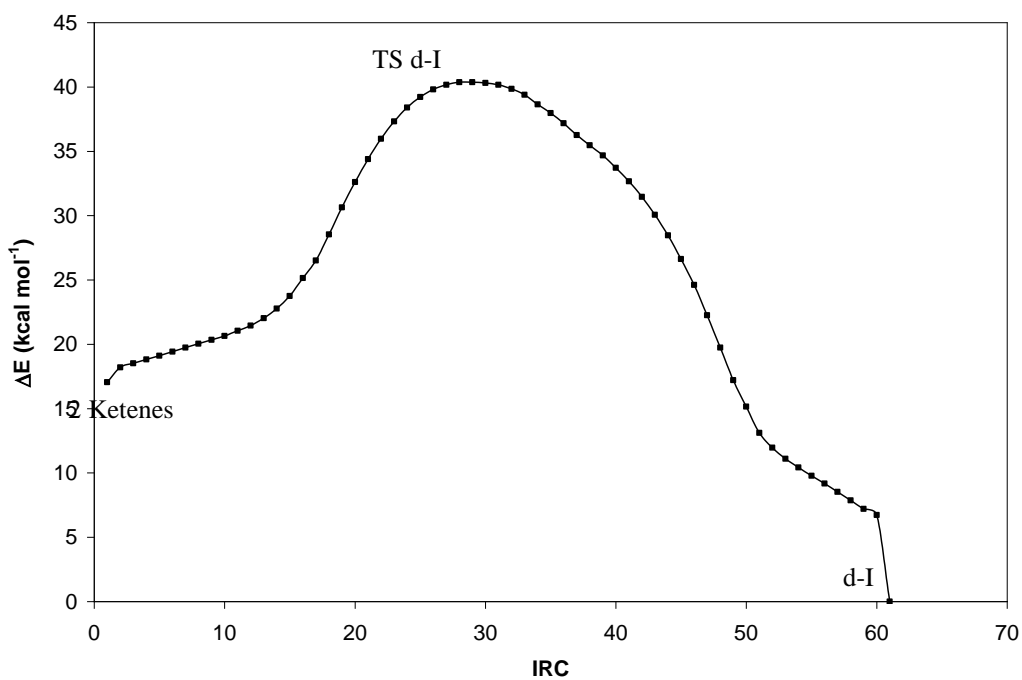
Graph 4.4. The IRC profile at the PW86x+PBEc/DZP level for the ketene dimerization toward diketene.
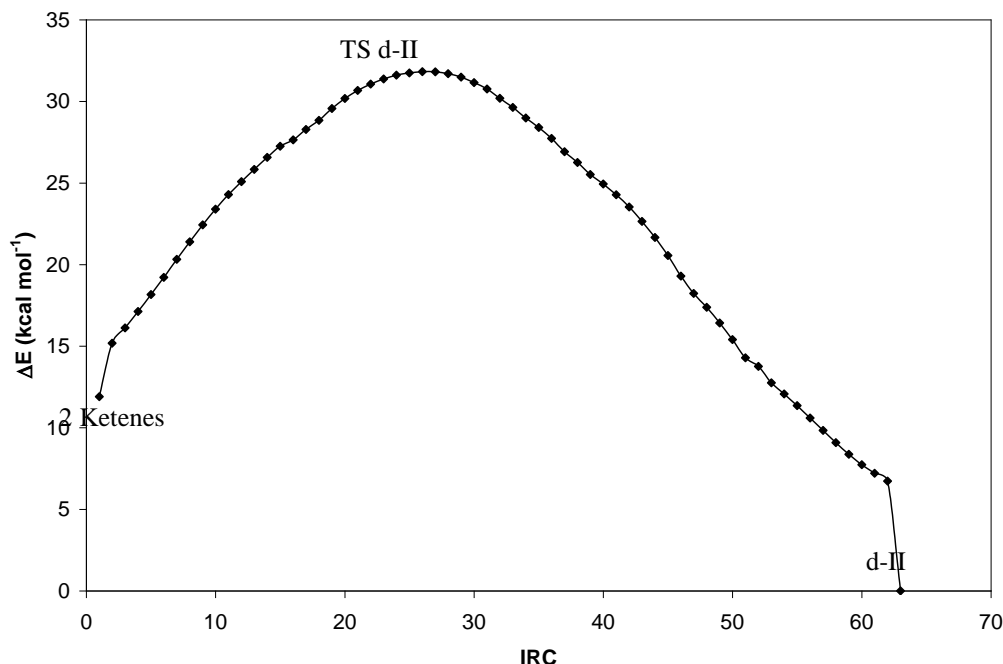
Graph 4.5. The IRC profile at the PW86x+PBEc/DZP level for the ketene dimerization toward cyclobutane-1,3-dione.

The dimerization towards the d-III and d-IV dimers has been studied to a lesser degree than the process towards the d-I and d-II dimers. In 1978, Jug and coworkers[14] using the semiempirical method SINDO, concluded that the reaction for the formation of the d-III dimer is not synchronous and that there might be formed an intermediate during the reactions for the dimers I and III. In 1988 Fu, Decai and Yanbo[15] analyzed the dimerization reaction using HF/STO-3G. These authors concluded that TS d-III is the result of a $[_{\pi}2_s+_{\pi}2_s]$ mechanism which is thermally forbidden according to Woodward-Hoffmann rules[41]. Very recently, Rode and Dobrowolski[18] analyzed the mechanisms for the production of the d-III and d-IV dimers using MP2/aug-cc-pVDZ. They obtained a synchronous non-planar quasi-formed ring for the geometry of TS d-III and a no synchronous planar structure with symmetry C_{2h} for the TS d-IV. These authors classified the reaction toward the d-III dimer as pericyclic and toward the d-IV dimer as pseudopericyclic according to the results of their AIM study. The geometry and the intrinsic reaction coordinate pathway (Graph 4.6) obtained in this work for the formation of the d-III dimer are in good agreement with the results of Rode and Dobrowolski[18]. We analyzed the synchronous planar TS for the d-III dimer proposed by Fu, Decai and Yanbo[15] and found that

136

according to the single point calculations the planar TS structure is approximately 1.5 kcal mol^{-1} less stable than the non planar one at the MPW1K level. That suggests that the TS d-III is non-planar but still synchronous (Table 4.2) and that the cycloaddition reaction towards the d-III dimer might be classified as pericyclic. TS d-III, yet with a slightly puckered transition state (ω(2,6,1,3)=-22.5), is consistent with a thermal forbidden [$_\pi$2$_s$+$_\pi$2$_s$] where the bond formation involves the two (π_{CO}/π^*_{CO}) sets of orbitals on the CO group (Chart 4.2).

The formation of d-IV is, according to our results for TS d-IV (Figure 4.7), asynchronous. As in TS d-I, the first step is C-C formation. However, in contrast to TS d-I where use was made of the occupied π_{CC} orbital and the virtual π^*_{CO} orbital (Chart 4.3), the process on TS d-IV involves the π_{CO} orbital on the monomer and the π^*_{CO} on the other hand. After formation of the 1C-2C bond in TS d-IV, the methylene group containing 1C has to rotate prior to formation of the 3O-4C bond. It is clear from Graph 4.5 where IRC energy profile for d-IV dimer is displayed that no intermediate (or second transition state) is located between TS d-IV and the product d-IV. Our structure for the TS d-IV is in disagreement with the planar structure proposed by Rode and Dobrowolski[18]. We carried out additional calculations enforcing the symmetry obtained for Rode and Dobrowolski. However, we could not find any transition state with the C_{2h} symmetry for the TS d-IV at the PW86x+PBEc/DZP level. Additionally, we applied single point calculations at the MPW1K level obtaining a barrier of 111.12 kcal mol^{-1} for the TS d-IV of Rode and Dobrowolski. This barrier is much greater than the value of 65.2 kcal per mol obtained in this work for the TS d-IV at the same level of theory. This relative stabilization of the TS d-IV may be explained by the short distance in the 1C–2C formed bond (Figure 4.3 and Table 4.2). The results above suggest a reclassification of the reaction toward the d-IV dimer as nonplanar-pseudopericyclic.

4.3.2 Energies

It has been reported that the experimental activation energy[11] and the heat of reaction[36] of diketene dimer (d-I) are 31 kcal per mol and -22.6 kcal per mol, respectively. Further on, d-I was found experimentally[11] to be less stable than d-II dimer by 1 kcal per mol in the gas phase. Experimental activation parameters in the gas phase have not been reported for the dimerization to d-II. We carried out single point calculations with different meta functionals and hybrid

functionals available in the ADF package based on the optimized structures at the PW86x+PBEc/DZP level in order to obtain the functional that best fits the reported experimental values. The complete list of the 58 studied functionals can be found in annexes. Table 4.3 shows the results for the activation energy and the heat of reaction of the best eleven functionals according to deviation in the activation energy for the d-I dimer. Similarly, Table 4.4 shows the results for the activation energy and the heat of reaction of the best eleven functionals according to deviation in the heat of reaction for the d-I dimer. The results of Tables 4.3 and 4.4 for the deviation of the theoretical predictions with respect to the experimental values for the d-I dimer can be best visualized in Graphs 8a and 8b respectively.

According to the results in Table 4.3 and Graph 4.8a, the XLP functional of Xu and Goddard[37] has the smallest deviation in the prediction of the activation energy barrier for the d-I dimer (+0.2 kcal mol^{-1}). However, the other eleven functionals have deviations which are between the expected theoretical and experimental errors. Thus, even the eleventh best functional, the modified Perdew-Wang 1-parameter model for kinetics (MPW1K) of Lynch and co-workers[38], with a deviation of +1.05 kcal mol^{-1} might reproduce adequately the value of the activation energy barrier for the d-I dimer. On the other hand, the results in Table 4.4 and Graph 4.8b show that the PBE0 functional[39] predicts with less deviation the experimental heat of reaction for the production of the d-I dimer. It is worth to say that the MPW1K functional is the second best in predicting the heat of reaction even though it was created to fit the activation energy barrier of reactions[38].

In what is likely the most extensive DFT study on ketene dimerization to date, it was found that the majority of the 58 tested functionals have better performance in predicting the activation energy barrier than the heat of reaction for the d-I dimer. As can be seen in Graph 4.8, the majority of the eleven functionals which reproduce the activation energy with high precision fail in reproducing the value for the heat of reaction. Only the hybrid MPW1K functional appears in the lists of the eleven functionals with less deviation in the prediction of both the activation energy and the heat of reaction (Tables 4.3 and 4.4).

138
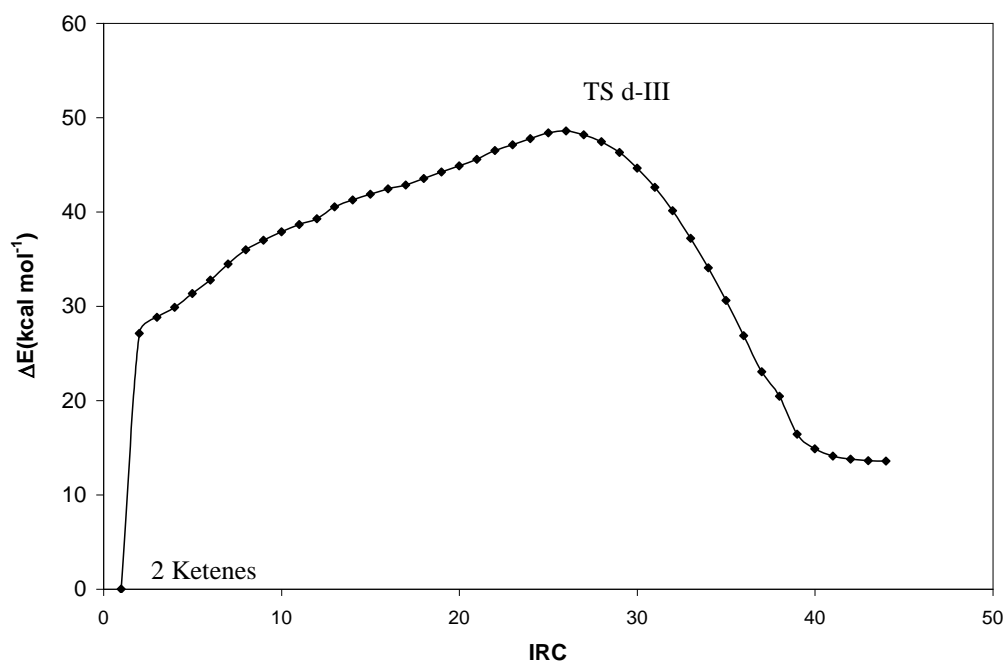
Graph 4.6. The IRC profile at the PW86x+PBEc/DZP level for the ketene dimerization toward d-III dimer.
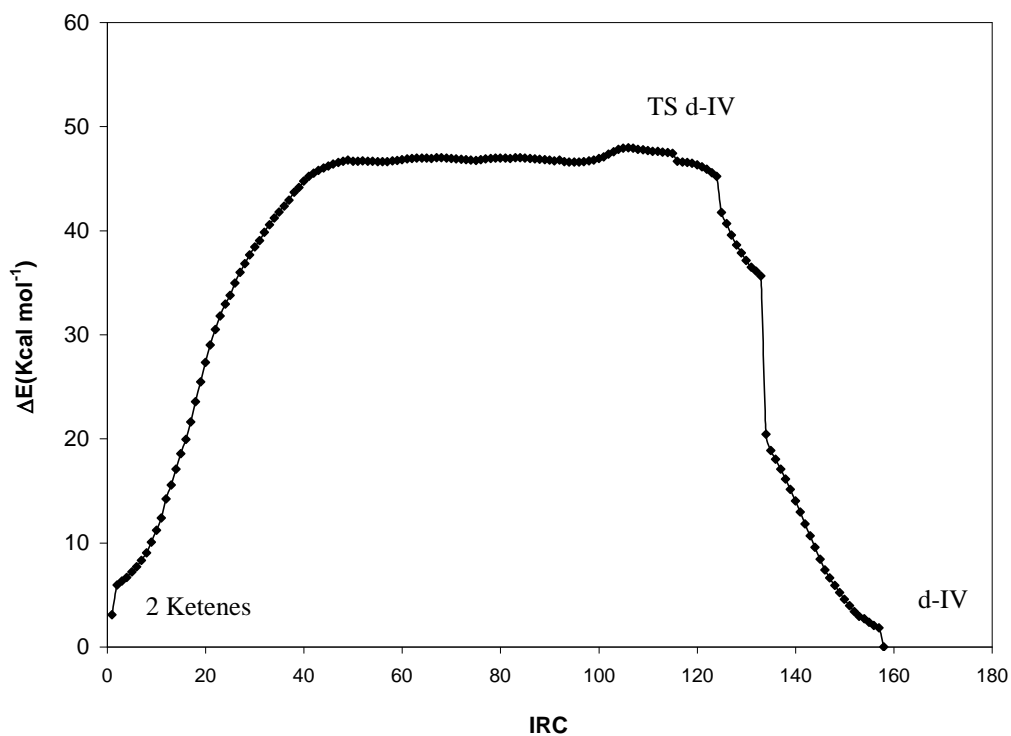
Graph 4.7. The IRC profile at the PW86x+PBEc/DZP level for the ketene dimerization toward d-IV dimer.

This functional reproduces with excellent agreement the experimental values for the diketene dimer and has the best overall performance among the tested functionals in this work (Table 4.5). Consequently, the MPW1K functional was selected to study the ketene dimerization reaction in both gas and liquid phase. The B1PW91[40] and the MPW1PW[41] functionals, which belong to the same family as the MPW1K functional, are in the second and third place, respectively, in the list of the best functionals for predicting the experimental values of the d-I dimer (Table 4.5).

Figure 4.4 shows the relative enthalpies for the ketene dimerization reaction at 298.15 K and 1 atm based on the energies calculated at the MPW1K/DZP//PW86x+PBEc/DZP level. According to this, the TS d-I is slightly less stable than the TS d-II by 0.92 kcal mol^{-1} and the TS d-III and TS d-IV have the largest values for the activation energy barrier. This suggests that both the d-I and d-II dimers are favored kinetically over both the d-III and d-IV dimers in gas phase. Similarly, for the heat of reaction, the d-I and d-II dimers were found to be the most stable dimers. Opposite to the tendency of the transition states, the d-I dimer was more stable than the d-II dimer. As a summary, the energetic of the reactions at the MPW1K/DZP level indicated that the d-I and d-II dimers are the principal product of the ketene dimerization in gas phase and that the d-I dimer may be the major product because of a thermodynamic control of the reaction.

The tendencies obtained with the MPW1K functional for the d-I and d-II dimers are also supported by the results with the other tested functionals. Of all the 58 studied functionals only three predicted an activation barrier for the d-I dimer lower than for the d-II dimer. These functionals are Becke00-x-only[42] with barriers of 43.59 and 44.39 kcal mol^{-1} for the d-I and d-II dimers respectively; KMLYP[43] with barriers of 29.47 and 29.76 kcal mol^{-1} for the d-I and d-II dimers respectively and BH&HLYP[44] with barriers of 36.12 and 36.15 kcal mol^{-1} for the d-I and d-II dimers respectively. The results of the 55 functionals suggest a high probability that the TS d-I is less stable than the TS d-II. On the other hand, all the functionals predicted that the d-I dimer is more stable than the d-II dimer. It has been controversial the relative energies between the d-I and d-II dimers and their corresponding transition states. Indeed, the results of the tendencies of the tested functionals in this work seem to be contradictory with the theoretical and experimental results.

Table 4.3. The best eleven functionals according to the deviation in the activation energy for the d-I dimer[*].

Functional	Activation Energy, kcal mol^{-1}				Heat of Reaction, kcal mol^{-1}			
	TS d-I	TS d-II	TS d-III	TS d-IV	d-I	d-II	d-III	d-IV
BLYP [7]	30.33	26.29	54.34	53.56	-7.09	-2.97	21.10	11.36
OLYP[12]	30.72	26.61	56.63	56.23	-10.68	-7.34	8.44	9.12
HCTH/93 [15]	31.41	27.39	57.48	57.41	-9.38	-5.79	19.79	10.65
HCTH/407 [18]	31.64	28.04	57.59	57.57	-8.43	-4.50	20.42	11.76
Becke00 [24]	31.75	28.66	57.78	58.17	-7.87	-4.50	21.29	11.55
XLYP [36]	30.80	26.81	54.83	53.70	-6.05	-2.02	22.17	12.14
B3LYP(VWN5) [40]	31.88	29.43	56.23	61.23	-12.42	-8.91	15.75	6.92
O3LYP(VWN5) [41]	30.11	27.20	56.05	59.50	-17.10	-13.62	12.03	3.48
B3LYP*(VWN5) [44]	30.09	27.21	54.29	58.24	-13.12	-9.30	14.93	6.27
MPW1K [55]	29.95	29.04	55.65	67.52	-24.24	-21.97	4.74	-3.10
X3LYP(VWN5) [57]	31.31	29.02	55.58	61.18	-13.65	-10.12	14.42	5.79

[*] The order of the functionals is given as in the ADF output file. Correction by ZPE is included in the results.

Table 4.4. The best eleven functionals according to the deviation in the heat of reaction for the d-I dimer[*].

Functional	Activation Energy, kcal mol^{-1}				Heat of Reaction, kcal mol^{-1}			
	TS d-I	TS d-II	TS d-III	TS d-IV	d-I	d-II	d-III	d-IV
PW91 [6]	22.01	17.64	46.90	47.31	-19.07	-15.12	9.59	0.84
PBE [9]	22.21	17.79	47.36	47.69	-18.87	-15.04	9.92	1.22
OPBE [31]	25.44	20.89	52.56	53.14	-19.48	-16.61	10.48	1.77
OPerdew [32]	24.37	19.98	50.84	51.67	-20.18	-16.88	9.33	0.90
TPSSh [39]	25.67	22.75	49.52	53.66	-19.27	-14.26	8.91	0.17
PBE0 [43]	25.81	23.42	51.33	58.55	-23.19	-20.24	5.66	-2.31
B97-1 [48]	27.02	24.31	52.87	57.42	-18.90	-16.63	10.30	0.81
MPBE0KCIS [50]	29.37	26.95	55.31	61.92	-17.75	-15.48	11.34	3.07
B1PW91(VWN5) [53]	28.36	25.96	53.88	60.89	-20.33	-17.50	8.70	0.30
MPW1PW [54]	27.74	25.39	53.17	60.09	-20.72	-17.85	8.23	-0.22
MPW1K [55]	29.95	29.04	55.65	67.52	-24.24	-21.97	4.74	-3.10

[*] The order of the functionals is given as in the ADF output file. Correction by ZPE is included in the results.

Table 4.5. Best functionals in predicting the experimental values for the d-I dimer in kcal mol^{-1}.

Functional	$\in E_a^*$	$\in \Delta H_r^*$	$\lvert \in E_a \rvert + \lvert \in \Delta H_r \rvert$
MPW1K [55]	1.05	1.57	2.61
B1PW91 [53]	2.64	-2.34	4.99
MPW1PW [54]	3.26	-1.95	5.21
PBE0 [43]	5.19	0.52	5.71
O3LYP [41]	0.89	-5.57	6.46

[*] Deviation for the corresponding value. $\in$ = Experimental – Calculated.
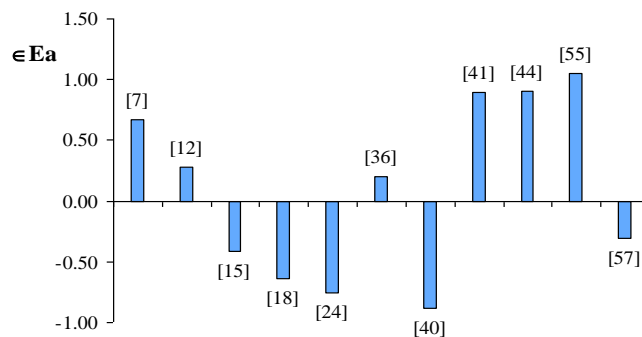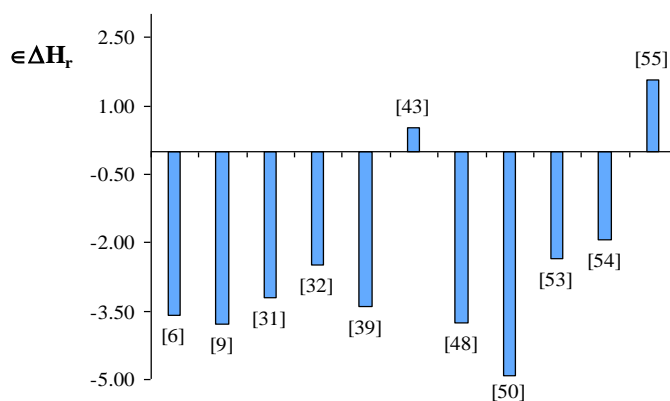
Graph 4.8. Deviations for the best eleven functionals with respect to the experimental values in kcal per mol. (a) Energy barrier. (b) Heat of reaction.

In 1990, Seidl & Schaefer[45] analyzed the relative stability of the d-I, d-II and d-III dimers at the CISD, CISD+Q and CCSD levels and they found that the d-I dimer was less stable than the d-II dimer and that the d-III dimer was not a thermodynamically-favorable product. In 1991, Seidl and Shaefer[16] analyzed the dimerization reaction applying energy calculations at the CISD+Q/DZP level among others. Their conclusion was that the TS d-I dimer was higher in energy than the TS d-II dimer and that the former was formed because of a kinetic control of reaction. However, the energy calculations of Seidl and Schaefer were based on the geometry at the SCF/DZP level which reproduced poorly agreement with the experimental values for the rotational constant of the d-I dimer[27] (it was discussed in the preceding section). Possibly, their

good agreement with the experimental data for the d-I dimer was obtained by error compensation.
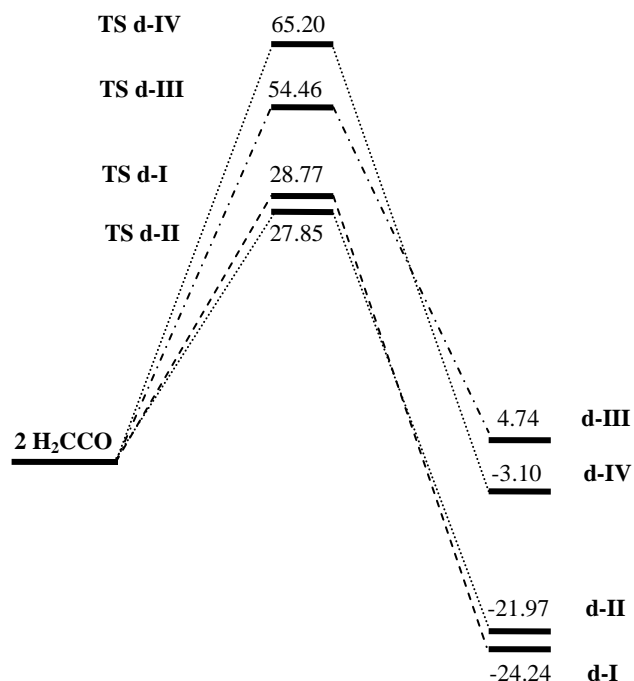
Figure 4.4. Relative enthalpies (1 atm and 298.15 K) for the ketene dimerization reaction according to the MPW1K/DZP//PW86x+PBEc/DZP level in kcal mol^{-1}. Correction by ZPE is included in the results.

In 1995, Salzner & Bachrach[17] studied the reaction for the d-I and d-II dimers using single point calculations at different levels of theory including CCSD and CCSD(T) on the optimized structures at MP2/6-31* level. They found that the energy difference between TS d-I and TS d-II was sensitive to the employed computational method and that the d-I dimer was less stable than the d-II dimer at all levels of theory that they used. In 2006, Rode and Dobrowolski[18] analyzed the system using the MP2/aug-cc-pVDZ level and the G3 multilevel method. They found that in the former level the TS d-I was less stable than the TS d-II, but in the latter level the TS d-I was more stable than the TS d-II by 0.4 kcal mol^{-1}. With respect to the heat of reaction, Rode and Dobrowolski[18] pointed out that dimer d-I was favored thermodynamically at the G3 level but the

d-II dimer was favored thermodynamically at the MP2/aug-cc-pVDZ level. Another calculation[46] at the CBS-Q multilevel obtained that the d-I dimer was more stable than the d-II dimer by ca. 3 kcal/mol. As a conclusion, it seems that both the prediction of the energy barrier and the heat of reaction for the d-I and d-II dimers are very sensitive to the level of applied theory.

In fact, the theoretical results suggest that the geometries predicted with medium-size basis sets (6-31G*)[17] and with low level of theories (HF and MP2)[27, 17] tend to favor the relative stability of TS d-I over TS d-II and to disfavor the relative stability of the d-I dimer over the d-II dimer. The tendencies that the TS d-I is disfavored kinetically and that the d-I dimer is favored thermodynamically obtained in this work are in agreement with the tendencies obtained in the dynamic study of Kelly and coworkers[19]. With respect to the other static studies, in general, our tendency agrees with the tendency obtained using medium-size gaussian basis set[17] for predicting the energy barrier and with the tendency obtained using multilevel methods for predicting the heat of reaction[18, 46]. However, the calculated differences for the activation barrier toward d-I and d-II and for the relative stability of these dimers are too small to make definitive conclusions.

Experimentally[11], the d-I dimer was found to be less stable than the d-II dimer for almost 1 kcal mol^{-1}. This seems to contradict our results; however, the differences between experiment and theory have been typical for the ketene compounds. An example of this disagreement appeared in the determination of the heat of formation for methylketene and dimethylketene[47, 48, 49]. Nonetheless, such differences in these results seem to be resolved by a measurement with the threshold mass spectrometry[49]. This last experimental value favored the theoretical-predicted values of the heat of formation for both the methylketene and the dimethylketene. This example and the historical-structure elucidation[4] of the d-I dimer provide an interesting insight into the difficulties associated with the experimental manipulation of this class of unstable compounds. Thus, there is a high probability that the d-I dimer is more stable than the d-II dimer as it is predicted by several high level theoretical methods.

By the other hand, the less stability of TS d-I may not be opposite to the experimental findings in gas phase since there is only one measurement for the energy barrier of the dimerization reaction based on the thermolysis of the d-I dimer in gas phase[11]. Thus, we do not have a direct

experimental point of comparison for the energy barrier of both the d-I and d-II dimers in gas phase. Since the dimerization reaction has been carried out in solution[10, 11, 13, 50, 51, 52], the inclusion of the solvent effects could clarify the energy barrier tendencies for the ketene dimerization reaction toward the different product dimers. According to the discussed facts, we suggest that new experimental measurements on the heat of formation for the d-I and d-II dimers and kinetic studies on the ketene dimerization with modern instrumental techniques of detection.

As it was mentioned in the preceding section, there are more studies for the d-I and d-II dimers than for the d-III and d-IV dimers. For the d-III dimer, Fu, Decay and Yanbo[15] found an activation barrier of 61.2 kcal per mol and a heat of reaction of 28.2 kcal per mol at MP2/4-31G level of theory. Rode and Dobrowolski[18] at MP2/aug-cc-pVDZ level predicted a free energy barrier of activation of 63.97 kcal mol^{-1} for TS d-III and energy of activation of 67.34 kcal mol^{-1} for TS d-IV. These authors predicted the heat of reactions of 12.53 kcal mol^{-1} and -0.82 kcal per mol for the d-III and d-IV dimers, respectively, at the same level of theory. Therefore, the tendencies obtained in this work for the d-III and d-IV dimers are in agreement with those in Rode and Dobrowolski. Nonetheless, the stabilities predicted with MPW1K are greater than those predicted by Rode and Dobrowolski at the MP2/aug-cc-pVDZ level for the d-III and d-IV dimers, as in the case for the d-I and d-II dimers. It is worth to say that the results for the energy barrier at the MP2/aug-cc-pVDZ level are in less qualitative agreement with the functional MPW1K for the TS d-I and d-II than for the TS d-III and d-IV. In general, the energy barriers predicted at the MP2/aug-cc-pVDZ level for the transition structure of the dimers seem to be lower than that predicted at the MPW1K/DZP level.

4.3.3 Extended Transition State Analysis

The extended transition state analysis[53] (ETS) gives information about the different interactions in the transition state and how these influence the activation barrier in the ketene dimerization reaction. In a first step of the ETS analysis, the energy of each reactant is calculated separately for the same geometry as in the transition state; accordingly, they are deformed from their equilibrium position and treated as single fragments. This first energy corresponds to the strain or deforming energy, ΔE_{str}. Table 4.10 shows the ETS analysis for the constituent fragments (F1 and F2) for the transition states of the ketene dimers in gas phase. For the case of the TS d-I and

the TS d-II, the F1 fragment has less strain energy than the F2 fragment. Therefore, the F1 fragment is less deformed than the F2 fragment. For the other transition states, the strain energies of the constituent F1 and F2 fragments have the same order of magnitude. The total strain energy is the sum of the strain energy of the constituent fragments in the transition state. The total strain energy for the transition state of the analyzed dimers has the following order TS d-IV > TS d-II > TS d-I > TS d-III. Thus, the formation of the ketenes for the generation of the TS d-IV involves the greatest strain energy (Table 4.6 and Graph 4.9).

In a second step of the ETS analysis, the fragments are allowed to interacting each other at the same distance as in the appropriate transition state. This calculation gives the interaction energy between the fragments, ΔE_{int}. This energy can be analyzed as the contribution from the electrostatic interaction, the repulsive interaction (Pauli principle) and the orbital interaction. The sum of ΔE_{str} and ΔE_{int} gives the energy barrier for the corresponding reaction. A better visualization of the results of the ETS analysis can be found in Graph 4.9. ETS analysis showed that the TS d-II is favored in gas phase by the interaction energy between the F1 and F2 fragments; particularly, the TS d-II is favored by the major orbital interaction[54] between its fragments. For doing this, the corresponding hydrogen orbitals of the methylene 5C group should be helping to favor the interaction of the monomers (Figure 4.3). Both the TS d-I and the TS d-II exhibit large electrostatic interactions which reinforced the concept of nucleophilic attack for representing the generation of the d-I and d-II dimers.

The strain energy for the TS d-III is comparable to the strain energy for the TS d-I and the TS d-II. However, the interaction energy between the fragments of the TS d-III is repulsive which makes the d-III dimer kinetically unfeasible. This can be explained by the low orbital interaction between its fragments[54] due to the high stereospecific arrangement in the $[_{\pi}2_s+_{\pi}2_s]$ mechanism[41]. The TS d-IV has the most favorable orbit interaction between the fragments[54] and its total interaction energy is the greatest energy among the analyzed dimers thereof (Table 4.6). However, the TS d-IV has the lowest value for the electrostatic interaction between the fragments as it has the most symmetric transition state (Table 4.6). In spite of the favorable value for the interaction energy, the large value of the total strain energy for the TS d-IV makes the d-IV dimer kinetically unfeasible. The TS d-IV proposed by Rode and Dobrowolski[18] was

analyzed using the ETS methodology. The results in Table 4.6 shows that the TS d-IV obtained in this work and the TS d-IV proposed by Rode and Dobrowolski[18] have comparable total strain energy. However, the interaction energy between the constituent fragments for the latter was found to be repulsive and therefore it makes its energy barrier higher. It was found that the orbital interaction energy is the term that affects most this repulsion interaction between the fragments[54].

Table 4.6. Extended transition state analysis[53]on the ketene dimers based on the MPW1K functional (in kcal mol^{-1})*.

TS	ΔE_{str} (F1)^a	ΔE_{str} (F2)^a	ΔE_{str} (Total)^b	ΔE_{ele}^{c}	$\Delta E_{Pauli} + \Delta E_{orb}$$^{d, e}$	ΔE_{int}^{f}	ΔE^g
d-I	11.60	34.61	46.21	-111.37	92.64	-18.73	27.49
d-II	15.71	36.34	52.02	-109.17	83.72	-25.45	26.60
d-III	22.65	22.65	45.30	-92.90	101.72	8.82	54.20
d-IV^h	51.84 (52)	59.43 (52)	111.27 (104)	-57.65	11.57	-46.08 (15.6)	65.19

* Energies based on the optimized geometries at the PW86x+PBEc/DZP level. Data for toluene and acetone are written in braces and brackets respectively. ^{a} Strain energy for the fragments. ^{b} Total strain energy. ^{c} Electrostatic interaction between F1 and F2. ^{d} Pauli repulsion and orbital interaction energy between F1 and F2. ^{e} The Pauli and orbital interaction terms in the gas phase could not be calculated separately for the MPW1K functional because the hybrid functionals are still not SCF calculated in the ADF package. Instead, the decomposition of the interaction energy at the PW86x+PBEc/DZP level is showed in Ref. 54. ^{f} Total interaction energy between F1 and F2. ^{g} Energy barrier. ^{h} Values in parenthesis correspond to the energies for the proposed transition state in the ref. 18.
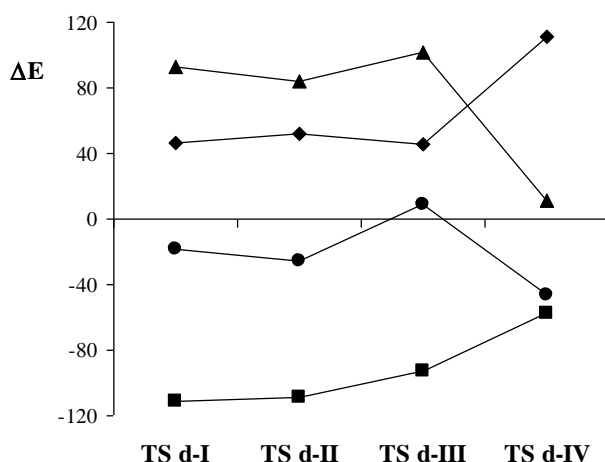
Graph 4.9. Contributions to the energy of the transition states in gas phase according to the ETS decomposition at the MPW1K level in kcal mol^{-1}. Energies based on the optimized geometries at the PW86x+PBEc/DZP level. ♦ Total strain. ■ Electrostatic interaction. ▲ (Pauli interaction + Orbital interaction). ● Total interaction between the fragments.

Conclusions

The results of this research give a better understanding of the ketene dimerization reaction in gas phase at the experimental conditions. The PW86x+PBEc/DZP calculated geometries predicted with excellent agreement the experimental rotational constants for the d-I dimer and therefore it is expected that the calculated geometries at the same level of theory for the other dimers and their transition states are well predicted. According to the TS structures and the IRC profiles in gas phase obtained in this work, the ketene dimerizations toward the d-I, d-II and d-IV dimers might be classified as nonplanar-pseudopericyclic reactions. The ketene dimerization toward the d-III dimer was found to be a pericyclic $[_\pi 2_s + _\pi 2_s]$ reaction with a nonplanar but still synchronous transition state.

The functional MPW1K had the best overall performance in predicting the experimental values for the activation energy barrier and the heat of reaction of the d-I dimer. The results obtained with the different functionals predicted that the TS d-I is less stable than the TS d-II in gas phase. Both the d-I and d-II dimers were found to be accessible and the d-I dimer appeared to be the major product because of a thermodynamic control of the reaction. All the 58 functionals used in this work predicted that the d-I dimer was more stable than the d-II dimer. This result could contradict the experimental data for the relative heat of combustion of these dimers. Therefore, new experimental measurements on the thermochemical properties for these dimers are called for.

The ETS analysis showed that that the TS d-I is slightly disfavored over the TS d-II by the less interaction energy between its constituent fragments, specifically, by the minor orbital interaction between its fragments. The d-III and d-IV dimers were found to be inaccessible in gas phase. The ETS analysis showed that the TS d-III was disfavored because of the large value of the Pauli repulsion term. Furthermore, the TS d-IV was found to be disfavored because of the large value of the total strain energy term and the small values of the orbital and electrostatic interaction terms.

148

References

(1) Ulrich Henri. *Cycloaddition Reactions of Heterocumulenes*. Academic Press: New York, London, 1967.

(2) (a) Holden, K. G. *Chemistry and Biology of β-Lactam Antibiotics*, Vol. 2; Morin, R. B.; Gorman, M., Eds.; Academic: New York, 1982. (b) Palomo, C.; Aizpurua, J. M.; Iñaki, G.; Oiarbide, M. "Asymmetric Synthesis of β-Lactams by Staudinger Ketene-Imine Cycloaddition Reaction", *Eur. J. Org. Chem.* 1999, 12, 3223–3235. (c) Tidwell, T. T. *Ketenes*; Wiley: New York, 1995 and references therein. (d) Collins, P. W.; Djuric, S. W. "Synthesis of Therapeutically Useful Prostaglandin and Prostaciclyn Analogs", *Chem. Rev.* 1993, 93, 1533–1564. (e) Foland, L. D.; Karlsson, J. O.; Perri, S. T.; Schwabe, R.; Xu, S. L.; Patil, S.; Moore, H. W. "Rearrangement of 4-Alkynylcyclobutenones. A New Synthesis of 1,4-Benzoquinones", *J. Am. Chem. Soc.* 1984, 111, 975–989. (f) Li, C. Y.; Wang, X. B.; Sun, X. L.; Tang, Y.; Zheng, J. C.: Xu, Z. H.; Zhou, Y. G.; Dai, L. X. "Iron Porphyrin-Catalized Olefination of Ketenes with Diazoacetate for the Enantioselective Synthesis of Allenes", *J. Am. Chem. Soc.* 2007, 129, 1494–1495. (g) Paull, D. H.; Alden-Danforth, E.; Wolfer, J.; Dogo-Isonagie, C.; Abraham, C. J.; Lectka, T. "An Asymmetric, Bifunctional Catalytic Approach to Non-Natural α-Amino Acid Derivatives", *J. Org. Chem.* 2007, 72, 5380–5382. (h) Ma, G.; Nguyen, H.; Romo, D. "Concise Total Synthesis of (±)-Salinosporamide A, (±)-Cinnabaramide A, and Derivatives via a Bis-cyclization Process: Implications for a Biosynthetic Pathway?", *Org. Lett.* 2007, 9, 2143–2146.

(3) Hyatt, J. A. and Raynolds, P. W. "Ketene Cycloadditions", *Org. Reactions*. 1994, 45, 160–246 and references therein.

(4) Clemens, R. J. "Diketene", *Chem. Rev.* 1986, 86, 241–318.

(5) Scholl, T. and Jackson, B. *"Process for the Production of Squaric Acid"*. US Patent 5.130.492, 1992.

(6) Naka, K.; Uemura, T; Chujo, Y. "Synthesis of Polymers Having cyclobutane-1,3-dione Unit in the Main Chain by Cycloaddition Polymerization of Bisketene", *Polym. Bull.* 1999, 42, 367–372.

(7) Kato, E. and Osawa, S. "Color Image Forming Method", *US Patent* 5.582.941, 1996.

(8) Nakazawa, Y.; Ishii, K.; Kato, E. *"Method of lithographic printing"*. US Patent 6.862.992, 2005.

(9) Dejaegher, Y.; Kuz'menok, N. M.; Zvonok, A. M.; De Kimpe, N. "The Chemistry of Azetidin-3-ones, Oxetan-3-ones, and Thietan-3-ones", *Chem. Rev.* 2002, 102, 29.

(10) Rice, F.O. and Greenberg, J. "Ketene II. Rate of Polymerization", *J. Am. Chem. Soc*. 1934, 56, 2132.

(11) Chickos, J. S.; Sherwood, D. E. Jr.; and Jug, K. "Mechanism of Thermolysis of Diketene in the Gas Phase", *J. Org. Chem*. 1978, 43, 1146.

(12) Barteau, M.; Huff, M.; Pogodda, U.; Martínez-Rey, R. *"Functionalized monolith catalyst and process for production of ketenes"*. US Patent 6.232.504, 1998.

(13) (a) Chick, F; Wilsmore, N. T. M. "Acetylketen: a Polymeride of Keten", *J. Chem. Soc.* 1908, 946–950. (b) Staudinger, H.; Klever, H. W. "Über Ketene. 6. Mitteilung: Keten", *Ber.* 1908, 41, 594–600. (c) Hallock, C. *"Process for Producing Ketene"*. US Patent 2.053.286, 1936.

(14) Jug, K.; Dwivedi, C. P. D.; Chickos, J. S. "Reaction Pathways for Various Ketene Dimers", *Theoret. Chim. Acta (Berl.)*. 1978, 49, 249.

(15) Fu, X. Y.; Decai, F.; Yanbo, D. "Theoretical Studies on the Reaction Mechanism of Ketene Dimerization Reactions", *J. Mol. Structure (THEOCHEM)*. 1988, 167, 349.

(16) Seidl, E. T. and Schaefer, H. F. III. "Theoretical Investigations on the Dimerization of Ketenes: Does the 2S + 2A Cycloaddition Reaction Exist?", *J. Am. Chem. Soc*. 1991, 113, 5195.

(17) Salzner, U. and Bachrach, M. S. "Ab Initio Studies of the Dimerization of Ketene and Phosphaketene", *J. Am. Chem. Soc*. 1994, 116, 6850.

(18) Rode, J. R. and Dobrowolski, J. Cz. "Reaction Paths of the [2 + 2] Cycloaddition of X=C=Y Molecules (X, Y = S or O or CH_2). Ab Initio Study", *J. Phys. Chem. A* 2006, 110, 207.

(19) Kelly, E.; Seth, M.; Ziegler, T. "Calculation of Free Energy Profiles for Elementary Bimolecular Reactions by ab Initio Molecular Dynamics: Sampling Methods and Thermostat Considerations", *J. Phys. Chem. A*, 2004, 108, 2167.

(20) Perdew, J.P. and Wang, Y. "Density-Functional Approximation for the Correlation Energy of the Inhomogeneous Electron Gas", *Physical Review B*. 1986, 33, 8822.

(21) Perdew, J.P.; Burke, K.; Ernzerhof, M. "Generalized Gradient Approximation Made Simple", *Physical Review Letters*. 1996, **77**, 3865.

(22) Baerends, E. J.; Ellis, D. E.; Ros, P. "Self-Consistent Molecular Hartree-Fock-Slater Calculations I. The Computational Procedure", *Chem. Phys.* 1973, 2, 41.

(23) Krijn, J. G. and Baerends, E. J. *Fit Functions in the HFS-Method*; Internal Report (in Dutch); Vrije Universiteit Amsterdam: Amsterdam, The Netherlands, 1984.

(24) McQuarrie, D. A. *Statistical Thermodynamics*; Harper: New York, 1973.

(25) Fukui, K. "The Path of Chemical Reactions – the IRC Approach", *Acc. Chem. Res*. 1981, 14, 363.

(26) Te Velde, G.; Bickelhaupt, F. M.; Baerends, E. J.; van Gisbergen, S.; Guerra, C. F.; Snijders, J. G.; Ziegler, T. "Chemistry with ADF", *J. Comput. Chem*. 2001, 22, 931.

(27) Seidl, E. T. and Schaefer, H. F. "Molecular Structure of Diketene: A Discrepancy between Theory and Experiments?", *J. Phys. Chem*. 1992, 96, 657.

(28) Bregman, J. and Bauer, S. H. "An Electron Diffraction Study of Ketene Dimer, Methylketene Dimer and β-Propiolactone", *J. Am. Chem. Soc*. 1955, 77, 1955.

(29) Kay, M.I. and Katz, L. "A Refinement of the Crystal Structure of Ketene Dimer", *Acta Crystallogr.* 1958, 11, 897.

(30) Mönnig, F.; Dreizler, H.; Rudolph, H. D. *Z. Naturforsch*, 1967, 22, 1471 – 1473.

(31) (a) Farnum, D. G.; Johnson, J. R.; Hess, R. E.; Marshall, T. B.;Webster, B. "Aldoketene Dimers and Trimers From Acid Chlorides. A Synthesis of Substituted 3-

Hydroxycyclobutenones", *J. Am. Chem. Soc*. 1965, 87, 5191–5197. (b) Hasek, R H.; Clark, R. D.; Elam, E. U.; Martin, J. C. "The Chemistry of Dimethylketene Dimer. IV. The Polyester and β-Lactone Dimer of Dimethylketene", *J. Org. Chem*. 1962, 27, 60.

(32) Wiberg, K. B. "Basis set effects on calculated geometries: 6-311++G** vs. aug-cc-pVDZ", *J. Comp. Chem*. 2004, 25, 1342 – 1346.

(33) Woodward, R. B. and Hoffmann, R. "The Conservation of Orbital Symmetry", *Angew. Chem. Int. Ed. Engl*. 1969, 8, 781 – 932.

(34) Deubel, D. V. "Transition States for the [2+2] Addition of $CH_2=CH_2$, $CH_2=O$, and [M]=O Across the C=C Double Bond of Ketene: Electronic Structure and Energy Decomposition", *J. Phys. Chem. A*, 2002, 106, 431 – 437.

(35) (a) Mayer, I. "Charge, Bond Order and Valence in the Ab Initio SCF Theory", *Chem. Phys. Lett*. 1983, 97, 270–274. (b) Mayer, I. "Comments on the Quantum Theory of Valence and Bonding: Choosing between Alternative Definitions", *Chem. Phys. Lett*. 1984, 110, 440–444.

(36) Mansson, M; Nakase, Y.; Sunner, S. "The Enthalpies of Combustion and Formation of Diketene", *Acta Chem. Scand*. 1968, 22, 171 – 174.

(37) Xu, X. and Goddard III, W.A. "From the Cover: The X3LYP Extended Density Functional for Accurate Descriptions of Nonbond Interactions, Spin States, and Thermochemical Properties", *Proc. Natl. Acad. Sci. U.S.A*. 2004, 101, 2673–2677.

(38) (*a*) Lynch, B. J.; Fast, P. L.; Harris, M.; Truhlar, D. G. "Adiabatic Connection for Kinetics", *J. Phys. Chem. A*, 2000, 104, 4811–4815. (*b*) Exact exchange based on: Watson, M. A.; Handy, N. C.; Cohen, A. J. "Density Functional Calculations, Using Slater Basis Sets, with Exact Exchange", *J. Chem. Phys*. 2003, 119, 6475-6481

(39) (a) Perdew, J. P.; Ernzerhof, M.; Burke, K. "Rationale for Mixing Exact Exchange with Density Functional Approximations", *J. Chem. Phys*. 1996, 105, 9982–9985. (b) Ernzerhof, M. and Scuseria, G. "Assessment of the Perdew–Burke–Ernzerhof Exchange-Correlation Functional", *J. Chem. Phys*. 1999, 110, 5029–5036. (c) Adamo, C. and Barone, V. "Toward

Reliable Density Functional Methods without Adjustable Parameters: The PBE0 Model", *J. Chem. Phys.* 1999, 110, 6158–6170. (d) Ref. 38b.

(40) (a) Adamo, C. and Barone, V. "Toward Reliable Adiabatic Connection Models Free from Adjustable Parameters", *Chem. Phys. Lett*. 1997, 274, 242 – 250. (b) Ref. 38b.

(41) (a) Adamo, C. and Barone, V. "Exchange Functionals with Improved Long-Range Behavior and Adiabatic Connection Methods without Adjustable Parameters: The *m*PW and *m*PW1PW Models", *J. Chem. Phys.* 1998, 108, 664 – 675. (b) Ref. 38b.

(42) Becke, A.D. "Simulation of delocalized exchange by local density functionals", *J. Chem. Phys*. 2000, 112, 4020.

(43) (a) Kang, J.K. and Musgrave, C.B. "Prediction of transition state barriers and enthalpies of reaction by a new hybrid density-functional approximation", *J. Chem. Phys*. 2001, 115, 11040. (b) Ref. 38b.

(44) 50% exact exchange and 50% Becke88 exchange, plus LYP correlation.

(45) Seidl, E. T. and Schaefer, H. F. "Diketene and its cyclic C4H4O2 isomers cyclobutane-1,3-dione and 2,4-dimethylene-1,3-dioxetane". *J. Am. Chem. Soc*. 1990, 112, 1493 – 1499.

(46) Morales, G. and Martinez, R. "Contribution groups for ketene polymers", *to be submitted*. Article based on the results of the chapter 6 of this thesis.

(47) Sumathi, R. and Green, W. H. Jr. "Thermodynamic Properties of Ketenes: Group Additivity Values from Quantum Chemical Calculations". *J. Phys. Chem. A* 2002, 106, 7937–7949.

(48) Nguyen, M. T. and Nguyen, H. M. T. "On the Heats of Formation of Methylketene, Dimethylketene and Related Cations", *Chem. Phys. Lett*. 1999, 300, 346–350.

(49) Traeger, J. C. "Neutral and Cationic Heats of Formation for Ketene, Methylketene, and Dimethylketene", *Int. J. Mass Spectrom.* 2000, 194, 261–267.

(50) Bergmin, R.; Quittmann, W.; Stoffel, J. *"Process for the reduction of the polymer portion in the dimerization of ketene"*, US Patent 4.999.438, 1990.

(51) Tenud, L.; Weilenmann, M.; Dallwigk, E. "1,3-Cyclobutanodionderivate aus Keten", *Helvetica Chimica Acta* 1977, 60, 975 – 977.

(52) Williams, J. W. and Krynitsky, J. A. "Ketene Dimer", *Org. Synth*. 1941, 21, 64-66.

(53) (a) Ziegler, T. and Rauk, A. "On the calculation of bonding energies by the Hartree Fock Slater method", *Theor. Chim. Acta* 1977, 46, 1-10. (b) Ziegler, T. and Rauk, A. "A theoretical study of the ethylene-metal bond in complexes between copper(1+), silver(1+), gold(1+), platinum(0) or platinum(2+) and ethylene, based on the Hartree-Fock-Slater transition-state method", *Inorg. Chem*. 1979, 18, 1558 – 1565. (c) Ziegler, T. and Rauk, A. "Carbon monoxide, carbon monosulfide, molecular nitrogen, phosphorus trifluoride, and methyl isocyanide as .sigma. donors and .pi. acceptors. A theoretical study by the Hartree-Fock-Slater transition-state method", *Inorg. Chem.* 1979, 18, 1755 – 1759.

(54) According to the decomposition of the interaction energy between the fragments using the PW86x+PBEc functional in gas phase (electrostatic, Pauli and orbital interactions in kcal mol^{-1}). TS d-I: -111.37, 235.56, -136.43; TS d-II: -109.17, 232.01, -144.43; TS d-III: -92.90, 218.24, -107.41; TS d-IV: -51.71, 230.01, -225.84; TS d-IV (ref. 18): -42.81, 200.72, -132.05.

Chapter 5

Parent Ketene Dimerization in Liquid Phase: Simulating Experimental Conditions

This research presents the first theoretical comparison between ketene dimerization in gas phase and ketene dimerization in solution. Density functional theory (DFT) calculations on the ketene dimerization were carried out considering the following product dimers: diketene (d-I), cyclobutane-1,3-dione (d-II), 2,4-dimethylene-1,3-dioxetane (d-III) and 2-methyleneoxetan-3-one (d-IV). Based on previous results with the MPW1K/DZP//PW86x+PBEc/DZP level (Chapter 4) it was found on both kinetic and thermodynamic grounds that only d-I and d-II are formed during ketene dimerization in gas phase. Results of the current chapter report that solvation makes dimerization more favorable. On the enthalpic surface this is due to a favorable interaction between the dimer dipole moment and solvent molecules. The dimer is stabilized further on the Gibbs energy surface by an increase of the dimerization entropy in solution compared to gas phase. The species d-I remains the most stable dimer in solution by 1 kcal/mol. Kinetically, the dimerization barriers for the relevant species d-I and d-II are cut in half by solvation both due to favorable dimer-dipole/solvent interactions ($\Delta H^{\neq}, \Delta G^{\neq}$) and an increase in the activation entropies ($\Delta S^{\neq}$). While the dimerization barrier for d-II is lowest for the gas phase and toluene the barrier for d-I formation becomes lowest for the more polar solvent acetone by 1 kcal/mol as d-I dimerization has the most polar transition state.

5.1 Introduction

Ketene dimerization is a process that deserves attention due to the research and commercial applications of the corresponding product dimers (Chapter 1). It is well known that the major product of the dimerization of the ketene in solution is the diketene (d-I) while high weight ketenes dimerize to their corresponding cyclobutanedione structure (d-II)[1]. On the other hand, the ketene in gas phase does not dimerize appreciably at room temperature[2, 3, 4] and it is supposed that liquid brown deposits produced during the storage of the ketene are caused by the dimerization in condensed acetone or acetic acid[5]. It is surprising that there are few experimental studies and no theoretical studies[1] about the role of the solvent in the diketene generation by dimerization due to it is possible only at room temperatures in the condensed phase[2, 3]. The two experimental available measurements about the dimerization in condensed phase are related to

the parent ketene[2] and to the dimethylketene[6]. In both measurements the polarity of the solvent increased the rate of the reaction and a second kinetic law fitted with excellent agreement the experimental data. Moreover, it is reported that in the dimerization in liquid phase does not intervene any external agent during the reaction[2, 7]. These results suggest that the ketene dimerization is a bimolecular process. However, it is remarkable that the formation of the unsubstituted d-I dimer in gas phase has a very high experimental activation energy[3] of 31 kcal mol^{-1}, whereas in acetone[2] the activation barrier is only 11 kcal mol^{-1}. This fact could indicate the intervention of an external agent on the reaction in the liquid phase since it is reported that the dimerization of ketenes can be affected by heat and acid or base catalysis[1]. Then, as the reaction is sensible to the external conditions, it was not clear whether the reaction was promoted by an identified catalyst or the solvation process made the reaction feasible in the liquid phase. Up to now, chapter 4 focused attention on the geometry and energetic of the dimerization process in gas phase. As a consequence, we shall now include solvation into our simulation to gain some insights related to the experimental conditions and for discarding the presence of an identified catalyst brought in the feed stream along with the raw ketene.

5.2 Computational details

Geometry optimizations and frequency calculations were applied using the exchange functional of Perdew-Wang (PW86x)[8] and the correlation functional of Perdew-Burke-Ernzerhof (PBEc)[9]. The standard double-ζ STO bases with one set of polarization functions were applied. The 1s electrons of C and O were treated within the frozen core approximation[10]. An auxiliary basis set of s, p, d, f and g STOs was utilized to fit the molecular densities to represent the Coulomb and exchange potentials in each SCF cycle[11]. Gas phase electronic enthalpies were calculated from Kohn-Sham energies and standard expressions[12] were used to calculate the remaining gas phase enthalpic and entropic contributions at nonzero temperature, including zero point energy (ZPE) contribution. Linear transit search were carried out to localize transition states for each kind of dimer. The intrinsic reaction coordinate (IRC)[13] calculation was applied to verify the TS structures for each dimer. Single point calculations using the MPW1K functional were applied on the optimized structures. The calculations were carried out using the Amsterdam Density Functional (ADF) program package[14] versions 2004.02 and 2005.02.

Solvation enthalpies in acetone and toluene were obtained using the COSMO method[15] as implemented in ADF[16]; the solvent excluding surface was constructed using the atomic radii of 1.16, 1.3 and 2.2 Å for H, O and C, respectively. The values for dielectric constant of 20.56 and 2.4 were used in the calculations for acetone and toluene respectively. The solvation enthalpy was calculated as the difference between the gas-phase energy and that calculated using the COSMO solvation model. The method of Wertz[17] was used to calculate the solvation entropies in each solvent. In the first step of this method, the ideal-gas solute is compressed from standard conditions ($V_{m, gas}$) to the standard volume of the solvent ($V_{m, liq}$). Then, the solute is transferred to the solvent forming a hypothetical solution which has the intermolecular interactions of a dilute solution. In this step the solute loses a fraction of its remaining entropy. This fraction can be calculated using the equation (1)[18] in which the numerator represents the change in entropy in the process of transferring. In the third step, the solute is expanded to the density of the solution at experimental conditions[2] (Acetone: 0.524 mol/l, Toluene: 0.910 mol/l). The solvation entropy is thus obtained with the sum of the entropy changes accompanying each step. Using the data reported in Table 5.1, we have the solvation entropy for acetone and toluene in equations 2 and 3 respectively.

Table 5.1. Experimental data used in Eqs (1, 2 and 3).

	[a]MW	[a] ρ g/ml	[a] S_{liq}^0 J/mol K	S_{gas}^0 J/mol K	α	$R \ln\left[\dfrac{V_{m,liq}}{V_{m,gas}}\right]$
Acetone	58.10	0.7845	199.80	[a] 250.27	0.20	-11.53
Toluene	92.14	0.8668	220.96	[b] 340.00	0.35	-10.81

[a] Ref. 18. [b] Ref. 19.

$$(1) \quad \alpha = \frac{S_{liq}^o - (S_{gas}^o + R \ln V_{m,liq} / V_{m,gas})}{(S_{gas}^o + R \ln V_{m,liq} / V_{m,gas})}$$

$$(2) \quad \Delta S_{Sol}^{Acetone} = -11.53 - 0.20 * (S_{gas}^o - 11.53) + 6.55$$

$$(3) \quad \Delta S_{Sol}^{Toluene} = -10.81 - 0.35 * (S_{gas}^o - 10.81) + 4.642$$

5.3 Results and Discussion

5.3.1 Geometries

Experimental moments of inertia for the diketene (d-I dimer) obtained from microwave spectrum[20] were reproduced with excellent agreement at the PW86x+PBEc/DZP level (Chapter 4). The experimental moments of inertia served as a benchmark for determining the most appropriate geometrical parameters that represent the d-I structure. The geometrical parameters calculated in this research were found to surpass the performance of previous theoretical calculations[21, 22, 23] as well as experimental measurements[24, 25] (Table 4.1). This fact gives high confidence about the results of the ketene dimerization at the PW86x+PBEc/DZP level in gas phase and also supports the study in liquid phase at this same level of theory.

Figure 5.1 compares some geometrical measurements of the gas-phase transition states with the transition states in liquid phase. The presence of a solvent reduces in a great magnitude the distance between 1C and 4C atoms in TS d-I and TS d-II. For the case of TS d-I that distance is reduced 5.2% when the solvent is toluene and 6.4% when the solvent is acetone (Figure 5.1). For TS d-II the reductions are 4.2% in toluene and 6.4% in acetone. These values seem to be quite small; however, an error in terms of distance with these magnitudes may affect seriously most of the molecular properties[26]. The distance between the 3O and 2C atoms in the case of TS d-I is increased instead of being reduced by 0.7% in toluene and 2.7% in acetone. It can be because of the increase of the dielectric constant. Large values of dielectric constant favored polarization of the environment around the 3O atom which reduces the attractive forces with 2C atom making longer the distance. On the other hand, in the case of TS d-II the distance 5C and 2C is reduced with the presence of the solvents. The reduction reaches 0.6% in toluene and 2.6% in acetone. The absolute magnitude of the dihedral angle involved in the creation of the cyclo compound in the TS d-I and the TS d-II is decreased by the presence of the solvent. The decreasing in the dihedral angle is greater in the TS d-I than in the TS d-II and it depends on the value of the dielectric constant. Evidently, more polar solvent may get further close the ketene molecules in the TS structures.

The bond orders in the formed and quasi-formed bond in TS d-I and TS d-II increase in going from gas phase to liquid phase according to the Mayer methodology[27] (Table 5.2). The bond order in the formed 1C–4C bond in the TS d-I is larger than in the TS d-II, but the opposite happens with the quasi-formed bond in the TS structures. The major increasing in bond order is found in the 1C–4C bond for both TS d-I and TS d-II. Therefore, we can conclude that the main factor in the stabilization of TS d-I and TS d-II corresponds to the reduction in the distance of the formed 1C–4C bond.

The geometry of TS d-III slightly changes with the presence of the solvent as it is expected for a synchronous pericyclic reaction[28]. The distance between the oxygen atoms and the carbon atoms remains practically unchanged in toluene. However, the TS d-III changes to an asynchronous transition state when the solvent is acetone. This may be explained by the fact that the TS d-III in gas phase has a non-zero dipole moment (due to the non-zero approaching dihedral angle) which is affected by the increasing of the dielectric constant of the solvent (Table 5.3).The geometry of TS d-IV in liquid phase is early related to the corresponding in the gas phase. This behavior of TS d-IV is opposite to the obtained for TS d-I and TS d-II. The main characteristic is that the bond length for the formed 1C–2C bond and the quasi- formed 3O–4C bond are increased by the presence of a solvent.

Table 5.2. Bond order for the transition states based on the Mayer methodology[27].

Structure	Bond	B. O. Gas Phase	B. O. Toluene	B. O. Acetone
TS d-I	1C-4C	0.680	0.766	0.783
	3O-2C	0.203	0.236	0.235
TS d-II	1C-4C	0.665	0.721	0.758
	5C-2C	0.255	0.270	0.300
TS d-III	1C-6O	0.455	0.448	0.471
	3O-2C	0.456	0.450	0.448
TS d-IV	1C-2C	0.873	0.896	0.875
	3O-4C	0.345	0.233	0.253
	7C-6O	0.103	0.150	0.152
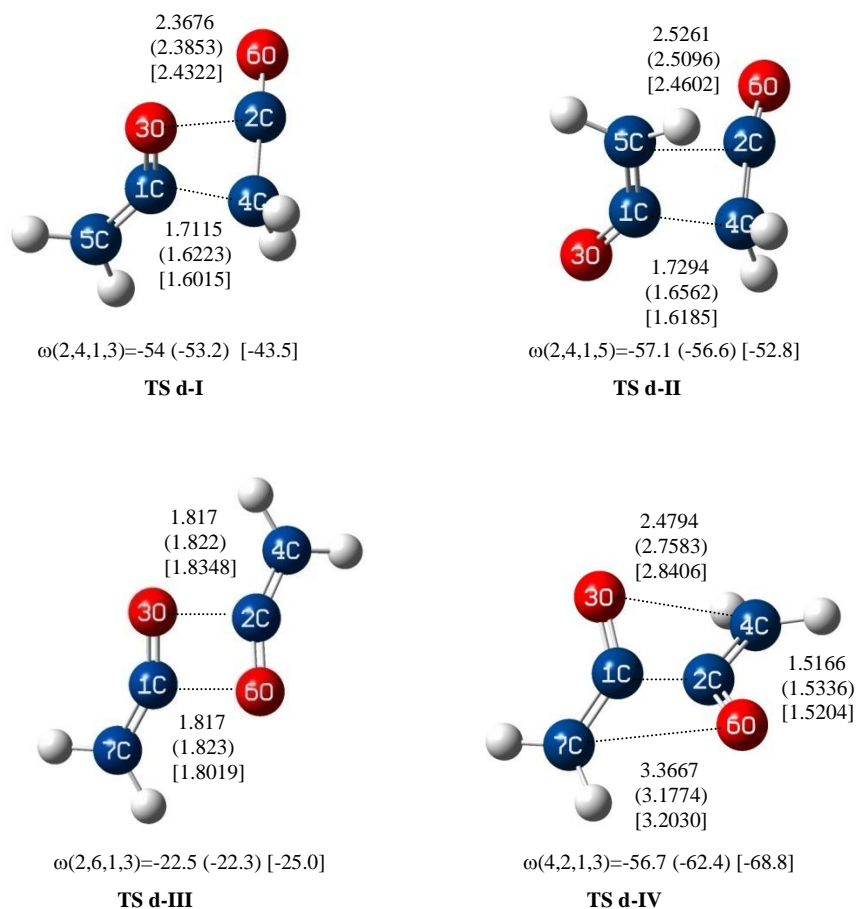
Figure 5.1. Some geometric measurements for transition state of ketene dimers in gas and liquid phase (bond lengths in Å). Parenthesis: toluene solvent. Brackets: acetone solvent.

The distance between the 7C atom and 6O atom is slightly increased by the presence of a solvent. In spite of the increasing in the distances of the bonds in going from gas to liquid phase, the bond order remains practically unchanged (Table 5.2). Thus, the stabilization of the TS d-IV in liquid phase is favored by the non-zero dipolar moment in gas phase (Table 5.3). The IRC calculations showed that the ketene dimerization reaction proceed in a concerted way in both gas and liquid phase (Graphs 1 and 2). The formation of a puckered pathway, as it is shown in the IRC Graphs, lower the energy for the formation of the corresponding dimer. It is more visible in

liquid phase in which the TS for the compounds are more puckered than in gas phase by the reduction of the distance of the formed bond in the corresponding dimer.

Table 5.3. Dipole moments (in Debyes) for the transition states in gas and liquid phase.

	Gas phase	Toluene	Acetone
TS(I)	4.331	5.715	7.532
TS(II)	3.777	5.023	6.086
TS(III)	0.900	1.080	1.070
TS(IV)	2.733	3.275	4.392
Monomer	1.462	1.734	2.000

5.3.2 Thermochemical properties in gas and liquid phase

The extensive DFT study presented in Chapter 4 demonstrated that the functional MPW1K[29] reproduced with excellent agreement the experimental values for the activation barrier[3] and the heat of dimerization[30] toward diketene dimer and had the best overall performance among the tested functional in this research (annexes). This study also obtained that in opposition to experimental combustion data, the d-I dimer, diketene, was more stable than the d-II dimer, cyclobutanedione. This section focus on the thermochemical properties obtained at the MPW1K/DZP// PW86x+PBEc/DZP level with the inclusion of COSMO model for solvation effects.

The differences in enthalpy, entropy and free energy for the dimers and their corresponding transition states in gas phase, toluene solvent and acetone solvent for the forward and backward reactions calculated at the MPW1K/DZP//PW86x+PBEc/DZP level are shown in Tables 4 and 5 respectively. In the gas phase, the TS states for the forward ketene dimerization reaction have large values for the entropy change. These values suggest that the TS states for the forward reactions are highly ordered which confirm that the ketene dimerization reactions take place in a concerted way. The high value of the free energy barriers for the transitions states of the dimers are in agreement with the experiments[2, 3, 4] indicating that the ketene dimerization reaction is not possible in gas phase at room or low temperatures at moderate times.
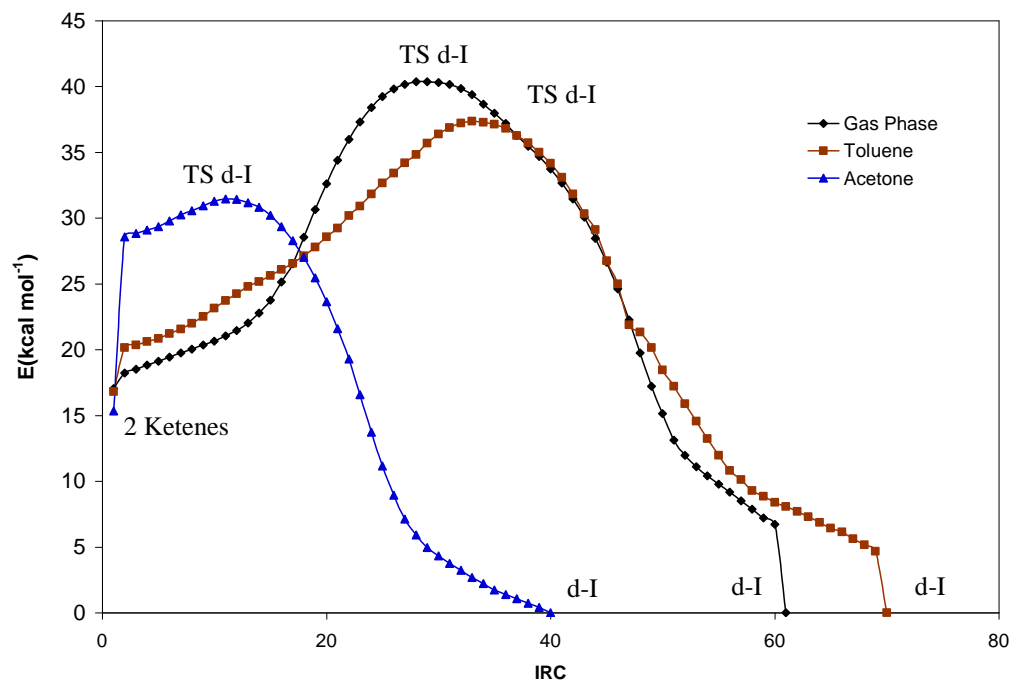
Graph 5.1. The IRC profile at the PW86x+PBEc/DZP level for the ketene dimerization toward the d-I dimer in gas, toluene and acetone.
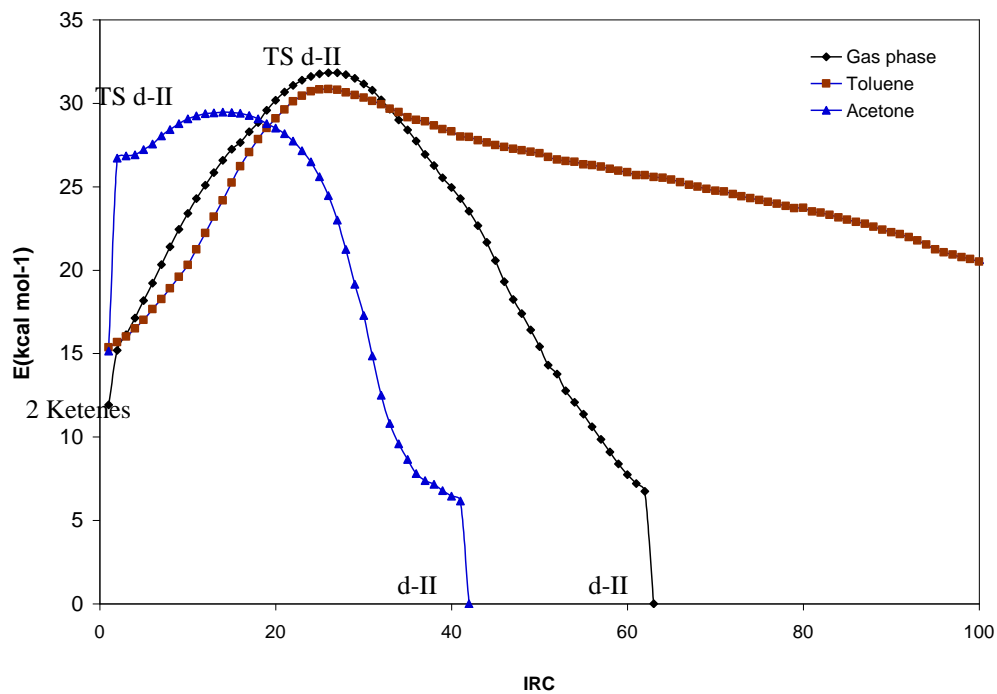
Graph 5.2. The IRC profile at the PW86x+PBEc/DZP level for the ketene dimerization toward the d-II dimer in gas, toluene and acetone. Note: 200 points in total for the IRC profile in toluene.

The transition structures for the d-I and d-II dimers have practically equal free energy barrier in gas phase and therefore both dimers should be accessible from the ketene dimerization reaction. By the other hand, the d-III and d-IV dimers are not accessible from the reaction in gas phase. The d-I dimer was found to be the major product in gas phase because of a thermodynamic control of the reaction.

The tendencies in the free energy barrier are maintained in toluene solvent as can be seen in Table 5.4 and in Figure 5.2. The entropies of solvation for the TS d-I and TS d-II correspond to 42% and 44% of the gas entropy respectively, whereas the enthalpies of solvation for TS d-I and TS d-II correspond to 27.8% and 28.5% of the enthalpy in the gas phase respectively. The calculated value for the free energy barrier of TS d-I in toluene differs by only 5.2 kcal/mol related to the available experimental value[2] (Table 5.4). The values of the free energy barriers for the dimers indicate that the ketene dimerization reaction is feasible in a nonpolar solvents as toluene at moderate times and that the d-I and d-II dimers are equally accessible in nonpolar solvents. The results in toluene also suggest that the d-I dimer is the major product because of a thermodynamic control of the reaction.

Table 5.4. Energetic for the forward reactions at 298.15 K and 1 atm calculated at the MPW1K/DZP//PW86x+PBEc/DZP level *.

	Gas phase			Toluene solution[+]			Acetone solution[+]		
	ΔH	ΔS	ΔG	ΔH	ΔS	ΔG	ΔH	ΔS	ΔG
TS d-I	28.77	-38.32	40.19	20.76	-22.13	27.36	13.83	-27.20	21.94
TS d-II	27.85	-39.53	39.64	19.92	-22.20	26.54	15.83	-28.01	24.18
TS d-III	55.88	-37.97	67.20	52.61	-21.12	58.91	52.92	-26.49	60.81
TS d-IV	66.33	-40.64	78.45	61.34	-25.90	69.06	57.38	-26.15	65.17
d-I	-24.24	-42.85	-11.46	-28.39	-24.10	-21.20	-28.62	-30.02	-19.67
d-II	-21.97	-41.95	-9.46	-26.77	-22.87	-19.95	-27.47	-28.80	-18.88
d-III	4.74	-42.71	17.48	3.10	-23.97	10.25	3.49	-29.91	12.41
d-IV	-3.10	-42.00	9.42	-6.66	-23.60	0.38	-6.53	-29.49	2.26

* Experimental data in parenthesis (gas phase from ref. 3 and liquid phase from ref. 2). ΔS in cal mol^{-1} K^{-1}. ΔH and ΔG in kcal mol^{-1}. [+] Experimental temperatures (ref. 2) for toluene and acetone were 273.15 K and 293.15 K respectively.

Table 5.5. Energetic for the reverse reactions at 298.15 K and 1 atm calculated at the MPW1K/DZP//PW86x+PBEc/DZP level *.

	Gas phase			Toluene solution			Acetone solution		
	ΔH	ΔS	ΔG	ΔH	ΔS	ΔG	ΔH	ΔS	ΔG
TS d-I	53.01	4.53	51.65	20.76	1.97	27.36	42.45	2.83	41.61
TS d-II	49.82	2.42	49.10	46.69	0.67	46.49	43.30	0.79	43.06
TS d-III	51.14	4.74	49.72	49.51	2.75	48.66	49.43	3.42	48.40
TS d-IV	69.43	1.36	71.03	68.00	-2.30	68.68	63.92	3.34	62.91
d-I →	24.24	42.85	11.46	28.39	24.10	21.20	28.62	30.02	19.67
d-II →	21.97	41.95	9.46	26.77	22.87	19.95	27.47	28.80	18.88
d-III →	-4.74	42.71	-17.48	-3.10	23.97	-10.25	-3.49	29.91	-12.41
d-IV →	3.10	42.00	-9.42	6.66	23.60	-0.38	6.53	29.49	-2.26

* Experimental data in parenthesis (ref. 3). ΔS in cal mol⁻¹ K⁻¹. ΔH and ΔG in kcal mol⁻¹.

Opposite to the tendency in gas phase and in toluene solvent, the results in acetone favor the relative stability of the TS d-I over the TS d-II. In this polar solvent, the enthalpies of solvation for the TS d-I and the TS d-II correspond to 52% and 43% of the corresponding enthalpy in gas phase respectively. The entropy of solvation for both TS d-I and TS d-II corresponds to 29% of the entropy in gas phase. The difference in enthalpies for both TS d-I and for TS d-II was found to be smaller in acetone than in toluene. The calculated value of 21.94 kcal mol⁻¹ for the free energy barrier of TS d-I in acetone is in excellent agreement with the experimental value[2] of 21.17 kcal mol⁻¹. Nevertheless, the activation energy and the entropy barrier calculated for that reaction differ in 4 kcal mol⁻¹ and 11 cal mol⁻¹ K⁻¹, respectively, to the experimental values (Table 5.4). These disagreements are explained by the fact that the weak intermolecular interactions between the reactants and products and between the solvent molecules themselves are not taken into account in the continuum solvation model. In spite of that, such interactions might cancel in the expression for the free energy of solvation and the systematic overestimation of the enthalpy of solvation and the entropy of solvation might be compensated[31, 32]. This phenomenon is known as the enthalpy-entropy compensation[33].

The results in acetone indicate that the d-I dimer is favored both kinetically and thermodynamically over the other dimers (Figure 5.2). However, the d-II dimer may be produced in a small amount during the ketene dimerization in acetone solvent. According to the values obtained in this work for the free energy barriers in acetone, the d-II dimer is produced in a yield of 3% approximately. This prediction is in excellent agreement with the results of Tenud and coworkers[34] who reported that a small amount of the symmetrical d-II dimer, cyclobutane-1,3-dione, was produced in a yield between 4% and 5% in acetone.

The excellent results obtained in this research in both gas phase and acetone suggest that the behavior of the reaction in toluene is also correct; thus, the d-II dimer may be produced in the same quantity, approximately, as the d-I dimer in toluene. In fact, since the structure of the diketene dimer was in doubt for almost 50 years[35], the studies done in that period of time about the ketene dimerization reaction did not consider the production of the different dimers due to parallel dimerization reactions. We only found the kinetic study of Rice and Greenberg[2] for the production of ketene dimer in different solvents. However, since this study was performed in the period of doubt about the structure of the diketene dimer, they only considered the production of a unique dimer measured by the reaction between that dimer and the oxalic anhydride[2]. Moreover, in that time the instrumental techniques of measurement and detection were not developed enough. Thus, new experimental measurements of the kinetic of ketene dimerization and new detecting methods for the d-II dimer are called for.

There is a direct relation between the feasibility of the dimerization reaction and the polarity of the solvent as it is reported in the literature[2, 6] (Figure 5.2). Nevertheless, the solvation effects whether in polar or nonpolar solvent make feasible the ketene dimerization reaction at room and low temperatures. Such stabilization of the reaction in liquid phase could obey to an increase of the flow of charge between the reactant ketenes in the corresponding transition state enhancing the nucleophilic character of the dimerization (Table 5.6 and Graph 5.3). The flow of negative charge in both the TS d-I and the TS d-II is increased with the increasing of the value of the dielectric constant (Graph 5.3a). However, the raising of the flow of charge is greater in the TS d-I than in the TS d-II. In gas phase, the difference in the flow of negative charge based on the Hirshfeld charges[36] (Table 5.6a) between the TS d-I and the TS d-II is -0.083 a.u. which is

comparable with that in toluene (-0.099 a.u.). These similar values of the flow of charge maintain the tendency of the free energy profile in toluene (Figure 5.2). On the other hand, the difference in the flow of charge between the TS d-I and the TS d-II is increased to -0.157 a.u. in acetone. Such increasing of the difference in the flow of charge increase the relative stability of the TS d-I compare with the TS d-II making the dimerization reaction toward the d-I dimer favored kinetically in acetone (Figure 5.2).
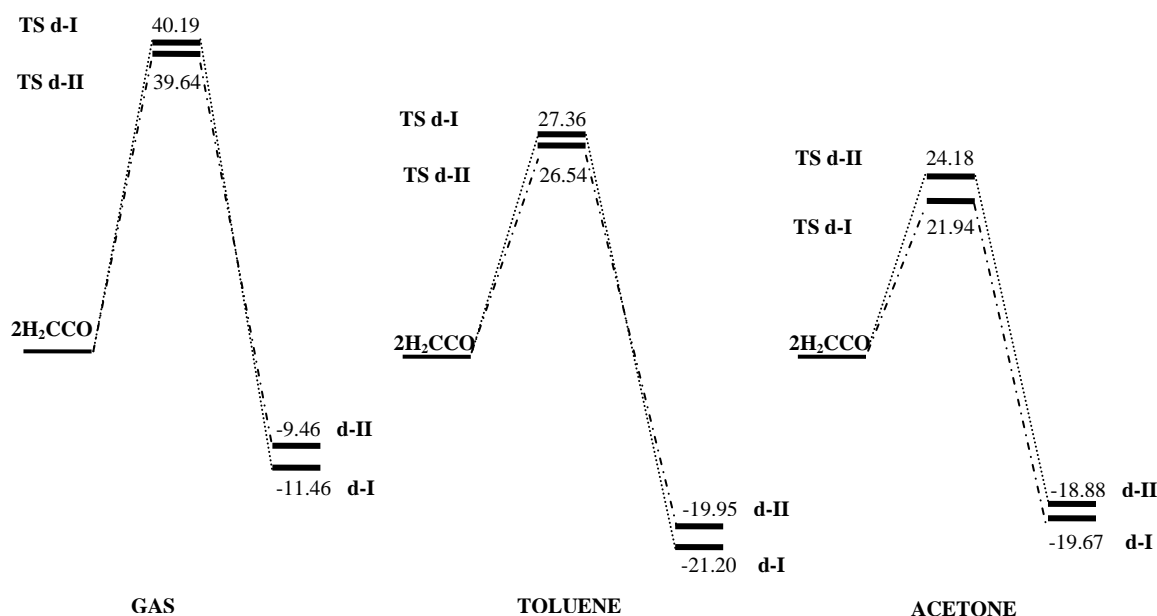
Figure 5.2. Free energies for the production of the d-I and d-II dimers at the MPW1K/DZP//PW86x+PBEc/DZP level. T=298.15 K, P=1 atm.

According to the Hirshfeld charges[36] (Table 5.6), the negative charge in TS d-I is transferred from the group CO, which form the 2C–6O bond (Figure 5.1), to the rest of the transition state, whereas the stabilization of TS d-II is done by a flow of negative charge to the eclipsed 3O atom (Figure 5.1). In both the TS d-I and the TS d-II, the non-ring-bonded oxygen atoms are participating in the stabilization of the corresponding transition state. However, the participation of the non-ring-bonded oxygen atom is less in the TS d-I than in the TS d-II. The major stabilization of the TS d-I over the TS d-II in polar solvent was predicted since the gas phase

dipole moment for the former was found to be greater than for the latter. The dipole moment in gas phase for the TS d-I and the TS d-II correspond to 4.33 and 3.78 Debye respectively. The value of the dipole moment for both the TS d-I and the TS d-II is increased 32% in toluene approximately. Whereas the values for the dipole moments of the TS d-I and the TS d-II are increased 74% and 61% respectively in acetone. In spite of the greater value for the dipole moment, the TS d-I only become more stable than the TS d-II for large values of the dielectric constant. The stabilization of the TS d-I in polar solvent was previously predicted with empirical solvation equations (Chapter 2).

Experimentally, the d-II dimer is the major product of the dimerization of substituted ketenes. Several investigations have proposed a step-wise process with a zwitterionic intermediate for explaining the mechanism of the substituted ketenes[1, 37]. The possibility of having a step-wise mechanism will depend on the distances of the 1C–4C and 5C–2C bonds (Graph 5.2) and particularly, on the relative formation of those bonds along the reaction coordinate. According to the results of this research, the possibility of a zwitterionic intermediate for the d-II dimer may be raised by increasing the solvent polarity and/or by an electron-withdrawing substituent. Methyl substituents will increase the negative charge on the nucleophilic carbon atom of the ketene group. This extra charge may become longer the formed 1C–4C bond on the TS d-II (Figure 5.3) favoring a concerted mechanism. This analysis agrees with the concerted mechanism proposed by Huisgen and Otto[6] who analyzed the dimerization of dimethylketene in different solvents. On the other hand, a step-wise mechanism for methyl substituted ketenes may be favored in strong polar solvents by the decreasing of the length of the formed 1C–4C bond.

Table 5.6a. Hirshfeld charges[36] (a.u.) for reactants and transition states of the d-I and d-II dimers in gas phase[*].

Reactants		TS d-I			TS d-II		
CH_2	CO	CH_2	CO	Σ	CH_2	CO	Σ
-0.042	0.042	-0.124 (-0.082)	-0.216 (-0.258)	-0.339 [-0.361]	-0.095 (-0.053)	-0.161 (-0.203)	-0.256 [0.240]
-0.042	0.042	0.106 (0.148)	0.233 (0.191)	0.340 [0.361]	0.099 (0.141)	0.156 (0.198)	0.255 [-0.240]

[*]Values in parenthesis correspond to the difference between the fragment in the TS and the fragment in the reactant. Numbers in brackets correspond to the Mulliken charges.

Table 5.6b. Hirshfeld charges[36] (a.u.) for reactants and transition states of the d-I and d-II dimers in toluene[*].

Reactants		TS d-I			TS d-II		
CH_2	CO	CH_2	CO	Σ	CH_2	CO	Σ
-0.026	0.026	-0.128 (-0.102)	-0.301 (-0.327)	-0.429 [-0.463]	-0.092 (-0.066)	-0.238 (-0.264)	-0.330 [0.325]
-0.026	0.026	0.153 (0.179)	0.276 (0.250)	0.429 [0.463]	0.146 (0.120)	0.184 (0.158)	0.330 [-0.325]

[*] Values in parenthesis correspond to the difference between the fragment in the TS and the fragment in the reactant. Numbers in brackets correspond to the Mulliken charges.

Table 5.6c. Hirshfeld charges[36] (a.u.) for reactants and transition states of the d-I and d-II dimers in acetone[*].

Reactants		TS d-I			TS d-II		
CH_2	CO	CH_2	CO	Σ	CH_2	CO	Σ
-0.010	0.010	-0.157 (-0.147)	-0.385 (-0.395)	-0.542 [-0.572]	-0.086 (-0.076)	-0.299 (-0.309)	-0.385 [0.384]
-0.010	0.010	0.199 (0.209)	0.344 (0.334)	0.543 [0.572]	0.178 (0.168)	0.207 (0.197)	0.385 [-0.384]

[*] Values in parenthesis correspond to the difference between the fragment in the TS and the fragment in the reactant. Numbers in brackets correspond to the Mulliken charges.

The results of this research suggest that the ketene dimerization in liquid phase is concerted. Since the free energy barriers in acetone fit very well with the experimental values, the mechanisms represent with high fidelity the reaction in solution. Thus, as it was reported by experimental measurements[2, 7] there are no diradicals intervening in the reaction. The stabilization of the transition states in liquid phase may be done by the increasing of the flow charge (nucleophilic character), the increasing of the dipole moment or by the increasing of the strength of the new formed bonds in the corresponding transition state. In the TS d-I and in the TS d-II all the aforementioned factors influence the stabilization of the transition states in liquid phase. The TS d-III is basically stabilized by the increasing of the flow of charge between the ketenes (Graph 5.3b) and the TS d-IV is fundamentally stabilized by the increasing of the dipole

moment (Table 5.3). The TS d-III and the TS d-IV have a small flow of charge between the reactant ketenes compared with that presented in the TS d-I and the TS d-II (Graph 5.3). But, the flow of negative charge in the TS d-IV is decreased in going from gas to liquid phase presumably by the early geometry of the transition states presented in the liquid phase.
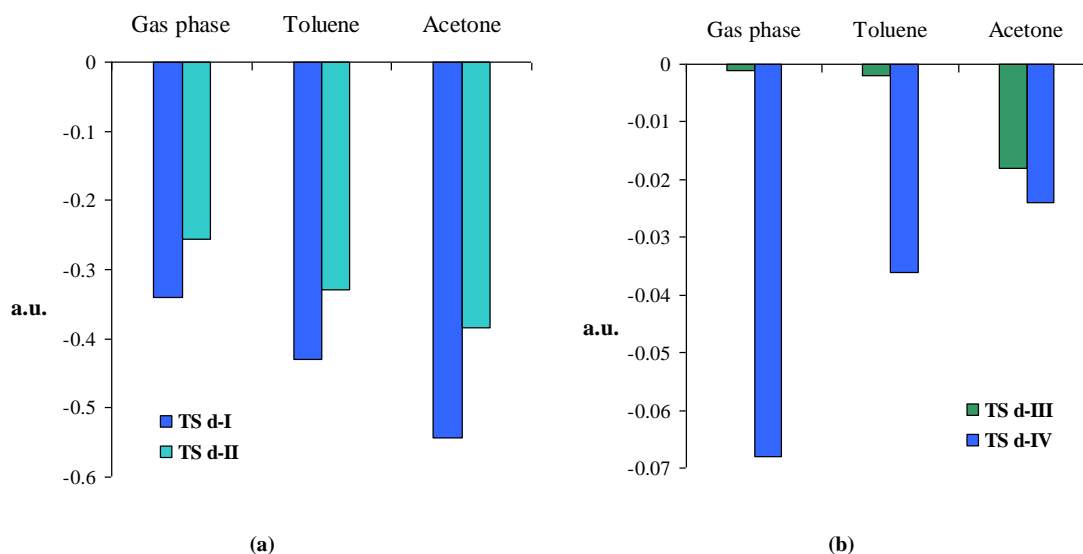
Graph 5.3. Flow of negative charge between the ketenes for the formation of the corresponding transition states. (a) d-I and d-II dimers. (b) d-III and d-IV dimers.

The solvents make the dimerization reactions more exothermic than the corresponding in gas phase. For the d-I and d-II dimers both solvents lower the enthalpy of the reaction with respect to that in gas phase by 4 and 5 kcal mol^{-1} respectively. The entropy of solvation is greater in toluene than in acetone. The entropy of the dimers d-I and d-II is lowered in toluene by 43.75% and 45.5% respectively, whereas the entropy of the d-I and d-II dimers is lowered in acetone by 30% and 31.4% respectively. The solvent reduces the free energy of reaction for both the d-I and d-II dimers. The free energy for the d-I dimer is lowered by 85% in toluene and 70% in acetone related to the corresponding value in the gas phase. The d-II dimer is more favored with the presence of the solvent than the other dimers. Toluene lowers the free energy of reaction for the d-II dimer in 111% of the corresponding value in gas phase. Acetone lowers the free energy

169

value by 99.6% of the value in gas phase. Thus, the difference between both the d-I and d-II dimers is lowered by the solvent. The differences between the free energy of the reaction for the d-I and d-II dimers are 2, 1.25 and 0.79 kcal mol^{-1} in gas phase, toluene and acetone respectively.

5.3.3 Extended Transition State Analysis

As it was described in the Chapter 4, the extended transition state analysis[38] (ETS) complements the information about the different interactions in the transition state. The first energy in the ETS analysis corresponds to the strain or deforming energy, ΔE_{str}. Table 5.7 shows the ETS analysis for the constituent fragments (F1 and F2) for the transition states of the ketene dimers in both gas and liquid phase. The presence of the liquid phase increases the strain energy involved in the formation of the TS d-I and the TS d-II. Particularly, toluene affects more the strain energy of the fragments in the TS d-I than in the TS d-II, but acetone affects less the strain energy of the fragments in the TS d-I than in the TS d-II. For the other transition states, the strain energies of the constituent F1 and F2 fragments have the same order of magnitude. The strain energies involved in the generation of the TS d-III and the TS d-IV are slightly affected with the presence of the liquid phase. The total strain energy is the sum of the strain energy of the constituent fragments in the transition state. The total strain energy for the transition state of the analyzed dimers has the following order TS d-IV > TS d-II > TS d-I > TS d-III in both gas and liquid phase. Thus, the formation of the ketenes for the generation of the TS d-IV involves the greatest strain energy (Table 5.7 and Graph 5.5).

The interaction energy between the fragments, second energy in the ETS analysis, for the case of the TS d-I and the TS d-II is favored in going from gas to liquid phase (Table 5.7). This improvement in the interaction energy, presumably by the electronic interaction which enhance the nucleophilic character of the reaction, overcompensates the total strain energy involved in the TS d-I and TS d-II formation, and the production of the d-I and d-II dimers is made feasible in the liquid phase therefrom. In the preceding section, it was demonstrated that the d-I dimer is favored kinetically over the d-II dimer in acetone by an increase of the flow of negative charge. Additional to these results, the ETS analysis shows that the TS d-I is favored in acetone by the minor strain energy between its fragments and that the TS d-II is favored in gas phase and in

toluene by the interaction energy between the F1 and F2 fragments; particularly, the TS d-II is favored by the major orbital interaction[39] between its fragments.

In chapter 2 we obtained that stabilization of the TS d-I with increasing polarity scale is not high enough to producing a zwitterionic intermediate. According to the ETS analysis, this lack of zwitterionic intermediate is due to the favorable interaction energy which overcompensate the strain total energy of the fragments. The fragments bend further in liquid phase compare to gas phase in order to allow increasing interaction between them. This interaction in liquid phase is more favorable than in gas phase, presumably by the electronic interaction since Hirshfield charge analysis reveled a raising in the flow of charge in going from gas to liquid phase (Graph 5.3), and lowers the energy for the formation of the transition states in liquid phase thereof.

Table 5.7. Extended transition state (ETS) Analysis[38] on the ketene dimers based on the MPW1K functional (in kcal mol^{-1})*.

TS	ΔE_{str} (F1)^a	ΔE_{str} (F2)^a	ΔE_{str} (Total)^b	$\Delta E_{ele}{}^c$	$\Delta E_{Pauli} + \Delta E_{orb}{}^{d, e}$	$\Delta E_{int}{}^{f, g}$	ΔE^h
d-I	11.60 {14.22} [13.55]	34.61 {42.93} [45.95]	46.21 {57.14} [59.50]	-111.37	92.64	-18.73 {-35.78} [-47.04]	27.49 {21.36} [12.46]
d-II	15.71 {16.32} [18.45]	36.34 {40.96} [44.91]	52.02 {57.27} [63.36]	-109.17	83.72	-25.45 {-36.73} [-48.95]	26.60 {20.54} [14.41]
d-III	22.65 {22.09} [19.51]	22.65 {22.21} [22.51]	45.30 {44.30} [42.02]	-92.90	101.72	8.82 {10.27} [10.86]	54.20 {54.57} [52.88]
d-IV	51.84 {54.98} [55.03]	59.43 {52.82} [54.65]	111.27 {107.80} [109.68]	-57.65	11.57	-46.08 {-45.18} [-52.97]	65.19 {62.62} [56.71]

* Energies based on the optimized geometries at the PW86x+PBEc/DZP level. Data for toluene and acetone are written in braces and brackets respectively. ^{a} Strain energy for the fragments. ^{b} Total strain energy. ^{c} Electrostatic interaction between F1 and F2. ^{d} Pauli repulsion and orbital interaction energy between F1 and F2. ^{e} The Pauli and orbital interaction terms in the gas phase could not be calculated separately for the MPW1K functional because the hybrid functionals are still not SCF calculated in the ADF package. Instead, the decomposition of the interaction energy at the PW86x+PBEc/DZP level is showed in Ref. 39. ^{f} Total interaction energy between F1 and F2. ^{g} The interaction energy between the fragments with the inclusion of the solvent effects is still not supported in the ADF package. ^{h} Energy barrier.

Conclusions

The results of this research give a better understanding of the ketene dimerization reaction in liquid phase at the experimental conditions. The calculated geometries predicted with excellent agreement the experimental rotational constants for the d-I dimer and therefore it is expected that the calculated geometries at the same level of theory for the other dimers and their transition states are well predicted. According to the TS structures and the IRC profiles in liquid phase obtained in this work at the PW86x+PBEc/DZP level with inclusion of solvent effects by the COSMO model, the ketene dimerizations toward the d-I, d-II and d-IV dimers might be classified as nonplanar-pseudopericyclic reactions. The ketene dimerization toward the d-III dimer was found to be a pericyclic reaction with a nonplanar but still synchronous transition state.

The experimental value for the free energy barriers of the d-I dimer in toluene and in acetone and the yield of the d-II dimer in acetone were reproduced with good agreement at the MPW1K/DZP//PW86x+PBEc/DZP level with the COSMO solvation model. These results suggest that the solvent effects play a major role in the feasibility of the ketene dimerization reaction at room and low temperatures and that an external agent, such as a catalyst, is not require to induce the progress of the reaction. The behavior of the reaction changes with the polarity of the solvent. Specifically, the toluene solvent maintains the behavior of the reaction as presented in gas phase, whereas the acetone solvent changes the tendency of the reaction and it makes the energy barrier for the TS d-I to be lower than for the TS d-II. Accordingly, the d-I dimer is disfavored and favored kinetically in toluene and acetone, respectively. The tendency in toluene was found to be in disagreement with the available experimental results since the experiments only predict the production of the d-I dimer. Modern techniques of detection could be used to establish the presence of the d-II dimer in different solvents.

The results of the Hirshfeld charges suggest that the transition states for the d-I and d-II dimers are stabilized in liquid phase because of the raising in the flow of charge between the reactant ketenes. This raising in the flow of charge was found to be greater in the TS d-I than in the TS d-II. Particularly, the difference in the flow of charge between the TS d-I and the TS d-II is greater in acetone than in toluene. Such difference in the flow of charge increases the relative stability of

the TS d-I compare with the TS d-II making the d-I dimer favored kinetically in acetone. Additional to the analysis of the flow of charge, the ETS analysis showed that that the relative stability of the TS d-I over the TS d-II is slightly disfavored in gas and in toluene by the less interaction energy between its constituent fragments, specifically, by the minor orbital interaction between its fragments. Furthermore, the relative stability of the TS d-I over the TS d-II is favored in acetone by the less total strain energy of its constituent fragments. The d-III and d-IV dimers were found to be inaccessible in either gas or liquid phase. The results of the Hirsfheld charges demonstrated that these dimers have a very low flow of charge between the reactant ketenes. The ETS suggested that the TS d-I is favored in acetone by the less strain energy and that zwitterionic intermediates for the d-I and d-II dimers are not formed owing to the orbital interaction that overcompensate the strain energy between the fragments.

References

(1) Tidwell, T. T. *Ketenes*; Wiley: New York, 1995.

(2) Rice, F.O. and Greenberg, J. "Ketene II. Rate of Polymerization", *J. Am. Chem. Soc*. 1934, 56, 2132.

(3) Chickos, J. S.; Sherwood, D. E. Jr.; and Jug, K. "Mechanism of Thermolysis of Diketene in the Gas Phase", *J. Org. Chem*. 1978, 43, 1146.

(4) Barteau, M.; Huff, M.; Pogodda, U.; Martínez-Rey, R. *"Functionalized monolith catalyst and process for production of ketenes"*. US Patent 6.232.504, 1998.

(5) (a) Chick, F; Wilsmore, N. T. M. "Acetylketen: a Polymeride of Keten", *J. Chem. Soc.* 1908, 946–950. (b) Staudinger, H.; Klever, H. W. "Über Ketene. 6. Mitteilung: Keten", *Ber.* 1908, 41, 594–600. (c) Hallock, C. *"Process for Producing Ketene"*. US Patent 2.053.286, 1936.

(6) Huisgen, R. and Otto, P. "The Mechanism of Dimerization of Dimethylketene", *J. Am. Chem. Soc*. 1968, 90, 5342.

(7) Rice, F. O. and Roberts, R. "The Structure of Diketene", *J. Am. Chem. Soc*. 1943, 65, 1677.

(8) Perdew, J.P. and Wang, Y. "Density-Functional Approximation for the Correlation Energy of the Inhomogeneous Electron Gas", *Physical Review B*. 1986, 33, 8822.

(9) Perdew, J.P.; Burke, K.; Ernzerhof, M. "Generalized Gradient Approximation Made Simple", *Physical Review Letters*. 1996, **77**, 3865.

(10) Baerends, E. J.; Ellis, D. E.; Ros, P. "Self-Consistent Molecular Hartree-Fock-Slater Calculations I. The Computational Procedure", *Chem. Phys.* 1973, 2, 41.

(11) Krijn, J. G. and Baerends, E. J. *Fit Functions in the HFS-Method*; Internal Report (in Dutch); Vrije Universiteit Amsterdam: Amsterdam, The Netherlands, 1984.

(12) McQuarrie, D. A. *Statistical Thermodynamics*; Harper: New York, 1973.

(13) Fukui, k. "The Path of Chemical Reactions – the IRC Approach", *Acc. Chem. Res*. 1981, 14, 363.

(14) Te Velde, G.; Bickelhaupt, F. M.; Baerends, E. J.; van Gisbergen, S.; Guerra, C. F.; Snijders, J. G.; Ziegler, T. "Chemistry with ADF", *J. Comput. Chem*. 2001, 22, 931.

(15) Klamt, A. and Schuurmann, G. "COSMO: A New Approach to Dielectric Screening in Solvents with Explicit Expressions for the Screening Energy and its Gradient", *J. Chem. Soc. Perkin. Trans*. 1993, 2, 799.

(16) Pye, C. C. and Ziegler, T. "An Implementation of the Conductor-Like Screening Model of Solvation within the Amsterdam Density Functional Package", *Theor. Chem. Acc.* 1999, 101, 396.

(17) Wertz, D. H. "Relationship between the Gas-Phase Entropies of Molecules and their Entropies of Solvation in Water and 1-Octanol", *J. Am. Chem. Soc*. 1980, 102, 5316.

(18) Cooper, J. and Ziegler, T. "A Density Functional Study of S_N2 Substitution at Square-Planar Platinum(II) Complexes", *Inorg. Chem*. 2002, 41, 6614.

(19) Lide, D. R., Ed. *CRC Handbook of Chemistry and Physics*, 86th ed.; CRC Press, 2006 (http://www.hbcpnetbase.com/).

(20) Mönnig, F.; Dreizler, H.; Rudolph, H. D. Z. *Naturforsch*, 1967, 22, 1471

(21) Salzner, U. and Bachrach, M. S. "Ab Initio Studies of the Dimerization of Ketene and Phosphaketene", *J. Am. Chem. Soc*. 1994, 116, 6850.

(22) Rode, J. R. and Dobrowolski, J. Cz. "Reaction Paths of the [2 + 2] Cycloaddition of X=C=Y Molecules (X, Y = S or O or CH_2). Ab Initio Study", *J. Phys. Chem. A* 2006, 110, 207.

(23) Seidl, E. T. and Schaefer, H. F. "Molecular Structure of Diketene: A Discrepancy between Theory and Experiments?", *J. Phys. Chem*. 1992, 96, 657.

(24) Bregman, J. and Bauer, S. H. "An Electron Diffraction Study of Ketene Dimer, Methylketene Dimer and β-Propiolactone", *J. Am. Chem. Soc*. 1955, 77, 1955.

(25) Kay, M.I. and Katz, L. "A Refinement of the Crystal Structure of Ketene Dimer", *Acta Crystallogr*. 1958, 11, 897.

(26) Cramer, C. J. *"Essentials of Computational Chemistry: Theories and Models"*. John Wiley & Sons, Ltd.: London, 2002.

(27) (a) Mayer, I. "Charge, Bond Order and Valence in the Ab Initio SCF Theory", *Chem. Phys. Lett.* 1983, 97, 270–274. (b) Mayer, I. "Comments on the Quantum Theory of Valence and Bonding: Choosing between Alternative Definitions", *Chem. Phys. Lett.* 1984, 110, 440–444.

(28) Pross, A. *"Theoretical and Physical Principles of Organic Reactivity"*. John Wiley & Sons, Inc.: New York, 1995.

(29) (*a*) Lynch, B. J.; Fast, P. L.; Harris, M.; Truhlar, D. G. "Adiabatic Connection for Kinetics", *J. Phys. Chem. A*, 2000, 104, 4811–4815. (*b*) Exact exchange based on: Watson, M. A.; Handy, N. C.; Cohen, A. J. "Density Functional Calculations, Using Slater Basis Sets, with Exact Exchange", *J. Chem. Phys*. 2003, 119, 6475-6481.

(30) Månsson, M; Nakase, Y.; Sunner, S. "The Enthalpies of Combustion and Formation of Diketene", *Acta Chem. Scand*. 1968, 22, 171.

(31) Williams, D. H. and Westwell, M. S. "Aspects of Weak Interactions", *Chem. Soc. Rev*. 1998, 27, 57.

(32) Yu, H.-A. and Karplus, M. "A Thermodynamic Analysis of Solvation", *J. Chem. Phys*. 1988, 89, 2366.

(33) Liu, L. and Guo, Q. X. "Isokinetic Relationship, Isoequilibrium Relationship, and Enthalpy–Entropy Compensation", *Chem. Rev*. 2001, 11, 673.

(34) Tenud, L.; Weilenmann, M.; Dallwigk, E. "1,3-Cyclobutanodionderivate aus Keten", *Helvetica Chimica Acta* 1977, 60, 975.

(35) Clemens, R. J. "Diketene", *Chem. Rev*. 1986, 86, 241.

(36) Hirshfeld, F. L. *Theoret. Chim. Acta* 1977, 44, 129.

(37) Roberts, J. D. and Sharts, C. M. *Org. Reactions*. 1962, 12, 26.

(38) (a) Ziegler, T. and Rauk, A. "On the calculation of bonding energies by the Hartree Fock Slater method", *Theor. Chim. Acta* 1977, 46, 1-10. (b) Ziegler, T. and Rauk, A. "A theoretical study of the ethylene-metal bond in complexes between copper(1+), silver(1+), gold(1+), platinum(0) or platinum(2+) and ethylene, based on the Hartree-Fock-Slater transition-state method", *Inorg. Chem.* 1979, 18, 1558 – 1565. (c) Ziegler, T. and Rauk, A. "Carbon monoxide, carbon monosulfide, molecular nitrogen, phosphorus trifluoride, and methyl isocyanide as .sigma. donors and .pi. acceptors. A theoretical study by the Hartree-Fock-Slater transition-state method", *Inorg. Chem.* 1979, 18, 1755 – 1759.

(39) According to the decomposition of the interaction energy between the fragments using the PW86x+PBEc functional in gas phase (electrostatic, Pauli and orbital interactions in kcal mol^{-1}). TS d-I: -111.37, 235.56, -136.43; TS d-II: -109.17, 232.01, -144.43; TS d-III: -92.90, 218.24, -107.41; TS d-IV: -51.71, 230.01, -225.84.

Chapter 6

Thermochemical Properties and Contribution Groups for Ketene Dimers and Related Structures from Theoretical Calculations

This chapter's main goals were to analyze ketene dimers' relative stability and expand group additivity value (GAV) methodology for estimating the thermochemical properties of high-weight ketene polymers (up to tetramers). The CBS-Q multilevel procedure and statistical thermodynamics were used for calculating the thermochemical properties of 20 cyclic structures, such as diketenes, cyclobutane-1,3-diones, cyclobut-2-enones and pyran-4-ones, as well as 57 acyclic base compounds organized into five groups. According to theoretical heat of formation predictions, diketene was found to be thermodynamically favored over cyclobutane-1,3-dione and its enol-tautomeric form (3-hydroxy-cyclobut-2-enone). This result did not agree with old combustion experiments. 3-hydroxy-cyclobut-2-enone was found to be the least stable dimer and its reported experimental detection in solution may have been due to solvent effects. Substituted diketenes had lower stability than substituted cyclobutane-1,3-diones with an increased number of methyl substituents, suggesting that cyclobutane-1,3-dione type dimers are the major products because of thermodynamic control of alkylketene dimerization. Missing GAVs for the ketene dimers and related structures were calculated through linear regression on the 57 acyclic base compounds. Corrections for nonnext neighbor interactions (such as gauche, eclipses and internal hydrogen bond) were needed for obtaining a highly accurate and precise regression model. To the best of our knowledge, the hydrogen bond correction for GAV methodology is the first reported in the literature; this correction was correlated to MP2/6-31G† and HF/6-31G† derived geometries to facilitate its application. GAVs assessed by the linear regression model were able to reproduce acyclic compounds' theoretical thermochemical properties and experimental heat of formation for acetylacetone. Ring formation and substituent position corrections were calculated by consecutively replacing the GAVs regarding the 20 cyclic structures' thermochemical properties.

6.1 Introduction

Ketenes can be polymerized in different routes due to their structures' double conjugated bonds $(nR_1R_2C=C=O)$. Diketenes (4-methylene-oxetan-2-ones) (n=2), cyclobutane-1,3-diones (n=2) and their enol-tautomeric forms (3-hydroxy-cyclobut-2-enones) and pyran-4-ones (n=3) are amongst the cyclic structures which can be generated from ketene polymerization.[1,2] Spontaneous alkylketene dimerization generally yields a greater percentage of cyclobutane-1,3-

diones whereas parent ketene dimerization yields diketene.[1a,3] Depending on the substituted groups, Cyclobutane-1,3-dione type dimer can isomerize to its enol-tautomeric form either spontaneously[4] or by using basic catalysts such as thrietylamine[5a] and aqueous sodium hydroxide[5b-c]. Further ketene incorporation into dimer compounds can yield ketene trimers[5,6] and ketene tetramers[2,6] which are both constituted by the pyran-4-one ring. The pyran-4-one ring is an important component of many biologically-active molecules, pharmaceutical substances and versatile building blocks in synthetic organic chemistry.[8] For example, the pyran-4-one ring has been detected as an odor-active component in the aroma of foods such as in cooked clam soup[8a], micro-waved rainbow trout[8b] and yogurt.[8c] The pyran-4-one ring has been used in deriving vanadyl complexes with insulin-like properties for diabetes therapy[8d] and new types of solvatochromic merocyanine dyes having potential applications for colorimetric sensor arrays for volatile organic compounds.[8e]

There are only a few experimental thermochemical property measurements for ketene dimers,[9,10] scarcely helping to evaluate these compounds' relative energetics. No experimental estimation for several other ketene polymer structures' thermochemical properties has been reported and an alternative method must therefore be used for predicting them. Benson's group additivity values (GAVs)[11-14] is one of the low computational cost and highly accurate methods (about 1 kcal per mol[11,12] for the heat of formation) for estimating thermochemical properties. However, several GAVs for estimating ketene polymer structures' thermochemical properties are missing, including ring corrections and substituent positions.[14] GAV methodology is based on the lineal adjustment of a set of reliable thermochemical data. It has been demonstrated that quantum mechanical and statistic thermodynamic calculations are able to reproduce thermochemical properties, having excellent agreement with experiments.[11,15-17] The following section analyzes the thermochemical properties of ketene dimers and related structures and assesses the GAVs missing for this class of cyclic compounds based upon theoretical procedures using a set of acyclic base molecules.

6.2 Theoretical Calculations

6.2.1 Molecular properties

Conformational isomers were calculated for the acyclic base compounds by using molecular mechanics' universal force field method, due to its broadly proven performance in obtaining conformers at low computational cost.[18] The conformers were reoptimized at the B3LYP/6-31+G(d) level of theory for discharging the most unstable isomers. The most stable isomers so obtained were further calculated with the CBS-Q multilevel method to assess accurate values for their molecular energies. CBS-Q level energies showed mean absolute deviations for the heat of formation at 0 K of ca. 1 kcal per mol which was better than the value of ca. 1.5 kcal per mol performed by the B3LYP method (B3LYP/6-311+G(3df,2p)//B3LYP/6-31G(d)).[19b] The CBS-Q method involves a sequence of optimizations using the restricted Hartree-Fock procedure and the second-order Moller-Plesset perturbational theory (MP2); the wave function is approximated in both levels by using the 6-31G† basis set. This basis set follows the 6-31G(d) mathematical structure and also includes d-type polarization functions on the heavy atoms, as in the 6-311G(d) basis set. After geometry optimization calculations, the energy is obtained by combining the extrapolated complete basis set second-order limit (CBS2) with higher order correlation (MP3, MP4, QCISD(T)) energies derived from a relatively smaller basis set. The method can be improved by an empirical correction due to bond additivity methodology and a correction for spin contamination.[19a-b] All the theoretical procedures were carried out using Gaussian package version 03W[20]. Harmonic vibrational frequencies and moments of inertia were estimated at HF/6-31G† and MP2/6-31G† levels, respectively. Zero point vibrational energies and vibrational frequencies were scaled by a factor of 0.91844 because of systematic overestimation of HF derivate frequencies.[15,19]

6.2.2 Thermochemical properties

Standard heats of formation were calculated within the atomization reaction framework.[21a,b] The experimental enthalpy change from 0 to 298 K for the elements in their standard state[21c], the heats of formation at 0 K for the atoms[21d] and the theoretical enthalpy change from 0 to 298 K for the compounds being studied were used in this reaction (Chart 6.1). Total partition function for all the substances was taken within the rigid-rotor-harmonic-oscillator framework corrected

by hindered internal rotation contributions. Anharmonic frequencies specifying internal rotations around single bonds were determined by Ayala and Schlegel's procedure.[22] The conformational ring movements (i.e. ring puckering and pseudorotations) were assumed to be harmonic. Such assumption was in good agreement with the diketene ring vibrational data;[23] no known studies have revealed the anharmonicity committed by ring movements for the other cyclic structures analyzed in this work.
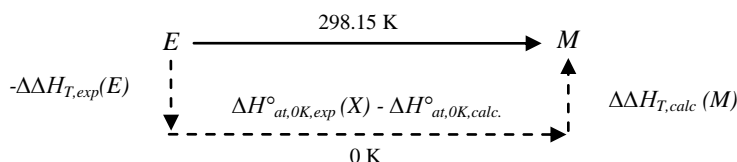
Chart 6.1. Atomization reaction procedure. X are the atoms of the elemen ts. E corresponds to the elements in their standard state. M is the studied compound.

Potential energy surfaces (V vs. ϕ) for the torsional movements were obtained at the HF/6-31G† level by optimized internal coordinate sequences, except for the corresponding dihedral angle which was varied in increments of 15° or 20°. The HF/6-31G(d) results have been shown to properly reproduce internal rotations' potential energy surface.[15b,24] Hindered rotor energies were subsequently obtained by solving the following Schrödinger equation:[25,26]

$$-\frac{\hbar^2}{2I_r}\frac{d^2\psi(\phi)}{d\phi^2} + V(\phi)\psi(\phi) = E\psi(\phi) \tag{1}$$

$$\psi_n(\phi) = \sum_m a_{nm}e^{-im\phi} \tag{2}$$

The reduced moment of inertia, I_r, was taken as the reduced moment for both the rotating group and the remainder molecule according to East and Radom's[27] $I(2,3)$ method; in this method, I_r is calculated on an axis passing through the center of gravity of both the rotating group and the other site. Though I_r is actually a function of dihedral angle, ϕ, it has been shown that a constant value for I_r can achieve acceptable approximations to hindered rotor contributions.[15b,26-28] The Schrödinger equation (eq. 1) was solved within the variational method's framework by the lineal combination of rigid-rotor basis functions (eq. 2, $m=0,\pm1,..,\pm200$).[26] The torsional partition function (Q_{int}) and torsional contribution to the thermochemical properties were calculated by

directly counting the energy levels (eq. 3) and by using the following widely-acknowledged statistical expressions (eqs. 4 - 6):[29,30]

$$Q_{int} = \frac{1}{\sigma_{int}} \sum e^{-E_i/RT} \tag{3}$$

$$S = Nk \left[\ln Q + T \frac{\partial}{\partial T}(\ln Q) \right] \tag{4}$$

$$C = NkT \frac{\partial^2}{\partial T^2}(T \ln Q) \tag{5}$$

$$H(T) - H(0) = \frac{RT^2}{Q} \frac{\partial Q}{\partial T} \tag{6}$$

6.2.3 Contribution groups

The procedure for obtaining the thermochemical properties stated was applied to ketene dimers and related structures (Table 6.1) as well as to acyclic base compounds (Table 6.2). The cyclic compounds (Table 6.1) contained some GAVS in their structure (Table 6.3) whose values had not been issued before; 57 acyclic compounds were thus calculated by the theoretical procedure to obtain these unknown GAVs (Table 6.3), covering a wide range of ketene polymer related structures. These compounds were classed into 5 groups (Table 6.2): group 1 contained alcohol and ether compounds, group 2 consisted of molecules containing carboxyl functional groups, group 3 comprised molecules with carbonyl, hydroxyl and alcoxyl functional groups, group 4 contained ester compounds and group 5 comprised molecules containing carboxylic functional groups.

Nonnext interactions or interactions between nonbonded atoms are not explicitly considered in the GAV methodology; several correction values (8 in total) were thus introduced, based on both the most stable conformers' calculated thermochemical properties and geometries. Unknown or missing groups for ketene dimers and related structures were obtained by using both cyclic (Table 6.1) and acyclic compounds (Table 6.2). A multivariate linear regression (MVLR) procedure was applied to the set of acyclic compounds; meanwhile, a sequential solving procedure assessed the corrections for ring formation (RC) and substituent position (SP) based upon the set of cyclic structures. This procedure for obtaining the missing GAVs was carried out to avoid possible alterations in GAV values due to ring formation strain forces.

Table 6.1. Ketene dimers and related structures analyzed in this chapter.

Diketenes	
1c) $-CH_2-CO-O-C(CH_2)-$	Diketene (4-methylene-oxetan-2-one)
2c) $-C(CH_3)H-CO-O-C(CH_2)-$	3-methyl-4-methylene-oxetan-2-one
3c) $-C(CH_3)_2-CO-O-C(CH_2)-$	3,3-dimethyl-4-methylene-oxetan-2-one
Cyclobutane-1,3-diones	
4c) $-CH_2-CO-CH_2-CO-$	Cyclobutane-1,3-dione
5c) $-C(CH_3)H-CO-CH_2-CO-$	2-methyl-cyclobutane-1,3-dione
6c) $-C(CH_3)_2-CO-CH_2-CO-$	2,2-dimethyl-cyclobutane-1,3-dione
7c) $-C(CH_3)H-CO-C(CH_3)H-CO-$	(Z)-2,4-dimethyl-cyclobutane-1,3-dione
Pyran-4-ones	
8c) $-CO-CH=CH-O-CH=CH-$	Pyran-4-one
9c) $-CO-C(CH_3)=CH-O-CH=CH-$	3-methyl-pyran-4-one
10c) $-CO-CH=C(CH_3)-O-CH=CH-$	2-methyl-pyran-4-one
11c) $-CO-CH=C(OH)-O-CH=CH-$	2-hydroxy-pyran-4-one
Cyclobut-2-enones	
12c) $-CH_2-CO-CH=CH-$	Cyclobut-2-enone
13c) $-C(CH_3)H-CO-CH=CH-$	4-methyl-cyclobut-2-enone
14c) $-CH_2-CO-C(CH_3)=CH-$	2-methyl-cyclobut-2-enone
15c) $-C(CH_3)_2-CO-CH=CH-$	4,4-dimethyl-cyclobut-2-enone
16c) $-CH_2-CO-CH=C(OH)-$	3-hydroxy-cyclobut-2-enone
17c) $-CH_2-CO-C(CH_3)=C(OH)-$	3-hydroxy-2-methyl-cyclobut-2-enone
18c) $-C(CH_3)H-CO-CH=C(OH)-$	3-hydroxy-4-methyl-cyclobut-2-enone
19c) $-C(CH_3)H-CO-C(CH_3)=C(OH)-$	3-hydroxy-2,4-dimethyl-cyclobut-2-enone
20c) $-C(CH_3)_2-CO-CH=C(OH)-$	3-hydroxy-4,4-dimethyl-cyclobut-2-enone

6.3 Results

6.3.1 Geometries and Energies

The parent ketene structure has been experimentally studied in some detail[1a] and it has been demonstrated that calculated geometries at the MP2 level are in good agreement with such experimental measurements.[15,31] Diketene has also been studied at both theoretical[32] and experimental[33] levels. The MP2/6-31G† geometrical parameters obtained in the current research were found to be in excellent agreement with theoretical calculations at different levels of theory (Figure 6.1). The theoretical predictions for the diketene ring were all found to disagree with both electron diffraction experiments and X-ray diffraction measurements. Electron diffraction-derived geometries predicted the same length for the C–C and C–O ring bonds, whereas X-ray data predicted much larger values for both bonds than other estimates. A more detailed discussion about differences in geometry predictions for diketene can be found in Seidl and Schaefer's work.[32] Discrepancies regarding geometric parameters for diketene can be resolved by comparing the predicted rotational constants with those directly obtained from microwave spectra.[33a] The rotational constants at MP2/6-31G† level obtained in this research reproduced the values obtained from microwave spectrum experiments with excellent agreement (Table 6.4). This result meant that the geometry obtained at this level suitably represented the diketene molecular structure.

Table 6.2. Acyclic base compounds calculated in this work.

Group 1. Ethers and alcohols	
(1) $CH_2C(OH)_2$	Ethene-1,1-diol
(2) $CH_2C(OH)OCH_3$	1-methoxy-ethenol
(3) $CH_2CHOC(OH)CH_2$	1-vinyloxy-ethenol
(4) $CH_2CHOC(CH_2)OCH_3$	1-methoxy-1-vinyloxy-ethene
(5) $CH_2C(OH)OC(OH)CH_2$	1-(1-hydroxy-vinyloxy)-ethenol
(6) $CH_3OC(CH_2)OC(CH_2)(OH)$	1-(1-methoxy-vinyloxy)-ethenol
(7) $CH_2CHOCHCH_2$	Vinyloxy-ethene
(8) CH_3OCHCH_2	Methoxy-ethene
(9) $(HO)CHC(OH)CH_3$	Propene-1,2-diol
(10) CH_2CHOH	Ethenol
(11) $CH_2C(OH)CH_3$	Propen-2-ol
(12) $CH_3CH_2OCHCH_2$	Ethoxy-ethene
(13) $(HO)CHCHOC(CH_2)OH$	1-(2-hydroxy-vinyloxy)-ethenol
(14) $CH_3OC(CH_2)OCH_3$	1,1-dimethoxy-ethene
(15) $CH_3CH_2OC(CH_2)OCH_3$	1-ethoxy-1-methoxy-ethene

Group 2. Aldehydes and ketones	
(16) $CH_2CHCOCHCH_2$	Penta-1,4-dien-3-one
(17) $HCOCHCH_2$	Propenal
(18) $HCOC(CH_2)CH_3$	2-methyl-propenal
(19) $HCOCH_2CHCH_2$	But-3-enal
(20) $HCOCH_2COH$	Malonaldehyde
(21) $HCOCH(CH_3)CHCH_2$	2-methyl-but-3-enal
(22) $HCOC(CH_3)_2CHCH_2$	2,2-dimethyl-but-3-enal
(23) $HCOCH_2COCH_3$	3-oxo-butyraldehyde
(24) $HCOCH(CH_3)COH$	2-methyl-malonaldehyde
(25) $HCOC(CH_3)COH$	2,2-dimethyl-malonaldehyde
(26) $CH_3CHOCHCH_2$	But-3-en-2-one
(27) $CH_2CHCOCH(CH_3)COH$	2-methyl-3-oxo-pent-4-enal
(28) $CH_2CHCOCH_2CHCH_2$	Hexa-1,5-dien-3-one
(29) $CH_3C(CH_2)COCHCH_2$	2-methyl-penta-1,4-dien-3-one
(30) $HCOCH_2COCH_2CHCH_2$	3-oxo-hex-5-enal
(31) $CH_2CHCOCH_2CH_3$	Pent-1-en-3-one
(32) $CH_3C(CH_2)COC(CH_2)CH_3$	2,4-dimethyl-penta-1,4-dien-3-one
(33) $CH_3C(CH_2)COCH_2CHCH_2$	2-methyl-hexa-1,5-dien-3-one

Group 3. Carbonyl, hydroxyl and alkoxyl groups	
(34) $CH_3C(OH)CHCOCHCH_2$	(Z)-5-hydroxy-hexa-1,4-dien-3-one
(35) $(HCO)CH(CH_3)C(OH)CH_2$	3-hydroxy-2-methyl-but-3-enal
(36) $(HCO)C(CH_3)_2C(OH)CH_2$	3-hydroxy-2,2-dimethyl-but-3-enal
(37) $(HO)CHCHCOCH_2COH$	(Z)-5-hydroxy-3-oxo-pent-4-enal
(38) $(HO)_2CCHCOH$	3,3-dihydroxy-propenal
(39) $CH_2CHOCHCHCOH$	(Z)-3-vinyloxy-propenal
(40) $(HCO)C(CH_3)HCHCH(OH)$	4-hydroxy-2-methyl-but-3-enal
(41) $(HO)CHCHC(COH)(CH_3)_2$	4-hydroxy-2,2-dimethyl-but-3-enal
(42) $CH_2CH(OH)CH_2COH$	3-hydroxy-but-3-enal
(43) $(HO)CHCHCH_2COH$	4-hydroxy-but-3-enal
(44) $(HCO)_2C(CH_3)CH_2(OH)$	2-hydroxymethyl-2-methyl-malonaldehyde
(45) $(HO)_2CCHCOCH_2CH_3$	1,1-dihydroxy-pent-1-en-3-one
(46) $(HO)CHCHCOCH_2CH_3$	(Z)-1-hydroxy-pent-1-en-3-one
(47) $(HO)CHCHCOCH_3$	(Z)-4-hydroxy-but-3-en-2-one
(48) $(HO)CHCHCOH$	(Z)-3-hydroxy-propenal
(49) $(HO)_2CCHCOCH_3$	4,4-dihydroxy-but-3-en-2-one
(50) $(HO)_2CCHCOCHCH_2$	1,1-dihydroxy-penta-1,4-dien-3-one
(51) $CH_3C(OH)CHCOH$	(Z)-3-hydroxy-butenal

Group 4. Ester group	
(52) $HCOOCHCH_2$	Formic acid vinyl ester
(53) $CH_2CHOCOCH_2COH$	3-oxo-propionic acid vinyl ester
(54) $CH_2CHCOOC(CH_2)CH_3$	2-methyl-acrylic acid vinyl ester

Group 5. Carboxylic acids	
(55) $CH_2CHCOOH$	Acrylic acid
(56) $HOCOC(CH_3)_2COH$	2,2-dimethyl-3-oxo-propionic acid
(57) $HOCOCH_2CHCH_2$	But-3-enoic acid

Table 6.3. List of unknown GAVS for the ketene cyclic structures and the acyclic base compounds[*].

	O/Cd/C	CO/O/Cd	O/Cd2	O/CO/Cd	CO/Cd2	C/(CO)2/C/H	C/(CO)2/C2	C/(CO)2/H2	C/CO/Cd/C/H	C/CO/Cd/C2	C/CO/Cd/H2	Cd/CO/C	Cd/CO/H	Cd/O/C	Cd/O/H	Cd/O2	CO/Cd/C	O/Cd/H
1c) Diketene (4-methylene-oxetan-				1							1			1				
2c) 3-methyl-4-methylene-oxetan-2-				1					1					1				
3c) 3,3-dimethyl-4-methylene-				1						1				1				
4c) Cyclobutane-1,3-dione								2										
5c) 2-methyl-cyclobutane-1,3-dione						1		1										
6c) 2,2-dimethyl-cyclobutane-1,3-							1	1										
7c) (E)-2,4-Dimethyl-cyclobutane-						2												
8c) Pyran-4-one			1		1								2		2			
9c) 3-methyl-pyran-4-one			1		1							1	1		2			
10c) 2-methyl-pyran-4-one			1		1								2	1	1			
11c) 2-hydroxy-pyran-4-one			1		1								2		1	1		1
12c) Cyclobut-2-enone											1		1				1	
13c) 4-methyl-cyclobut-2-enone									1				1				1	
14c) 2-methyl-cyclobut-2-enone											1	1					1	
15c) 4,4-dimethyl-cyclobut-2-enone										1			1				1	
16c) 3-hydroxy-cyclobut-2-enone											1		1	1			1	1
17c) 3-hydroxy-2-methyl-cyclobut-											1	1		1			1	1
18c) 3-hydroxy-4-methyl-cyclobut-									1				1	1			1	1
19c) 3-hydroxy-2,4-dimethyl-									1			1		1			1	1
20c) 3-hydroxy-4,4-dimethyl-										1			1	1			1	1
(1) Ethene-1,1-diol																1		2
(2) 1-methoxy-ethenol	1															1		1
(3) 1-vinyloxy-ethenol			1												1	1		1
(4) 1-methoxy-1-vinyloxy-ethene	1		1												1	1		
(5) 1-(1-hydroxy-vinyloxy)-ethenol			1													2		2
(6) 1-(1-methoxy-vinyloxy)-ethenol	1		1													2		1
(7) Vinyloxy-ethene			1												2			
(8) Methoxy-ethene	1														1			
(9) Propene-1,2-diol														1	1			2
(10) Ethenol															1			1
(11) Propen-2-ol														1				1
(12) Ethoxy-ethene	1														1			
(13) 1-(2-hydroxy-vinyloxy)-ethenol			1												2	1		2
(14) 1,1-dimethoxy-ethene	2															1		
(15) 1-ethoxy-1-methoxy-ethene	2															1		
(16) Penta-1,4-dien-3-one					1								2					
(17) Propenal													1					
(18) 2-methyl-propenal												1						
(19) But-3-enal											1							
(20) Malonaldehyde								1										
(21) 2-methyl-but-3-enal									1									
(22) 2,2-dimethyl-but-3-enal										1								
(23) 3-oxo-butyraldehyde								1										
(24) 2-methyl-malonaldehyde						1												
(25) 2,2-dimethyl-malonaldehyde							1											
(26) But-3-en-2-one													1				1	
(27) 2-methyl-3-oxo-pent-4-enal													1				1	

[*] CO/O/Cd, O/Cd2 and O/CO/Cd are unknown GAVs for both entropy and specific heat. O/Cd/C is an unknown GAV for specific heat.

Table 6.3. List of unknown GAVS for the ketene cyclic structures and the acyclic base compounds (continuation)[*].

	O/Cd/C	CO/O/Cd	O/Cd2	O/CO/Cd	CO/Cd2	C/(CO)2/C/H	C/(CO)2/C2	C/(CO)2/H2	C/CO/Cd/C/H	C/CO/Cd/C2	C/CO/Cd/H2	Cd/CO/C	Cd/CO/H	Cd/O/C	Cd/O/H	Cd/O2	CO/Cd/C	O/Cd/H
(28) Hexa-1,5-dien-3-one												1	1				1	
(29) 2-methyl-penta-1,4-dien-3-one					1							1	1					
(30) 3-oxo-hex-5-enal								1			1							
(31) Pent-1-en-3-one													1				1	
(32) 2,4-dimethyl-penta-1,4-dien-3-					1						2							
(33) 2-methyl-hexa-1,5-dien-3-one												1	1				1	
(34) 5-hydroxy-hexa-1,4-dien-3-one					1								2	1				1
(35) 3-hydroxy-2-methyl-but-3-enal									1					1				1
(36) 3-hydroxy-2,2-dimethyl-but-3-										1				1				1
(37) 5-hydroxy-3-oxo-pent-4-enal								1						1	1		1	1
(38) 3,3-dihydroxy-propenal														1		1		2
(39) 3-vinyloxy-propenal			1											1	2			
(40) 4-hydroxy-2-methyl-but-3-enal									1						1			1
(41) 4-hydroxy-2,2-dimethyl-but-3-										1					1			1
(42) 3-hydroxy-but-3-enal												1			1			1
(43) 4-hydroxy-but-3-enal												1			1			1
(44) 2-hydroxymethyl-2-methyl-							1											
(45) 1,1-dihydroxy-pent-1-en-3-one														1		1	1	2
(46) 1-hydroxy-pent-1-en-3-one														1	1		1	1
(47) 4-hydroxy-but-3-en-2-one														1	1		1	1
(48) 3-hydroxy-propenal														1	1			1
(49) 4,4-dihydroxy-but-3-en-2-one														1		1	1	2
(50) 1,1-dihydroxy-penta-1,4-dien-					1									2		1		2
(51) 3-hydroxy-butenal														1	1			1
(52) Formic acid vinyl ester				1													1	
(53) 3-oxo-propionic acid vinyl ester				1				1									1	
(54) 2-methyl-acrylic acid vinyl ester		1	1												1	1		
(55) Acrylic acid	1														1			
(56) 2,2-dimethyl-3-oxo-propionic								1										
(57) But-3-enoic acid													1					

[*] CO/O/Cd, O/Cd2 and O/CO/Cd are unknown GAVs for both entropy and specific heat. O/Cd/C is an unknown GAV for specific heat.

(a) 4-Methyleneoxetan-2-one

(b) Cyclobutane-1,3-dione
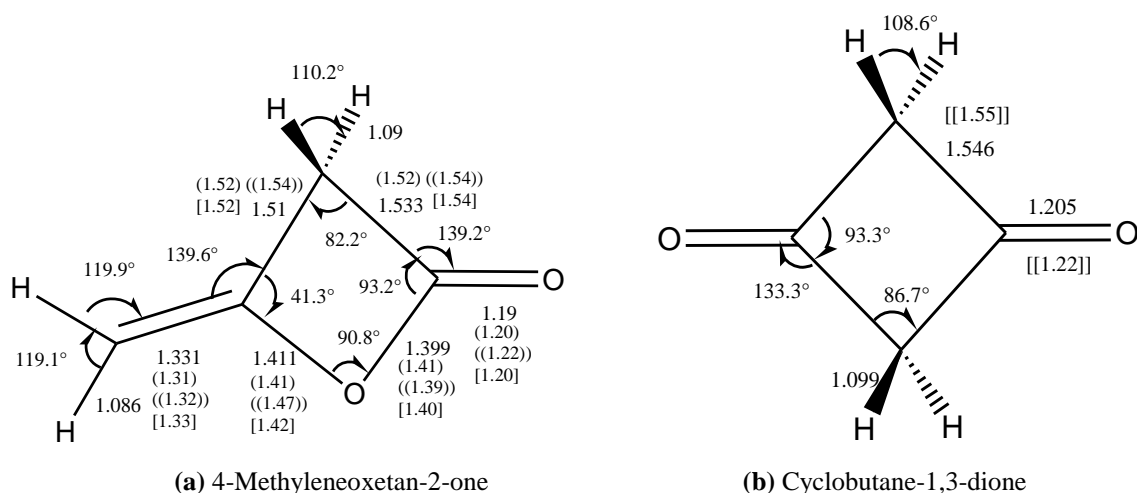
Figure 6.1. Some geometrical parameters for ketene dimers (lengths in Å) compared to other estimates: electron diffraction (33b), in parentheses; X-ray structures (33d), in double parentheses; Seidl and Schaefer's theoretical predictions (32), in brackets; theoretical predictions at MP2/aug-cc-pVDZ level (34a), in double brackets.

No experiments have been reported in the literature for cyclobutane-1,3-dione; however, the geometrical parameters obtained at MP2/6-31G† level coincided with other theoretical estimations[34] (Figure 6.2). Regarding the acyclic compounds, the geometrical parameters for acrolein and ethoxy-ethene[35] found in this work agreed with experimental measurements[36,37] (Figures in the supporting information material). For the other compounds, the theoretical measurements found in this work agreed with theoretical estimations at different levels of theory; ethyl vinyl ether, ethylene ether, geometrical parameters were in excellent agreement with geometrical parameters at other levels of theory.[35]

Table 6.4. Rotational constants for the d-I dimer in MHz[*].

Method	A	B	C	Absolute deviation
Microwave spectrum[33a]	12141.36 ± 0.04	2781.27 ± 0.01	2296.59 ± 0.01	-----
Electron diffraction[33b]	11711 (-430)	2846 (65)	2323 (26)	521
X-ray crystallography[33d]	11757 (-387)	2736 (-45)	2250 (-47)	479
MP2/aug-cc-pVDZ[34a]	12 053 (-88)	2716 (-65)	2249 (-47)	200
CCSD/DZd[32]	12 051 (-90)	2747 (-34)	2270 (-27)	151
MP2/6-31G†	12063 (-78)	2766 (-14)	2283 (-13)	105

* Numbers in parenthesis indicate the deviation from experimental microwave results. Rotational constants for the electron diffraction and X-ray structures were taken from ref 32.

According to the current research's geometrical results, the diketene (1c) and cyclobut-2-one rings (12c) as well as the pyran-4-one ring (8c), maintained their planarity independently of the number and characteristics of the substituent groups (Me or OH) (Figure 6.2). The symmetric cyclobutane-1,3-dione ring (4c) slightly puckered when it had either one or two Me substituents in the *cis* or (Z) 2,4 position (Tables in the supporting information material). For the acyclic compounds, the group 2 molecules (i.e. aldehydes and ketones) showed conformations of the oxygen atom from the CO functional group eclipsing the carbon atom. The oxygen atom preferred eclipsing the carbon atom in the following order CO>CH3>Cd>H. Exceptions to this rule were acrolein, 17, and but-3-en-2-one, 26, due to them preferring the CO---H eclipse to the CO---Cd eclipse. Compounds having branches in the main backbond, as happens in compounds 25 and 27, also showed alterations to this rule. Group 3 molecules exhibited internal hydrogen bonds having less than 1.8 Å lengths. Tables S1 and S2 show the most stable conformers and their Cartesian coordinates obtained at the MP2/6-31G† level for the ketene cyclic structures and the acyclic base compounds calculated in this work.

| 1c) Diketene | 4c) Cyclobutane-1,3-dione | 8c) Pyran-4-one |
| 11c) 2-Hydroxy-pyran-4-one | 12c) Cyclobut-2-enone | 16c) 3-hydroxy-cyclobut-2-enone |
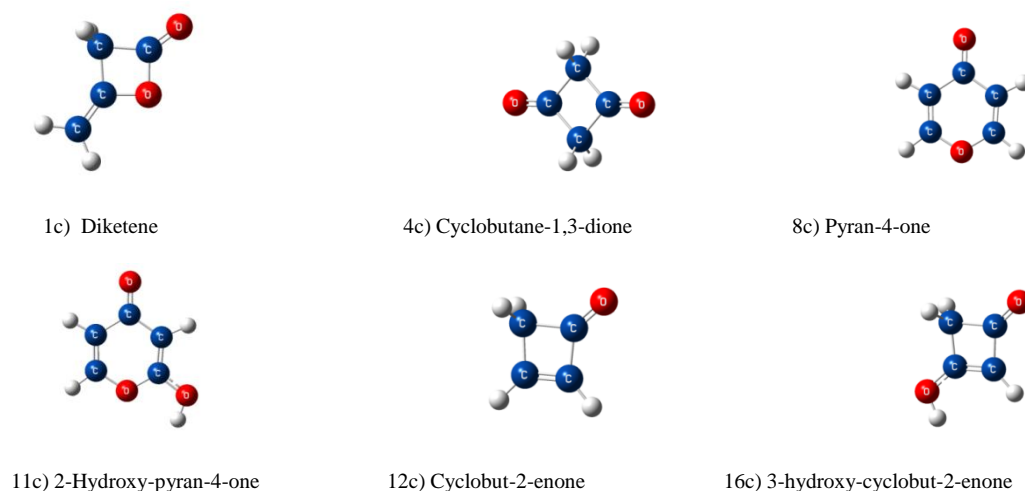
Figure 6.2. The cyclic structures analyzed in this work.

6.3.2 Hindered rotor potentials

Internal rotations' energetic barriers were calculated as being the difference between restricted optimized geometry and global equilibrium conformers. Potential surfaces were interpolated by using finite Fourier series containing the minimum number of terms possible (eq. 7). The usefulness of the Fourier-series in quantum chemistry is wide acknowledged not

only for the proper representation of internal rotation potential but also as a means of elucidating the computed potential functions' electronic molecular features.[38,39]

$$V(\phi) = \sum_{i=0}^{k} a_i \cos(i\phi) + b_i \, sen\,(i\phi) \tag{7}$$

Figure 6.3 illustrates the potential energy surfaces calculated at the HF/6-31G(d') level for some rotors accounted for by the single bonds of the compounds listed in Table 6.2. Tables S15–S19 in the supporting information show the Fourier-series coefficients for the adjusted internal rotor surfaces for the acyclic compounds. According to the internal rotation potentials obtained in this work, some rotors can be acceptably approximated within the frame of harmonic vibrations due to the large value of their energy barriers. This is the case for compounds undergoing internal hydrogen bond; e.g. the Cd−OH internal rotation in 3-hydroxy-propenal (compound 48 from group 3) occurred at 819 cm^{-1} frequency (Figure 6.3), exhibiting a ca. 65 kJ/mol energy barrier which forced the rotamer to stay in the well potential in a position very close to the lowest energy point ($\phi = 0°$).
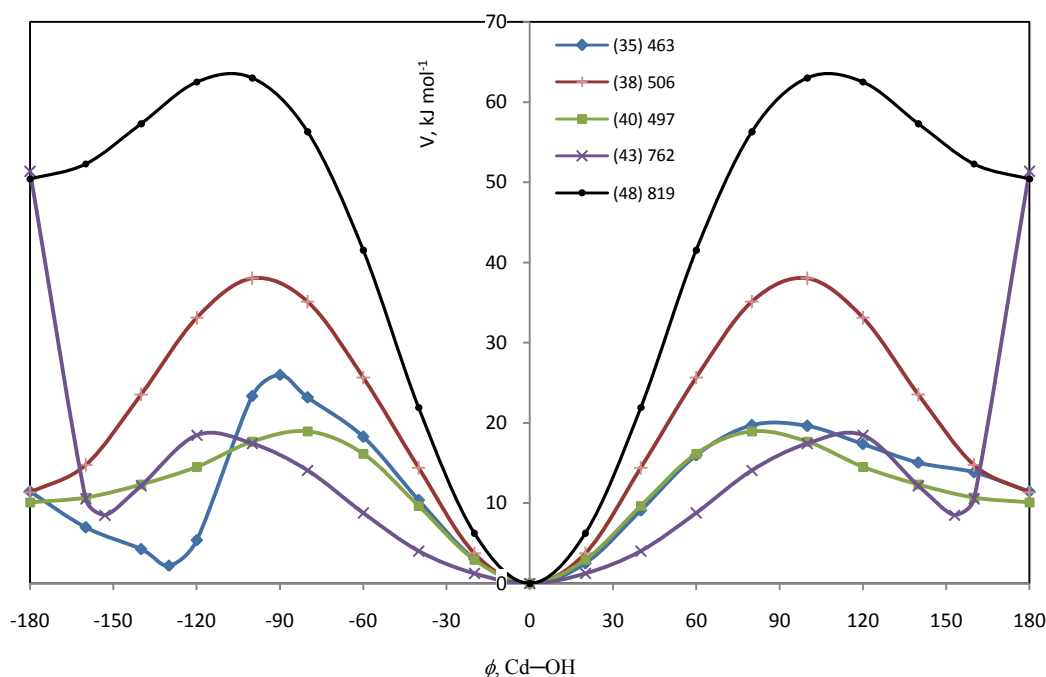
Figure 6.3. PES for internal rotations around Cd–OH bonds for some group 3 compounds (ZPE correction included). The legend illustrates the number of compounds with corresponding vibrational frequencies given in cm^{-1}.

6.3.3 Thermochemical Properties

6.3.3.1 Heats of formation

Tables 5 and 6 show the calculated values for the thermodynamic properties of the compounds studied in this work. The heats of formation for the studied compounds were also assessed by using widely-known heat of formation for several reference compounds (Table 6.7) in isodesmic reaction methodology (Table 6.8).[40] Isodesmic reactions are usually fictitious reactions conserving the type of chemical bonds and their numbers; this quality cancels out computational errors which can arise from a lack of electron correlation and deficiencies in the basis sets in both reactants and products[40]. The heat of formation values obtained with the isodesmic reactions for each compound analyzed here (Tables 6.8 and in the supporting information) were in excellent agreement (±1 kcal per mol of deviation) with the results obtained by using atomization reaction methodology (Tables 6.5 and 6.6). Such agreement between both methodologies provided confidence in the theoretical calculation results since the isodesmic reaction procedure made use of the experimental heat of formation for the reference compounds (Table 6.7). The correct heats of formation values for the analyzed compounds were taken as being those assessed by the atomization reaction procedure (Tables 6.5 and 6.6).

Table 6.5. Thermochemical properties for ketene cyclic structures from quantum mechanical calculations.

	ΔH_f^o, kcal/mol	S^o, cal/mol K	Cp, cal/mol K						
			300 K	400 K	500 K	600 K	800 K	1000 K	1500 K
Diketenes									
1c) Diketene (4-methylene-oxetan-2-one)	-47.81	72.64	20.40	25.79	30.29	33.92	39.30	43.05	48.51
2c) 3-Methyl-4-methylene-oxetan-2-one	-57.46	81.98	26.09	32.78	38.49	43.19	50.27	55.29	62.72
3c) 3,3-Dimethyl-4-methylene-oxetan-2-one	-67.37	87.22	32.35	40.45	47.34	53.01	61.63	67.80	77.05
Cyclobutane-1,3-diones									
4c) Cyclobutane-1,3-dione	-44.34	74.57	21.26	26.43	30.75	34.27	39.56	43.27	48.68
5c) 2-methyl-cyclobutane-1,3-dione	-54.02	82.83	26.88	33.21	38.67	43.24	50.25	55.28	62.75
6c) 2,2-dimethyl-cyclobutane-1,3-dione	-72.26	90.40	33.14	40.81	47.45	52.99	61.56	67.75	77.06
7c) (E)-2,4-dimethyl-cyclobutane-1,3-dione	-68.24	91.50	32.57	40.10	46.72	52.32	61.04	67.36	76.86
Pyran-4-ones									
8c) Pyran-4-one	-39.19	73.97	21.65	27.93	33.19	37.43	43.62	47.83	53.86
9c) 3-methyl-pyran-4-one	-50.00	81.86	27.70	34.90	41.17	46.38	54.27	59.82	67.93
10c) 2-methyl-pyran-4-one	-54.13	81.91	27.69	35.00	41.31	46.53	54.40	59.91	67.97
11c) 2-hydroxy-pyran-4-one	-86.87	79.30	26.61	33.31	38.77	43.06	49.13	53.16	58.91
Cyclobut-2-enones									
12c) Cyclobut-2-enone	10.32	67.70	16.87	21.69	25.83	29.20	34.23	37.75	42.91
13c) 4-methyl-cyclobut-2-enone	0.98	76.83	22.80	28.91	34.20	38.59	45.25	50.01	57.11
14c) 2-methyl-cyclobut-2-enone	-6.39	76.77	22.28	28.10	33.33	37.77	44.63	49.56	56.90
15c) 4,4-dimethyl-cyclobut-2-enone	-68.31	84.91	33.85	41.93	48.66	54.14	62.38	68.19	76.82
16c) 3-hydroxy-cyclobut-2-enone	-38.32	72.10	21.79	27.08	31.44	34.93	39.99	43.41	48.28
17c) 3-hydroxy-2-methyl-cyclobut-2-enone	-56.59	82.03	26.88	33.11	38.60	43.19	50.12	54.97	62.08
18c) 3-hydroxy-4-methyl-cyclobut-2-enone	-54.70	81.15	27.69	34.35	39.90	44.40	51.09	55.74	62.52
19c) 3-hydroxy-2,4-dimethyl-cyclobut-2-enone	-68.60	89.76	32.94	40.41	47.03	52.60	61.14	67.22	76.27
20c) 3-hydroxy-4,4-dimethyl-cyclobut-2-enone	-68.31	84.91	33.85	41.93	48.66	54.14	62.38	68.19	76.82

Diketene (1c) appeared to be the most stable ketene dimer according to the heat of formation values for the different cyclic structures analyzed in this work (Table 6.5). This dimer's relative stability contradicted experimental measurements by Chickos et al.,[9] who claimed that cyclobutane-1,3-dione dimer (4c) was more stable than diketene (1c) by about 1 kcal per mol. The reportedly favorable experimental stability of cyclobutane-1,3-dione over diketene was based on both combustion and sublimation data which might have been erroneous due to this compound's tautomeric instability in condensed phase.[4]

Table 6.6. Thermochemical properties for acyclic base compounds from quantum mechanical calculations.

	$\Delta H_f°$, kcal/mol	$S°$, cal/mol K	Cp, cal/mol K						
			300 K	400 K	500 K	600 K	800 K	1000 K	1500 K
Group 1. Ethers and alcohols.									
(1) Ethene-1,1-diol	-75.62	64.98	18.97	23.27	26.50	28.77	31.61	33.45	36.46
(2) 1-methoxy-ethenol	-71.84	72.73	23.75	29.30	33.88	37.42	42.35	45.71	50.89
(3) 1-vinyloxy-ethenol	-48.39	81.60	27.27	33.45	38.12	41.65	46.72	50.33	56.03
(4) 1-methoxy-1-vinyloxy-ethene	-42.78	91.04	30.18	37.42	43.58	48.59	56.14	61.57	69.89
(5) 1-(1-hydroxy-vinyloxy)-ethenol	-91.75	93.71	27.08	33.05	38.45	43.06	50.33	55.72	64.03
(6) 1-(1-methoxy-vinyloxy)-ethenol	-88.05	100.96	37.18	44.34	50.03	54.60	61.54	66.64	74.70
(7) Vinyloxy-ethene	-2.09	73.76	21.53	26.67	31.04	34.65	40.21	44.30	50.66
(8) Methoxy-ethene	-25.05	67.58	20.13	24.26	27.83	30.87	35.75	39.44	45.31
(9) Propene-1,2-diol	-78.77	76.90	25.00	29.06	32.59	35.59	40.34	43.93	49.75
(10) Ethenol	-28.89	60.22	14.69	18.15	20.81	22.80	25.67	27.77	31.23
(11) Propen-2-ol	-40.10	66.32	19.97	25.05	29.13	32.28	36.84	40.14	45.48
(12) Ethoxy-ethene	-33.15	73.95	26.57	32.14	36.89	40.90	47.34	52.23	59.95
(13) 1-(2-hydroxy-vinyloxy)-ethenol	-88.66	87.35	31.30	38.73	44.34	48.40	53.59	56.81	61.66
(14) 1,1-dimethoxy-ethene	-65.72	84.24	27.08	33.05	38.45	43.06	50.33	55.72	64.03
(15) 1-ethoxy-1-methoxy-ethene	-74.06	90.52	33.69	40.52	46.96	52.57	61.51	68.14	78.38
Group 2. Aldehydes and ketones									
(16) Penta-1,4-dien-3-one	-0.83	76.96	25.60	31.01	35.86	39.91	46.06	50.41	56.89
(17) Propenal	-15.08	65.16	16.80	20.37	23.46	26.06	30.09	32.97	37.23
(18) 2-Methyl-propenal	-25.02	73.23	21.53	26.67	31.04	34.65	40.21	44.30	50.66
(19) But-3-enal	-17.69	80.95	21.39	26.14	30.44	34.11	39.90	44.17	50.72
(20) Malonaldehyde	-60.60	75.47	18.62	22.35	25.71	28.60	33.14	36.43	41.33
(21) 2-methyl-but-3-enal	-25.82	83.64	29.06	34.40	39.40	43.82	51.01	56.44	64.88
(22) 2,2-dimethyl-but-3-enal	-34.48	92.94	33.16	40.69	47.51	53.32	62.43	69.12	79.38
(23) 3-oxo-butyraldehyde	-74.53	86.50	23.99	29.11	33.74	37.71	43.95	48.51	55.40
(24) 2-methyl-malonaldehyde	-67.96	86.60	25.40	30.13	34.44	38.20	44.23	48.71	55.52
(25) 2,2-dimethyl-malonaldehyde	-77.19	90.91	31.62	37.82	43.33	48.05	55.57	61.18	69.80
(26) But-3-en-2-one	-26.46	73.82	21.61	26.41	30.77	34.50	40.31	44.54	50.94
(27) 2-methyl-3-oxo-pent-4-enal	-57.75	98.44	34.20	41.04	47.22	52.51	60.76	66.72	75.65
(28) Hexa-1,5-dien-3-one	-5.84	90.07	31.89	38.15	43.91	48.85	56.56	62.19	70.77
(29) 2-methyl-penta-1,4-dien-3-one	-10.53	86.14	31.34	38.41	44.30	49.15	56.62	62.11	70.62
(30) 3-oxo-hex-5-enal	-53.76	103.45	32.92	40.05	46.39	51.74	60.04	66.08	75.20
(31) Pent-1-en-3-one	-32.60	80.17	29.06	34.92	40.14	44.62	51.76	57.07	65.26
(32) 2,4-dimethyl-penta-1,4-dien-3-one	-19.10	95.07	36.80	44.96	51.95	57.84	67.09	73.97	84.63
(33) 2-methyl-hexa-1,5-dien-3-one	-15.74	96.69	37.49	45.73	52.85	58.79	67.97	74.71	85.07
Group 3. Carbonyl, hydroxyl and alkoxyl groups									
(34) (Z)-5-hydroxy-hexa-1,4-dien-3-one	-71.16	85.55	33.38	41.06	47.76	53.37	62.04	68.46	78.79
(35) 3-hydroxy-2-methyl-but-3-enal	-71.91	92.54	32.25	38.83	44.58	49.35	56.64	61.92	70.06
(36) 3-hydroxy-2,2-dimethyl-but-3-enal	-83.37	98.36	37.81	46.28	53.49	59.39	68.33	74.75	84.59
(37) (Z)-5-hydroxy-3-oxo-pent-4-enal	-101.83	90.33	30.03	36.73	42.53	47.37	54.92	60.58	69.45
(38) 3,3-dihydroxy-propenal	-119.12	72.70	22.62	28.02	32.47	35.99	41.08	44.60	50.19
(39) (Z)-3-vinyloxy-propenal	-31.72	84.59	27.71	33.74	39.06	43.50	50.25	55.03	62.01
(40) 4-hydroxy-2-methyl-but-3-enal	-67.66	91.50	35.10	41.51	46.61	50.74	57.21	62.12	70.00
(41) 4-hydroxy-2,2-dimethyl-but-3-enal	-77.72	96.04	37.28	46.74	55.02	61.62	70.93	77.12	86.09
(42) 3-hydroxy-but-3-enal	-63.43	83.91	26.22	31.95	36.83	40.82	46.77	50.90	56.90
(43) 4-hydroxy-but-3-enal	-61.04	82.69	24.33	29.93	34.74	38.71	44.77	49.12	55.70
(44) 2-hydroxymethyl-2-methyl-malonal	-114.04	96.53	37.53	45.39	51.72	56.73	63.99	68.99	76.37
(45) 1,1-dihydroxy-pent-1-en-3-one	-140.54	88.21	33.11	41.28	48.24	53.93	62.44	68.48	77.95
(46) (Z)-1-hydroxy-pent-1-en-3-one	-85.58	83.55	29.36	36.42	42.68	48.01	56.47	62.92	73.31
(47) (Z)-4-hydroxy-but-3-en-2-one	-78.94	75.79	23.52	29.25	34.35	38.66	45.45	50.62	59.10
(48) (Z)-3-hydroxy-propenal	-65.23	68.10	18.52	22.84	26.68	29.95	35.17	39.17	45.28
(49) 4,4-dihydroxy-but-3-en-2-one	-133.13	80.73	27.41	34.28	40.04	44.70	51.54	56.32	63.84
(50) 1,1-dihydroxy-penta-1,4-dien-3-one	-110.12	82.67	32.01	39.59	45.77	50.66	57.70	62.53	70.03
(51) (Z)-3-hydroxy-butenal	-78.98	75.33	24.24	29.72	34.64	38.87	45.64	50.82	59.12
Group 4. Ester group									
(52) Formic acid vinyl ester	-61.94	70.29	19.51	24.08	28.00	31.19	35.86	39.03	43.27
(53) 3-oxo-propionic acid vinyl ester	-96.92	93.56	31.69	38.30	43.92	48.54	55.63	60.77	68.16
(54) 2-methyl-acrylic acid vinyl ester	-58.27	94.07	33.74	41.15	47.86	53.67	62.76	69.09	77.58
Group 5. Carboxylic acids									
(55) Acrylic acid	-76.88	69.86	30.86	38.47	44.15	48.24	53.48	56.74	61.63
(56) 2,2-dimethyl-3-oxo-propionic acid	-140.11	97.64	33.25	40.46	46.86	52.31	60.89	67.22	76.52
(57) But-3-enoic acid	-81.49	82.13	24.86	30.34	35.18	39.29	45.77	50.56	57.53

Several investigations have recently criticized such experimental relative stability and it seems that the heat of formation for both compounds must be reassessed.[34,42] The values calculated in this research coincided with theoretical works[34,42] regarding diketene's relative stability over cyclobutane-1,3-dione. In fact, diketene was found to have a -47.81 kcal per mol heat of formation at the CBS-Q level which is ca. 2 kcal per mol more stable than the -45.47±0.3 kcal per mol experimental value.[10]

Table 6.7. Experimental $\Delta H_f°$ (kJ/mol)[(a)] and CBS-Q energies (au) at 298 K for the reference species in the isodesmic reactions.

Species	$\Delta H_f°$, kJ/mol	E^{298} (a.u.)	Species	$\Delta H_f°$, kJ/mol	E^{298} (a.u.)
CH4	-74.60	-40.405770	(CH3)2CHCHCH2	-27.20	-196.091909
CH3CHO	-166.10[(b)]	-153.575967	(CH3)2CHCHO	-213.17[(c)]	-232.026087
CH2CHOCH3	-104.60	-231.999290	H2O	-241.83	-76.332730
C2H6	-84.00	-79.625293	CH3CHCO	-63.35[(c)]	-191.592801
CH3COC2H5	-238.60	-232.036918	HCOOH	-378.65	-189.521474
CH2CHOC2H5	-140.16	-231.999290	CH3COOCH3	-413.30	-267.967415
CH2CHCH3	19.70	-117.639993	CH2CHCHCH2	108.78	-155.660066
CH2CHCH2CH3	-0.50	-156.863963	Oxetane	-80.50[(d)]	-192.759516
H2CO	-108.60	-114.338952	Oxirane	-52.60[(d)]	-153.533011
C2H4	52.40	-78.411728	Propiolactone	-282.90[(d)]	-266.757641
HCOOCH3	-352.40	-228.731354	Cyclobutene	156.70[(d)]	-155.640421
H2	0.00	-1.162781	Cyclobutane	28.40[(d)]	-156.854156
CH3COCH3	-217.10	-192.812053	Cyclobutanone	-101.25[(d)]	-230.819403
CH3OH	-201.00	-115.534033	Cyclohexane	-123.14[(d)]	-235.344221
C2H5OC2H5	-252.10	-233.198893	Cyclohexanone	-226.10[(d)]	-309.305669
CO2	-393.51	-188.367756	Furan	-34.89[(d)]	-229.635986
H2CCO	-47.70[(c)]	-152.370823	3,4-Dihydro-2H-pyran	-125.10[(d)]	-270.045343
CH3CH2CHO	-188.66	-192.800567	Tetrahydro-2H-pyran	-223.38[(d)]	-271.247122

[(a)] Ref. 35. [(b)] Ref. 41a,b. [(c)] Ref. 15. [(d)] Ref. 41d.

Table 6.8. Checking of $\Delta H_f°$ in kcal/mol for some compounds by using isodesmic reactions.[*]

				$\Delta H_{rxn}{}^{298}$	$\Delta H_f°$
1c) Diketene (Dik)	→	2H2C=C=O		24.59	-47.39
Dik + 3CH4	→	CH3CHO + CH3OCHCH2 + C2H6		17.00	-48.03
Dik + 2C2H6	→	CH2CHCH2CH3 + CH3COOCH3		-18.17	-48.10
Dik + 2CH4	→	Oxetane + H2CO + C2H4		51.56	-48.60
Dik + 3C2H6	→	Oxetane + CH3COCH2CH3 + C2H4 + CH4		26.84	-48.18
Dik + CH4	→	Oxetan-2-one + C2H4		10.81	-48.07
			Average (-47.81)		-48.06
4c) Cyclobutane-1,3-dione (Cy13one) →		2H2C=C=O		20.49	-43.28
Cy13one + 2CH4	→	Cyclobutane + 2H2CO		33.74	-43.26
Cy13one + CH4	→	Cyclobutanone + 2H2CO		13.62	-45.97
Cy13one + 2CH4	→	Cyclobutane + OCHCHO		19.54	-43.35
Cy13one + CH4	→	CH3CH=C=O + CH3CHO		7.10	-44.24
			Average (-44.34)		-44.02
16c) 3-Hydroxy-cyclobut-2-enone (3HCy):					
3HCy + 2CH4	→	CH3COCH2CH3 + CH2CHOH		-12.28	-37.97
3HCy + 3CH4	→	CH3CHC=C=O + CH3CH2OH + C2H6		0.88	-38.77
3HCy + C2H6	→	Cyclobutanone + CH2CHOH		7.33	-40.34
3HCy + H2CO	→	Cyclobutanone + HCOOH + CO2		-54.34	-40.80
			Average (-38.32)		-39.47

[*] Results from atomization reaction procedure shown in parenthesis.

Likewise, cyclobutane-1,3-dione was found to have a -44.34 kcal per mol heat of formation which is ca. 2 kcal per mol less stable than the experimentally obtained value.[9] Experimental and theoretical heat of formation values for ketene compounds have typically been in

contradiction. So far, theoretical calculations have appeared to properly assess the heat of formation for this class of compounds.[15] Experimental discrepancies in determining heat of formation is proof of the inherent difficulties of working with ketenes and ketene derivative compounds. Generating cyclobutane-1,3-dione structure ketene dimers has also been a matter of controversy due to it being unknown whether they are produced as just a result of a kinetic effect.[1a] Based on this work's results, diketene was found to be the major product of ketene dimerization in gas phase due to thermodynamic control of the reaction. This conclusion is in agreement with results of chapter 4[42].

The 3-hydroxy-cyclobut-2-enone (16c) was found to be the least stable ketene dimer that has been reported (Tables 6.5 and 6.8). 3-hydroxy-cyclobut-2-enone compound can be generated by tautomerization of cyclobutane-1,3-dione[4] (4c). Based on the values calculated in this work, the appearance of the cyclobutane-1,3-dione acidic or enolized form was thermodynamically disfavored in gas phase; the heat of tautomerization for cyclobutane-1,3-dione to 3-hydroxy-cyclobut-2-enone was calculated to be 6.0 kcal per mol in gas phase. Comparatively, the tautomerization enthalpy of acetaldehyde ($\Delta H°_f$=-40.80 kcal per mol[35]) to ethenol ($\Delta H°_f$=-28.89 kcal per mol, Table 6.6) is ca. 12 kcal per mol (the enthalpy lowers to 10.9 kcal per mol when considering the reviewed value for acetaldehyde by Holmes et al[41b]), while tautomerization enthalpy of propanal ($\Delta H°_f$=-45.10 kcal per mol[35]) to propen-1-ol ($\Delta H°_f$ =-41.60 kcal per mol[43]) is 3.5 kcal per mol (ca. 8 kcal/mol when considering $\Delta H°_f$ =-36.20 kcal per mol[41c] for propen-1-ol) and tautomerization enthalpy of acetone ($\Delta H°_f$ =-51.9 kcal per mol[35]) to propen-2-ol ($\Delta H°_f$ =-40.1 kcal per mol, Table 6.6) is 11.8 kcal per mol. The carbonyl form was more stable than the hydroxide form in gas phase in all the preceding cases. On the other hand, tautomeric cyclobutane-1,3-dione species have been reported in substantial amounts in polar solvents.[4] This favorable appearance of 4c enol-tautomeric species in polar solvents can only be plausibly explained due to the lack of kinetic information. From the thermodynamic point of view (and in the absence of any catalyst) favorable interactions in polar media mainly due to the OH group may enable cyclobutane-1,3-dione to afford its enol-tautomeric species.

The more relative stability of cyclobutane-1,3-dione compared to its enol tautomer is not characteristic of acyclic β-diketones (Figure 6.4). Both the symmetrical and unsymmetrical enol-tauromeric forms of β-diketones generally appear to be more stable than the keto form.[44]

Such relatively more stable enol forms may be explained by the fact that nonbonding orbitals can interact by connecting σ bonds (through-bond interaction) in these tautomers to a greater extent than interactions by direct overlap (through-space interaction).[45] Despite experimental and theoretical analysis finding that the symmetrical enol-tautomer for acyclic β-diketones is the most stable,[45b,46] the unsymmetrical one was analyzed in this work (in group 3) to enable correct O/Cd/H and CO/Cd/C group calculations.
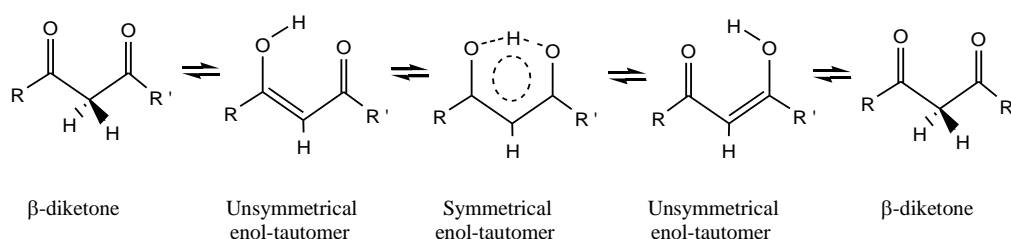
Figure 6.4. β-diketone tautomerization.

Substituent methyl groups modify relative energies for different dimer species as well as for the tautomeric reaction in gas phase (Table 6.5). Figure 6.5 shows the different stabilizations achieved by the dimers with H, Me and 2Me substituents. Based on these results, the increased number of Me substituents lowered the energy gap between the different dimers. When the rings contained 2Me substituents, the diketene form became thermodynamically unfavorable. This fact suggests that the greater the alkyl substituents' molecular weight the more the relative stabilization of the cyclobutane-1,3-diones and their enol-tautomeric forms compared to the corresponding diketene forms. The relative stabilization of cyclobutane-1,3-diones and their enol-tautomeric forms by the methyl groups could be due to increased through-bond interactions.[45c] Accordingly, spontaneous alkylketene dimerization towards cyclobutane-1,3-dione forms tended to be thermodynamically favored over dimerization towards 4-methylene-oxetan-2-one forms having increased alkyl substituent weight (Table 6.5).
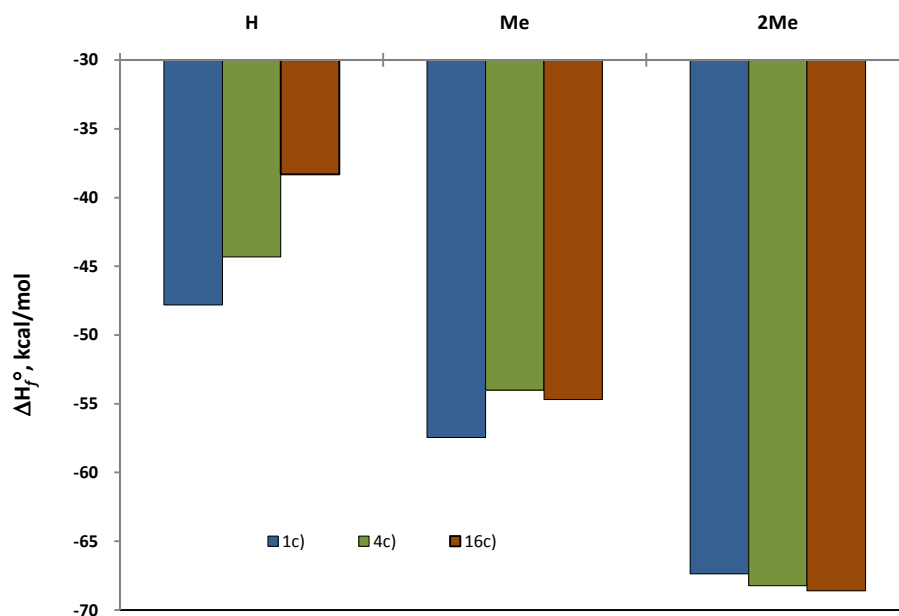
Figure 6.5. Substituent stabilization in 1c) diketene, 2c) cyclobutane-1,3-dione and 16c) 3-hydroxy-cyclobut-2-enone.

6.3.3.2 Entropies and heat capacities

The entropies and specific heats assessed by using MP2/6-31G† geometries and scaled frequencies at HF/6-31G† level are summarized in Tables 6.5 and 6.6. Tables in the supporting information summarize contributions to entropy and specific heat from each class of movement, namely translation, rotation and normal vibrations (TRV) and internal rotations (IR). Final values for the compounds' entropies must consider the mixture of energetically equivalent conformers. An additional mixture entropy term corrects the entropy for properly estimating this property; the entropy generated by 1 mol of mixture can be calculated according to[14], $\Delta S_{mix} = -R \sum n_i \ln(n_i)$, Where n_i corresponds to the equilibrium mol fraction of the ith conformer in the mixture. The entropy of mixture was reduced to the well-known formula of $\Delta S_{mix} = -R \ln(2)$ for the mixture of two energetically equivalent conformers. It is worth mentioning that the effects of hindrance potential were prominent in calculating entropy and low temperature specific heat. This is a consequence of both potential barrier medium values in most of the rotors and low internal rotator frequency values. The symmetry numbers and other information, such as optical conformers, hindered frequencies and the potential energy barriers required for calculating the entropies of the analyzed compounds, can be consulted in Table 6.9.

6.3.4 GAVS assessment

6.3.4.1 Nonnext neighbor interactions

The corrections for the proper GAV calculations were based on final thermochemical property values (Table 6.6). The first correction analyzed here concerns the preferable spatial configuration of ether compounds (Figure 6.6). Group 1 ether compounds 14 and 15 showed different eclipsed atom trends, increasing from hydrogen to methyl substituent in the alkoxy group. The 14 and 15 dioxy compounds possessed the methyl group eclipsed by the methylene group; the methoxyl substituents were thus in *syn* position (Figure 6.6). The most stable conformers having low molecular weight for this group were 1 and 2; in line with expressing these molecules in terms of GAVs, the Cd/O2 group took the O---H eclipse into account. Thus, the GAVs for compounds 14 and 15 had to be corrected for the lack of this eclipse (NN_{G1}^{I}). Likewise, ether compounds 4, 5, 6 and 13, which included another methylene group, showed spatial distortions (NN_{G1}^{II}) compared to most stable low-weight diether conformers. GAV corrections for the heat of formation (kcal per mol) in the preceding ether compounds were obtained as follows: $NN_{G1}^{I} = T14 + (T1 - 2*T2)$, $NN_{G1}^{I}=2.34$; $NN_{G1}^{I} = T15 + T1 - 2*T2 - T12 + T8$, $NN_{G1}^{I}=2.1$; $NN_{G1}^{II-4} = T4 - T7 + T10 - T2$, $NN_{G1}^{II-4}=2.27$; $NN_{G1}^{II-5} = T5 - T1 + T10 - T2 + T8 - T7$, $NN_{G1}^{II-5}=3.87$; $NN_{G1}^{II-6} = T6 - T1 + 2*T10 - T2 - T7$, $NN_{G1}^{II-6}=3.73$; $NN_{G1}^{II-13} = T13 - T1 - T7 + 2*Cd/H2$, $NN_{G1}^{II-13}=1.58$.

(1) Ethene-1,1-diol   (2) 1-Methoxy-ethenol   (14) 1,1-Dimethoxy-ethene   (15) 1-Ethoxy-1-methoxy-ethene
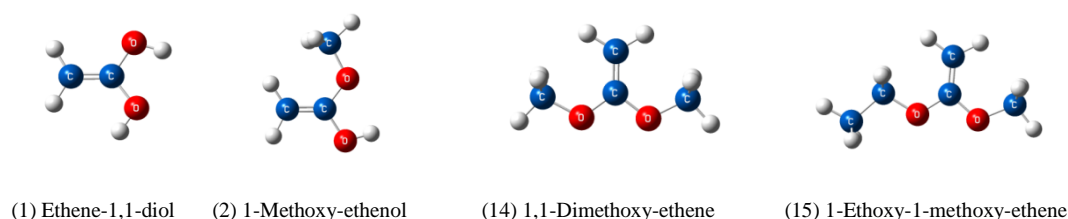
Figure 6.6. Conformers for some group 1 compounds.

The correction for the lack of the O---H eclipse, NN_{G1}^{I}, thus corresponded to the mean value of 2.22 kcal per mol for the heat of formation for compounds 14 and 15. Similarly, group 2 compounds 27, 28 and 31 and group 3 compounds 37, 45 and 46 as well as compound 55

Table 6.9. Symmetry numbers, optical isomers, hindered internal frequencies, reduced moment of inertia and potential energies.

	σint	σext	OI	Hind. Freq. (cm⁻¹)	I_r (amu Å)	V_{max}, kcal/mol
Group 1. Ethers and alcohols						
(1) Ethene-1,1-diol	2	1	1	257(Cd-O); 417(Cd-O)	0.755; 0.657	5.13; 8.76
(2) 1-methoxy-ethenol	6	2	1	131 (Cd-OCH3); 254 (O-C); 298 (Cd-OH)	2.8; 8.156; 0.814	9.0; 3.54; 5.62
(3) 1-vinyloxy-ethenol	1	1	2	86 (O-Cd); 116 (O-Cd); 301 (Cd-O)	0.83; 9.74; 5.81	3.11; 5.13; 5.10
(4) 1-methoxy-1-vinyloxy-ethene	6	1	2	45 (O-Cd); 64 (Cd-O); 123 (O-Cd); 266 (O-C)	4.25; 11.84; 4.71; 3.05	3.84; 1.67; 3.11; 3.43
(5) 1-(1-hydroxy-vinyloxy)-ethenol	1	2	2	65 (O-Cd); 71 (Cd-O); 256 (Cd-O); 257 (Cd-O)	25.8; 25.8; 0.83; 0.83	2.52; 2.52; 3.43; 3.43
(6) 1-(1-methoxy-vinyloxy)-ethenol	3	1	2	44(O-Cd); 70(O-Cd); 105(O-Cd); 262(O-C); 282(O-H)	29.82; 31.42; 5.56; 3.02; 0.84	3.61; 2.18; 3.57; 2.91; 4.49
(7) Vinyloxy-ethene	1	2	1	57 (Cd-O); 78 (Cd-O)	3.60; 3.60	2.36; 2.36
(8) Methoxy-ethene	6	2	1	237 (O-Cd); 269 (O-C)	6.53; 2.60	4.5; 3.73
(9) Propene-1,2-diol	3	1	2	209 (Cd-C); 321(Cd-O); 555 (Cd-O)	2.96; 0.54; 0.84	2.74; 3.52; 3.54
(10) Ethenol	2	1	1	476 (Cd-O)	0.76	5.29
(11) Propen-2-ol	6	2	1	204 (Cd-C); 463 (O-H)	2.93; 0.66	2.32; 5.18
(12) Ethoxy-ethene	6	2	1	115 (O-C); 214 (O-Cd); 287 (C-C)	5.10; 7.13; 2.71	11.8; 4.21; 3.58
(13) 1-(2-hydroxy-vinyloxy)-ethenol	4	1	2	59 (O-Cd); 92 (O-Cd); 309 (Cd-O); 461 (Cd-O)	19.4; 21.05; 0.83; 0.61	6.20; 4.80; 4.51; 6.0
(14) 1,1-dimethoxy-ethene	9	1	1	100 (Cd-O); 141 (Cd-O); 265 (O-C); 282 (O-C)	2.83; 2.83; 7.46; 7.46	3.03; 3.03; 3.89; 3.89
(15) 1-ethoxy-1-methoxy-ethene	9	2	1	79(Cd-O); 127(O-C); 135(Cd-O); 274(O-C); 276(C-C)	6.36; 11.3; 10.55; 2.91; 2.76	2.96; 2.76; 5.92; 3.68; 3.91
Group 2. Aldehydes and ketones						
(16) Penta-1,4-dien-3-one	4	2	1	71 (Cd-CO); 119 (Cd-CO)	7.22; 7.22	5.70; 5.70
(17) Propenal	2	1	1	173 (Cd-CO)	2.76	7.67
(18) 2-methyl-propenal	6	2	1	158 (Cd-O); 189 (Cd-C)	6.44; 2.90	8.04; 1.86
(19) But-3-enal	1	1	2	85 (C-C); 156 (C-Cd)	5.59; 7.61	2.91; 2.86
(20) Malonaldehyde	1	1	2	66 (CO-C); 129 (CO-C)	3.86; 7.48	2.89; 2.56
(21) 2-methyl-but-3-enal	3	1	2	84 (C-CO); 96 (C-Cd); 237 (C-C)	5.67; 6.13; 3.00	2.87; 3.07; 3.22
(22) 2,2-dimethyl-but-3-enal	9	1	2	78 (C-CO); 100 (C-Cd); 254 (C-C); 292 (C-C)	5.29; 7.18; 3.06; 3.06	2.91; 2.60; 3.80; 4.73
(23) 3-oxo-butyraldehyde	3	1	2	34 (C-CO); 69 (C-CO); 125 (CO-CH3)	13.44; 4.48; 2.94	3.29; 1.90; 0.77
(24) 2-methyl-malonaldehyde	3	1	2	79 (CO-C); 96 (CO-C); 222 (C-C)	8.40; 5.93; 2.91	2.88; 3.62; 2.88
(25) 2,2-dimethyl-malonaldehyde	9	2	2	62 (CO-C); 68 (CO-C); 222 (C-C); 254 (C-C)	5.48; 5.48; 3.06; 3.06	2.63; 2.65; 3.29; 3.29
(26) But-3-en-2-one	6	2	1	128 (CO-Cd); 160 (CO-C)	8.07; 2.95	5.49; 1.44
(27) 2-methyl-3-oxo-pent-4-enal	3	1	2	53 (CO-C); 65 (CO-C); 98 (CO-Cd); 223 (C-C)	5.57; 41.22; 7.55; 2.97	3.95; 2.61; 6.51; 3.03
(28) Hexa-1,5-dien-3-one	2	1	2	54 (CO-C); 81 (Cd-C); 119 (CO-Cd)	14.50; 6.60; 7.10	2.78; 3.21; 5.36
(29) 2-methyl-penta-1,4-dien-3-one	3	1	1	55 (CO-Cd); 78 (CO-Cd); 191 (Cd-C)	26.43; 6.77; 2.85	4.10; 3.71; 2.01
(30) 3-oxo-hex-5-enal	1	1	2	39 (CO-C); 44 (CO-C); 68 (CO-C); 98 (Cd-C)	16.50; 14.72; 5.20; 7.47	2.14; 3.31; 2.21; 3.34
(31) Pent-1-en-3-one	6	2	1	68 (CO-Cd); 113 (CO-C); 236 (C-C)	11.33; 7.31; 2.66	3.69; 5.32; 2.87
(32)2,4-dimethyl-penta-1,4-dien-3-one	9	2	2	47(CO-Cd); 92(CO-Cd); 181(Cd-C); 188(Cd-C)	34.54; 34.54; 2.89; 2.89	5.12; 5.12; 1.96; 1.96
(33) 2-methyl-hexa-1,5-dien-3-one	3	1	2	49(CO-Cd); 74(CO-C); 101(Cd-C); 195 (Cd-C)	29.65; 16.30; 7.40; 2.81	4.80; 5.36; 3.56; 2.07
Group 3. Carbonyl, hydroxyl and alkoxyl groups						
(34) (Z)-5-hydroxy-hexa-1,4-dien-3-one	12	2	1	71(CO-Cd); 159(Cd-C); 210(CO-Cd); 649	7.49; 3.01; 21.64; 0.66	5.86; 1.64; 14.92; 18.64
(35) 3-hydroxy-2-methyl-but-3-enal	3	1	2	67(Cd-C); 94(CO-C); 245(C-C); 463(Cd-OH)	28.02; 5.38; 2.94; 0.17	3.54; 4.10; 3.10; 5.58
(36) 3-hydroxy-2,2-dimethyl-but-3-enal	9	1	2	70 (Cd-C); 89 (CO-C); 261 (C-C); 321 (C-C); 455 (Cd-OH)	34.3; 5.04; 3.03; 3.07; 0.21	3.36; 4.35; 3.49; 5.20; 5.42
(37) (Z)-5-hydroxy-3-oxo-pent-4-enal	4	1	2	36(CO-C); 57(CO-C); 116(CO-Cd); 802(Cd-OH)	15.00; 4.62; 18.80; 0.52	3.55; 2.03; 15.80; 15.52
(38) 3,3-dihydroxy-propenal	4	1	1	313 (CO-Cd); 506 (Cd-OH); 901 (Cd-OH)	8.91; 0.69; 0.84	22.70; 9.09; 22.51
(39) (Z)-3-vinyloxy-propenal	2	1	1	47 (Cd-O); 92 (Cd-O); 168 (Cd-CO)	4.23; 4.62; 3.14	2.06; 4.25; 9.76
(40) 4-hydroxy-2-methyl-but-3-enal	6	1	2	74(CO-C); 203(Cd-C); 228(C-C); 497 (Cd-OH)	4.78; 7.93; 2.97; 0.84	3.05; 3.80; 3.40; 4.53
(41) 4-hydroxy-2,2-dimethyl-but-3-enal	9	1	2	104(CO-C); 112(Cd-C); 253(C-C); 291(C-C); 623(C-C)	9.25; 31.26; 2.84; 3.05; 0.60	6.40; 7.03;3.75; 4.60; 4.88
(42) 3-hydroxy-but-3-enal	1	1	2	87 (CO-C); 143 (Cd-C); 522 (Cd-OH)	9.36; 20.10; 0.79	6.12; 7.57; 6.50
(43) 4-hydroxy-but-3-enal	1	1	1	52 (Cd-C); 159 (CO-C); 762 (Cd-OH)	22.88; 10.0; 0.56	3.71; 3.66; 12.28
(44)2-hydroxymethyl-2-methyl-malonal	3	1	2	73 (CO-C); 102 (CO-C); 152 (C-C); 230 (C-C); 549 (C-OH)	7.54; 7.58; 15.58; 3.08; 0.84	7.10; 4.52; 9.34; 3.85; 6.63
(45) 1,1-dihydroxy-pent-1-en-3-one	12	1	1	45(CO-C); 118(CO-Cd); 243(C-C); 491(Cd-OH); 782(Cd-OH)	12.62; 21.44; 2.67; 0.65; 0.57	1.20; 21.90; 2.96; 23.10; 8.87
(46) (Z)-1-hydroxy-pent-1-en-3-one	12	1	1	62(CO-C); 106(CO-Cd); 238(C-C); 822(Cd-OH)	12.45; 17.96; 2.62; 0.45	1.28; 15.64; 2.92; 15.96
(47) (Z)-4-hydroxy-but-3-en-2-one	12	1	1	101 (CO-C); 122 (CO-Cd); 834 (Cd-H)	2.97; 17.33; 0.63	0.80; 16.10; 16.25
(48) (Z)-3-hydroxy-propenal	4	1	1	251 (CO-Cd); 819 (Cd-OH)	8.78; 0.65	15.80; 15.06
(49) 4,4-dihydroxy-but-3-en-2-one	12	1	1	69 (CO-C); 137 (CO-Cd); 494 (Cd-OH); 908 (Cd-OH)	2.99; 20.62; 0.60; 0.76	0.33; 22.34; 8.91; 23.30
(50) 1,1-dihydroxy-penta-1,4-dien-3-one	8	1	1	77 (CO-Cd); 150 (CO-Cd); 502 (Cd-OH); 939 (Cd-OH)	7.54; 20.55; 0.57; 0.67	6.05; 22.60; 9.05; 23.86
(51) (Z)-3-hydroxy-butenal	12	1	1	155 (Cd-C); 186 (CO-Cd); 828 (Cd-OH)	2.98; 8.91; 0.81	1.63; 17.40; 16.96

197

Table 6.9. Symmetry numbers, optical isomers, hindered internal frequencies, reduced moment of inertia and potential energies (continuation).

	σ_{int}	σ_{ext}	OI	Hind. Freq. (cm^{-1})	I_r (amu Å)	V_{max}, kcal/mol
Group 4. Ester group						
(52) Formic acid vinyl ester	4	1	1	69 (CO-O); 304 (O-Cd)	3.83; 5.75	3.83; 11.66
(53) 3-oxo-propionic acid vinyl ester	4	1	2	33 (CO-C); 52 (CO-C); 71 (O-Cd); 152 (CO-O)	12.08; 4.50; 5.72; 7.37	2.26; 2.98; 3.93; 11.97
(54) 2-methyl-acrylic acid vinyl ester	6	1	2	70(CO-Cd); 72(O-Cd); 144(CO-O); 205(Cd-C)	25.11; 24.61; 7.35; 2.61	9.84; 2.97; 6.92; 2.23
Group 5. Carboxylic acids						
(55) Acrylic acid	4	1	1	124 (CO-Cd); 706 (CO-OH)	7.50; 0.60	6.89; 13.86
(56) 2,2-dimethyl-3-oxo-propionic acid	9	1	2	44(CO-C); 68(CO-C); 235(C-C); 280(C-C); 655(CO-OH)	31.60; 5.40; 3.03; 3.05; 0.30	2.24; 2.56; 3.75; 3.66; 14.27
(57) But-3-enoic acid	2	1	2	54 (CO-C); 95 (Cd-C); 560 (CO-OH)	14.00; 6.33; 0.53	2.13; 3.05; 13.71

belonging to group 5 took different conformations from those exhibited by the corresponding low-weight compounds; i.e. low-weight compounds such as 17, 18 and 26 showed that the carbonyl group preferred the *syn* position and the CO group (Figure 6.7) therefore appeared to eclipse the hydrogen and methyl group instead of the methylene group. By contrast, compounds 27, 28, 31, 37, 45, 46 and 55 showed the *anti* conformation to be the most stable (Figure 6.7 and Tables in the supporting information). The correction for the heat of formation in these compounds due to this class of nonnext neighbor interaction corresponded to, $NN_{G2}^{I} + C/CO/C/H_2 = T31 - T26$, $NN_{G2}^{I} = -0.96$ kcal/mol. Likewise, the most stable conformers for 23, 27, 30, 44 and 56 compounds exhibited nonbonding interactions which were different to that in the *syn* and *anti* position; this type of correction was due to the CO---X eclipse where X = {H, CO} (in kcal per mol): $NN_{G2}^{II-23} + C/CO/H_3 + CO/C_2 - CO/C/H = T23 - T20$, $NN_{G2}^{II-23} = -1.43$; $NN_{G2}^{II-27} - CO/C/H - C/CO/H_3 + NN_{G2}^{I} = T27 - T24 - T26$, $NN_{G2}^{II-27} = -1.67$; $NN_{G2}^{II-30} + CO/C_2 - 2*CO/C/H = T30 - T20 - T19$, $NN_{G2}^{II-30} = -2.25$; $NN_{G2}^{II-44} + O/C/H - C/C/H_3 = T44 - T25 - T12 + T8$, $NN_{G2}^{II-44} = -1.04$; $NN_{G2}^{II-56} - CO/C/H + CO/O/C + O/C/H = T56 - T25$, $NN_{G2}^{II-56} = 1.20$.

Group 3 presented molecules which underwent an internal hydrogen bond (internal H-bond) having appreciably short distances of less than 1.8 Å at the MP2/6-31G† level. Molecules 34, 37, 38, 43, 45, 46, 47, 48, 49, 50 and 51 exhibited short C=O---H–O distances, further contributing towards their stability (see the unsymmetrical enol-tautomer depicted in Figure 6.4). Among these compounds, molecules 34, 46, 47 and 48 increased their stability by adopting the *cis* or (*Z*) conformation (Figure 6.8). CIS conformations were preferred due to both a resonance effect of the C=C and C=O bonds and the interaction between the hydroxyl hydrogen orbitals and the π-CO systems.[5b-d,47] Effects and interactions of this type (known as resonance-assisted hydrogen bonding) are significant for strengthening hydrogen bonding

and increasing the resonance energy of many systems having biological activity, such as several enzymatic reaction mechanisms[48a-c] and chemical inversion of L-amino acids to D-amino acids which are important neurotransmitters (D-serine)[48d-e] and building blocks (D-alanine) for bacterial cell wall synthesis.[48f] Considering the extra stability in the *cis* or (*Z*) conformers for molecules 34, 46, 47 and 48 (NN_{CIS}^{OH} in kcal per mol), it was possible to estimate H-bond interactions, NN_x^{OH} (in kcal per mol), in x distances as follows:

$$NN_{CIS}^{OH} + NN_{1.725}^{OH-34} = T34 - T11 - T16 + 2*Cd/H_2 = -17.70$$

$$NN_{1.652}^{OH-38} - 2*Cd/H_2 = T38 - T1 - T17, \ NN_{1.652}^{OH-38} = -15.9$$

$$NN_{1.788}^{OH-43} - 2*Cd/H_2 = T43 - T19 - T10, \ NN_{1.788}^{OH-43} = -1.94$$

$$NN_{1.643}^{OH-45} - 2*Cd/H_2 + C/CO/C/H_2 + NN_{G2}^{I} = T45 - T1 - T26, \ NN_{1.635}^{OH-45} = -19.78$$

$$NN_{CIS}^{OH} + NN_{1.775}^{OH-46} = T46 - T31 - T10 + 2*Cd/H_2 = -11.59$$

$$NN_{CIS}^{OH} + NN_{1.771}^{OH-47} = T47 - T26 - T10 + 2*Cd/H_2 = -11.03$$

$$NN_{CIS}^{OH} + NN_{1.792}^{OH-48} = T48 - T17 - T10 + 2*Cd/H_2 = -8.81$$

$$NN_{1.635}^{OH-49} - 2*Cd/H_2 = T49 - T1 - T26, \ NN_{1.635}^{OH-49} = -18.53$$

$$NN_{1.615}^{OH-50} - 2*Cd/H_2 = T50 - T1 - T16, \ NN_{1.615}^{OH-50} = -21.15$$

$$NN_{CIS}^{OH} + NN_{1.759}^{OH-51} = T51 - T17 - T11 + 2*Cd/H_2 = -11.28$$
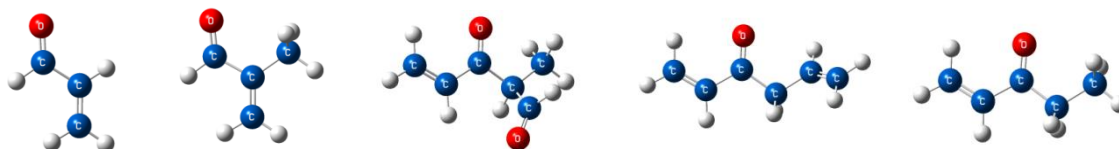
(17) Acrolein   (18) 2-Me-propenal   (27) 2-Me-3-oxo-pent-4-enal   (28) Hexa-1,5-dien-3-one   (31) Pent-1-en-3-one

Figure 6.7. Conformers for some group 2 compounds.

Assessment of both NN_{CIS}^{OH} and NN_x^{OH} for compounds 34, 46, 47, 48 and 51 involved a linear system of equations. The value of one variable had to be defined to solve this linear system. This can be done by assuming a distance for a null value for the internal H-bond interaction. Figure in the supporting information shows the correction values for the distances calculated by using compounds 38, 43, 45, 49 and 50 (Figure 6.8). According to lineal fitting with the H-bond interaction values in the preceding compounds, it could be assumed that there were null interactions in distances greater than ca. 1.79 Å (at the MP2/6-31G† level). Therefore, $NN_{1.792}^{OH-48}$ was assumed to be null and the linear system could be solved to assess the following values in kcal per mol: $NN_{CIS}^{OH} = -8.81$, $NN_{1.725}^{OH-34} = -8.89$, $NN_{1.759}^{OH-51} = -2.47$, $NN_{1.771}^{OH-47} = -2.22$, $NN_{1.775}^{OH-46} = -2.78$. The values obtained for the

H-bond correction including the resonance effect of the *cis* conformers in enol form of β-diketones were in the intramolecular hydrogen bond energy range in malonaldehyde enol derivatives assessed by Musin and Mariam.[49] Figure 6.9a and 6.9b show the adjustment for the NN_x^{OH} correction found in this work. Figure 6.9a presents the results for the distances based on the MP2/6-31G† level whereas Figure 6.9b presents the results for the distances based on the HF/6-31G† level. This last adjustment can be used for preliminary evaluations of this interaction at low levels of theory.

(34) 5-hydroxy-hexa-1,4-dien-3-one   (37) (Z)-5-hydroxy-3-oxo-pent-4-enal   (38) 3,3-dihydroxy-propenal   (43) 4-hydroxy-but-3-enal   (49) 4,4-dihydroxy-but-3-en-2-one
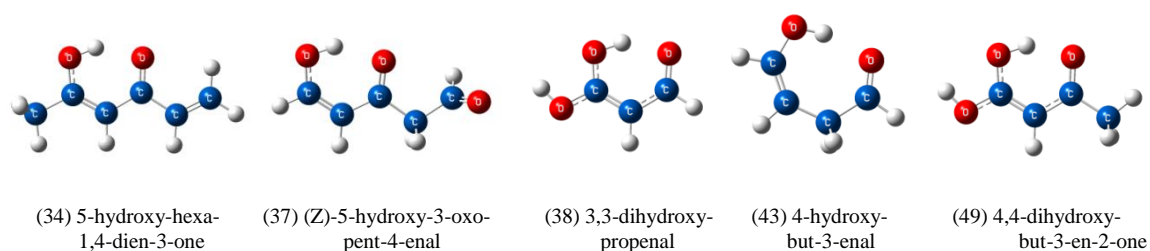
Figure 6.8. Conformers for some group 3 compounds.

Compounds 37 and 43 from group 3 possessed internal H-bonds (Figure 6.8). Molecule 37 contained several nonnext neighbor corrections. H-bond correction for compound 37 at 1.783 Å can be calculated to be $NN_{1.783}^{OH-37}$ = -1.45 kcal/mol by using the linear fitting shown in Figure 6.9a. Correction due to the CO---CO eclipse for this molecule could be calculated as: $NN_{G2}^{II-37} - C/CO/H_3 - CO/C/H - 2Cd/H_2 + NN_{CIS}^{OH} + NN_{1.783}^{OH-37} + NN_{G2}^{I} = T37 - T20 - T10 - T26$, $NN_{G2}^{II-37} = -1.45$ kcal/mol. NN_x^{OH} value for a 1.788 Å distance occurring in compound 43 was assessed as being -1.61 kcal per mol. The most stable conformer for compound 43 show that the NN value also contained some correction for methylene distortion. The CO----Cd eclipse for the $C/CO/Cd/H_2$ group possessed the normal orientation as shown in compound 19 (supporting information) whereas it had ca. 160° distortion in compound 43. This distortion prolonged the H---H distances, thereby giving extra stability which was already included in the NN_x^{OH} correction. The true value for this NN_x^{OH} for a 1.788 Å distance was less than the value supposed in this work, as shown by linear adjustment tendency in Figures 6.9a and 6.9b. This supports the consideration that the H-bond GAV correction was null at distances greater than 1.79 Å (Figure 6.9a). It is important to mention that contributions of weak internal H-bonding to the molecular stability (such as

contributions in polyols[13c]) are already considered in the value of the constituent GAVs; e.g. in ethylene glycol O----H distance is 2.267 Å at the MP2/6-31G† level.
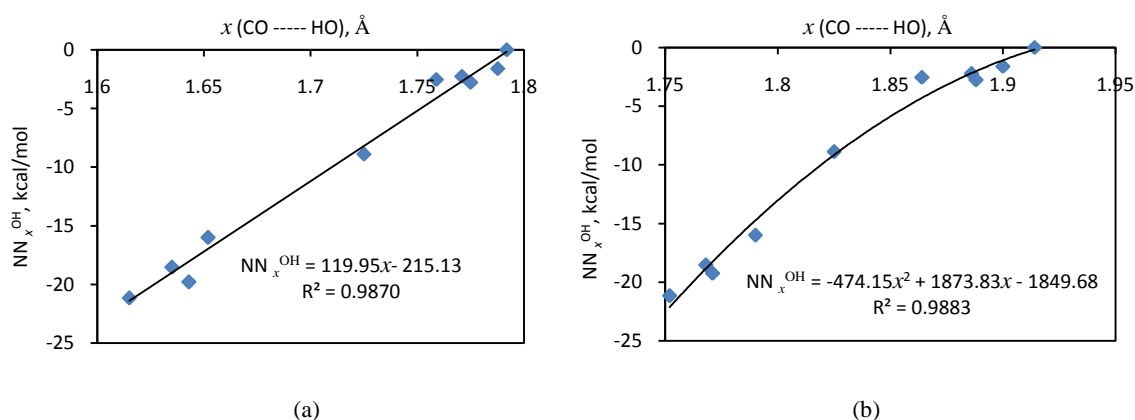
Figure 6.9. Correction for ΔH_f in molecules with both NN_x^{OH} and $NNcis^{OH}$ interactions. Distances based on (a) MP2/6-31G† and (b) HF/6-31G† calculations.

Appreciable magnitude nonnext neighbor interactions were also present in compounds 9, 32 and 53. Compound 9 needed a nonnext neighbor correction due to the hydroxyl groups' *cis* position. This interaction can be assessed as follows: $NN_{G1}^{I-9} = T9 - T10 - T11 + 2*Cd/H2$, $NN_{G1}^{I-9} = 2.74$ kcal/mol. Compound 32 had to be corrected due to the CH_3---CO---CH_3 eclipse that differed from the Cd---CO---Cd eclipse of the lowest isomer of compound 16: $NN_{G2}^{II-32} = T32 - 2*T18 - T16 + 2*T17$, $NN_{G2}^{II-32} = 1.61$ kcal/mol. Compound 53 presented the CO---CO eclipse as in compounds 23 and 37 (Group 2); however, its value was a little lower than in this group due to the oxy group attached to one of the CO groups: NN_{G2}^{I-53} + $C/O/H_3 + CO/C/H + O/Cd/C - CO/O/C - O/CO/Cd = T53 - T20 - T8$, $NN_{G4}^{I-53} = -0.48$ kcal/mol. Likewise, compounds 3, 33, 35, 36, 41, 42 and 54 were corrected by including Gauche interactions (NN_{GE}). The corresponding nonnext neighbor corrections could be obtained by using the following figures (in kcal per mol): $NN_{GE}^{3} = T3 - T2 + T8 - T7$, $NN_{GE}^{3} = 0.50$; $NN_{GE}^{33} = T33 - T19 - T18 - CO/Cd/C + 2*CO/Cd/H$, $NN_{GE}^{33} = -0.90$; $NN_{GE}^{35} = T35 - T21 - T11 + Cd/H_2 + C/Cd/H_3 + Cd/C/H$, $NN_{GE}^{35} = -1.32$; $NN_{GE}^{36} = T36 - T22 - T11 + Cd/H_2 + C/Cd/H_3 + Cd/C/H$, $NN_{GE}^{36} = -4.13$; $NN_{GE}^{41} = T41 - T22 - T10 + 2*Cd/H_2$, $NN_{GE}^{41} = -1.83$; $NN_{GE}^{42} = T42 - T19 - T11 + Cd/H_2 + C/Cd/H_3 + Cd/C/H$, $NN_{GE}^{42} = -0.97$; $NN_{GE}^{54} = T54 - T11 + T10 - T52 + O/CO/H + CO/O/H + NN_{G2}^{I}$, $NN_{GE}^{54} = 0.61$.

An additional improvement to the equations so derived must be considered for correctly assessing the unknown GAVS. Correction due to possible errors accounted for by CBS-Q energy predictions (NN_{CBS-Q}) were considered for compounds 7, 17 and 39. The balance of heat of formation values for these related compounds by using GAVs must fulfill: T39 – T17 – T7 + 2*Cd/H_2 = 0. Nevertheless, heat of formation values with CBS-Q energies gave: T39 – T17 – T7 + 2*Cd/H_2 = -2.03 kcal/mol. This error in predicting these compounds' heat of formation can be set up as a correction (NN_{CBS-Q}) for compound 39. Some other appreciable deviations in predicting heat of formation based on energies at the CBS-Q multilevel have been reported elsewhere.[15,19] Table of the supporting material gives a summary of the NN corrections for calculating heat of formation GAVs. The preceding corrections were also applied for the calculation of GAVS for intrinsic entropy and specific heat at different temperatures. Tables and Figures of the supplementary material summarize and illustrate the correction values for the nonnext neighbor interactions. It should be stressed that NN_x^{OH} corrections for specific heat at different temperatures agreed with the assumption that internal hydrogen bonds become weakened with increasing temperature.[50]

6.3.4.2 Acyclic compound-based GAVS

Estimating entropy by the GAV method (so-called intrinsic entropy) needs correction due to high temperatures (statistical thermodynamic classical limits) in addition to nonnext neighbor interactions.[14] Such correction is obtained by considering both the number of indistinguishable configurations which the compounds may have and the contribution from the mixture of energetically-equivalent conformers. The correction can be done mathematically by using the following expression:

$$S_{int}^{o} = S_{calc}^{o} + R \sum \ln \left(\frac{\sigma_i}{n_i} \right) \tag{9}$$

Where σ_i corresponds to the total symmetry number ($\sigma_i^{ext} * \sigma_i^{int}$) and n_i corresponds to the number of energetically equivalent conformers (Table 6.9). Calculated total entropy was thus further modified while deriving GAVs to work with the intrinsic value instead (eq. 9). All final thermochemical properties were expressed in terms of GAVs and the corresponding nonnext neighbor corrections. The values for known GAVs can be found in Table 6.10. The unknown groups were assumed to be the independent variables of the derived linear systems of equations, one for each property. MVLR methodology was used for determining values for

the unknown groups which best fit the systems of equations. The common feature for all groups of acyclic compounds when using the MVLR method was that estimating the thermochemical properties was successful. The data's agreement indicated that GAV methodology was applicable for calculating standard enthalpies of formation, standard entropies and specific heat at several temperatures and suggested that it could provide reliable data for other ketene polymer structures which were not considered in this study.

GAV methodology was capable of reproducing the 57 ab initio thermochemical data having 0.065 kcal/mol, 0.12 cal/mol K, 0.09 cal/mol K average deviation for heat of formation at 298 K, 298 K standard entropy and 300 K specific heat (Table 6.11). The highest deviation was found to be 0.25 kcal/mol for heat of formation, 0.6 cal/mol K for entropy and 0.48 cal/mol K for specific heat at 300 K. Table 6.11 gives a summary of main regression process features; it also shows a comparison between the fitting process without using nonnext neighbor corrections (NN) and when using them. The fitting process without NN showed good R-squared coefficient, although the deviations were appreciable for all properties and this model was therefore inaccurate; for example, maximum positive deviation for 9 kcal/mol heat of formation cannot be accepted for reproducing this property. The fitting process with the use of NN showed both good R-squared coefficient and very low deviation; Table 6.11 shows a 0.66 kcal per mol root mean square deviation for adjusting heat of formation for the process with NN. Considering NN gives both a precise and accurate model. This improvement suggested that including the NN interactions derived in this work in regression were essential for correctly determining the unknown GAVs (Table 6.3). Table 6.12 compares the values for the unknown GAVs obtained with and without including NN. The main differences in the values of the different GAVS obtained without NN and with NN were found in Cd/CO/H,

Table 6.10. Known GAVS (Ref. 14).

	ΔH_f^o, kcal/mol	S_{intr}, cal/mol K	Cp, cal/mol K						
			300 K	400 K	500 K	600 K	800 K	1000 K	1500 K
C/C/H3	-10.2	30.4	6.2	7.8	9.4	10.8	13.0	14.8	17.6
C/Cd/H3	-10.2	30.4	6.2	7.8	9.4	10.8	13.0	14.8	17.6
C/CO/H3	-10.2	30.4	6.2	7.8	9.4	10.8	13.0	14.8	17.6
C/O/H3	-10.2	30.4	6.2	7.8	9.4	10.8	13.0	14.8	17.6
Cd/C/H	8.6	8.0	4.2	5.0	5.8	6.5	7.6	8.5	9.6
Cd/H2	6.3	27.6	5.1	6.4	7.5	8.5	10.1	11.3	13.2
C/CO/C/H2	-5.2	9.6	6.2	7.7	8.7	9.5	11.1	12.2	13.5*
CO/C/H	-29.1	34.9	7.0	7.8	8.8	9.7	11.2	12.2	13.6*
CO/C2	-31.4	15.0	5.6	6.3	7.1	7.8	8.9	9.6	10.1*
CO/Cd/H	-29.1	34.9	7.0	7.8	8.8	9.7	11.2	12.2	13.6*
CO/O/C	-35.1	14.8	6.0	6.7	7.3	8.0	8.9	9.4	10.4*
CO/O/H	-32.1	34.9	7.0	7.9	8.8	9.7	11.2	12.2	13.6*
O/C/H	-37.9	29.1	4.3	4.4	4.8	5.2	6.0	6.6	7.6*
O/CO/H	-58.1	24.5	3.8	5.0	5.8	6.3	7.2	7.8	8.2*

* Values estimated from extrapolation.

Table 6.11. Summary of regressions processes' main features.

	$\Delta H_f{}^\circ$, kcal/mol		S_{intr}, cal/mol K		Cp at 300 K, cal/mol K	
	Without NN	With NN	Without NN	With NN	Without NN	With NN
Average deviation	0.294	0.010	0.097	0.002	0.107	-0.001
Mean absolute deviation	2.669	0.065	1.102	0.120	1.080	0.092
Maximum positive deviation	9.060	0.266	3.992	0.556	4.336	0.374
Maximum negative deviation	-7.493	-0.245	-3.249	-0.598	-4.336	-0.486
Root mean square deviation	26.876	0.664	10.902	1.411	10.356	1.087
R-squared coefficient	0.989	0.999	0.981	0.999	0.950	0.999

Table 6.12. Comparison between the assessed GAVs without NN and with NN.

	$\Delta H_f{}^\circ$, kcal/mol		S_{intr}, cal/mol K		Cp at 300 K,	
	Without	With NN	Without	With NN	Without	With NN
CO/Cd2	-28.3	-28.9	17.2	17.9	8.0	5.9
C/(CO)2/C/H	2.4	0.4	-11.5	-12.8	5.8	5.2
C/(CO)2/C2	1.5	1.4	-36.5	-35.4	5.3	5.2
C/(CO)2/H2	-4.4	-2.4	7.5	7.0	5.5	4.6
C/CO/Cd/C/H	-0.1	-1.5	-13.1	-13.7	7.2	6.6
C/CO/Cd/C2	0.0	0.2	-36.1	-35.4	5.0	4.5
C/CO/Cd/H2	-2.3	-3.5	9.1	9.1	6.1	5.1
Cd/CO/C	8.9	8.1	-15.6	-14.7	3.5	3.6
Cd/CO/H	3.0	7.8	2.9	4.1	3.2	4.7
Cd/O/C	11.2	8.3	-14.1	-16.7	3.5	1.8
Cd/O/H	11.1	9.2	5.1	4.2	5.0	2.8
Cd/O2	10.6	6.9	-16.8	-19.9	5.1	0.0
CO/Cd/C	-32.1	-30.3	15.0	16.7	6.2	5.6
O/Cd/H	-49.6	-44.4	27.7	29.9	4.0	6.9

Cd/O/C, Cd/O/H, Cd/O2 and O/Cd/H due to these groups being involved in most compounds corrected by interactions. The inductive and resonance effects[51] which might have been present in the molecules analyzed here containing these GAVS may have been responsible for the NN interactions. Table 6.13 presents the final values for the GAVs calculated in this work (standard error at 99% confidence). The confidence intervals showed that the model is very precise (0.48 kcal per mol as maximum confidence size for heat of formation). The condition number, defined as $\|A\|\,\|A^{-1}\|$ where A is the coefficient matrix associated with the GAV-adjusting problem, indicates how well-defined the regression problem was.[52] The condition number was calculated to be 9.4 and therefore indicated that errors in predicting theoretical properties would be amplified by up to nine times in derived Benson group values; for example, the lack of NN_{CBS-Q} for compound 39 would assess a ca. 1.5 kcal per mol value for heat of formation for this compound, this being greater than that estimated from the CBS-Q energies. It seems that values for the condition number less than 10 were sufficient for considering the GAV-regression problem as being well conditioned (see Ref. 16b). The randomly distributed residuals, found when predicting thermochemical properties from

GAVs, suggested that error deviations were uncorrelated (Figures 6.12, 6.13 and 6.14); the Durbin-Watson test[53] score (d=1.78) was found to be inconclusive in identifying the autocorrelation in the residuals for this regression model.

Table 13. GAVs calculated in this work (standard errors 99% confidence).

	$\Delta H_f{}^o$, kcal/mol	S_{intr}, cal/mol K	Cp, cal/mol K						
			300 K	400 K	500 K	600 K	800 K	1000 K	1500 K
C/O/C/H2[(c)]	-8.1[(a)]	7.8	6.5	7.9	9.1	10.0	11.6	12.8	14.6
O/Cd/C [(b)]	-30.5[(a)]	9.7[(a)]	5.7±0.4	6.7±0.5	6.7±0.4	6.5±0.5	6.6±0.5	6.0±0.5	5.2±0.5
CO/O/Cd	-32.0[(a)]	18.4±0.6	16.0±0.4	20.6±0.6	23.5±0.5	25.3±0.5	27.2±0.6	28.0±0.5	29.6±0.6
O/CO/Cd	-45.2[(a)]	6.4±0.5	4.6±0.4	6.2±0.6	6.9±0.5	7.3±0.5	7.6±0.5	7.6±0.5	6.7±0.5
O/Cd2	-33.0[(a)]	14.1±0.5	5.7±0.4	6.7±0.5	6.7±0.4	6.5±0.5	6.3±0.5	6.0±0.5	5.2±0.5
CO/Cd2	-28.9±0.2	17.9±0.6	5.9±0.5	5.9±0.6	6.5±0.5	7.1±0.6	8.1±0.6	8.7±0.6	9.4±0.6
C/(CO)2/C/H	0.4±0.2	-12.8±0.4	5.2±0.3	6.7±0.5	7.5±0.4	8.0±0.4	8.8±0.4	9.5±0.4	10.7±0.4
C/(CO)2/C2	1.4±0.2	-35.4±0.4	5.2±0.3	6.9±0.4	7.2±0.3	7.3±0.3	7.3±0.4	7.4±0.3	7.4±0.4
C/(CO)2/H2	-2.4±0.1	7.0±0.3	4.6±0.2	6.8±0.3	8.1±0.3	9.2±0.3	10.8±0.3	12.1±0.3	14.1±0.3
C/CO/Cd/C/H	-1.5±0.2	-13.7±0.4	6.6±0.3	7.4±0.4	7.9±0.3	8.4±0.4	9.1±0.4	9.8±0.4	10.9±0.4
C/CO/Cd/C2	0.2±0.2	-35.4±0.4	4.5±0.3	5.8±0.4	6.6±0.3	7.1±0.4	7.5±0.4	7.7±0.4	7.8±0.4
C/CO/Cd/H2	-3.5±0.1	9.1±0.2	5.1±0.2	6.9±0.3	8.3±0.2	9.4±0.2	11.0±0.3	12.3±0.2	14.3±0.3
Cd/CO/C	8.1±0.2	-14.7±0.3	3.6±0.3	5.0±0.4	5.9±0.3	6.4±0.3	7.0±0.3	7.1±0.3	7.1±0.3
Cd/CO/H	7.8±0.1	4.1±0.3	4.7±0.2	6.2±0.3	7.1±0.2	7.9±0.3	8.8±0.3	9.5±0.3	10.4±0.3
Cd/O/C	8.3±0.1	-16.7±0.3	1.8±0.4	2.5±0.5	3.6±0.4	4.3±0.5	5.1±0.5	5.6±0.5	6.2±0.5
Cd/O/H	9.2±0.1	4.2±0.2	2.8±0.3	3.6±0.4	4.7±0.3	5.6±0.3	6.9±0.3	7.9±0.3	9.5±0.3
Cd/O2	6.9±0.1	-19.9±0.3	0.0±0.6	0.4±0.8	1.8±0.6	3.0±0.7	4.5±0.7	5.2±0.7	6.4±0.7
CO/Cd/C	-30.3±0.1	16.7±0.3	5.6±0.3	6.0±0.4	6.7±0.3	7.3±0.3	8.4±0.3	9.0±0.3	9.7±0.3
O/Cd/H	-44.4±0.1	29.9±0.2	6.9±0.3	8.3±0.4	8.6±0.4	8.7±0.4	8.6±0.4	8.5±0.4	8.5±0.4

[(a)] From Ref. 10. [(b)] Estimated to be equal to O/Cd$_2$. [(c)] Recalculated for S_{int} and Cp based upon compounds (12) and (8).
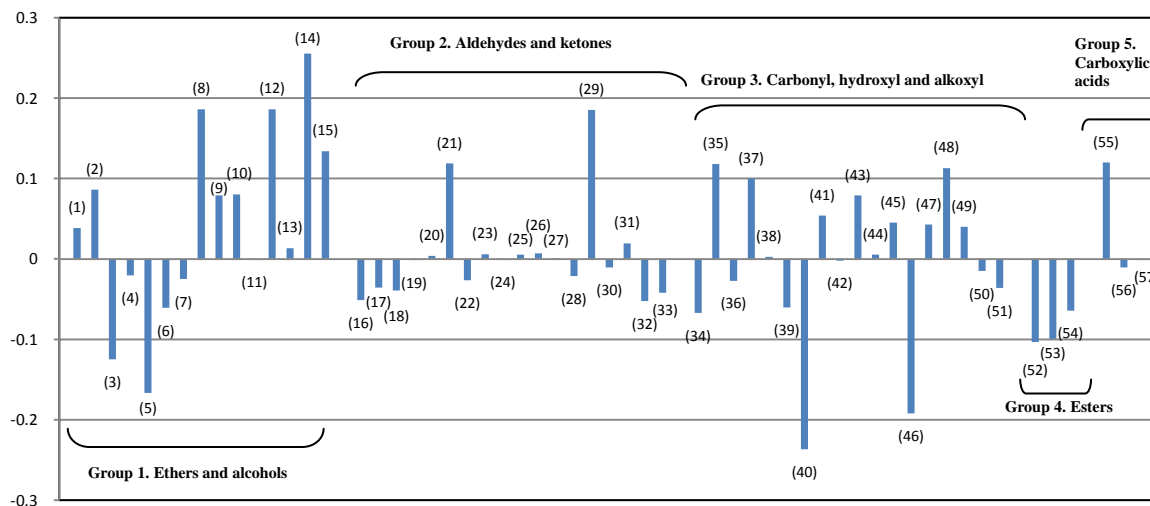
Figure 6.10. Deviations in ΔH_f (in kcal per mol) predictions for the acyclic base compounds from GAVs.
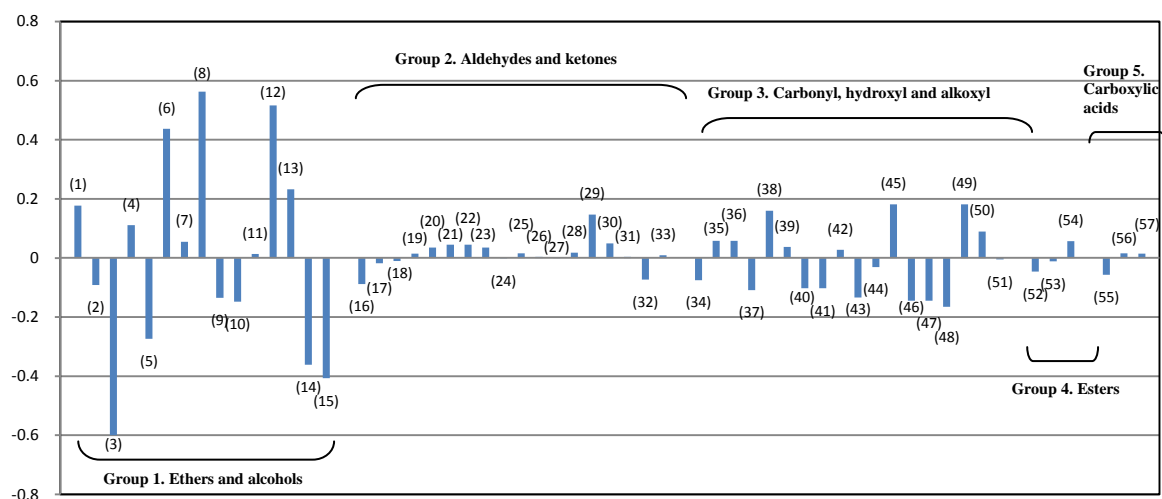
Figure 6.11. Deviations in intrinsic entropy (in cal/mol K) predictions for the acyclic base compounds from GAVs.
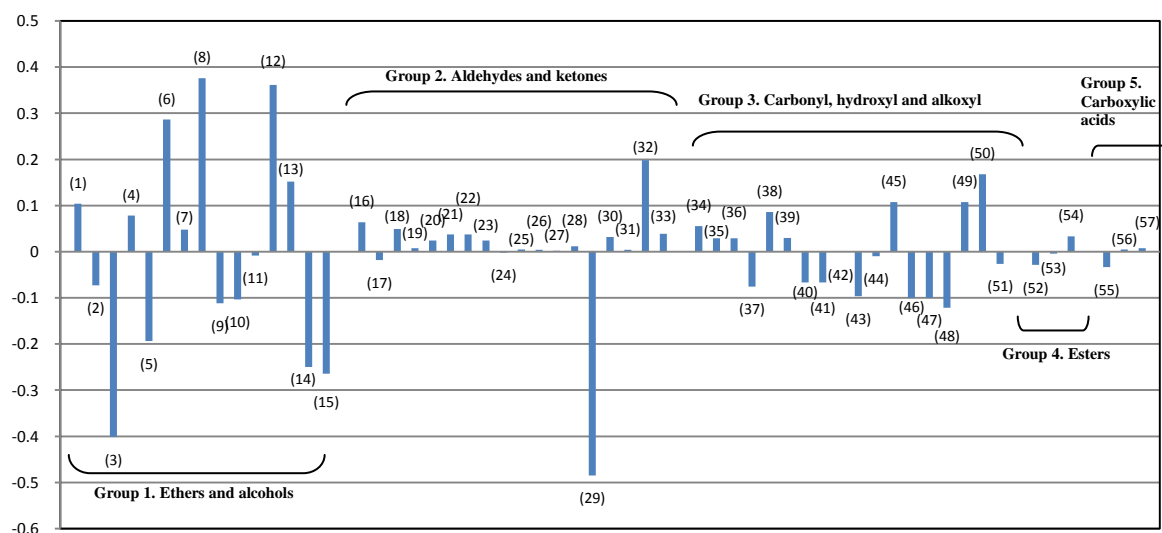
Figure 6.12. Deviations in Cp at 300 K (in cal/mol K) predictions for the acyclic base compounds from GAVs.

Some heat-of-formation GAVs assessed in this work have been reported elsewhere. The 8.27 kcal per mol value for Cd/O/C (Table 6.13) was in excellent agreement with the value calculated by Sebbar et al. (8.20 kcal per mol).[54] Likewise, the -44.43 kcal per mol value for O/Cd/H is in excellent agreement with the -44.80 kcal per mol value recently calculated by da Silva et al.[55a] The O/Cd/H value has been recalculated several times since being first estimated by Benson et al based on alcohols (-37.9 kcal per mol).[13a] Several newer more stable values for O/Cd/H have been reported by other authors[41c,55b-f] and it has been found that these estimations differed from those of Benson et al by values ranging from -6.7 to -11.4

kcal per mol, into which the data calculated in the current research fall precisely (Table 6.13). Similarly, the 9.21 kcal per mol value for Cd/O/H differed from the value initially obtained by Benson et al [13a,14] (8.60 kcal per mol), presumably due to differences in O/Cd/H group.

The 7.79 kcal per mol value for Cd/CO/H assessed in the current research differed from that calculated by Benson et al (4.32 kcal per mol) based on crotonaldehyde.[13a] Differences in Cd/CO/H values were mainly due to uncertainties in heat of formation for this compound. Benson et al[13a] used a -25.5 kcal per mol value whereas a recent experiment assessed -24.36±0.12 kcal per mol for crotonaldehyde's heat of formation.[56] This recent experimental data suggested (agreeing with the results of this research) that the actual Cd/CO/H group value must be greater than 4.32 kcal per mol. The 6.49 kcal per mol value for Cd/O_2 diverged from that assessed by Sebbar et al[57] (12.41 kcal per mol) at the B3LYP/6-311G(d,p) level. Differences in Cd/O_2 group values were related to ethane-1,1-diol heat of formation[57] (Table 6.2) and assumed O/Cd/H group value, which was reduced to ethenol heat of formation[55e] (Table 6.2). Experiments for determining ethene-1,1-diol and ethenol heat of formation are called for to assign correct figures for O/Cd/H and Cd/O_2.

The validity of the GAVs calculated in the current research can be verified by comparing the results for acetylacetone ($CH_3COCH_2COCH_3$) and malonic acid ($HOCOCH_2COOH$) heats of formation. According to GAV methodology (Tables 6.10 and 6.13), these compound's heats of formation were -85.6 kcal per mol and -188.8 kcal per mol respectively. The result for acetylacetone was in excellent agreement with the -85.78 kcal per mol reported by Temprado et al[58a] based on analyzing recent NMR studies and correlations for pure tautomer vaporization enthalpies in gas chromatography experiments. The result for malonic acid was also in excellent agreement with the -187.8 kcal per mol based on both experimental heat of sublimation (105.1±0.8 kJ/mol)[59a] and experimental ΔH_f in solid phase (-891 kJ/mol)[59b]. Such agreements between GAV methodology and experiments suggested that the $C/(CO)_2/H_2$ value must be -2.4 kcal per mol instead of the data initially estimated by Benson et al (-7.6 kcal per mol).[13a,14] Discrepancies in Benson et al's estimation done by can be explained by errors in the acetylacetone thermochemical data which was seemingly referred to its enol-tautomeric form instead (Figure 6.4). Additional calculations in current research at CBS-Q multilevel have predicted -17.6 kJ per mol tautomerization enthalpy for acetylacetone,

agreeing with a -19.3±2.8 kJ per mol experimental value by Temprado et al[58a] and -19.5±0.75 kJ per mol by Folkendt et al.[58b]

6.3.4.3 Ring and substituent position corrections for ketene dimers and related structures

Ring corrections (RC) derived in this work had a high confidence level due to the CBS-Q method's good performance.[19] Ring strain energies calculated by the CBS-Q model, particularly in four-membered rings, had one of the best performances, according to Petersson et al's evaluation.[19] RC for ketene dimers and related structures derived with the GAVs listed in Tables 6.10 and 6.13 are shown in Table 6.14. The RC value for diketene was found to be 1 kcal per mol more stable than the 22.5 kcal per mol value estimated by Månsson et al.[10] The RC values for the other ring compounds assessed in the current work represent the first ones reported in the literature. Enthalpy corrections for the four-membered ring compounds had positive values, whereas the enthalpy corrections for pyran-4-one type ring compounds had negative values (Table 6.14). According to Benson, the ring correction derived from GAVs reflects the strain energy of the corresponding cyclic compound since group values were derived from open-chain-zero-strained compounds.[14] However, this RC value may also contain contributions from resonance energy. The pyran-4-ones negative enthalpy corrections may have resulted from combining resonance energy and ring strain energy, such as that occurring in furan, phenol and other vinyl or unsaturated ether compounds.[15] Resonance through chemical bonds on unsaturated carbon and adjacent oxygen atoms was evidenced by the weaker O-H bonds (ca. 85 kcal per mol[60a]) in CH_2=CHOH, CH≡COH and phenol, compared to that in CH_3OH and CH_3CH_2OH (ca. 104 kcal per mol[60b]).

Regarding cyclobut-2-enones, resonance energy's effect on total correction value for heat of formation could be partly seen in the OH value and methyl substituent corrections (Table 6.14, column SP). 3-hydroxy-cyclobut-2-enone lowered its energy by ca. 12 kcal per mol in the presence of a methyl substituent (Table 6.5), whereas two methyl substituent groups lowered energy by ca. 16 kcal per mol. Better electron-withdrawing groups presumably further stabilize 3-hydroxy-cyclobut-2-enones. It is also worth mentioning that substituent position corrections (SP) were more important in cyclobutane-1,3-dione than in the diketene ring. The tendency of these SP agreed with the conclusion that alkylketene dimerization produced cyclobutane-1,3-dione structure as being the major product because of

thermodynamic control of the reaction. Ketene dimerization tendencies cannot be explained and separated within the GAV framework in terms of strain and resonance energy or steric effects. As Lay et al[61] have stated, additional studies are needed to separate and identify ring strain and resonance effects in oxygenated hydrocarbon species.

Table 6.14. Ring formation (RC) and substituent position (SP) corrections for ketene dimers and related cyclic structures.

	ΔH_f^o, kcal/mol		S_{intr}, cal/ mol K		Cp 300 K, cal/ mol K	
	RC	SP	RC	SP	RC	SP
Diketenes						
1c) Diketene (4-methylene-oxetan-2-one)	21.4	---	31.5	---	-2.3	---
2c) 3-methyl-4-methylene-oxetan-2-one	21.4	-1.4	31.5	2.6	-2.3	-2.0
3c) 3,3-dimethyl-4-methylene-oxetan-2-one	21.4	-2.8	31.5	2.6	-2.3	0.2
Cyclobutane-1,3-diones						
4c) Cyclobutane-1,3-dione	23.3	---	30.5	---	0.9	---
5c) 2-methyl-cyclobutane-1,3-dione	23.3	-2.3	30.5	-0.2	0.9	-1.2
6c) 2,2-dimethyl-cyclobutane-1,3-dione	23.3	-11.3	30.5	1.7	0.9	-1.1
7c) (E)-2,4-dimethyl-cyclobutane-1,3-dione	23.3	-9.2	30.5	0.1	0.9	-2.3
Pyran-4-ones						
8c) Pyran-4-one	-11.3	---	25.4	---	-5.0	---
9c) 3-methyl-pyran-4-one	-11.3	-3.8	25.4	0.6	-5.0	0.9
10c) 2-methyl-pyran-4-one	-11.3	-0.7	25.4	-1.5	-5.0	1.0
11c) 2-hydroxy-pyran-4-one	-11.3	-1.0	25.4	0.9	-5.0	0.9
Cyclobut-2-enones						
12c) Cyclobut-2-enone	27.7	---	29.9	---	-2.7	---
13c) 4-methyl-cyclobut-2-enone	27.7	-1.1	29.9	2.3	-2.7	-1.7
14c) 2-methyl-cyclobut-2-enone	27.7	-6.8	29.9	-0.4	-2.7	0.4
15c) 4,4-dimethyl-cyclobut-2-enone	27.7	-8.3	29.9	2.5	-2.7	0.5
16c) 3-hydroxy-cyclobut-2-enone	27.7	-3.9	29.9	0.5	-2.7	0.4
17c) 3-hydroxy-2-methyl-cyclobut-2-enone	27.7	-12.2	29.9	1.0	-2.7	0.4
18c) 3-hydroxy-4-methyl-cyclobut-2-enone	27.7	-12.0	29.9	2.8	-2.7	-1.4
19c) 3-hydroxy-2,4-dimethyl-cyclobut-2-enone	27.7	-16.0	29.9	1.2	-2.7	-1.1
20c) 3-hydroxy-4,4-dimethyl-cyclobut-2-enone	27.7	-17.1	29.9	0.6	-2.7	0.7

Substituent position corrections for intrinsic entropy and specific heat were particularly lower than for heat of formation. Such low substituent effect values showed that the main concern in intrinsic entropy and specific heat corrections for ring formation is the loss in internal rotation modes of acyclic compounds.[14] The RC and SP corrections assessed in this work clearly helped in calculating the thermochemical data for ketene dimers and related structures and were particularly valuable when no other data was available.

Conclusions

The most relevant results concerning ketene dimers' geometries and thermochemistry have been discussed above. According to the thermochemical data in gas phase assessed in this work, the diketene dimer was more stable than cyclobutane-1,3-dione dimer by ca. 3.5 kcal per mol and therefore the diketene dimer was found to be the major product for parent ketene dimerization due to thermodynamic control of the reaction. Such relative stability for ketene

dimers found at CBS-Q multilevel contradicts combustion experiments. New experimental measurements regarding parent ketene dimer thermochemistry are called for to clarify dimerization energetics. On the other hand, alkylketene dimer stability was found to favor cyclobutane-1,3-dione structure and its enol-tautomeric species when increasing the number of methyl substituents. Such relative alkyldimer stability suggested that alkylketene dimerization was thermodynamically controlled regarding cyclobutane-1,3-dione structure and its enol tauromer.

Despite its relatively simple approach, the GAV method proved to be a powerful and relatively accurate technique for estimating heat of formation, entropy and specific heat for ketene dimers and other cyclic structures. The GAV method was particularly useful when no other data or theoretical methods were available. This work has led to 19 new GAVs, 4 ring corrections and 16 substituent position corrections needed for estimating the thermochemical properties of ketene dimers and related structures (i.e. cyclobut-2-enones and pyran-4-ones) based on quantum chemical calculations using a set of 57 acyclic compounds and 20 cyclic molecules. NN interactions derived from gauche positions, eclipse positions and hydrogen internal bonds were found to significantly affect the properties of the compounds analyzed here. The GAVs assessed by using such NN corrections accurately reproduced the theoretical thermochemical properties for the set of 57 acyclic compounds and experimental heat of formation for acetylacetone. Ring and substituent corrections derived from the new GAV values were found to contain resonance and strain energies reflecting the relative stability of the different cyclic species. The protocol outlined here provides support for applying GAVs to high-weight ketene polymers and for expanding this methodology to other polymer structures which were not considered in this research.

References

(1) a) Tidwell, T.T. *Ketenes*. John Wiley & Sons: New York, 1995 and references therein. b) Holden, K. G. *Chemistry and biology of β-lactam antibiotics*, Vol. 2; Morin, R. B., Gorman, M., Eds.; Academic: New York, 1982. c) Palomo, C.; Aizpurua, J. M.; Iñaki, G.; Oiarbide, M. Asymmetric synthesis of β-lactams by Staudinger ketene-imine cycloaddition reaction. *Eur. J. Org. Chem.* 1999, 12, 3223–3235. d) Collins, P. W.; Djuric, S. W. Synthesis of therapeutically useful prostaglandin and prostaciclyn analogs. *Chem. Rev.* 1993, 93, 1533–1564. e) Paull, D. H.; Alden-Danforth, E.; Wolfer, J.; Dogo-Isonagie, C.; Abraham, C. J.; Lectka, T. An asymmetric, bifunctional catalytic approach to non-natural α-amino acid derivatives. *J. Org. Chem.* 2007, 72, 5380–5382. f) Ma, G.; Nguyen, H.; Romo, D. Concise total synthesis of (±)-salinosporamide A, (±)-cinnabaramide A, and derivatives via a bis-cyclization process: Implications for a biosynthetic pathway? *Org. Lett.* 2007, 9, 2143–2146.

(2) Rothman, R. S. Process for preparation of hexadecilcetena. USP. 3,535,383. 1970.

(3) a) Naka, K.; Uemura, T; Chujo, Y. Synthesis of polymers having 1,3-cyclobutanedione unit in the main chain by cycloaddition polymerization of bisketene. *Polym. Bull.* 1999, 42, 367–372. b) Hasek, R H.; Clark, R. D.; Elam, E. U.; Martin, J. C. The chemistry of dimethylketene dimer. IV. The polyester and β-lactone dimer of dimethylketene. *J. Org. Chem.* 1962, 27, 60–64. c) Scholl, T.; Jackson, B. Process for the production of squaric acid. U.S. Patent 5,130,492, 1992.

(4) Wasserman, H. H.; Dehmlow, E. V. Cyclobutane-1,3-dione. *J. Am. Chem. Soc.* 1962, 84, 3786–3787.

(5) a) Farnum, D. G.; Johnson, J. R.; Hess, R. E.; Marshall, T. B.; Webster, B. Aldoketene dimers and trimers from acid chlorides. A synthesis of substituted 3-hydroxycyclobutenones. *J. Am. Chem. Soc.* 1965, 87, 5191–5197. b) Baldwin, J. E.; Roberts, J. D. Structure and rearrangement of neutral phenylketene dimer. *J. Am. Chem. Soc.* 1963, 85, 2444–2446. c) Chickos, J. S; Winter, R. E. K. Nuclear magnetic resonance studies of the mechanism of keto-enol tautomerism in 3-hydroxy-2,4-dimethylcyclobutenone. II. Solvent and ph effects. *J. Am. Chem. Soc.* 1973, 95, 506–511. d) Bertolasi, V; Pretto, L.; Gilli, G.; Gilli, P. π-bond cooperativity and anticooperativity effects in resonance-assisted hydrogen bonds (RAHBs). *Acta Cryst.* 2006, B62, 850–863.

(6) a) Hyatt, J. A.; Raynolds, P. W. Ketene cycloadditions. *Org. React.* 1994, 45, 160–246. b) Clemens, R. J. Diketene. *Chem. Rev.* 1986, 86, 241–318.

(7) a) Mitchell, James A. Moisture-proof wrapping material. US Patent 2,281,589. 1942. b) Karademir, A. T. Quantitative determination of alkyl ketene dimer (AKD) retention in paper made on a pilot paper machine. *J. Agric. For.* 2002, 26, 253–260.

(8) a) Sekiwa, Y.; Kubota, K.; Kobayashi, A. Characteristic flavor components in the brew of cooked clam (*Meretrix Lusoria*) and the effect of storage on flavor formation. *J. Agric. Food Chem.* 1997, 45, 826–830. b) Selli, S.; Prost, C.; Serot, T. Odour-active and off-odour components in rainbow trout (*Oncorhynchus mykiss*) extracts obtained by microwave assisted distillation-solvent extraction. *Food Chemistry*, 2009, 114, 317–322. c) Saint-Eve, A.; Lévy, C.; Le Moigne, M.; Ducruet, V.; Souchon, I. Quality changes in yogurt during storage in different packaging materials. *Food Chemistry*, 2008, 110, 285–293. d) Yuen, V. G.; Caravan, P.; Gelmini, L.; Glover, N.; McNeill, J. H.; Setyawati, I. A.; Zhou, Y.; Orvig, C. Glucose-lowering properties of vanadium compounds: comparison of coordination complexes with maltol or kojic acid as ligands. *J. Inorg. Biochem.* 1997, 68, 109–116. e) Wang, S.; Kim, S. H. New solvatochromic merocyanine dyes based on barbituric acid and Meldrum's acid. *Dyes and Pigments*, 2009, 80, 314–320.

(9) Chickos, J. S.; Sherwood, D. E.; Jug, K. Mechanistic of thermolysis of diketene in the gas phase. *J. Org. Chem.* 1978, 43, 1146.

(10) Månsson, M; Nakase, Y.; Sunner, S. The enthalpies of combustion and formation of diketene. *Acta Chem. Scand.* 1968, 22, 171–174.

(11) Pooling, B. E.; Prausnitz, J. M.; O'Connell, J. P. *The properties of gases and liquids*. International editions 2001. Fifth edition. MacGraw Hill, USA.

(12) Sabbe, M. K.; Saeys, M; Reyniers, M.F; Marin, G. B.; Van Speybroeck, V.; Waroquier, M. Group additivity values for the gas phase standard enthalpy of formation of hydrocarbons and hydrocarbon radicals. *J. Phys. Chem. A* 2005, 109, 7466–7480.

(13) a) Benson, S. W.; Cruickshank, F. R.; Golden, D. M.; Haugen, G. R.; O'Neal, H. E.; Rodgers, A. S.; Shaw, R.; Walsh, R. Additivity rules for the estimation of thermochemical properties. *Chem. Rev.* 69, 279-324, 1969. b) Benson, S. W.; Cohen, N. Estimation of heats of formation of organic compounds by additivity methods. *Chem Rev.* 1993, 93, 2419. c) Eigenmann, H. K.; Golden, D. M.; Benson, S. W. Revised group additivity parameters for the enthalpies of formation of oxygen-containing organic compounds. *J. Phys. Chem.* 1973, 77, 1687-1691.

(14) Benson, S. W. *Thermochemical kinetics. Methods for the estimation of thermochemical data and rate parameters*. John Wiley & Sons. USA 1976.

(15) a) Sumathi, R.; Carstensen, H. H.; Green, W. H. Reaction rate prediction via group additivity. Part 1: H Abstaction from alkanes by H and CH3. *J. Phys. Chem. A* 2001, 105, 6910. b) Sumathi, R.; Green, W. H. Thermodynamic properties of ketenes: group additivity values from quantum chemical calculations. *J. Phys. Chem. A* 2002, 106, 7937–7949.

(16) Benson, S. W. *Current status of group additivity*. Symposium on Computational Thermochemistry, Orlando, Florida, August 25-29, 1996.

(17) a) Aubry, C.; Holmes, J. L.; Terlouw, J. K. Effect of methyl substitution on the thermochemistry of ketene. *J. Phys. Chem. A* 1997, 101, 5958–5961. b) Nguyen, M. T.; Nguyen, H. M. T. On the heats of formation of methylketene, dimethylketene and related cations. *Chem. Phys. Lett.* 1999, 300, 346–350. c) Traeger, J. C. Neutral and cationic heats of formation for ketene, methylketene, and dimethylketene. *Int. J. Mass Spectrom.* 2000, 194, 261–267.

(18) Casewit, C. J.; Colwell, K. S.; Rappé, A. K. Application of a universal force field to organic molecules. *J. Am. Chem. Soc.* 1992, 114, 10035–10046.

(19) a) Petersson, G. A.; Tensfeldt, T. G.; Montgomery Jr., J. A. A complete basis set model chemistry. III. The complete basis set-quadratic configuration interaction family of methods. *J. Chem. Phys.* 1991, 94, 6091. b) Montgomery Jr., J. A.; Frisch, M. J.; Ochterski, J. W.; Petersson, G. A. A complete basis set model chemistry. VII. Use of the minimum population localization method. *J. Chem. Phys.* 2000, 112, 6532. c) Petersson, G.; Malick, D.; Wilson, G.; Ochterski, J.; Montgomery, J.; Frisch, M. Calibration and comparison of the Gaussian-2, complete basis set, and density functional methods for computational thermochemistry. *J. Chem. Phys.* 1998, 109, 10570.

(20) Frisch, M. J.; Trucks, G. W.; Schlegel, H. B.; Scuseria, G. E.; Robb, M. A.; Cheeseman, J. R.; Montgomery, Jr., J. A.; Vreven, T.; Kudin, K. N.; Burant, J. C.; Millam, J. M.; Iyengar, S. S.; Tomasi, J.; Barone, V.; Mennucci, B.; Cossi, M.; Scalmani, G.; Rega, N.; Petersson, G. A.; Nakatsuji, H.; Hada, M.; Ehara, M.; Toyota, K.; Fukuda, R.; Hasegawa, J.; Ishida, M.; Nakajima, T.; Honda, Y.; Kitao, O.; Nakai, H.; Klene, M.; Li, X.; Knox, J. E.; Hratchian, H. P.; Cross, J. B.; Adamo, C.; Jaramillo, J.; Gomperts, R.; Stratmann, R. E.; Yazyev, O.; Austin, A. J.; Cammi, R.; Pomelli, C.; Ochterski, J. W.; Ayala, P. Y.; Morokuma, K.; Voth, G. A.; Salvador, P.; Dannenberg, J. J.; Zakrzewski, V. G.; Dapprich, S.; Daniels, A. D.; Strain, M. C.; Farkas, O.; Malick, D. K.; Rabuck, A.

D.; Raghavachari, K.; Foresman, J. B.; Ortiz, J. V.; Cui, Q.; Baboul, A. G.; Clifford, S.; Cioslowski, J.; Stefanov, B. B.; Liu, G.; Liashenko, A.; Piskorz, P.; Komaromi, I.; Martin, R. L.; Fox, D. J.; Keith, T.; Al-Laham, M. A.; Peng, C. Y.; Nanayakkara, A.; Challacombe, M.; Gill, P. M. W.; Johnson, B.; Chen, W.; Wong, M. W.; Gonzalez, C.; Pople, J. A. Gaussian, Inc., Wallingford CT, (Gaussian 03, Revision C.02), 2004.

(21) a) Pople, J. A.; Luke, T. B.; Frisch, M. J.; Binckely, J. S. Theoretical thermochemistry. 1. heats of formation of neutral AHn molecules (A=Li to Cl). *J. Phys. Chem.*, 1985, 89, 2198–2203. b) Nicolaides, A.; Rauk, A.; Glukhovtsev, M.; Radom, L. Heats of formation from G2, G2(MP2), and G2(MP2,SVP) total energies. *J. Phys. Chem.* 1996, 100, 17460. c) Wagman, D. D.; Evans, W. H.; Parker, V. B.; Schumm, R. H.; Halows, I.; Bailey, S. M.; Churney, K. L.; Nuttall, R. N. *J. Phys. Chem. Ref. Data* 1982, 11, suppl. 2. d) Lias, S. G.; Bartmess, J. E.; Liebman, J. F.; Holmes, J. L.; Levin, R. D.; Mallard, W. G. *J. Phys. Chem. Ref. Data* 1988, 17, suppl. 1.

(22) Ayala, P. Y.; Schlegel, H. B. Identification and treatment of internal rotation in normal mode vibrational analysis. *J. Chem. Phys.* 1998, 108, 2314.

(23) a) Durig, J.; Green, W. H.; Hammond, N.C. Raman and far-infrared spectra of some four-membered ring molecules. *J. Phys. Chem.* 1966, 70, 1989–1997. b) Carreira, L.A.; Lord, R. C. Far-Infrared spectra of ring compounds. V. Ring-puckering potential functions of some oxygen-containing molecules. *J. Chem. Phys.* 1969, 51, 3225–3231.

(24) Yamada, T.; Lay, T. H.; Bozelli, J. W. Ab initio calculations and internal rotor: contribution for thermodynamic properties $S°_{298}$ and Cp(T)'s ($300 \leq T/K \leq 1500$): group additivity for fluoroethanes. *J. Phys. Chem. A* 1998, 102, 7286–7293.

(25) Pitzer, K. S.; Gwinn, W. D. Energy levels and thermodynamic functions for molecules with internal rotation I. Rigid frame with attached tops. *J. Chem. Phys.* 1942, 10, 428.

(26) a) Wong, M. W.; Radom, L. Radical addition to alkenes: further assessment of theoretical procedures. *J. Phys. Chem. A* 1998, 102, 2237–2245. b) Parker, C.L. ; Cooksy, A. L. Ab initio study of the 1,3-butadienyl radical isomers. *J. Phys. Chem. A* 1998, 102, 6186–6190. c) Van Speybroeck, V.; Van Neck, D.; Waroquier, M.; Wauters, S.; Saeys, M.; Marin, G. B. Ab initio study of radical addition reactions: addition of a primary ethylbenzene radical to ethene (I). *J. Phys. Chem. A.* 2000, 104, 10939.

(27) East, A.; Radom, L. Ab initio statistical thermodynamical models for the computation of third-law entropies. *J. Chem. Phys.* 1997, 106, 6655.

(28) Ercolani, G. Numerical evaluation of energy levels and wave functions for hindered internal rotation. *J. Chem. Educ.* 2000, 77, 1495.

(29) McQuarrie, D.A. *Statistical mechanics*. Harper and Row, New York, 1976.

(30) Irikura, K. K.; Frurip, D. J. *Computational thermochemistry: prediction and estimation of molecular thermodynamics.* American Chemical Society, 1998.

(31) Woodward, R. B.; Small, G. Jr. The structure of the acidic dimer of methylketene. *J. Am. Chem. Soc.* 1950, 72, 1297–1304.

(32) Seidl, E. T.; Schaefer, H. F. Molecular structure of diketene: A discrepancy between theory and experiments? *J. Phys. Chem.* 1992, 96, 657–661.

(33) a) Mönnig, F.; Dreizler, H.; Rudolph, H. D. *Naturforsch. A* 1967, 22, 1471–1473. b) Bregman, J.; Sauer, S. H. An electron diffraction study of ketene dimer, methylketene dimer and β-propiolactone. *J. Am. Chem. Soc.* 1955, 77, 1955–1965. c) Katz, L.; Lipscomb, W. N. J. Org. Chem. 1952, 17, 515–517. d) Kay, M. I.; Katz, L. A refinement of the crystal structure of ketene dimer. *Acta Crystallogr.* 1958, 11, 897–898.

(34) a) Rode, J. R.; Dobrowolski, J. Cz. Reaction paths of the [2 + 2] cycloaddition of X=C=Y molecules (X, Y = S or O or CH2). Ab initio study. *J. Phys. Chem. A* 2006, 110, 207–218. b) Kelly, E.; Seth, M.; Ziegler, T. Calculation of free energy profiles for elementary bimolecular reactions by ab initio molecular dynamics: sampling methods and thermostat considerations. *J. Phys. Chem. A* 2004, 108, 2167–2180.

(35) Computational chemistry comparison and benchmark database. National Institute of Standards and Technology. http://srdata.nist.gov/cccbdb/default.htm.

(36) Hellwege, K.H.; Hellwege, A.M. (ed.). Landolt-Bornstein: Group II: Atomic and molecular physics Volume 7: Structure data of free polyatomic molecules. Springer-Verlag. Berlin. 1976.

(37) Kuchitsu (ed.), Landolt-Bornstein: Group II: Atomic and molecular physics, Volume 21: Structure data of free polyatomic molecules. Springer-Verlag, Berlin, 1992.

(38) a) Radom, L.; Pople, J. A. Molecular orbital theory of the electronic structure of organic compounds. IV. Internal rotation in hydrocarbons using a minimal Slater-type basis. *J. Am. Chem. Soc.* 1970, 92, 4786. b) Radom, L.; Lathan, W. A.; Hehre, W. J.; Pople, J. A. Molecular orbital theory of the electronic structure of organic compounds. XVII. Internal rotation in 1,2-disubstituted ethanes. *J. Am. Chem. Soc.* 1973, 95, 693.

(39) Chung-Phillips, A. A Study of the Fourier-series representation for internal rotation. *J. Chem. Phys.* 1988, 88, 1764.

(40) Hehre, W. J.; Ditchfield, R.; Radom. L.; Pople, J. A. Molecular orbital theory of the electronic structure of organic compounds. V. Molecular theory of bond separation. *J. Am. Chem. Soc.* 1970, 92, 4796.

(41) a) Pedley, J. B.; Naylor, R. D.; Kirby, S. P. *Thermochemical data of organic compounds.* Chapman and Hall, London, 1986. b) Holmes, J. L.; Aubry, C.; Wang, X. Assessing thermochemical data. *Int. J. Mass Spectrom.* 2007, 267, 263-267. c) Holmes, J. L.; Jobst, K. J.; Terlow, J. K. Small (poly)unsaturated oxygen containing ions and molecules: a brief assessment of their thermochemistry based on computational chemistry. Eur. J. Mass Spectrom. 2009, 15, 261-273. d) Lide, D. R., Ed. *CRC Handbook of Chemistry and Physics*, 86th ed.; CRC Press: Boca Raton, FL, 2006 (http://www.hbcpnetbase.com/).

(42) Morales, G.; Martínez, R.; Ziegler, T. Theoretical comparison of ketene dimerization in the gas and liquid phase. *J. Phys. Chem. A* 2008, 112, 3192–3200.

(43) Turecek, F. (E)- and (Z)-prop-1-en-1-ol: gas-phase generation and determination of heats of formation by mass spectrometry. *J. Chem. Soc., Chem. Commun.* 1984, 1374.

(44) Gomes, J. R. B.; Ribeiro da Silva, M. A. V. Computational study on the bond dissociation enthalpies in the enolic and ketonic forms of β-diketones: their influence on metal−ligand bond Enthalpies. *J. Phys. Chem. A*, 2006, 110, 13948–13955.

(45) a) Hoffman, R. Interaction of orbital through space and through bonds. *Acc. Chem. Res.* 1971, 4, 1–9. b) Houk, K. N.; Davis, L. P; Newkome, G. R.; Duke, R. E. Jr.; Nauman, R. V. Photoelectron spectroscopy of cyclic β-diketones and their enolone tautomers. *J. Am. Chem. Soc.*, 1973, 95, 8364–8371. c) Pasto, D. J.; Chipman, D. M.; Worman, J. J. Comparison of through-space and through-bond interactions in four-membered ring systems. *J. Phys. Chem.* 1982, 86, 3981–3989.

(46) a) Lowrey , A. H.; George, C; Antonio, P. D.; Karle, J. Structure of acetylacetone by electron diffraction. *J. Am. Chem. Soc.*, 1971, 93, 6399 –6403. b) Gordon, M. S.; Koob, R. D. An INDO investigation of the structure and bonding of acetylacetone and trifluoroacetylacetone. *J. Am. Chem. Soc.*, 1973, 95, 5863–5867.

(47) a) Huggins, M. L. Hydrogen bridges in organic compounds. *J. Org. Chem.*, 1936, 1, 407–456. b) Gilli, G.; Bertolasi, V. *Structural chemistry* in *The chemistry of enols*, Ed. Rappoport, Wiley, 1989. c) Kojić-Prodić, B.; Molčanov, K. The nature of hydrogen bond: new insights into old theories. *Acta Chim. Slov.* 2008, 55, 692–708.

(48) a) Jeffrey, G. A.; Saenger, W. *Hydrogen bonding in biological structures*, Springer, 1991. b) Cleland, W. W.; Kreevoy, M. M. Low-barrier hydrogen bonds and enzymic catalysis. *Science* 1994, 264, 1887–1890. c) Gerlt, G. A.; Kreevoy, M. M.; Cleland, W.

W.; Frey, P. A. Understanding enzymatic catalysis: the importance of short, strong hydrogen bonds. *Chem. Biol.* 1997, 4, 259–267. d) Wickelgren, I. Key brain receptor gets an unusual regulator. *Science* 1999, 286, 1265–1266. e) Fujii, K.; Maedal, K.; Hikida, T.; Mustafa, A. K.; Balkissoon, R.; Xia, J.; Yamada, T.; Ozekil, Y.; Kawahara, R.; Okawa, M.; Huganir, R. L.; Ujike, H.; Snyder, S. H.; Sawa, A. Serine racemase binds to PICK1: potential relevance to schizophrenia. *Mol. Psychiatry* 2006, 11, 150–157. f) Stryer, L. *Biochemistry*, 4th ed. W. H. Freeman and Co.: New York, 2000.

(49) Musin, R. N.; Mariam, Y. H. An integrated approach to the study of intramolecular hydrogen bonds in malonaldehyde enol derivatives and naphthazarin: trend in energetic versus geometrical consequences. *J. Phys. Org. Chem.* 2006, 19, 425–444.

(50) a) Muller, N.; Reiter, R. C. Temperature dependence of chemical shifts of protons in hydrogen bonds. *J. Chem. Phys*. 1965, 42, 3265–3269. b) Dougherty, R. C. Temperature and pressure dependence of hydrogen bond strength: A perturbation molecular orbital approach. *J. Chem. Phys.* 1998, 109, 7372–7378.

(51) Exner, O.; Bhm, S. Theory of substituent effects: recent advances. *Curr. Org. Chem.*, 2006, 10, 763–778.

(52) a) Wilkinson, J. H. *The algebraic eigenvalue problem.* Clarendon Press, Oxford, 1965. b) Schwarz, H. R. *Numerical analysis. A comprehensive introduction*. Wiley, Chichester, New York, 1989.

(53) a) Durbin, J.; Watson, G. S. Testing for Serial Correlation in Least Squares Regression I. *Biometrika*, 1950, 37, 409-428. b) Durbin, J.; Watson, G. S. Testing for Serial Correlation in Least Squares Regression II. *Biometrika*, 1951, 38, 159-178. c) Durbin, J.; Watson, G. S. Testing for Serial Correlation in Least Squares Regression III. *Biometrika*, 1971, 58, 1-19.

(54) Sebbar, N.; Bozzelli, J. W.; Bockhorn, H. thermochemical properties, rotation barriers, bond energies, and group additivity for vinyl, phenyl, ethynyl, and allyl peroxides. *J. Phys. Chem. A*, 2004, 108, 8353–8366.

(55) a) da Silva, G.; Kim, C. H.; Bozzelli, J. W. Thermodynamic properties (enthalpy, bond energy, entropy, and heat capacity) and internal rotor potentials of vinyl alcohol, methyl vinyl ether, and their corresponding radicals. *J. Phys. Chem. A* 2006, 110, 7925–7934. b) Chen, C.; Wong, D.; Bozzelli, J. W. Standard chemical thermodynamic properties of multichloro alkanes and alkenes: a modified group additivity scheme. *J. Phys. Chem. A* 1998, 102, 4551–4558. c) Holmes, J. L.; Lossing, F. P. Heats of formation of ionic and neutral enols of acetaldehyde and acetone. *J. Am. Chem. Soc.* 1982, 104, 2648. d)

Turecek, F.; Havlas, Z. J. Thermochemicstry of unstable enols: the O-(Cd)(H) group equivalent. *J. Org. Chem.* 1986, 51, 4066. e) Zhu, L.; Chen, C. J.; Bozzelli, J. W. Structures, rotational barriers, and thermodynamic properties of C2 Vinyl and chlorovinyl alcohols and additivity groups. *J. Phys. Chem. A*, 2000, 104, 9197. f) Cohen, N. *J. Phys. Chem. Ref. Data* 1996, 25, 1411.

(56) Steele, W. V.; Chirico, R. D.; Cowell, A. B.; Knipmeyer, S. E.; Nguyen, A. Thermodynamic properties and ideal-gas enthalpies of formation for methyl benzoate, ethyl benzoate, (R)-(+)-limonene, tert-amyl methyl ether, trans-crotonaldehyde, and diethylene glycol. *J. Chem. Eng. Data* 2002, 47, 667–688.

(57) Sebbar, N.; Bockhorn, H.; Bozzelli, J.W. Thermochemical properties, rotation barriers, and group additivity for unsaturated oxygenated hydrocarbons and radicals resulting from reaction of vinyl and phenyl radical systems with O2. *J. Phys. Chem. A* 2005, 109, 2233–2253.

(58) a) Tamprado, M; Roux, M. V.; Umnahanant, P.; Zhao, H.; Chickos, J. S. The thermochemistry of 2,4-pentanedione revisited: observance of a nonzero enthalpy of mixing between tautomers and its effects on enthalpies of formation. *J. Phys. Chem. B*, 2005, 109, 12590–12595. b) Folkendt, M. M.; Weiss-Lopez, B. E.; Chauvel, J. P. Jr.; True, N. S. Gas-Phase ^{1}H-NMR studies of keto-enol tautomerism of acetylacetone, methyl acetoacetate, and ethyl acetoacetate. *J. Phys. Chem*. 1985, 89, 3347–3352.

(59) a) Al-Takhin, G.; Pilcher, G.; Bickerton, J.; Zaki, A. A. Standard enthalpies of formation of diamine(dicarboxylato)platinum(II) complexes and of bis(pentane-2,4-dionato)platinum(II): the mean Pt-O bond dissociation enthalpies. *J. Chem. Soc., Dalton Trans*. 1983, 12, 2657-2659. b) Wilhoit, R. C.; Shiao, D. Thermochemistry of biologically important compounds. Heats of combustion of solid organic acids. *J. Chem. Eng. Data*, 1964, 9, 596-599.

(60) a) Yu, T.; Mebel, A. M.; Lin, M. C. Reaction of phenoxy radical with nitric oxide. *J. Phys. Org. Chem.* 1995, 8, 47. b) Berkowitz, J.; Ellison, G. B.; Gutman, D. Three methods to measure RH bond energies. *J. Phys. Chem.* 1994, 98, 2744.

(61) Lay, T. H.; Yamada, T.; Tsai, P. L.; Bozzelli, J. W. Thermodynamic parameters and group additivity ring corrections for three- to six-membered oxygen heterocyclic hydrocarbons. *J. Phys. Chem. A* 1997, 101, 2471–2477.

CONCLUDING REMARKS

Molecular Modeling of Ketene Dimerization Reaction

The first extensive density functional study of the ketene dimerization in both gas and liquid phase is presented in this work. The four dimerization products considered are diketene, cyclobutane-1,3-dione, 2,4-dimethylene-1,3-dioxetane, and 2-methyleneoxetan-3-one. It was found in both gas phase and solution that all four dimerization processes involve a single transition state without intermediates. For diketene, cyclobutane-1,3-dione, and 2-methyleneoxetan-3-one, dimerization is asynchronous with the formation of one bond preceding formation of the other. On the other hand, dimerization leading to 2,4-dimethylene-1,3-dioxetane is synchronous with both bonds forming at the same time. The ketene dimerizations toward the diketene, cyclobutane-1,3-dione, and 2-methyleneoxetan-3-one dimers might be classified as nonplanar pseudopericyclic reactions. The ketene dimerization process leading to the 2,4-dimethylene-1,3-dioxetane dimer is, on the other hand, a pericyclic reaction with a nonplanar but still synchronous transition state.

Solvation makes dimerization more favorable in solution than in gas phase as the products, especially diketene, cyclobutane-1,3-dione, and 2-methyleneoxetan-3-one, are stabilized by interactions between the solute dipoles and the solvent. Similar interactions in the transition states towards diketene, cyclobutane-1,3-dione, and 2-methyleneoxetan-3-one help lower the activation enthalpies compared to the gas phase. An increase in the entropy of dimerization and activation in solution compared to gas phase help further ease the formation of the dimers kinetically as well as thermodynamically in solution. The species 2,4-dimethylene-1,3-dioxetane and 2-methyleneoxetan-3-one have higher energies and dimerization barriers than diketene and cyclobutane-1,3-dione. As a consequence, 2,4-dimethylene-1,3-dioxetane and 2-methyleneoxetan-3-one are unlikely products from ketene dimerization in gas phase as well as in solution.

The species diketene is calculated to be more stable than cyclobutane-1,3-dione in gas phase as well as solution. However, the calculated margin is reduced from 2 kcal/mol in gas phase

to 1 kcal/mol in acetone. On the other hand, whereas cyclobutane-1,3-dione is calculated to have the lowest dimerization barrier in gas phase and modestly nonpolar solvents, diketene has the lowest barrier in polar solvents such as acetone. Our results are in good agreement with experiments carried out in solvents. However, in gas-phase experiments cyclobutane-1,3-dione is more stable than diketene, in contrast to our calculation as well as other recent studies.

Completion of the ketene dimerization study is done by calculating the gas-phase thermochemistry of substituted ketene dimers at the CBS-Q multilevel method. Results based on the thermochemistry of substituted ketene dimers suggest that the dimerization of aldoketenes and ketoketenes toward the cyclobutane-1,3-dione dimer structure is controlled thermodynamically. Enol-tautomeric form for the low weight cyclobutane-1,3-dione dimer is found to be disfavored thermodynamically. Favorable solvent interaction may explain the experimental detection of this tautomeric form. The group additivity method of Benson (GAVs) appears to reproduce accurately the thermochemical properties for the ketene dimers. The GAV method is extended to the ketene dimer structures such as diketene, cyclobutane-1,3-dione and its enol-tautomeric form by assessing 19 new contribution groups. The new GAVs are based upon a linear regression over a set of 57 acyclic compounds. Successive replacements of the new GAVs on the derived thermochemical property equations of the substituted dimers allow determining the corrections for ring formation and substitutent position. The new GAVS and the ring and substituent corrections for the substituted diketene dimer, cyclobutane-1,3-dione dimer and its enol-tautomeric form are particularly useful when no other data are available.

PUBLICATIONS AND CONFERENCES

"Theoretical Comparison of Ketene Dimerization in the Gas and Liquid Phase". *The Journal of Physical Chemistry A*. 2008, 112, 3192-3200.

"Thermochemical Properties and Contribution Groups for Ketene Dimers and Related Structures from Theoretical Calculations". Submitted to *The Journal of Physical Chemistry*.

6th Canadian Conference on Computational Chemistry.
    Vancouver, 26th - 31st July 2006.
    Poster Presentation: "Static Modeling of Ketene Dimerization Reaction
                in Gas and Liquid Phase".

7th deMon Developers Annual Workshop.
    Kananaskis Country, Alberta, Canada, 21st – 25th April 2006.
    Poster Presentation: "Static Modeling of Ketene Dimerization Reaction
              Using ADF".

Course book: "Introduction to Molecular Modeling in Chemical Engineering"
        Chemical Engineering Department.
        Universidad Industrial de Santander. 2005.

XXXI International Congress of Theoretical Chemist of Latin Expression, Quitel.
    Margarita Island, Venezuela, 1st – 6th October 2005.
    Poster Presentation: "Contribution Groups for Ketene Polymers from
             Theoretical Calculations".

1st Colombian Congress of Theoretical Chemist.
    Universidad de Pamplona, Pamplona, July 2004.
    Oral Presentation: "Thermodynamic Properties of Ketene Compounds".

SUPPORTING INFORMATION FOR

CHAPTERS 4 AND 5

Table S1. Names, molecule numbering and structures of the studied dimers.
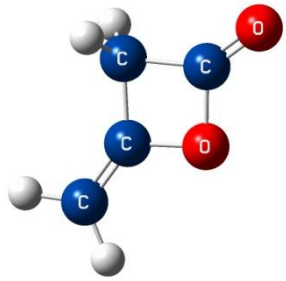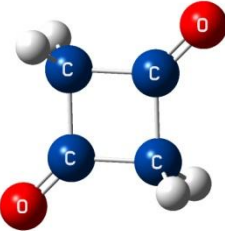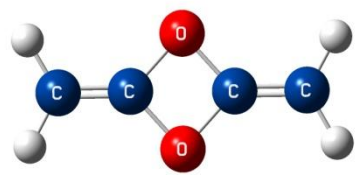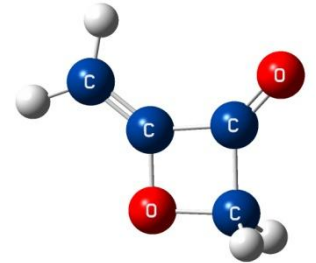
Diketene (d-I)	1,3-Cyclobutanedione (d-II)	2,4-methylene-1,3-Dioxetane (d-III)	2-methylene-3-oxetanone (d-IV)

Table S2. The cartesian coordinates (in Å) for the ketene dimers at the PW86x+PBEc/DZP level.

	d-I			d-II			d-III			d-IV		
	X	Y	Z	X	Y	Z	X	Y	Z	X	Y	Z
C	-0.060	-1.321	0.000	0.000	0.000	-0.019	0.031	0.000	0.000	0.067	0.051	0.000
C	-0.898	-2.344	-0.001	0.792	-0.790	-1.080	1.350	1.374	0.000	1.560	0.066	-0.001
C	-0.058	0.182	0.003	-0.792	0.790	-1.080	2.255	2.336	0.000	1.496	-1.468	-0.001
C	1.456	0.012	0.001	0.000	0.000	-2.140	-0.869	-0.968	0.000	-0.928	0.939	0.001
O	2.447	0.678	0.001	0.000	0.000	-3.348	1.432	-0.019	0.000	2.434	0.899	-0.001
O	1.363	-1.400	-0.002	0.000	0.000	1.189	-0.052	1.393	0.000	0.020	-1.350	0.001
H	-0.528	-3.366	-0.003	-1.878	0.603	-1.080	3.310	2.084	0.000	1.857	-1.963	-0.911
H	-1.971	-2.171	0.001	-0.618	1.878	-1.080	1.938	3.373	0.000	1.859	-1.963	0.909
H	-0.451	0.667	0.906	1.878	-0.603	-1.080	-0.542	-2.002	0.000	-1.973	0.637	0.002
H	-0.453	0.671	-0.898	0.618	-1.878	-1.080	-1.927	-0.726	0.000	-0.677	1.997	0.000

Table S3. The cartesian coordinates (in Å) for transition states in gas phase at the PW86x+PBEc/DZP level *.

	TS d-I (438i)			TS d-II (319i)			TS d-III (795i)			TS d-IV (127i)		
	X	**Y**	**Z**	**X**	**Y**	**Z**	**X**	**Y**	**Z**	**X**	**Y**	**Z**
C	1.654	0.018	-0.009	-0.160	-0.003	0.503	0.029	0.015	0.066	0.049	-0.049	-0.001
C	-0.103	1.390	0.035	2.330	0.022	0.079	2.123	2.183	-1.162	1.561	-0.147	0.039
C	-0.057	-0.005	-0.027	2.010	-1.172	0.726	1.697	1.149	-0.474	2.024	1.206	-0.162
C	2.255	-0.686	0.975	0.402	-1.206	0.090	-0.526	-1.175	0.040	-0.817	-0.624	-0.893
O	1.957	0.782	-0.963	0.124	-2.105	-0.690	-0.037	1.277	0.052	2.290	-1.103	0.311
O	-0.173	2.489	0.369	2.865	0.805	-0.598	1.846	-0.007	0.017	-0.168	0.809	0.928
H	1.691	-1.287	1.679	2.667	-2.012	0.459	-1.600	-1.222	-0.131	3.089	1.435	-0.065
H	3.344	-0.723	0.987	1.875	-1.056	1.807	0.053	-2.078	0.188	-1.883	-0.425	-0.809
H	-0.691	-0.458	0.753	-1.136	0.287	0.111	1.547	3.098	-1.223	-0.473	-1.431	-1.538
H	-0.255	-0.393	-1.032	0.169	0.466	1.428	3.081	2.091	-1.671	1.381	1.912	-0.685

* Corresponding imaginary frequencies are given in parenthesis.

Table S4. The cartesian coordinates (in Å) for transition states in toluene at the PW86x+PBEc/DZP level*.

	TS d-I (354i)			TS d-II (287i)			TS d-III (817i)			TS d-IV (100i)		
	X	**Y**	**Z**	**X**	**Y**	**Z**	**X**	**Y**	**Z**	**X**	**Y**	**Z**
C	2.243	-0.703	0.964	-0.155	0.000	0.496	2.221	-0.167	0.303	-0.033	-0.027	-0.020
C	-0.003	-0.006	-0.013	2.318	0.014	0.070	1.024	0.227	-0.066	1.498	-0.095	0.048
C	1.620	0.006	-0.009	1.979	-1.184	0.710	-1.025	-0.226	-0.068	2.003	1.212	-0.208
C	-0.098	1.405	0.038	0.436	-1.198	0.110	-2.221	0.164	0.303	-0.735	-0.727	-1.002
O	-0.202	2.502	0.364	0.137	-2.098	-0.683	0.170	1.130	-0.310	-0.492	0.741	0.871
O	1.973	0.782	-0.969	2.857	0.805	-0.590	-0.169	-1.127	-0.318	2.178	-1.122	0.205
H	-0.276	-0.391	-1.006	2.624	-2.029	0.422	-2.919	-0.603	0.642	3.070	1.339	-0.415
H	-0.598	-0.470	0.795	1.902	-1.069	1.800	-2.518	1.208	0.277	-1.826	-0.691	-1.010
H	1.682	-1.283	1.693	-1.126	0.282	0.084	2.517	-1.210	0.275	1.315	2.032	-0.411
H	3.332	-0.743	0.985	0.175	0.501	1.405	2.920	0.600	0.642	-0.217	-1.473	-1.606

Table S5. The cartesian coordinates (in Å) for transition states in acetone at the PW86x+PBEc/DZP level*.

	TS d-I (357i)			TS d-II (296i)			TS d-III (808i)			TS d-IV (53i)		
	X	Y	Z	X	Y	Z	X	Y	Z	X	Y	Z
C	0.034	0.030	0.126	-0.125	0.011	0.461	0.020	0.001	0.029	-0.020	-0.029	0.001
C	1.630	-0.031	0.009	2.302	0.023	0.059	2.227	2.328	-0.498	1.498	-0.092	0.047
C	-0.137	1.432	0.063	1.972	-1.199	0.678	1.722	1.210	-0.036	1.999	1.194	-0.302
C	2.279	-0.875	0.846	0.453	-1.208	0.117	-0.502	-1.143	-0.353	-0.714	-0.664	-1.038
O	-0.297	2.553	0.203	0.103	-2.124	-0.653	1.806	-0.022	0.262	-0.515	0.687	0.918
O	1.998	0.798	-0.915	2.863	0.833	-0.554	-0.084	1.243	0.281	2.177	-1.115	0.264
H	-0.360	-0.429	-0.799	2.629	-2.024	0.355	-1.547	-1.139	-0.671	1.311	2.029	-0.445
H	1.740	-1.489	1.565	1.953	-1.104	1.777	0.076	-2.063	-0.367	-1.804	-0.585	-1.085
H	3.365	-0.967	0.785	-1.089	0.300	0.036	1.678	3.265	-0.470	3.052	1.308	-0.583
H	-0.496	-0.365	1.016	0.209	0.533	1.358	3.236	2.286	-0.918	-0.196	-1.375	-1.684

* Corresponding imaginary frequencies are given in parenthesis.

Table S6. The Hirshfeld charges (in a.u.) and dipole moments (in Debye) for the transition states in gas and liquid phase.

	TS d-I			TS d-II			TS d-III			TS d-IV		
	Gas phase	Toluene	Acetone	Gas phase	Toluene	Acetone	Gas phase	Toluene	Acetone	Gas phase	Toluene	Acetone
C	0.059	-0.185	-0.020	-0.155	-0.158	-0.158	0.166	-0.139	0.161	0.063	0.077	0.075
C	0.274	-0.031	0.024	0.234	0.252	0.266	-0.142	0.160	-0.136	0.011	0.097	0.090
C	-0.049	0.038	0.330	-0.060	-0.044	-0.034	0.166	0.160	0.168	0.032	0.023	0.037
C	-0.181	0.297	-0.021	0.087	0.071	0.062	-0.141	-0.139	-0.143	-0.077	-0.035	-0.007
O	-0.274	-0.021	0.014	-0.248	-0.309	-0.361	-0.151	-0.164	-0.145	-0.197	-0.204	-0.239
O	-0.041	-0.339	-0.409	-0.077	-0.068	-0.059	-0.152	-0.162	-0.160	-0.156	-0.227	-0.264
H	0.022	0.092	0.109	0.078	0.098	0.111	0.064	0.073	0.063	0.060	0.077	0.075
H	0.036	0.092	0.026	0.081	0.092	0.101	0.063	0.070	0.061	0.051	0.065	0.075
H	0.076	0.025	0.023	0.038	0.037	0.035	0.062	0.069	0.065	0.068	0.066	0.087
H	0.080	0.032	0.110	0.022	0.029	0.036	0.064	0.072	0.066	0.050	0.062	0.072
Dipole moment	4.331	5.715	7.532	3.777	5.023	6.086	0.900	1.080	1.070	2.733	3.275	4.392

Table S7. The Hirhfeld charges (in a.u.), the dipole moment (in Debye) and the cartesian coordinates (in Å) for the ketene at the PW86x+PBEc/DZP level.

	Hirshfeld charges			Gas phase coordinates		
	Gas phase	**Toluene**	**Acetone**	**X**	**Y**	**Z**
C	-0.166	-0.164	-0.160	0	0	-0.163
C	0.178	0.175	0.172	0	0	-1.474
O	-0.136	-0.148	-0.162	0	0	-2.648
H	0.062	0.069	0.075	0	-0.944	0.371
H	0.062	0.069	0.075	0	0.944	0.371
Dipole moment	1.462	1.734	2.000			

Table S8. Total Bonding Energy from various XC functionals and the predicted heat of reaction and the activation energy for the ketene dimerization toward the d-I dimer based on the optimized structures at the PW86x+PBEc/DZP level[*].

	XC Functional	**2Ketene**	**d-I**			**TS d-I**		
		E (0 K)	**E (0 K)**	**ΔHr (298 K)**	**(ΔHr - ΔHr[exp])[+]**	**E (0 K)**	**Ea (298 K)**	**(Ea - Ea[exp])°**
[1]	KCIS-modified	-1326.31	-1339.30	-9.22	-13.45	-1300.41	28.35	2.65
[2]	KCIS-original	-1352.00	-1368.10	-12.33	-10.34	-1327.91	26.53	4.47
[3]	PKZB	-1353.01	-1369.43	-12.64	-10.03	-1328.86	26.60	4.40
[4]	VS98	-1417.37	-1429.33	-8.18	-14.49	-1392.33	27.48	3.52
[5]	LDA(VWN)	-1498.33	-1535.74	-33.64	10.97	-1488.47	12.30	18.70
[6]	PW91	-1414.87	-1437.72	-19.07	-3.60	-1395.30	22.01	8.99
[7]	BLYP	-1351.44	-1362.30	-7.09	-15.58	-1323.55	30.33	0.67
[8]	BP	-1395.15	-1415.51	-16.59	-6.08	-1373.61	23.98	7.02
[9]	PBE	-1408.38	-1431.03	-18.87	-3.80	-1388.62	22.21	8.79
[10]	RPBE	-1365.49	-1381.54	-12.28	-10.39	-1340.84	27.09	3.91
[11]	revPBE	-1371.45	-1388.23	-13.01	-9.66	-1347.12	26.78	4.22
[12]	OLYP	-1368.65	-1383.10	-10.68	-11.99	-1340.38	30.72	0.28
[13]	FT97	-1350.06	-1360.84	-7.00	-15.67	-1323.93	28.58	2.42
[14]	BLAP3	-1416.91	-1425.51	-4.82	-17.85	-1383.97	35.39	-4.39
[15]	HCTH/93	-1379.56	-1392.72	-9.38	-13.29	-1350.59	31.41	-0.41
[16]	HCTH/120	-1395.75	-1411.85	-12.32	-10.35	-1370.32	27.87	3.13
[17]	HCTH/147	-1394.89	-1410.69	-12.03	-10.64	-1368.87	28.46	2.54
[18]	HCTH/407	-1387.84	-1400.04	-8.43	-14.24	-1358.64	31.64	-0.64
[19]	BmTau1	-1407.14	-1414.33	-3.42	-19.25	-1373.49	36.10	-5.10
[20]	BOP	-1337.67	-1345.72	-4.28	-18.39	-1307.23	32.89	-1.89
[21]	PKZBx-KCIScor	-1338.53	-1352.57	-10.27	-12.40	-1312.96	28.01	2.99
[22]	VS98-x(xc)	-1304.13	-1285.90	22.00	-44.67	-1248.11	58.47	-27.47
[23]	VS98-x-only	-1310.37	-1314.37	-0.23	-22.44	-1279.81	33.00	-2.00
[24]	Becke00	-1443.92	-1455.57	-7.87	-14.80	-1414.61	31.75	-0.75
[25]	Becke00x(xc)	-1344.85	-1337.35	11.27	-33.94	-1303.69	43.60	-12.60
[26]	Becke00-x-only	-1548.37	-1552.58	-0.44	-22.23	-1507.22	43.59	-12.59
[27]	Becke88x+BR89c	-1400.99	-1409.46	-4.70	-17.97	-1371.05	32.39	-1.39
[28]	OLAP3	-1434.12	-1446.31	-8.41	-14.26	-1400.80	35.77	-4.77

[*]Energies in kcal mol^{-1}. Functionals ordered according to the ADF output file. [+] Experimental value (-22.67 kcal mol^{-1}) from *J. Org. Chem.*, 1978, 43, 1146. ° Experimental value (-31 kcal mol^{-1}) from *Acta Chem. Scand.* 1968, 22, 171.

Table S8. Total Bonding Energy from various XC functionals and the predicted heat of reaction and the activation energy for the ketene dimerization toward the d-I dimer based on the optimized structures at the PW86x+PBEc/DZP level (continuation)[*].

	XC Functional	2Ketene	d-I			TS d-I		
		E (0 K)	E (0 K)	ΔHr (298 K)	(ΔHr - ΔHr[exp])[+]	E (0 K)	Ea (298 K)	(Ea - Ea[exp])[°]
[29]	TPSS	-1427.90	-1449.23	-17.57	-5.10	-1406.00	24.34	6.66
[30]	mPBE	-1396.88	-1417.72	-17.07	-5.60	-1375.81	23.51	7.49
[31]	OPBE	-1410.88	-1434.13	-19.48	-3.19	-1387.89	25.44	5.56
[32]	OPerdew	-1412.36	-1436.31	-20.18	-2.49	-1390.44	24.37	6.63
[33]	mPBEKCIS	-1372.93	-1389.68	-12.97	-9.70	-1349.29	26.09	4.91
[34]	mPW	-1398.51	-1418.07	-15.78	-6.89	-1376.31	24.64	6.36
[35]	tau-HCTH	-1410.23	-1429.05	-15.04	-7.63	-1386.30	26.38	4.62
[36]	XLYP	-1347.06	-1356.88	-6.05	-16.62	-1318.70	30.80	0.20
[37]	KT1	-1421.49	-1458.65	-33.39	10.72	-1414.78	9.15	21.85
[38]	KT2	-1471.24	-1510.86	-35.85	13.18	-1464.79	8.90	22.10
[39]	TPSSh	-1562.73	-1585.78	-19.27	-3.40	-1539.51	25.67	5.33
[40]	B3LYP(VWN5)	-1638.53	-1654.73	-12.42	-10.25	-1609.09	31.88	-0.88
[41]	O3LYP(VWN5)	-1586.92	-1607.79	-17.10	-5.57	-1559.25	30.11	0.89
[42]	KMLYP(VWN5)	-2188.29	-2221.37	-29.31	6.64	-2161.27	29.47	1.53
[43]	PBE0	-1752.33	-1779.30	-23.19	0.52	-1728.96	25.81	5.19
[44]	B3LYP*(VWN5)	-1577.60	-1594.50	-13.12	-9.55	-1549.95	30.09	0.91
[45]	BhandH	-2132.68	-2170.78	-34.33	11.66	-2111.10	24.03	6.97
[46]	BHandHLYP	-2046.69	-2067.69	-17.22	-5.45	-2013.01	36.12	-5.12
[47]	B97	-1643.88	-1664.74	-17.09	-5.58	-1617.96	28.36	2.64
[48]	B97-1	-1671.57	-1694.25	-18.90	-3.77	-1646.99	27.02	3.98
[49]	B97-2	-1682.28	-1703.80	-17.74	-4.93	-1655.50	29.23	1.77
[50]	mPBE0KCIS	-1719.76	-1741.28	-17.75	-4.92	-1692.84	29.37	1.63
[51]	mPBE1KCIS	-1618.48	-1638.61	-16.35	-6.32	-1592.52	28.41	2.59
[52]	B1LYP(VWN5)	-1699.06	-1714.99	-12.16	-10.51	-1668.28	33.23	-2.23
[53]	B1PW91(VWN5)	-1740.92	-1765.02	-20.33	-2.34	-1715.00	28.36	2.64
[54]	mPW1PW	-1744.83	-1769.33	-20.72	-1.95	-1719.53	27.74	3.26
[55]	**mPW1K**	**-1991.42**	**-2019.42**	**-24.24**	**1.57**	**-1963.91**	**29.95**	**1.05**
[56]	tau-HCTH-hybrid	-1601.16	-1623.81	-18.88	-3.79	-1577.86	25.75	5.25
[57]	X3LYP(VWN5)	-1667.48	-1684.91	-13.65	-9.02	-1638.62	31.31	-0.31

[*]Energies in kcal mol^{-1}. Functionals ordered according to the ADF output file. [+] Experimental value (-22.67 kcal mol^{-1}) from *J. Org. Chem.*, 1978, 43, 1146. [°] Experimental value (-31 kcal mol^{-1}) from *Acta Chem. Scand.* 1968, 22, 171.

Table S9. The MPW1K/DZP energies, the thermal energy corrections and the change in entropies based on the optimized structures and frequencies at the PW86x+PBEc/DZP level.

	ΔE (kcal mol^{-1})			Δ(U(298 K)-U(0 K)) (kcal mol^{-1})			ΔS (cal mol^{-1} K^{-1})		
	Gas phase	Toluene	Acetone	Gas phase	Toluene	Acetone	Gas phase	Toluene	Acetone
d-I	-28.01	-29.95	-32.13	4.37	2.16	4.10	-42.85	-24.09	-30.02
TS d-I	27.51	21.36	12.46	1.85	-0.01	1.97	-38.32	-22.13	-27.20
d-II	-24.60	-27.24	-29.96	3.22	1.06	3.08	-41.95	-22.87	-28.80
TS d-II	26.59	20.54	14.41	1.86	-0.03	2.02	-39.52	-22.21	-28.01
d-III	1.61	1.73	0.63	3.72	1.96	3.45	-42.71	-23.98	-29.91
TS d-III	54.24	54.14	52.76	0.81	-1.55	0.50	-38.38	-20.92	-26.76
d-IV	-6.62	-7.62	-9.85	4.11	1.56	3.91	-42.00	-23.60	-29.49
TS d-IV	65.20	62.62	56.71	1.48	-0.69	1.26	-40.99	-25.90	-35.27

SUPPORTING INFORMATION FOR

CHAPTER 6

231

Table S1. Cyclic structures, geometries and rotational constants in GHz at the MP2/6-31G(d') level and CBS-Q energies.

1c) Diketene

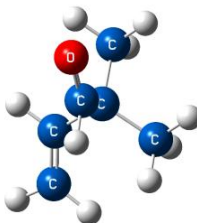|	X	Y	Z
C	-0.0532	1.1577	0.0001
C	-1.0509	-0.0067	0.0000
C	0.9505	0.0305	0.0000
O	-2.2283	-0.1851	-0.0002
O	-0.0400	-0.9751	0.0002
C	2.2695	-0.1539	-0.0001
H	2.6937	-1.1542	-0.0001
H	2.9360	0.7031	-0.0002
H	-0.0892	1.7837	-0.8988
H	-0.0891	1.7836	0.8990
ABC	12.0633	2.7664	2.2835

CBS-Q (0 K)=-304.786907 a.u.
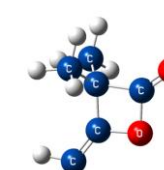
2c) 3-Methyl-4-methylene- oxetan-2-one

	X	Y	Z
C	0.0706	0.6857	0.4962
C	1.0114	-0.4518	0.0786
C	-0.9827	-0.3190	0.0889
O	2.1808	-0.6649	-0.0091
O	-0.0428	-1.3146	-0.2529
C	-2.3086	-0.4082	-0.0081
H	-2.7859	-1.3119	-0.3771
H	-2.9291	0.4332	0.2855
C	0.1854	1.9805	-0.3032
H	-0.6340	2.6626	-0.0466
H	1.1355	2.4805	-0.0795
H	0.1418	1.7779	-1.3797
H	0.1112	0.8701	1.5787
ABC	4.1569	2.6263	1.7179

CBS-Q (0 K)= -344.019765 a.u.
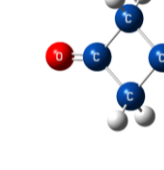
3c) 3,3-Dimethyl-4-methylene- oxetan-2-one

	X	Y	Z
C	-0.0910	0.5905	0.0000
C	-0.9523	-0.6803	0.0000
C	1.0286	-0.4280	0.0000
O	-2.1061	-0.9821	0.0000
O	0.1576	-1.5385	0.0000
C	2.3612	-0.4592	0.0000
H	2.9040	-1.4005	0.0000
H	2.9219	0.4712	0.0000
C	-0.2283	1.4257	-1.2722
H	-1.2108	1.9148	-1.2960
H	0.5468	2.2029	-1.2961
H	-0.1242	0.8059	-2.1711
C	-0.2283	1.4257	1.2722
H	0.5468	2.2029	1.2961
H	-1.2108	1.9148	1.2960
H	-0.1241	0.8059	2.1711
ABC	2.6436	2.1119	1.5781

CBS-Q (0 K)= -383.252994 a.u.

4c) Cyclobutane-1,3-dione

	X	Y	Z
C	0.0000	-1.125	0.000
C	0.0000	1.1245	0.000
H	0.0000	-1.766	-0.893
H	0.0000	-1.766	0.8928
H	0.0000	1.7664	-0.893
H	0.0000	1.7663	0.8928
C	-1.061	0.0000	0.0000
C	1.061	0.0000	0.0000
O	-2.266	0.0000	0.0000
O	2.2663	0.0000	0.0000
ABC	10.954	2.5977	2.1573

CBS-Q (0 K)= -304.780686 a.u.
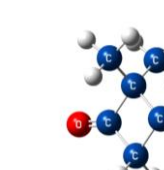
5c) 2-Methyl-cyclobutane-1,3-dione

	X	Y	Z
H	0.0000	0.7879	1.5727
C	0.0000	0.6541	0.4766
C	-1.0552	-0.4006	0.0736
C	1.0552	-0.4006	0.0736
C	0.0000	-1.5113	-0.1365
H	0.0000	-2.2750	0.6556
H	0.0000	-2.0152	-1.1122
O	-2.2502	-0.3477	-0.0830
O	2.2502	-0.3477	-0.0830
C	0.0000	1.9999	-0.2409
H	-0.8917	2.5770	0.0311
H	0.0000	1.8621	-1.3290
H	0.8917	2.5770	0.0311
ABC	4.0462	2.5237	1.6556

CBS-Q (0 K)= -344.013645 a.u.

6c) 2,2-Dimethyl-cyclobutane-1,3-dione
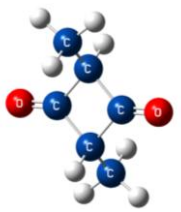
	X	Y	Z
C	0.0000	0.5683	0.0000
C	-1.0567	-0.5601	0.0001
C	1.0567	-0.5601	-0.0001
C	0.0000	-1.6900	0.0001
H	0.0002	-2.3334	0.8919
H	-0.0002	-2.3335	-0.8918
O	-2.2640	-0.5476	0.0000
O	2.2640	-0.5476	-0.0002
C	-0.0002	1.4205	-1.2708
H	-0.8938	2.0581	-1.2916
H	-0.0003	0.8007	-2.1775
H	0.8934	2.0581	-1.2918
C	0.0002	1.4205	1.2708
H	-0.8934	2.0581	1.2919
H	0.8938	2.0581	1.2916
H	0.0003	0.8007	2.1775
ABC	2.6676	2.0165	1.5465

CBS-Q (0 K)= -383.260285 a.u.

Table S1. Cyclic structures, geometries and rotational constants in GHz at the MP2/6-31G(d') level and CBS-Q energies (continuation).
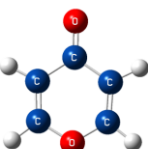
7c) (Z)-2,4-Dimethyl-cyclobutane-1,3-dione				
		X	Y	Z
	C	-1.0169	0.0000	0.4918
	C	0.0000	1.0555	0.0000
	C	0.0000	-1.0555	0.0000
	C	1.0170	0.0000	-0.4918
	H	1.1162	0.0000	-1.5900
	H	-1.1160	0.0000	1.5900
	O	0.0000	2.2636	-0.0001
	O	0.0000	-2.2636	-0.0001
	C	-2.3927	0.0000	-0.1774
	H	-2.9581	0.8921	0.1174
	H	-2.9581	-0.8921	0.1174
	H	-2.2986	0.0000	-1.2707
	C	2.3927	0.0000	0.1776
	H	2.9581	0.8921	-0.1171
	H	2.9581	-0.8921	-0.1171
	H	2.2985	0.0000	1.2708
	ABC	2.4202	2.2399	1.2493

CBS-Q (0 K)= -383.253897 a.u.

8c) Pyran-4-one				
		X	Y	Z
	H	2.0177	-1.7292	0.0000
	C	1.1572	-1.0639	0.0000
	H	2.1896	0.7815	0.0000
	C	1.2188	0.2902	0.0000
	C	0.0000	1.1103	0.0000
	C	-1.2188	0.2902	0.0000
	H	-2.1896	0.7815	0.0000
	C	-1.1572	-1.0639	0.0000
	O	0.0000	-1.7756	0.0000
	O	0.0000	2.3404	0.0000
	H	-2.0177	-1.7292	0.0000
	ABC	5.8999	2.6704	1.8384

CBS-Q (0 K)= -342.828903 a.u.
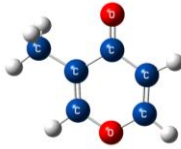
9c) 3-Methyl-pyran-4-one				
		X	Y	Z
	C	-1.3691	-0.4526	0.0000
	O	-2.4083	-1.1125	0.0000
	C	-0.0271	-1.0446	0.0000
	H	0.0595	-2.1295	0.0000
	C	-1.3327	1.0155	0.0000
	H	-2.2668	1.5731	0.0000
	C	1.1011	-0.2862	0.0000
	C	-0.1536	1.6814	0.0000
	O	1.0650	1.0802	0.0000
	C	2.5114	-0.7853	0.0000
	H	2.5282	-1.8799	0.0000
	H	3.0459	-0.4198	0.8862
	H	3.0459	-0.4197	-0.8862
	H	-0.0463	2.7641	0.0000
	ABC	3.9442	1.8205	1.2554

CBS-Q (0 K)= -382.070272 a.u.
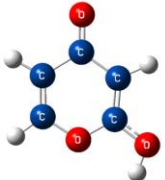
10) 2-Methyl-pyran-4-one				
		X	Y	Z
	C	-0.4537	0.9107	0.0000
	O	-1.3791	1.7256	0.0000
	C	0.9635	1.2790	0.0000
	H	1.2392	2.3315	0.0000
	C	-0.6773	-0.5450	0.0000
	C	1.9339	0.3317	0.0000
	C	0.3863	-1.3909	0.0000
	O	1.6898	-1.0008	0.0000
	H	3.0035	0.5300	0.0000
	C	-2.0937	-1.0407	0.0000
	H	-2.6258	-0.6581	0.8799
	H	-2.1427	-2.1363	0.0000
	H	-2.6258	-0.6581	-0.8799
	H	0.3123	-2.4771	0.0000
	ABC	3.3388	2.2255	1.3465

CBS-Q (0 K)= -382.063729 a.u.
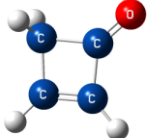
11c) 2-Hydroxy-pyran-4-one				
		X	Y	Z
	C	1.3530	-0.3941	0.0000
	O	2.4431	-0.9644	0.0000
	C	1.2207	1.0776	0.0000
	H	2.1207	1.6884	0.0000
	C	0.0656	-1.0801	0.0000
	H	0.0217	-2.1655	0.0000
	H	-0.1800	2.7435	0.0000
	C	0.0102	1.6736	0.0000
	C	-1.0951	-0.3750	0.0000
	O	-1.1729	0.9787	0.0000
	O	-2.3092	-0.9440	0.0000
	H	-2.9770	-0.2410	0.0000
	ABC	4.0541	1.8674	1.2785

CBS-Q (0 K)= -417.986776 a.u.
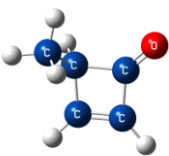
12c) Cyclobut-2-enone				
		X	Y	Z
	C	0.4829	1.0849	0.0000
	H	0.4951	1.7197	0.8966
	H	0.4951	1.7197	-0.8966
	C	-0.6166	-0.0373	0.0000
	C	1.4285	-0.1125	0.0000
	H	2.5158	-0.1643	0.0000
	C	0.4688	-1.0767	0.0000
	H	0.4860	-2.1650	0.0000
	O	-1.8217	-0.0326	0.0000
	ABC	12.4684	5.2608	3.7897

CBS-Q (0 K)= -229.612135 a.u.

Table S1. Cyclic structures, geometries and rotational constants in GHz at the MP2/6-31G(d') level and CBS-Q energies (continuation).
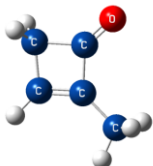
13c) 4-methyl-cyclobut-2-enone			
	X	Y	Z
C	1.0634	1.0755	-0.2666
C	-0.1976	1.4367	0.0968
C	-0.6792	0.0425	0.4972
H	-0.8552	-0.0801	1.5774
C	0.7764	-0.3603	0.0685
O	1.3679	-1.4103	0.0091
H	1.9272	1.6167	-0.6490
C	-1.8035	-0.5913	-0.3168
H	-2.7728	-0.1293	-0.0884
H	-1.8752	-1.6630	-0.0923
H	-1.6134	-0.4788	-1.3920
H	-0.7115	2.3973	0.0964
ABC	5.2284	4.0278	2.5027

CBS-Q (0 K)= -268.844454 a.u.

14c) 2-methyl-cyclobut-2-enone			
	X	Y	Z
C	0.6685	-0.1959	0.0000
C	0.0369	-1.4046	0.0000
C	-1.3927	-0.8705	0.0000
H	-1.9951	-1.0746	-0.8962
C	-0.6578	0.5140	0.0000
O	-1.0215	1.6653	0.0000
H	0.4192	-2.4251	0.0000
H	-1.9951	-1.0747	0.8963
C	2.0799	0.2870	0.0000
H	2.2728	0.9107	-0.8828
H	2.2728	0.9104	0.8831
H	2.7892	-0.5491	-0.0002
ABC	5.3661	3.8063	2.2912

CBS-Q (0 K)= -268.856328 a.u.
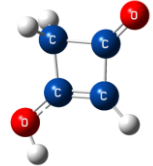
15c) 4,4-dimethyl-cyclobut-2-enone			
	X	Y	Z
C	-1.3986	1.0379	0.0000
C	-0.1098	1.4765	0.0000
C	0.5546	0.0967	0.0000
C	-0.9387	-0.3916	0.0000
O	-1.4552	-1.4830	0.0000
C	1.3251	-0.2708	1.2669
H	2.2887	0.2564	1.3068
H	1.5276	-1.3501	1.2851
H	0.7534	-0.0135	2.1681
H	0.3238	2.4768	0.0000
C	1.3251	-0.2708	-1.2669
H	2.2887	0.2564	-1.3068
H	1.5276	-1.3501	-1.2851
H	0.7534	-0.0135	-2.1681
H	-2.3681	1.5339	0.0000
ABC	3.5002	2.6460	2.2377

CBS-Q (0 K)= -308.086838 a.u.
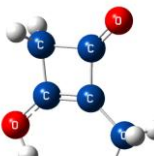
16c) 3-Hydroxy-cyclobut-2-enone			
	X	Y	Z
C	-0.0695	1.1160	0.0000
H	-0.0683	1.7461	0.8992
H	-0.0683	1.7461	-0.8992
C	0.9022	-0.0425	0.0000
C	-0.0167	-1.0580	0.0000
H	0.0353	-2.1445	0.0000
C	-1.1143	-0.0594	0.0000
O	-2.3225	-0.0892	0.0000
O	2.2315	0.0576	0.0000
H	2.6188	-0.8318	0.0000
ABC	12.1229	2.5374	2.1270

CBS-Q (0 K)= -304.771267 a.u.
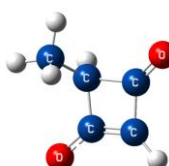
17c) 3-Hydroxy-2-methyl-cyclobut-2-enone			
	X	Y	Z
C	0.0116	0.6359	0.0000
C	-0.8891	-0.3993	0.0000
C	0.0979	-1.5433	0.0000
H	0.1087	-2.1747	0.8988
H	0.1086	-2.1747	-0.8987
C	1.1204	-0.3499	0.0000
O	-2.2216	-0.5120	0.0000
H	-2.6136	0.3758	-0.0002
O	2.3298	-0.2919	0.0000
C	-0.0534	2.1282	0.0000
H	0.4484	2.5418	0.8845
H	-1.0904	2.4920	0.0000
H	0.4484	2.5418	-0.8845
ABC	3.9267	2.4998	1.5576

CBS-Q (0 K)= -344.018045 a.u.

18c) 3-Hydroxy-4-methyl- cyclobut-2-enone			
	X	Y	Z
C	0.0525	-1.3796	-0.2860
C	0.9321	-0.3906	0.0671
C	-0.0818	0.6532	0.4840
H	-0.0857	0.8602	1.5652
C	-1.0792	-0.4874	0.0689
O	2.2565	-0.2310	0.0812
H	2.6811	-1.0380	-0.2499
O	-2.2874	-0.5484	0.0384
H	0.1461	-2.3925	-0.6722
C	-0.1516	1.9396	-0.3313
H	0.7028	2.5942	-0.1174
H	-1.0730	2.4850	-0.0921
H	-0.1562	1.7158	-1.4060
ABC	4.3196	2.4139	1.6533

CBS-Q (0 K)= -344.014813 a.u.

Table S1. Cyclic structures, geometries and rotational constants in GHz at the MP2/6-31G(d') level and CBS-Q energies (continuation).
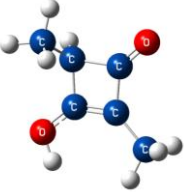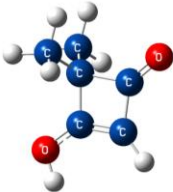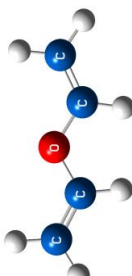
19c) 3-Hydroxy-2,4-dimethyl-cyclobut-2-enone					20c) 3-Hydroxy-4,4-dimethyl-cyclobut-2-enone				
		X	Y	Z			X	Y	Z
	C	-0.9954	-0.1068	0.0154		C	-0.1329	-1.6129	0.0000
	C	-0.0888	0.9037	-0.1879		C	-0.9679	-0.5268	0.0000
	C	1.1357	0.0513	-0.4354		C	0.0922	0.5567	0.0000
	H	1.5071	0.0921	-1.4715		C	1.0371	-0.6992	0.0000
	C	0.0909	-1.0955	-0.1953		O	-2.2851	-0.3129	0.0000
	O	-0.1207	2.2414	-0.1817		H	-2.7502	-1.1645	0.0000
	H	-1.0227	2.5370	0.0212		O	2.2426	-0.8122	0.0000
	O	0.1837	-2.3039	-0.1667		H	-0.2726	-2.6922	0.0000
	C	2.2807	0.1415	0.5678		C	0.1690	1.4027	-1.2686
	H	2.8381	1.0801	0.4540		H	-0.6546	2.1288	-1.3059
	H	2.9771	-0.6933	0.4192		H	1.1170	1.9562	-1.2897
	H	1.8981	0.0888	1.5954		H	0.1191	0.7743	-2.1675
	C	-2.4533	-0.2078	0.3259		C	0.1690	1.4027	1.2686
	H	-2.9145	0.7817	0.4512		H	1.1170	1.9562	1.2897
	H	-2.6165	-0.7751	1.2513		H	-0.6546	2.1288	1.3059
	H	-2.9903	-0.7299	-0.4768		H	0.1191	0.7743	2.1675
	ABC	2.3332	2.2177	1.2274		ABC	2.7415	1.9779	1.5311
CBS-Q (0 K)= -383.254740 a.u.					CBS-Q (0 K)= -383.253929 a.u.				

Table S2. Acyclic structures, XYZ coordinates and rotational constants (GHz) at the MP2/6-31G(d') level and CBS-Q energies.

(1) Ethene-1,1-diol

	X	Y	Z
H	0.3735	2.1478	0.0000
C	-0.3799	1.3702	0.0000
H	-1.4288	1.6461	0.0000
C	0.0000	0.0817	0.0000
O	1.2931	-0.3075	0.0000
H	1.3018	-1.2751	0.0000
O	-0.8215	-1.0079	0.0000
H	-1.7397	-0.7065	0.0000
ABC	11.0428	10.0550	5.2629

CBS-Q (0 K)= -228.719825 a.u.

(2) 1-Methoxy-ethenol

	X	Y	Z
H	1.6610	1.7888	0.0000
C	1.3242	0.7590	0.0000
H	2.0573	-0.0357	0.0000
C	0.0000	0.5225	0.0000
O	-0.9126	1.5241	0.0000
H	-1.7870	1.1093	0.0000
O	-0.6350	-0.6795	0.0000
C	0.2119	-1.8242	0.0000
H	0.8445	-1.8369	0.8972
H	0.8445	-1.8369	-0.8972
H	-0.4558	-2.6893	0.0000
ABC	9.4460	4.3594	3.0410

CBS-Q (0 K)= -267.931876 a.u.

(3) 1-Vinyloxy-ethenol

	X	Y	Z
C	-1.3400	0.1262	0.3494
H	-1.1324	0.8364	1.1503
H	-2.6927	-0.8136	-0.9796
C	-2.5503	-0.1011	-0.1720
H	-3.4126	0.4257	0.2246
O	-0.2415	-0.6018	-0.0643
C	0.9607	0.0580	-0.0495
H	2.1484	1.7814	-0.0716
C	1.1410	1.3865	-0.1289
H	0.3100	2.0553	-0.3148
O	1.9801	-0.8262	0.0279
H	1.6024	-1.6787	0.2887
ABC	8.9352	2.2747	1.8758

CBS-Q (0 K)= -305.950930 a.u.

(4) 1-Methoxy-1-vinyloxy-ethene

	X	Y	Z
H	2.5666	-0.7142	1.0202
C	2.2693	-1.0464	0.0166
H	2.8859	-0.5383	-0.7366
H	2.3891	-2.1286	-0.0745
O	0.8858	-0.7904	-0.2101
C	0.5081	0.5021	-0.0697
H	0.7999	2.5396	0.2888
C	1.2814	1.5753	0.1780
H	2.3606	1.5166	0.2330
O	-0.8331	0.6498	-0.2683
C	-1.6533	-0.3059	0.2969
H	-1.1790	-0.9659	1.0199
H	-3.5925	-1.0892	0.4587
C	-2.9511	-0.3600	-0.0251
H	-3.3786	0.3145	-0.7617
ABC	5.6975	1.6550	1.3292

CBS-Q (0 K)= -345.160085 a.u.

(5) 1-(1-Hydroxy-vinyloxy)-ethenol

	X	Y	Z
C	0.0000	1.1485	0.1229
H	0.9132	2.9947	-0.3053
C	0.9680	2.0674	0.2535
H	1.7648	1.9044	0.9694
O	0.0000	0.0000	0.9000
C	0.0000	-1.1485	0.1229
H	-1.7648	-1.9044	0.9694
C	-0.9680	-2.0674	0.2535
H	-0.9132	-2.9947	-0.3053
O	-1.0332	1.2522	-0.7392
H	-1.6185	0.4882	-0.6093
O	1.0332	-1.2522	-0.7392
H	1.6185	-0.4882	-0.6093
ABC	4.9093	2.0415	1.8040

CBS-Q (0 K)= -381.102938 a.u.

(6) 1-(1-Methoxy-vinyloxy)-ethenol

	X	Y	Z
C	-0.7160	0.4807	-0.2698
H	-2.4396	1.5640	0.3684
C	-1.3871	1.5805	0.1135
H	-0.8544	2.5240	0.1409
O	0.5878	0.5618	-0.6965
C	1.5237	-0.0269	0.1373
H	0.5929	0.3055	1.9998
C	1.4338	-0.1256	1.4704
H	2.2262	-0.6244	2.0154
O	-1.1509	-0.7910	-0.3736
O	2.5908	-0.4363	-0.5815
H	2.3089	-0.4867	-1.5064
C	-2.4661	-1.0208	0.1246
H	-3.2106	-0.4742	-0.4701
H	-2.5391	-0.7162	1.1774
H	-2.6347	-2.0962	0.0314
ABC	3.7944	1.3138	1.2382

CBS-Q (0 K)= -420.314464 a.u.

Table S2. Acyclic structures, XYZ coordinates and rotational constants (GHz) at the MP2/6-31G(d') level and CBS-Q energies (continuation).

(7) Vinyloxy-ethene			
	X	Y	Z
H	0.0000	2.4440	1.3149
C	0.0000	2.3606	0.2318
H	0.0000	3.2644	-0.3682
C	0.0000	1.1665	-0.3745
H	0.0000	1.0510	-1.4605
O	0.0000	0.0000	0.3425
C	0.0000	-1.1665	-0.3745
H	0.0000	-1.0510	-1.4605
H	0.0000	-3.2644	-0.3682
C	0.0000	-2.3606	0.2318
H	0.0000	-2.4440	1.3149
ABC	34.6740	2.5002	2.3320

CBS-Q (0 K)= -230.795502 a.u.
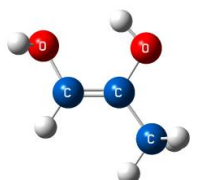
(8) Methoxy-ethene			
	X	Y	Z
H	0.1541	-1.5629	0.8961
C	-0.4532	-1.3706	0.0000
H	0.1541	-1.5629	-0.8961
H	-1.3307	-2.0224	0.0000
O	-0.9517	-0.0401	0.0000
C	0.0000	0.9275	0.0000
H	-0.4748	1.9080	0.0000
H	1.9518	1.6808	0.0000
C	1.3385	0.7852	0.0000
ABC	18.0413	6.4174	4.8816

CBS-Q (0 K)= -192.775508 a.u.
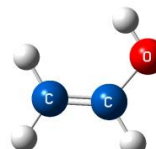
(9) Propene-1,2-diol			
	X	Y	Z
C	-0.6905	-0.7392	0.0030
H	-0.6904	-1.8267	-0.0347
C	0.4331	0.0031	0.0108
C	1.8220	-0.5446	-0.0001
H	2.3549	-0.2167	-0.9019
H	1.8127	-1.6398	0.0263
H	2.3819	-0.1722	0.8673
O	0.3885	1.3674	0.0145
H	-0.5550	1.6009	-0.0148
O	-1.9124	-0.0741	-0.0923
H	-2.5002	-0.4078	0.5973
ABC	9.9293	3.8146	2.8192

CBS-Q (0 K)= -267.942663 a.u.
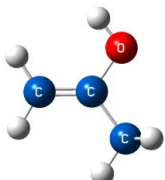
(10) Ethenol			
	X	Y	Z
C	1.2198	-0.1194	0.0000
H	2.1036	0.5096	0.0000
H	1.3635	-1.1990	0.0000
C	0.0000	0.4421	0.0000
H	-0.1526	1.5199	0.0000
O	-1.1998	-0.2015	0.0000
H	-1.0346	-1.1554	0.0000
ABC	60.2675	10.4496	8.9055

CBS-Q (0 K)= -153.563925 a.u.
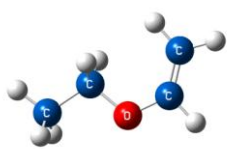
(11) Propen-2-ol			
	X	Y	Z
H	-0.2580	2.2156	0.0000
C	0.4316	1.3722	0.0000
H	1.4936	1.5929	0.0000
C	0.0000	0.0972	0.0000
O	-1.3184	-0.2720	0.0000
H	-1.8595	0.5307	0.0000
C	0.8821	-1.1145	0.0000
H	0.6749	-1.7304	0.8842
H	1.9391	-0.8311	0.0000
H	0.6749	-1.7304	-0.8842
ABC	10.0358	9.0455	4.9030

CBS-Q (0 K)=   -192.798875 a.u.
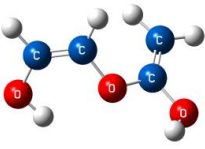
(12) Ethoxy-ethene			
	X	Y	Z
C	-2.2353	-0.0578	0.0000
H	-2.4647	0.5395	0.8891
H	-2.8770	-0.9473	0.0000
H	-2.4647	0.5395	-0.8891
C	-0.7727	-0.4647	0.0000
H	-0.5218	-1.0624	0.8907
H	-0.5218	-1.0624	-0.8907
O	0.0000	0.7346	0.0000
C	1.3461	0.5614	0.0000
H	1.8410	1.5323	0.0000
H	3.1280	-0.5352	0.0000
C	2.0438	-0.5900	0.0000
H	1.5890	-1.5749	0.0000
ABC	16.1751	2.8222	2.4782

CBS-Q (0 K)= -232.006345 a.u.

Table S2. Acyclic structures, XYZ coordinates and rotational constants (GHz) at the MP2/6-31G(d') level and CBS-Q energies (continuation).
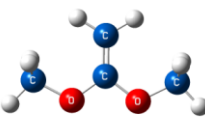
(13) 1-(2-Hydroxy-vinyloxy)-ethenol

	X	Y	Z
H	0.7627	1.9722	-0.6671
C	1.5708	1.2659	-0.5259
H	2.5819	1.5321	-0.8103
C	1.3360	0.0293	-0.0611
O	0.1296	-0.4624	0.3821
O	2.2816	-0.9347	0.0116
H	1.9511	-1.6177	0.6133
C	-0.8273	0.4971	0.7128
H	-0.5256	1.2695	1.4147
C	-2.0649	0.3616	0.2087
O	-2.4504	-0.5989	-0.6674
H	-1.6687	-1.1418	-0.8575
H	-2.8745	1.0296	0.4886
ABC	6.0409	1.5020	1.3575

CBS-Q (0 K)= -381.096715 a.u.
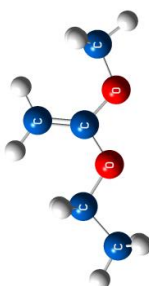
(14) 1,1-Dimethoxy-ethene

	X	Y	Z
H	-0.8970	2.4643	0.5246
C	0.0000	2.3412	-0.0976
H	0.8970	2.4643	0.5246
H	0.0000	3.0845	-0.8988
O	0.0000	1.0781	-0.7492
C	0.0000	0.0000	0.0654
H	0.0000	-0.9240	1.9800
C	0.0000	0.0000	1.4176
H	0.0000	0.9240	1.9800
O	0.0000	-1.0781	-0.7492
C	0.0000	-2.3412	-0.0976
H	-0.8970	-2.4643	0.5246
H	0.8970	-2.4643	0.5246
H	0.0000	-3.0845	-0.8988
ABC	9.0192	2.3251	1.8935

CBS-Q (0 K)= -307.140582 a.u.
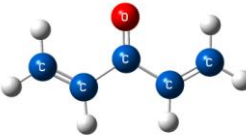
(15) 1-Ethoxy-1-methoxy-ethene

	X	Y	Z
H	2.1245	0.6189	0.0000
C	1.2029	1.1854	0.0000
H	1.2817	2.2643	0.0000
C	0.0000	0.5677	0.0000
O	-0.2339	-0.7631	0.0000
O	-1.2171	1.1569	0.0000
C	0.9189	-1.6054	0.0000
H	1.5290	-1.3942	0.8915
H	1.5290	-1.3942	-0.8915
C	-1.2121	2.5782	0.0000
H	-0.7142	2.9713	0.8969
H	-2.2639	2.8752	0.0000
H	-0.7142	2.9713	-0.8969
C	0.4169	-3.0380	0.0000
H	1.2639	-3.7349	0.0000
H	-0.1939	-3.2279	-0.8891
H	-0.1939	-3.2279	0.8891
ABC	7.4236	1.3458	1.1645

CBS-Q (0 K)= -346.371718 a.u.
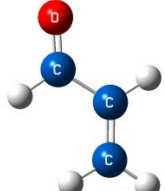
(16) Penta-1,4-dien-3-one

	X	Y	Z
C	0.0000	0.0000	0.1137
C	0.0000	1.2715	-0.6749
H	0.0000	1.2050	-1.7634
H	0.0000	2.5064	1.0354
C	0.0000	2.4648	-0.0528
H	0.0000	3.4025	-0.6048
C	0.0000	-1.2715	-0.6749
H	0.0000	-1.2050	-1.7634
H	0.0000	-2.5064	1.0354
C	0.0000	-2.4648	-0.0528
H	0.0000	-3.4025	-0.6048
O	0.0000	0.0000	1.3396
ABC	10.3270	2.2609	1.8548

CBS-Q (0 K)= -268.849370 a.u.
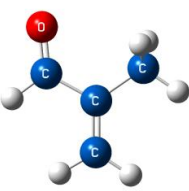
(17) Propenal (Acrolein)

	X	Y	Z
H	2.1230	0.6660	0.0000
C	1.2246	1.2843	0.0000
H	1.3696	2.3627	0.0000
C	0.0000	0.7241	0.0000
H	-0.9144	1.3170	0.0000
C	-0.1532	-0.7473	0.0000
H	0.8071	-1.3147	0.0000
O	-1.2267	-1.3247	0.0000
ABC	47.3813	4.6082	4.1997

CBS-Q (0 K)= -191.597998 a.u.

(18) 2-Methyl-propenal

	X	Y	Z
H	-1.7872	1.6449	0.0000
C	-0.6964	1.6478	0.0000
H	-0.2061	2.6205	0.0000
C	0.0000	0.4920	0.0000
C	-0.7671	-0.7789	0.0000
H	-1.8763	-0.6637	0.0000
O	-0.2491	-1.8832	0.0000
C	1.4985	0.3811	0.0000
H	1.8402	-0.1790	0.8797
H	1.9722	1.3693	0.0000
H	1.8402	-0.1790	-0.8797
ABC	8.5810	4.3742	2.9500

CBS-Q (0 K)= -230.831099 a.u.

Table S2. Acyclic structures, XYZ coordinates and rotational constants (GHz) at the MP2/6-31G(d') level and CBS-Q energies (continuation).
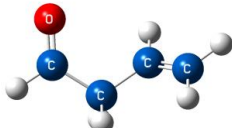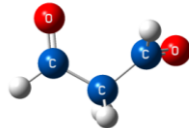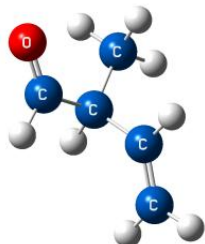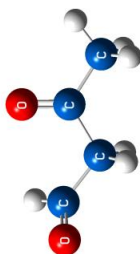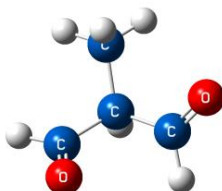
(19) But-3-enal

	X	Y	Z
H	2.8388	-0.9663	0.8823
C	2.3915	-0.4875	0.0000
H	2.6712	0.5722	0.0000
H	2.8388	-0.9663	-0.8823
C	0.9024	-0.6620	0.0000
H	0.5281	-1.6911	0.0000
H	0.2988	1.3906	0.0000
C	0.0000	0.3412	0.0000
C	-1.4463	0.0524	0.0000
H	-1.7038	-1.0338	0.0000
O	-2.3197	0.9038	0.0000
ABC	32.6089	2.1617	2.0531

CBS-Q (0 K)= -230.831078 a.u.

(20) Malonaldehyde

	X	Y	Z
H	0.0464	1.6513	0.8785
C	0.0075	0.9114	0.0612
H	-0.2725	1.4523	-0.8542
C	-1.0372	-0.1467	0.3651
H	-0.8477	-0.7521	1.2761
C	1.3886	0.3038	-0.1016
H	2.2118	1.0303	-0.2818
O	1.6105	-0.8907	-0.0499
O	-2.0219	-0.3334	-0.3209
ABC	13.0375	3.2535	2.7944

CBS-Q (0 K)= -266.751882 a.u.

(21) 2-Methyl-but-3-enal

	X	Y	Z
H	2.5878	-0.4785	-1.1310
C	2.4226	-0.3997	-0.0566
H	3.2692	-0.6230	0.5903
C	1.2316	-0.0316	0.4464
H	1.1015	0.0412	1.5298
C	0.0081	0.2723	-0.3846
H	0.3100	0.2765	-1.4463
C	-0.6469	1.6009	-0.0044
H	-1.5462	1.7792	-0.6054
H	0.0529	2.4307	-0.1575
H	-0.9523	1.5900	1.0485
C	-0.9592	-0.8940	-0.2183
H	-0.5538	-1.8788	-0.5486
O	-2.0758	-0.8032	0.2531
ABC	6.1081	2.4082	1.9055

CBS-Q (0 K)= -270.050468 a.u.

(22) 2,2-Dimethyl-but-3-enal

	X	Y	Z
H	-2.6550	-0.1428	-0.7952
C	-2.3234	-0.6988	0.0790
H	-3.0550	-1.3555	0.5467
C	-1.0820	-0.5836	0.5842
H	-0.8163	-1.1737	1.4664
C	0.0397	0.2747	0.0362
C	-0.4276	1.2205	-1.0778
H	0.4091	1.8414	-1.4237
H	-1.2186	1.8842	-0.7060
H	-0.8218	0.6701	-1.9424
C	0.7125	1.0479	1.1742
H	1.5758	1.6122	0.7999
H	1.0764	0.3643	1.9503
H	0.0010	1.7494	1.6279
C	1.0287	-0.7131	-0.5821
H	0.6290	-1.2524	-1.4744
O	2.1485	-0.9353	-0.1664
ABC	3.6730	1.9803	1.8239

CBS-Q (0 K)= -309.281222 a.u.

(23) 3-Oxo-butyraldehyde

	X	Y	Z
C	-0.9239	0.1690	0.0009
O	-0.7849	1.3802	-0.0456
C	-2.2772	-0.5036	-0.1105
H	-3.0524	0.2535	-0.2619
H	-2.4928	-1.0763	0.8015
H	-2.2823	-1.2132	-0.9485
C	0.2804	-0.7570	0.1684
H	0.3786	-1.4154	-0.7062
H	0.1193	-1.4029	1.0473
C	1.5627	0.0347	0.3408
H	1.5763	0.7324	1.2041
O	2.5225	-0.0723	-0.3961
ABC	8.8950	2.0479	1.7703

CBS-Q (0 K)= -305.991492 a.u.

(24) 2-Methyl-malonaldehyde

	X	Y	Z
C	0.0020	0.4346	0.5254
H	0.0176	0.6839	1.6026
C	-0.5779	1.6135	-0.2654
H	0.0316	2.5154	-0.1297
H	-1.5981	1.8295	0.0682
H	-0.6201	1.3721	-1.3332
C	1.4428	0.1797	0.1141
H	2.1391	1.0317	0.2911
C	-0.8128	-0.8381	0.3548
H	-0.4317	-1.7253	0.9037
O	-1.8191	-0.9051	-0.3230
O	1.8362	-0.8506	-0.3989
ABC	5.1501	3.0298	2.1558

CBS-Q (0 K)= -305.981272 a.u.

Table S2. Acyclic structures, XYZ coordinates and rotational constants (GHz) at the MP2/6-31G(d') level and CBS-Q energies (continuation).

(25) 2,2-Dimethyl-malonaldehyde

	X	Y	Z
C	0.0000	0.0000	0.2895
C	0.0000	1.2791	1.1306
H	0.9078	1.3269	1.7439
H	-0.8728	1.3037	1.7955
H	-0.0130	2.1716	0.4939
C	0.0000	-1.2791	1.1306
H	-0.9078	-1.3269	1.7439
H	0.8728	-1.3037	1.7955
H	0.0130	-2.1716	0.4939
C	1.2140	-0.0152	-0.6406
H	1.3897	-0.9893	-1.1536
C	-1.2140	0.0152	-0.6406
H	-1.3897	0.9893	-1.1536
O	1.9437	0.9364	-0.8361
O	-1.9437	-0.9364	-0.8361
ABC	3.7009	2.0288	1.8629

CBS-Q (0 K)= -345.213486 a.u.

(26) But-3-en-2-one

	X	Y	Z
H	-0.5855	-2.1528	0.0000
C	0.4712	-1.8910	0.0000
H	1.1788	-2.7186	0.0000
C	0.8941	-0.6122	0.0000
H	1.9586	-0.3738	0.0000
C	0.0000	0.5807	0.0000
C	-1.5042	0.3675	0.0000
H	-1.9943	1.3456	0.0000
H	-1.8183	-0.1987	0.8864
H	-1.8183	-0.1987	-0.8864
O	0.4891	1.7033	0.0000
ABC	8.8859	4.2445	2.9251

CBS-Q (0 K)= -230.833595 a.u.

(27) 2-Methyl-3-oxo-pent-4-enal

	X	Y	Z
H	-3.1731	-0.5538	-0.3702
C	-2.8267	0.3887	0.0517
H	-3.5649	1.1602	0.2612
C	-1.5167	0.5739	0.2997
H	-1.1376	1.5056	0.7180
C	-0.5347	-0.5123	0.0084
O	-0.8449	-1.5644	-0.5295
C	0.9187	-0.2302	0.4280
H	0.8955	0.1320	1.4675
C	1.4153	0.9347	-0.4189
H	1.9101	0.6398	-1.3732
O	1.2800	2.1059	-0.1205
C	1.8004	-1.4658	0.2679
H	1.8194	-1.7928	-0.7780
H	1.4058	-2.2975	0.8613
H	2.8274	-1.2590	0.5932
ABC	2.7111	1.6921	1.1228

CBS-Q (0 K)= -383.239172 a.u.

(28) Hexa-1,5-dien-3-one

	X	Y	Z
H	3.0160	1.0415	-0.3168
C	2.9865	-0.0426	-0.2171
H	3.9226	-0.5926	-0.2909
C	1.8097	-0.6608	-0.0098
H	1.7513	-1.7453	0.0921
C	0.5393	0.1280	0.0837
O	0.5243	1.3465	-0.0076
C	-0.7289	-0.6869	0.3185
H	-0.6017	-1.2062	1.2854
H	-0.7860	-1.4834	-0.4402
C	-1.9751	0.1496	0.3169
H	-1.9760	1.0182	0.9761
H	-3.9365	0.5167	-0.4117
C	-3.0497	-0.1133	-0.4438
H	-3.0749	-0.9648	-1.1237
ABC	8.3170	1.3069	1.1816

CBS-Q (0 K)= -308.074808 a.u.

(29) 2-Methyl-penta-1,4-dien-3-one

	X	Y	Z
H	-0.5114	2.3128	-0.3028
C	-1.3164	1.5942	-0.1689
H	-2.3305	1.9909	-0.2100
C	-1.0952	0.2736	0.0074
C	0.2866	-0.3050	0.0039
C	-2.2092	-0.7322	0.1349
H	-2.1615	-1.4579	-0.6856
H	-3.1880	-0.2395	0.1231
H	-2.1098	-1.3052	1.0655
O	0.4344	-1.5150	-0.1500
C	1.4673	0.5969	0.1928
H	1.3101	1.6207	0.5256
H	2.8584	-0.9008	-0.3389
C	2.7114	0.1299	-0.0199
H	3.5906	0.7553	0.1220
ABC	5.0089	1.9181	1.4145

CBS-Q (0 K)= -308.081770 a.u.

(30) 3-Oxo-hex-5-enal
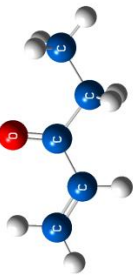
	X	Y	Z
H	3.4885	-1.0259	1.1943
C	3.4887	-0.0915	0.6332
H	4.3428	0.5675	0.7754
C	2.4833	0.2347	-0.1947
H	2.5058	1.1826	-0.7325
C	1.2848	-0.6393	-0.4309
H	1.2690	-1.0127	-1.4706
H	1.3134	-1.5358	0.2070
C	-0.0358	0.0913	-0.2140
C	-1.2882	-0.7813	-0.1667
H	-1.2824	-1.3941	0.7461
H	-1.2890	-1.4718	-1.0260
C	-2.5449	0.0687	-0.1833
H	-2.6462	0.7448	-1.0586
O	-0.1069	1.3030	-0.0935
O	-3.3968	0.0283	0.6814
ABC	6.7490	0.8466	0.8095

CBS-Q (0 K)= -383.232701 a.u.

Table S2. Acyclic structures, XYZ coordinates and rotational constants (GHz) at the MP2/6-31G(d') level and CBS-Q energies (continuation).

(31) Pent-1-en-3-one

	X	Y	Z
C	1.7834	-1.6746	0.0000
H	1.9520	-2.7581	0.0000
H	2.2703	-1.2457	0.8825
H	2.2703	-1.2457	-0.8825
C	0.2905	-1.3585	0.0000
H	-0.2127	-1.7995	0.8759
H	-0.2127	-1.7995	-0.8759
C	0.0000	0.1341	0.0000
C	-1.4477	0.5223	0.0000
H	-2.1938	-0.2738	0.0000
H	-1.0456	2.5921	0.0000
C	-1.8114	1.8175	0.0000
H	-2.8553	2.1250	0.0000
O	0.8924	0.9701	0.0000
ABC	9.5526	2.0993	1.7584

CBS-Q (0 K)= -270.061059 a.u.

(32) 2,4-Dimethyl-penta-1,4-dien-3-one

	X	Y	Z
H	1.1933	-0.3256	-1.9264
C	0.9349	-1.2556	-1.4257
H	1.2351	-2.1834	-1.9127
C	0.3018	-1.2711	-0.2326
C	0.0000	0.0000	0.5039
C	-0.3018	1.2711	-0.2326
H	-1.1933	0.3256	-1.9264
C	-0.9349	1.2556	-1.4257
H	-1.2351	2.1834	-1.9127
C	0.0000	2.5379	0.5250
H	-0.2937	3.4225	-0.0516
H	1.0708	2.6070	0.7581
H	-0.5321	2.5374	1.4836
C	0.0000	-2.5379	0.5250
H	0.5321	-2.5374	1.4836
H	0.2937	-3.4225	-0.0516
H	-1.0708	-2.6070	0.7581
O	0.0000	0.0000	1.7343
ABC	3.2921	1.5624	1.1853

CBS-Q (0 K)= -347.313018 a.u.
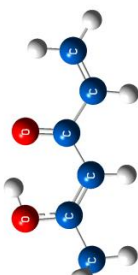
(33) 2-Methyl-hexa-1,5-dien-3-one

	X	Y	Z
H	4.2577	-0.4066	0.3969
C	3.3268	0.1527	0.4668
H	3.2836	0.9460	1.2129
H	2.3511	-0.9355	-1.0535
C	2.2804	-0.1256	-0.3271
C	0.9784	0.6225	-0.2812
H	0.8240	1.1889	-1.2150
H	0.9904	1.3653	0.5296
C	-0.2175	-0.3138	-0.0995
C	-1.5931	0.2672	0.0348
H	-1.0068	2.3186	-0.1547
C	-1.8105	1.5988	-0.0167
H	-2.8165	2.0068	0.0771
C	-2.6988	-0.7387	0.2222
H	-3.6705	-0.2406	0.3161
H	-2.5203	-1.3458	1.1182
H	-2.7343	-1.4352	-0.6243
O	-0.0691	-1.5300	-0.0749
ABC	4.4973	1.1245	0.9397

CBS-Q (0 K)= -347.307911 a.u.
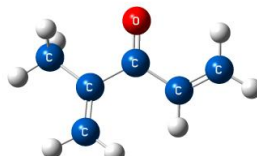
(34) 5-Hydroxy-hexa-1,4-dien-3-one

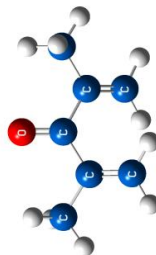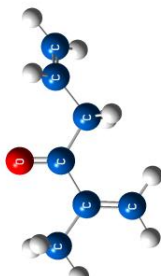|	X	Y	X
C	-1.3732	0.8423	0.0000
C	0.0000	0.8337	0.0000
H	0.5321	1.7807	0.0000
C	0.7432	-0.4147	0.0000
C	2.2322	-0.3239	0.0000
H	2.6819	0.6695	0.0000
H	2.5223	-2.4141	0.0000
C	2.9941	-1.4328	0.0000
H	4.0811	-1.3827	0.0000
C	-2.2029	2.0884	0.0000
H	-1.5776	2.9864	0.0000
H	-2.8535	2.0976	0.8837
H	-2.8535	2.0976	-0.8837
O	-2.1092	-0.2673	0.0000
H	-1.4691	-1.0260	0.0000
O	0.1812	-1.5286	0.0000
ABC	5.7698	1.0993	0.9287

CBS-Q (0 K)= -383.259669 a.u.
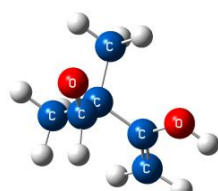
(35) 3-Hydroxy-2-methyl-but-3-enal

	X	Y	Z
H	2.2043	0.1046	-1.8169
C	2.2236	-0.1610	-0.7651
H	3.1735	-0.4913	-0.3459
C	1.1078	-0.0642	-0.0176
O	1.0266	-0.3744	1.3124
H	1.9006	-0.6554	1.6224
C	-0.2392	0.3675	-0.5305
H	-0.1292	0.5677	-1.6094
C	-1.1953	-0.8168	-0.4119
H	-0.7992	-1.7735	-0.8254
O	-2.3060	-0.7559	0.0741
C	-0.7867	1.6026	0.1883
H	-1.7719	1.8686	-0.2103
H	-0.1073	2.4528	0.0565
H	-0.8971	1.4000	1.2580
ABC	4.2441	1.8303	1.7288

CBS-Q (0 K)= -345.205402 a.u.

(36) 3-Hydroxy-2,2-dimethyl-but-3-enal
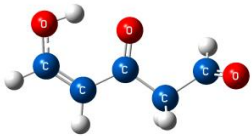
	X	Y	Z
H	2.2875	1.4553	-0.5742
C	2.2714	0.3883	-0.3891
H	3.2143	-0.1494	-0.4879
C	1.1373	-0.2471	-0.0374
O	1.0580	-1.5954	0.1993
H	1.9358	-1.9869	0.0754
C	-0.2304	0.3699	0.1360
C	-1.1559	-0.3483	-0.8485
H	-0.7634	-0.3931	-1.8927
O	-2.2460	-0.8022	-0.5686
C	-0.7335	0.1749	1.5713
H	-1.7557	0.5592	1.6656
H	-0.0837	0.7140	2.2725
H	-0.7417	-0.8862	1.8387
C	-0.2541	1.8570	-0.2520
H	-1.2704	2.2529	-0.1303
H	0.0563	2.0125	-1.2934
H	0.4158	2.4326	0.3989
ABC	2.7285	1.7444	1.4577

CBS-Q (0 K)= -384.440701 a.u.

(37) 5-Hydroxy-3-oxo-pent-4-enal

	X	Y	Z
C	-2.5238	0.4526	-0.0651
H	-3.4279	1.0613	-0.1131
C	-1.2764	1.0098	-0.0085
H	-1.1818	2.0917	-0.0147
C	-0.0936	0.1655	0.0467
C	1.2682	0.8433	0.0736
H	1.2770	1.6160	0.8595
H	1.4573	1.3463	-0.8853
C	2.3773	-0.1606	0.3312
H	2.2745	-0.7496	1.2666
O	3.3270	-0.3170	-0.4095
O	-0.1576	-1.0764	0.0581
O	-2.7926	-0.8460	-0.0681
H	-1.9231	-1.3131	-0.0247
ABC	6.7365	0.9742	0.8728

CBS-Q (0 K)= -419.172286 a.u.
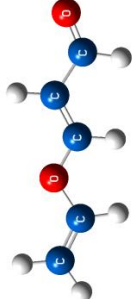
(38) 3,3-Dihydroxy-propenal

	X	Y	Z
C	1.0326	-0.1139	0.0000
H	2.0590	0.2331	0.0000
C	0.0000	0.7985	0.0000
C	0.7026	-1.5073	0.0000
H	1.5472	-2.2210	0.0000
O	-0.4597	-1.9648	0.0000
O	-1.2770	0.4679	0.0000
H	-1.2963	-0.5402	0.0000
O	0.2262	2.1104	0.0000
H	-0.6370	2.5559	0.0000
ABC	8.7861	2.7511	2.0951

CBS-Q (0 K)= -341.926097 a.u.
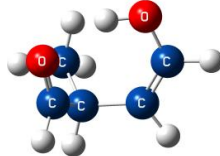
(39) 3-Vinyloxy-propenal

	X	Y	Z
C	-2.3908	0.6457	0.0000
H	-2.1227	1.7300	0.0000
C	-1.2476	-0.2701	0.0000
H	-1.4219	-1.3442	0.0000
H	0.1745	1.3270	0.0000
C	0.0000	0.2463	0.0000
O	1.1019	-0.5339	0.0000
C	2.3241	0.1033	0.0000
H	2.2824	1.1938	0.0000
H	4.4123	-0.0745	0.0000
C	3.4623	-0.5986	0.0000
H	3.4560	-1.6848	0.0000
O	-3.5605	0.2955	0.0000
ABC	26.0349	0.8872	0.8579

CBS-Q (0 K)= -343.980664 a.u.
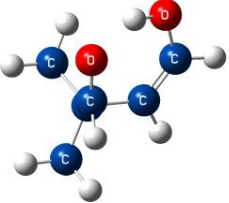
(40) 4-Hydroxy-2-methyl-but-3-enal

	X	Y	Z
H	-1.9607	0.0137	1.4469
C	-1.8858	-0.0448	0.3612
C	-0.7172	0.1027	-0.2926
H	-0.6907	0.0434	-1.3852
C	0.5973	0.3313	0.4114
H	0.3940	0.4300	1.4923
C	1.3418	1.5645	-0.1031
H	2.3040	1.6842	0.4088
H	0.7390	2.4663	0.0546
H	1.5500	1.4658	-1.1750
C	1.4302	-0.9336	0.2469
H	0.9603	-1.8496	0.6762
O	2.5001	-0.9889	-0.3277
O	-3.1099	-0.2680	-0.1864
H	-3.0144	-0.3199	-1.1489
ABC	5.6126	1.2814	1.1237

CBS-Q (0 K)= -345.198529 a.u.
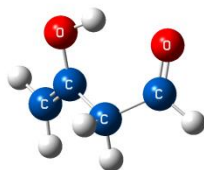
(41) 4-Hydroxy-2,2-dimethyl-but-3-enal

	X	Y	Z
C	-1.5753	-1.0613	-0.3058
C	-0.2328	-1.1671	-0.4571
H	0.1285	-2.0652	-0.9573
C	0.7997	-0.1637	0.0399
C	0.7286	0.0153	1.5653
H	1.4434	0.7785	1.9026
H	0.9736	-0.9360	2.0529
H	-0.2714	0.3135	1.8957
C	0.4612	1.1356	-0.6737
H	0.9900	1.3176	-1.6365
O	-0.3730	1.9380	-0.2790
C	2.2032	-0.6160	-0.3792
H	2.9666	0.0987	-0.0430
H	2.2791	-0.7157	-1.4706
H	2.4313	-1.5925	0.0665
H	-2.2359	-1.8621	-0.6388
O	-2.2883	-0.0536	0.2460
H	-1.7221	0.7316	0.3567
ABC	2.7286	1.7840	1.4518

CBS-Q (0 K)= -384.431396 a.u.

(42) 3-Hydroxy-but-3-enal

	X	Y	Z
H	-2.2787	-1.4913	-0.5377
C	-2.0858	-0.4303	-0.4143
H	-2.8706	0.2788	-0.6626
C	-0.9095	0.0074	0.0668
O	-0.7017	1.3357	0.3122
H	0.2432	1.5137	0.1724
C	0.2116	-0.9272	0.4639
H	-0.0308	-1.9633	0.1970
C	1.5623	-0.5563	-0.1196
H	2.2711	-1.3942	-0.2928
O	1.9084	0.5890	-0.3645
H	0.3406	-0.9026	1.5613
ABC	6.8954	2.6764	2.1194

CBS-Q (0 K)= -305.974130 a.u.

Table S2. Acyclic structures, XYZ coordinates and rotational constants (GHz) at the MP2/6-31G(d') level and CBS-Q energies (continuation).
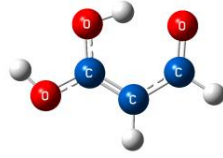
(43) 4-Hydroxy-but-3-enal			
	X	Y	Z
C	1.6025	0.2321	0.0000
C	0.6449	1.1874	0.0000
H	1.0404	2.2029	0.0000
C	-0.8633	1.1404	0.0000
H	-1.2595	1.7035	-0.8661
C	-1.6387	-0.1515	0.0000
H	-2.7402	0.0018	0.0001
O	-1.2067	-1.2929	0.0000
H	-1.2595	1.7035	0.8661
H	2.6462	0.5475	0.0000
O	1.5219	-1.1123	0.0000
H	0.5794	-1.3681	0.0000
ABC	5.3695	3.1967	2.0281

CBS-Q (0 K)= -305.970231 a.u.

(44) 2-Hydroxymethyl-2-methyl-malonaldehyde			
	X	Y	Z
C	-0.3024	0.4251	-0.1110
C	0.9046	0.4710	-1.0602
H	1.5520	1.3175	-0.7740
H	0.5565	0.6498	-2.0868
C	-1.1562	1.6987	-0.2377
H	-1.5929	1.7697	-1.2429
H	-0.5421	2.5937	-0.0716
H	-1.9779	1.7036	0.4905
C	0.1493	0.2445	1.3296
H	-0.6477	0.3246	2.0992
C	-1.1570	-0.7785	-0.4904
H	-1.4945	-0.7809	-1.5535
O	1.3045	0.0331	1.6562
O	-1.4738	-1.6668	0.2751
O	1.6074	-0.7535	-1.0853
H	2.0114	-0.8461	-0.2105
ABC	2.1761	1.8191	1.7942

CBS-Q (0 K)=
   -420.353761 a.u.

(45) 1,1-Dihydroxy-pent-1-en-3-one			
	X	Y	Z
C	1.7192	-0.1354	0.0000
C	0.5200	-0.8074	0.0000
H	0.5212	-1.8918	0.0000
C	-0.7032	-0.0453	0.0000
O	1.8362	1.1805	0.0000
H	0.8896	1.5280	0.0000
O	-0.7215	1.2063	0.0000
C	-2.0117	-0.8170	0.0000
H	-2.0100	-1.4833	-0.8764
H	-2.0100	-1.4833	0.8764
C	-3.2428	0.0860	0.0000
H	-4.1598	-0.5155	0.0000
H	-3.2514	0.7340	0.8827
H	-3.2514	0.7340	-0.8827
O	2.8846	-0.7856	0.0000
H	3.5885	-0.1167	0.0000
ABC	5.8493	1.0572	0.9054

CBS-Q (0 K)= -420.394892 a.u.

(46) 1-Hydroxy-pent-1-en-3-one			
	X	Y	Z
C	-2.1174	0.5387	0.0000
C	-0.8373	1.0147	0.0000
H	-0.6766	2.0893	0.0000
C	0.2995	0.0984	0.0000
O	-2.4665	-0.7438	0.0000
H	-1.6219	-1.2572	0.0000
O	0.1489	-1.1352	0.0000
C	1.6917	0.7051	0.0000
H	1.7692	1.3679	-0.8762
H	1.7692	1.3679	0.8762
H	-2.9838	1.2020	0.0000
C	2.8028	-0.3417	0.0000
H	3.7870	0.1417	0.0000
H	2.7311	-0.9859	0.8828
H	2.7311	-0.9859	-0.8827
ABC	7.3258	1.4863	1.2547

CBS-Q (0 K)= -345.225886 a.u.

(47) 4-Hydroxy-but-3-en-2-one			
	X	Y	Z
C	-1.5118	0.7081	0.0000
C	-0.1721	0.9749	0.0000
H	0.1568	2.0102	0.0000
C	0.8031	-0.1113	0.0000
O	-2.0595	-0.5022	0.0000
H	-1.3063	-1.1430	0.0000
O	0.4569	-1.3046	0.0000
C	2.2703	0.2615	0.0000
H	2.5078	0.8668	-0.8849
H	2.5078	0.8668	0.8849
H	2.8801	-0.6467	0.0000
H	-2.2619	1.5006	0.0000
ABC	8.3291	2.5544	1.9790

CBS-Q (0 K)= -305.998046 a.u.

(48) 3-Hydroxy-propenal			
	X	Y	Z
C	-1.1910	0.4255	0.0000
C	0.0000	1.0974	0.0000
H	0.0018	2.1832	0.0000
C	1.2518	0.3646	0.0000
O	-1.3286	-0.8947	0.0000
H	-0.4161	-1.2728	0.0000
O	1.3307	-0.8725	0.0000
H	-2.1527	0.9404	0.0000
H	2.1856	0.9614	0.0000
ABC	9.8427	4.9526	3.2948

CBS-Q (0 K)= -266.758869 a.u.

Table S2. Acyclic structures, XYZ coordinates and rotational constants (GHz) at the MP2/6-31G(d') level and CBS-Q energies (continuation).

(49) 4,4-Dihydroxy-but-3-en-2-one

	X	Y	Z
C	-1.2098	-0.1634	0.0000
C	0.0191	-0.7810	0.0000
H	0.0668	-1.8640	0.0000
C	1.2048	0.0373	0.0000
O	-2.3439	-0.8660	0.0000
H	-3.0777	-0.2300	0.0000
O	-1.3846	1.1450	0.0000
H	-0.4524	1.5336	0.0000
C	2.5448	-0.6661	0.0000
H	2.6371	-1.3087	0.8852
H	3.3475	0.0771	-0.0001
H	2.6370	-1.3089	-0.8850
O	1.1645	1.2885	0.0000
ABC	6.0784	1.7454	1.3676

CBS-Q (0 K)= -381.165638 a.u.

(50) 1,1-Dihydroxy-penta-1,4-dien-3-one

	X	Y	Z
C	-0.1719	-1.6128	0.0000
C	-0.8067	-0.3893	0.0000
H	-1.8900	-0.3546	0.0000
C	0.0000	0.8001	0.0000
C	-0.7125	2.1077	0.0000
H	-1.8028	2.0894	0.0000
H	1.0536	3.2631	0.0000
C	-0.0349	3.2696	0.0000
H	-0.5457	4.2305	0.0000
O	1.2558	0.7721	0.0000
O	-0.8611	-2.7536	0.0000
H	-0.2174	-3.4811	0.0000
O	1.1364	-1.7655	0.0000
H	1.5098	-0.8225	0.0000
ABC	6.1260	1.1254	0.9507

CBS-Q (0 K)= -419.185536 a.u.

(51) 3-Hydroxy-butenal

	X	Y	Z
C	0.7694	0.0090	0.0000
C	-0.1986	0.9824	0.0000
H	0.0919	2.0288	0.0000
C	-1.6027	0.6326	0.0000
O	0.4911	-1.2941	0.0000
H	-0.4955	-1.3761	0.0000
O	-2.0372	-0.5298	0.0000
H	-2.3265	1.4722	0.0000
C	2.2404	0.2852	0.0000
H	2.7009	-0.1743	0.8837
H	2.7009	-0.1743	-0.8837
H	2.4464	1.3597	0.0000
ABC	8.3859	2.5707	1.9920

CBS-Q (0 K)= -305.998155 a.u.

(52) Formic acid vinyl ester

	X	Y	Z
C	1.3298	0.4119	0.0001
H	1.8962	1.3564	0.0001
O	0.0066	0.7211	-0.0002
O	1.8109	-0.6922	0.0002
C	-0.8850	-0.3464	-0.0003
H	-0.4241	-1.3303	-0.0009
H	-2.8954	-0.9368	0.0001
C	-2.1991	-0.1039	0.0002
H	-2.5905	0.9098	0.0008
ABC	20.3328	3.1588	2.7341

CBS-Q (0 K)= -266.754867 a.u.

(53) 3-Oxo-propionic acid vinyl ester

	X	Y	Z
H	3.2875	-1.7601	0.0355
C	3.3547	-0.7108	-0.2385
H	4.3117	-0.3117	-0.5595
C	2.2902	0.0955	-0.1910
H	2.2809	1.1502	-0.4505
O	1.0647	-0.4186	0.2214
C	0.0136	0.4467	0.2452
O	0.0635	1.6118	-0.0792
C	-1.2386	-0.2505	0.7243
H	-1.1034	-1.3300	0.8365
H	-1.4940	0.1801	1.7058
C	-2.4063	0.0411	-0.2126
H	-2.4448	1.0808	-0.5999
O	-3.2431	-0.7858	-0.5088
ABC	5.6659	0.9451	0.8599

CBS-Q (0 K)= -419.165946 a.u.

(54) 2-Methyl-acrylic acid vinyl ester

	X	Y	Z
H	-3.1898	0.7472	0.8314
C	-3.1847	0.0215	0.0198
H	-4.1405	-0.3099	-0.3801
C	-2.0198	-0.4430	-0.4629
H	-1.9679	-1.1696	-1.2711
C	-0.7346	0.0345	0.1133
O	-0.6097	0.8384	1.0105
O	0.3063	-0.5820	-0.5194
C	1.5962	-0.1907	-0.1057
H	3.3627	-0.8513	0.8352
C	2.3381	-1.0843	0.5599
H	1.9315	-2.0534	0.8355
C	2.0166	1.1692	-0.5735
H	3.0647	1.3550	-0.3151
H	1.3943	1.9417	-0.1078
H	1.9016	1.2450	-1.6627
ABC	4.9477	1.1784	1.1090

CBS-Q (0 K)= -383.240468 a.u.

244

Table S2. Acyclic structures, XYZ coordinates and rotational constants (GHz) at the MP2/6-31G(d') level and CBS-Q energies (continuation).

<table>
<tr><td colspan="4">(55) Acrylic Acid</td></tr>
<tr><td></td><td>X</td><td>Y</td><td>Z</td></tr>
<tr><td>H</td><td>1.4961</td><td>-1.7021</td><td>0.0000</td></tr>
<tr><td>C</td><td>0.4299</td><td>-1.9229</td><td>0.0000</td></tr>
<tr><td>H</td><td>0.1202</td><td>-2.9657</td><td>0.0000</td></tr>
<tr><td>C</td><td>-0.4655</td><td>-0.9214</td><td>0.0000</td></tr>
<tr><td>H</td><td>-1.5395</td><td>-1.0951</td><td>0.0000</td></tr>
<tr><td>C</td><td>0.0000</td><td>0.4901</td><td>0.0000</td></tr>
<tr><td>O</td><td>1.1545</td><td>0.8625</td><td>0.0000</td></tr>
<tr><td>O</td><td>-1.0534</td><td>1.3436</td><td>0.0000</td></tr>
<tr><td>H</td><td>-0.6727</td><td>2.2387</td><td>0.0000</td></tr>
<tr><td>ABC</td><td>10.9642</td><td>4.2471</td><td>3.0613</td></tr>
</table>

CBS-Q (0 K)= -266.777714 a.u.

(56) 2,2-Dimethyl-3-oxo-propionic acid

<table>
<tr><td></td><td>X</td><td>Y</td><td>Z</td></tr>
<tr><td>C</td><td>-0.2703</td><td>0.2264</td><td>0.2782</td></tr>
<tr><td>C</td><td>-0.7962</td><td>1.5927</td><td>-0.1486</td></tr>
<tr><td>H</td><td>-0.1552</td><td>2.3875</td><td>0.2483</td></tr>
<tr><td>H</td><td>-1.8165</td><td>1.7316</td><td>0.2260</td></tr>
<tr><td>H</td><td>-0.8185</td><td>1.6808</td><td>-1.2395</td></tr>
<tr><td>C</td><td>-0.2449</td><td>0.0768</td><td>1.8162</td></tr>
<tr><td>H</td><td>-1.2505</td><td>0.2518</td><td>2.2199</td></tr>
<tr><td>H</td><td>0.4340</td><td>0.8185</td><td>2.2560</td></tr>
<tr><td>H</td><td>0.0905</td><td>-0.9217</td><td>2.1188</td></tr>
<tr><td>C</td><td>1.1389</td><td>0.0148</td><td>-0.2559</td></tr>
<tr><td>C</td><td>-1.1621</td><td>-0.8949</td><td>-0.2653</td></tr>
<tr><td>H</td><td>-0.8501</td><td>-1.9232</td><td>0.0193</td></tr>
<tr><td>O</td><td>-2.1573</td><td>-0.7001</td><td>-0.9337</td></tr>
<tr><td>O</td><td>1.7969</td><td>0.8254</td><td>-0.8685</td></tr>
<tr><td>O</td><td>1.5958</td><td>-1.2294</td><td>0.0445</td></tr>
<tr><td>H</td><td>2.4908</td><td>-1.2871</td><td>-0.3345</td></tr>
<tr><td>ABC</td><td>2.7113</td><td>1.6544</td><td>1.5658</td></tr>
</table>

CBS-Q (0 K)= -420.394850 a.u.

(57) But-3-enoic acid

<table>
<tr><td></td><td>X</td><td>Y</td><td>Z</td></tr>
<tr><td>H</td><td>-3.4652</td><td>0.5474</td><td>-0.3876</td></tr>
<tr><td>C</td><td>-2.5965</td><td>-0.1073</td><td>-0.3621</td></tr>
<tr><td>H</td><td>-2.6748</td><td>-1.0522</td><td>-0.8994</td></tr>
<tr><td>H</td><td>-1.4264</td><td>1.1938</td><td>0.8194</td></tr>
<tr><td>C</td><td>-1.4812</td><td>0.2363</td><td>0.3010</td></tr>
<tr><td>C</td><td>-0.2608</td><td>-0.6365</td><td>0.3809</td></tr>
<tr><td>H</td><td>-0.3544</td><td>-1.5252</td><td>-0.2567</td></tr>
<tr><td>H</td><td>-0.1097</td><td>-1.0110</td><td>1.4066</td></tr>
<tr><td>C</td><td>1.0033</td><td>0.1088</td><td>0.0050</td></tr>
<tr><td>O</td><td>1.1216</td><td>1.3095</td><td>-0.1005</td></tr>
<tr><td>O</td><td>2.0328</td><td>-0.7540</td><td>-0.1794</td></tr>
<tr><td>H</td><td>2.8073</td><td>-0.2049</td><td>-0.3917</td></tr>
<tr><td>ABC</td><td>8.7920</td><td>2.0679</td><td>1.7792</td></tr>
</table>

CBS-Q (0 K)= -306.002665 a.u.

Table S3. List of known GAVS for the acyclic base compounds.

	C/C/H3	C/Cd/H3	C/CO/C/H2	C/CO/H3	C/O/C/H2	C/O/H3	Cd/C/H	Cd/H2	CO/C/H	CO/C2	CO/Cd/H	CO/O/C	CO/O/Cd*	CO/O/H	O/C/H	O/Cd2*	O/CO/Cd*	O/CO/H	O/Cd/C*
(1)								1											
(2)						1		1											1
(3)								2								1			
(4)						1		2								1			1
(5)								2								1			
(6)						1		2								1			1
(7)								2								1			
(8)						1		1											1
(9)		1																	
(10)								1											
(11)		1						1											
(12)	1			1				1											1
(13)								1								1			
(14)						2		1											2
(15)	1			1		1		1											2
(16)								2											
(17)								1			1								
(18)		1						1			1								
(19)							1	1	1										
(20)								2											
(21)	1						1	1	1										
(22)	2						1	1	1										
(23)			1						1	1									
(24)	1								2										
(25)	2								2										
(26)				1				1											
(27)	1							1	1										
(28)							1	2											
(29)		1						2											
(30)							1	1	1	1									
(31)	1		1					1											
(32)		2						2											
(33)		1					1	2											
(34)		1						1											
(35)	1							1	1										
(36)	2							1	1										
(37)									1										
(38)												1							
(39)								1				1					1		
(40)	1						1	1											
(41)	2						1	1											
(42)								1	1										
(43)							1	1											
(44)	1			1					2							1			
(45)	1		1																
(46)	1		1																
(47)			1																
(48)												1							
(49)			1																
(50)								1											
(51)		1										1							
(52)								1								1		1	
(53)								1	1			1						1	
(54)		1						2					1					1	
(55)								1					1						1
(56)	2								1			1						1	
(57)							1	1			1							1	

* Unknown GAVS for the specific heat. † C/O/C/H2 was recalculated based on (8) and (12).

Table S4. Contribution of each movement to the thermochemical properties for cyclic compounds.

	ΔH$_f$°, kcal/mol		S°, cal/mol K			Cp 300 K, cal/mol K	
	TRV	IR	TRV	IR	S$_{mix}$	TRV	IR
Diketenes							
1c) Diketene (4-methylene-oxetan-2-one)	-47.81	---	72.64	---	0.00	20.40	---
2c) 3-Methyl-4-methylene-oxetan-2-one	-57.83	0.37	78.35	2.25	1.38	24.16	1.93
3c) 3,3-Dimethyl-4-methylene-oxetan-2-one	-68.09	0.72	82.99	4.22	0.00	28.36	4.00
Cyclobutane-1,3-diones							
4c) Cyclobutane-1,3-dione	-44.34	---	74.57	---	---	21.26	---
5c) 2-Methyl-cyclobutane-1,3-dione	-54.43	0.41	80.31	2.52	0.00	24.84	2.04
6c) 2,2-Dimethyl-cyclobutane-1,3-dione	-73.01	0.75	85.87	2.54	0.00	29.12	4.02
7c) (E)-2,4-Dimethyl-cyclobutane-1,3-dione	-69.04	0.80	86.63	4.88	0.00	28.44	2.07
Pyran-4-ones							
8c) Pyran-4-one	-39.19	---	73.97	---	0.00	21.65	---
9c) 3-Methyl-pyran-4-one	-54.56	0.44	79.11	2.80	0.00	25.81	1.88
10c) 2-Methyl-pyran-4-one	-50.44	0.44	78.98	2.88	0.00	25.72	1.98
11c) 2-Hydroxy-pyran-4-one	-87.27	0.39	78.25	1.06	0.00	24.56	2.05
Cyclobut-2-enones							
12c) Cyclobut-2-enone	10.32	---	67.70	---	0.00	16.87	---
13c) 4-methyl-cyclobut-2-enone	0.60	0.38	73.27	2.18	1.38	20.70	2.10
14c) 2-methyl-cyclobut-2-enone	-6.81	0.42	73.47	3.30	0.00	20.90	1.38
15c) 4,4-dimethyl-cyclobut-2-enone	-15.43	0.74	77.95	4.24	0.00	24.96	4.16
16c) 3-Hydroxy-cyclobut-2-enone	-38.62	0.30	72.02	0.08	0.00	19.43	2.36
17c) 3-Hydroxy-2-methyl-cyclobut-2-enone	-57.33	0.74	77.93	4.10	0.00	23.49	3.39
18c) 3-Hydroxy-4-methyl-cyclobut-2-enone	-55.33	0.63	77.74	2.03	1.38	23.33	4.36
19c) 3-Hydroxy-2,4-dimethyl-cyclobut-2-enone	-69.71	1.10	83.60	4.79	1.38	27.39	5.55
20c) 3-Hydroxy-4,4-dimethyl-cyclobut-2-enone	-69.29	0.98	82.24	2.69	0.00	27.55	6.30

Table S5. Nonnext neighbor correction for ΔH$_f$° (in kcal/mol).

	NN$_{Ca}$^{I}	NN$_{CT}$	NN$_{cis}$^{OH}	NN^{OH}	NN$_{Ca}$^{I}	NN$_{Ca}$^{II}	NN$_{Ca}$^{II}	NN$_{cpco}$
Group 1. Ethers and alcohols.								
(3) 1-Vinyloxy-ethenol		0.50						
(4) 1-Methoxy-1-vinyloxy-ethene						2.27		
(5) 1-(1-Hydroxy-vinyloxy)-ethenol						3.87		
(6) 1-(1-Methoxy-vinyloxy)-ethenol						3.73		
(9) Propene-1,2-diol					2.74			
(13) 1-(2-Hydroxy-vinyloxy)-ethenol						1.58		
(14) 1,1-Dimethoxy-ethene					2.22			
(15) 1-Ethoxy-1-methoxy-ethene					2.10			
Group 2. Aldehydes and ketones.								
(23) 3-Oxo-butyraldehyde							-1.43	
(27) 2-Methyl-3-oxo-pent-4-enal	-0.96						-1.67	
(28) Hexa-1,5-dien-3-one	-0.96							
(30) 3-Oxo-hex-5-enal							-2.25	
(31) Pent-1-en-3-one	-0.96							
(32) 2,4-Dimethyl-penta-1,4-dien-3-one							1.61	
(33) 2-Methyl-hexa-1,5-dien-3-one		-0.90						
Group 3. Carbonyl, hydroxyl and alkoxyl groups.								
(34) (Z)-5-Hydroxy-hexa-1,4-dien-3-one			-8.81	-8.89				
(35) 3-Hydroxy-2-methyl-but-3-enal		-1.32						
(36) 3-Hydroxy-2,2-dimethyl-but-3-enal		-4.13						
(37) (Z)-5-Hydroxy-3-oxo-pent-4-enal	-0.96		-8.81	-1.45			-1.45	
(38) 3,3-Dihydroxy-propenal				-15.90				
(39) (Z)-3-Vinyloxy-propenal								-2.03
(40) 4-Hydroxy-2-methyl-but-3-enal								
(41) 4-Hydroxy-2,2-dimethyl-but-3-enal		-1.83						
(42) 3-Hydroxy-but-3-enal		-0.97						
(43) 4-Hydroxy-but-3-enal				-1.94				
(44) 2-Hydroxymethyl-2-methyl-malonal							-1.04	
(45) 1,1-Dihydroxy-pent-1-en-3-one	-0.96			-19.78				
(46) (Z)-1-Hydroxy-pent-1-en-3-one	-0.96		-8.81	-2.78				
(47) (Z)-4-Hydroxy-but-3-en-2-one			-8.81	-2.22				
(48) (Z)-3-Hydroxy-propenal			-8.81					
(49) 4,4-Dihydroxy-but-3-en-2-one				-18.53				
(50) 1,1-Dihydroxy-penta-1,4-dien-3-one				-21.15				
(51) (Z)-3-Hydroxy-butenal			-8.81	-2.47				
Group 4. Ester group.								
(53) 3-Oxo-propionic acid vinyl ester							-0.48	
(54) 2-Methyl-acrylic acid vinyl ester		0.61						
Group 5. Carboxylic acids.								
(55) Acrylic acid	-0.96							
(56) 2,2-Dimethyl-3-oxo-propionic acid							1.20	

Table S6. Contribution of each movement to the thermochemical properties for the acyclic base compounds.

	ΔH_f^o, kcal/mol		S^o, cal/mol K			Cp 300 K, cal/mol K	
	TRV	IR	TRV	IR	S_{mix}	TRV	IR
Group 1. Ethers and alcohols.							
(1) Ethene-1,1-diol	-76.25	0.63	64.50	3.24	0.00	14.38	4.59
(2) 1-Methoxy-ethenol	-73.06	1.22	66.73	7.37	0.00	16.72	7.04
(3) 1-Vinyloxy-ethenol	-49.78	1.39	71.37	11.61	1.38	19.71	7.56
(4) 1-Methoxy-1-vinyloxy-ethene	-44.73	1.95	74.71	17.71	1.38	22.19	7.99
(5) 1-(1-Hydroxy-vinyloxy)-ethenol	-94.34	2.59	73.09	19.24	1.38	22.03	10.40
(6) 1-(1-Methoxy-vinyloxy)-ethenol	-90.83	2.78	77.14	22.44	1.38	24.47	12.72
(7) Vinyloxy-ethene	-2.98	0.89	66.77	9.74	0.00	17.53	4.00
(8) Methoxy-ethene	-25.72	0.99	63.25	5.70	0.00	14.26	5.87
(9) Propene-1,2-diol	-80.03	1.26	70.04	8.24	1.38	18.03	6.97
(10) Ethenol	-29.18	0.29	66.92	1.39	0.00	12.04	2.65
(11) Propen-2-ol	-40.75	0.64	64.05	3.64	0.00	15.68	4.29
(12) Ethoxy-ethene	-34.73	1.58	67.48	9.22	0.00	17.41	9.16
(13) 1-(2-Hydroxy-vinyloxy)-ethenol	-86.54	2.07	75.72	14.89	1.38	22.19	10.40
(14) 1,1-Dimethoxy-ethene	-67.78	2.06	71.20	15.56	0.00	19.03	8.05
(15) 1-Ethoxy-1-methoxy-ethene	-76.94	2.87	73.80	20.85	0.00	22.20	11.49
Group 2. Aldehydes and ketones.							
(16) Penta-1,4-dien-3-one	-2.12	1.30	70.75	8.96	0.00	20.26	5.34
(17) Propenal	-15.52	0.45	64.08	2.47	0.00	13.95	2.85
(18) 2-Methyl-propenal	-25.89	0.87	69.07	5.54	0.00	17.55	4.36
(19) But-3-enal	-18.92	1.23	68.82	10.75	1.38	17.06	4.33
(20) Malonaldehyde	-61.53	0.93	67.85	10.93	1.38	15.15	3.47
(21) 2-Methyl-but-3-enal	-27.68	1.86	73.01	12.00	1.38	20.70	8.36
(22) 2,2-Dimethyl-but-3-enal	-36.50	2.02	76.77	14.79	1.38	24.85	8.31
(23) 3-Oxo-butyraldehyde	-75.97	1.44	71.93	14.58	1.38	18.93	5.06
(24) 2-Methyl-malonaldehyde	-69.54	1.58	72.08	13.14	1.38	18.71	6.69
(25) 2,2-Dimethyl-malonaldehyde	-79.23	2.04	74.79	14.74	1.38	22.93	8.69
(26) But-3-en-2-one	-27.47	1.01	67.55	7.65	0.00	17.71	3.90
(27) 2-Methyl-3-oxo-pent-4-enal	-60.15	2.40	79.18	19.25	1.38	25.21	8.99
(28) Hexa-1,5-dien-3-one	-7.72	1.88	75.95	15.34	1.38	23.49	7.34
(29) 2-Methyl-penta-1,4-dien-3-one	-12.05	1.52	75.88	13.01	0.00	23.94	7.41
(30) 3-Oxo-hex-5-enal	-56.22	2.46	78.55	23.53	1.38	24.75	8.17
(31) Pent-1-en-3-one	-34.34	1.74	71.39	11.53	0.00	20.68	8.38
(32) 2,4-Dimethyl-penta-1,4-dien-3-one	-21.19	2.09	78.37	18.07	1.38	27.65	9.15
(33) 2-Methyl-hexa-1,5-dien-3-one	-18.08	2.34	79.52	18.54	1.38	27.14	10.35
Group 3. Carbonyl, hydroxyl and alkoxyl groups.							
(34) (Z)-5-Hydroxy-hexa-1,4-dien-3-one	-72.75	1.59	79.02	10.67	0.00	25.64	7.74
(35) 3-Hydroxy-2-methyl-but-3-enal	-74.02	2.11	76.47	14.69	1.38	23.23	9.02
(36) 3-Hydroxy-2,2-dimethyl-but-3-enal	-85.66	2.29	80.14	16.84	1.38	27.48	10.33
(37) (Z)-5-Hydroxy-3-oxo-pent-4-enal	-103.39	1.56	77.85	15.24	1.38	23.28	6.75
(38) 3,3-Dihydroxy-propenal	-119.73	0.61	72.07	3.38	0.00	18.14	4.49
(39) (Z)-3-Vinyloxy-propenal	-33.18	1.45	75.72	13.01	0.00	21.71	5.99
(40) 4-Hydroxy-2-methyl-but-3-enal	-69.52	2.09	78.92	12.58	1.38	23.19	11.90
(41) 4-Hydroxy-2,2-dimethyl-but-3-enal	-78.50	2.51	81.54	16.03	1.38	27.33	11.92
(42) 3-Hydroxy-but-3-enal	-64.92	1.49	71.78	12.13	1.38	19.44	6.78
(43) 4-Hydroxy-but-3-enal	-60.40	1.60	73.54	13.04	0.00	19.41	7.63
(44) 2-Hydroxymethyl-2-methyl-malonal	-116.44	2.41	79.09	16.06	1.38	24.70	12.83
(45) 1,1-Dihydroxy-pent-1-en-3-one	-142.15	1.61	79.40	12.94	0.00	24.74	8.37
(46) (Z)-1-Hydroxy-pent-1-en-3-one	-87.31	1.42	73.62	11.93	0.00	21.29	6.93
(47) (Z)-4-Hydroxy-but-3-en-2-one	-79.89	0.95	71.97	6.57	0.00	19.40	4.12
(48) (Z)-3-Hydroxy-propenal	-65.70	0.47	68.01	2.84	0.00	15.66	2.86
(49) 4,4-Dihydroxy-but-3-en-2-one	-134.15	1.01	75.87	7.62	0.00	21.87	5.54
(50) 1,1-Dihydroxy-penta-1,4-dien-3-one	-111.38	1.26	78.85	7.95	0.00	24.51	7.50
(51) (Z)-3-Hydroxy-butenal	-79.90	0.92	72.32	5.76	0.00	19.45	4.78
Group 4. Ester group.							
(52) Formic acid vinyl ester	-62.80	0.86	67.28	5.77	0.00	15.03	4.48
(53) 3-Oxo-propionic acid vinyl ester	-99.00	2.09	77.43	17.51	1.38	22.78	8.91
(54) 2-Methyl-acrylic acid vinyl ester	-60.46	2.20	78.17	17.28	1.38	25.12	8.62
Group 5. Carboxylic acids.							
(55) Acrylic acid	-77.53	0.65	67.92	4.69	0.00	16.03	3.04
(56) 2,2-Dimethyl-3-oxo-propionic acid	-142.22	2.11	78.96	17.30	1.38	25.06	8.19
(57) But-3-enoic acid	-82.83	1.34	71.96	11.55	1.38	19.30	5.56

Table S7. Nonnext neighbor correction (in cal/mol K) for the intrinsic entropy at 298 K, S^o_{intr}.

		NN_{G2}^{I}	NN_{Gauche}	NN_{CIS}^{OH}	NN^{OH}	NN_{G1}^{I}	NN_{G1}^{II}	NN_{G2}^{II}	NN_{Other}
Group 1. Ethers and alcohols.								
(3)	1-Vinyloxy-ethenol		-0.06						
(4)	1-Methoxy-1-vinyloxy-ethene						0.65		
(5)	1-(1-Hydroxy-vinyloxy)-ethenol						4.54		
(6)	1-(1-Methoxy-vinyloxy)-ethenol						1.68		
(9)	Propene-1,2-diol					2.83			
(13)	1-(2-Hydroxy-vinyloxy)-ethenol						-1.67		
(14)	1,1-Dimethoxy-ethene					3.75			
(15)	1-Ethoxy-1-methoxy-ethene					5.04			
Group 2. Aldehydes and ketones.								
(23)	3-Oxo-butyraldehyde							1.33	
(27)	2-Methyl-3-oxo-pent-4-enal	-1.88						1.64	
(28)	Hexa-1,5-dien-3-one	-0.20							
(29)	2-Methyl-penta-1,4-dien-3-one	-1.88							
(30)	3-Oxo-hex-5-enal							0.45	
(31)	Pent-1-en-3-one	-1.88							
(32)	2,4-Dimethyl-penta-1,4-dien-3-one		-2.16						
(33)	2-Methyl-hexa-1,5-dien-3-one								-4.39
Group 3. Carbonyl (C=O) and hydroxyl and alkoxyl groups.								
(34)	5-Hydroxy-hexa-1,4-dien-3-one			-3.88					
(35)	3-Hydroxy-2-methyl-but-3-enal		0.88						
(36)	3-Hydroxy-2,2-dimethyl-but-3-enal		0.16						
(37)	5-Hydroxy-3-oxo-pent-4-enal	-1.88			-2.55			0.83	
(38)	3,3-Dihydroxy-propenal				-3.60				
(39)	3-Vinyloxy-propenal								-0.48
(40)	4-Hydroxy-2-methyl-but-3-enal								0.10
(41)	4-Hydroxy-2,2-dimethyl-but-3-enal		-3.28						
(42)	3-Hydroxy-but-3-enal		-0.93						
(43)	4-Hydroxy-but-3-enal				0.86				
(44)	2-Hydroxymethyl-2-methyl-							-4.35	
(45)	1,1-Dihydroxy-pent-1-en-3-one	-1.88			-4.47				
(46)	1-Hydroxy-pent-1-en-3-one	-1.88		-3.00					
(47)	4-Hydroxy-but-3-en-2-one			-4.41					
(48)	3-Hydroxy-propenal			-2.06					
(49)	4,4-Dihydroxy-but-3-en-2-one				-5.60				
(50)	1,1-Dihydroxy-penta-1,4-dien-3-one				-6.80				
(51)	3-Hydroxy-butenal			-2.30					
Group 4. Ester group.								
(53)	3-Oxo-propionic acid vinyl ester		0.04						
(54)	2-Methyl-acrylic acid vinyl ester		-0.15						
Group 5. Carboxylic acids.								
(55)	Acrylic acid	-1.88							
(56)	2,2-Dimethyl-3-oxo-propionic acid							0.95	
(57)	But-3-enoic acid								-0.47

Table S8. Nonnext neighbor correction (in cal/mol K) for the specific heat at 300 K, Cp.

		NN_{G2}^{I}	NN_{Gauche}	NN_{CIS}^{OH}	NN^{OH}	NN_{G1}^{I}	NN_{G1}^{II}	NN_{G2}^{II}	NN_{Other}
Group 1. Ethers and alcohols.								
(3)	1-Vinyloxy-ethenol		2.12						
(4)	1-Methoxy-1-vinyloxy-ethene						-0.41		
(5)	1-(1-Hydroxy-vinyloxy)-ethenol						3.00		
(6)	1-(1-Methoxy-vinyloxy)-ethenol						2.31		
(9)	Propene-1,2-diol					0.53			
(13)	1-(2-Hydroxy-vinyloxy)-ethenol						1.00		
(14)	1,1-Dimethoxy-ethene					-1.45			
(15)	1-Ethoxy-1-methoxy-ethene					-1.28			
Group 2. Aldehydes and ketones.								
(23)	3-Oxo-butyraldehyde							0.57	
(27)	2-Methyl-3-oxo-pent-4-enal	1.26						-0.88	
(28)	Hexa-1,5-dien-3-one	2.08							
(29)	2-Methyl-penta-1,4-dien-3-one	1.26							
(30)	3-Oxo-hex-5-enal							1.30	
(31)	Pent-1-en-3-one	1.26							
(32)	2,4-Dimethyl-penta-1,4-dien-3-one		1.00						
(33)	2-Methyl-hexa-1,5-dien-3-one								2.60
Group 3. Carbonyl (C=O) and hydroxyl and alkoxyl groups.								
(34)	5-Hydroxy-hexa-1,4-dien-3-one			-1.99					
(35)	3-Hydroxy-2-methyl-but-3-enal		-1.33						
(36)	3-Hydroxy-2,2-dimethyl-but-3-enal		0.13						
(37)	5-Hydroxy-3-oxo-pent-4-enal	1.26			-2.34			-0.42	
(38)	3,3-Dihydroxy-propenal				-2.95				
(39)	3-Vinyloxy-propenal								-0.43
(40)	4-Hydroxy-2-methyl-but-3-enal								1.54
(41)	4-Hydroxy-2,2-dimethyl-but-3-enal		-0.37						
(42)	3-Hydroxy-but-3-enal		0.30						
(43)	4-Hydroxy-but-3-enal				-1.56				
(44)	2-Hydroxymethyl-2-methyl-							1.37	
(45)	1,1-Dihydroxy-pent-1-en-3-one	1.26			-4.73				
(46)	1-Hydroxy-pent-1-en-3-one	1.26		-4.20					
(47)	4-Hydroxy-but-3-en-2-one			-2.58					
(48)	3-Hydroxy-propenal			-2.78					
(49)	4,4-Dihydroxy-but-3-en-2-one				-2.97				
(50)	1,1-Dihydroxy-penta-1,4-dien-3-one				-2.36				
(51)	3-Hydroxy-butenal			-2.34					
Group 4. Ester group.								
(53)	3-Oxo-propionic acid vinyl ester		1.56						
(54)	2-Methyl-acrylic acid vinyl ester		-9.86						
Group 5. Carboxylic acids.								
(55)	Acrylic acid	1.26							
(56)	2,2-Dimethyl-3-oxo-propionic acid							-1.17	
(57)	But-3-enoic acid								0.66

Table S9. Nonnext neighbor correction for the specific heat (in cal/mol K) at 400 K.

		NN_{G2}^{I}	NN_{Gauche}	NN_{CIS}^{O-H}	NN^{O-H}	NN_{G1}^{I}	NN_{G1}^{II}	NN_{G2}^{II}	NN_{Other}
	Group 1. Ethers and alcohols.								
(3)	1-Vinyloxy-ethenol		1.73						
(4)	1-Methoxy-1-vinyloxy-ethene						-0.40		
(5)	1-(1-Hydroxy-vinyloxy)-ethenol						0.81		
(6)	1-(1-Methoxy-vinyloxy)-ethenol						1.40		
(9)	Propene-1,2-diol					-1.43			
(13)	1-(2-Hydroxy-vinyloxy)-ethenol						1.51		
(14)	1,1-Dimethoxy-ethene					-2.28			
(15)	1-Ethoxy-1-methoxy-ethene					-2.70			
	Group 2. Aldehydes and ketones.								
(23)	3-Oxo-butyraldehyde							0.43	
(27)	2-Methyl-3-oxo-pent-4-enal	0.82						-0.67	
(28)	Hexa-1,5-dien-3-one	1.25							
(29)	2-Methyl-penta-1,4-dien-3-one	0.82							
(30)	3-Oxo-hex-5-enal							0.87	
(31)	Pent-1-en-3-one	0.82							
(32)	2,4-Dimethyl-penta-1,4-dien-3-one		0.59						
(33)	2-Methyl-hexa-1,5-dien-3-one								2.17
	Group 3. Carbonyl (C=O) and hydroxyl and alkoxyl groups.								
(34)	5-Hydroxy-hexa-1,4-dien-3-one			-2.29					
(35)	3-Hydroxy-2-methyl-but-3-enal		-1.39						
(36)	3-Hydroxy-2,2-dimethyl-but-3-enal		-0.23						
(37)	5-Hydroxy-3-oxo-pent-4-enal	0.82		-2.46				-0.16	
(38)	3,3-Dihydroxy-propenal				-2.90				
(39)	3-Vinyloxy-propenal								-0.58
(40)	4-Hydroxy-2-methyl-but-3-enal								1.68
(41)	4-Hydroxy-2,2-dimethyl-but-3-enal		0.62						
(42)	3-Hydroxy-but-3-enal		-0.01						
(43)	4-Hydroxy-but-3-enal				-1.63				
(44)	2-Hydroxymethyl-2-methyl-malonaldehyde							3.12	
(45)	1,1-Dihydroxy-pent-1-en-3-one	0.82			-4.20				
(46)	1-Hydroxy-pent-1-en-3-one	0.82		-3.94					
(47)	4-Hydroxy-but-3-en-2-one			-2.59					
(48)	3-Hydroxy-propenal			-2.95					
(49)	4,4-Dihydroxy-but-3-en-2-one				-2.68				
(50)	1,1-Dihydroxy-penta-1,4-dien-3-one				-1.98				
(51)	3-Hydroxy-butenal			-2.98					
	Group 4. Ester group.								
(53)	3-Oxo-propionic acid vinyl ester		0.78						
(54)	2-Methyl-acrylic acid vinyl ester		-14.68						
	Group 5. Carboxylic acids.								
(55)	Acrylic acid	0.82							
(56)	2,2-Dimethyl-3-oxo-propionic acid							-1.27	
(57)	But-3-enoic acid								0.30

Table S10. Nonnext neighbor correction for the specific heat (in cal/mol K) at 500 K.

		NN_{G2}^{I}	NN_{Gauche}	NN_{CIS}^{O-H}	NN^{O-H}	NN_{G1}^{I}	NN_{G1}^{II}	NN_{G2}^{II}	NN_{Other}
	Group 1. Ethers and alcohols.								
(3)	1-Vinyloxy-ethenol		1.03						
(4)	1-Methoxy-1-vinyloxy-ethene						-0.54		
(5)	1-(1-Hydroxy-vinyloxy)-ethenol						-0.94		
(6)	1-(1-Methoxy-vinyloxy)-ethenol						0.22		
(9)	Propene-1,2-diol					-2.34			
(13)	1-(2-Hydroxy-vinyloxy)-ethenol						1.05		
(14)	1,1-Dimethoxy-ethene					-2.81			
(15)	1-Ethoxy-1-methoxy-ethene					-3.36			
	Group 2. Aldehydes and ketones.								
(23)	3-Oxo-butyraldehyde							0.33	
(27)	2-Methyl-3-oxo-pent-4-enal	0.67						-0.46	
(28)	Hexa-1,5-dien-3-one	0.90							
(29)	2-Methyl-penta-1,4-dien-3-one	0.67							
(30)	3-Oxo-hex-5-enal							0.74	
(31)	Pent-1-en-3-one	0.67							
(32)	2,4-Dimethyl-penta-1,4-dien-3-one		-0.23						
(33)	2-Methyl-hexa-1,5-dien-3-one								1.69
	Group 3. Carbonyl (C=O) and hydroxyl and alkoxyl groups.								
(34)	5-Hydroxy-hexa-1,4-dien-3-one			-2.21					
(35)	3-Hydroxy-2-methyl-but-3-enal		-1.24						
(36)	3-Hydroxy-2,2-dimethyl-but-3-enal		-0.43						
(37)	5-Hydroxy-3-oxo-pent-4-enal	0.67		-2.21				0.01	
(38)	3,3-Dihydroxy-propenal				-2.47				
(39)	3-Vinyloxy-propenal								-0.43
(40)	4-Hydroxy-2-methyl-but-3-enal								1.42
(41)	4-Hydroxy-2,2-dimethyl-but-3-enal		1.73						
(42)	3-Hydroxy-but-3-enal		-0.02						
(43)	4-Hydroxy-but-3-enal				-1.48				
(44)	2-Hydroxymethyl-2-methyl-							3.94	
(45)	1,1-Dihydroxy-pent-1-en-3-one	0.67				-3.38			
(46)	1-Hydroxy-pent-1-en-3-one	0.67		-3.24					
(47)	4-Hydroxy-but-3-en-2-one			-2.21					
(48)	3-Hydroxy-propenal			-2.56					
(49)	4,4-Dihydroxy-but-3-en-2-one				-2.21				
(50)	1,1-Dihydroxy-penta-1,4-dien-3-one				-1.57				
(51)	3-Hydroxy-butenal			-2.93					
	Group 4. Ester group.								
(53)	3-Oxo-propionic acid vinyl ester		0.51						
(54)	2-Methyl-acrylic acid vinyl ester		-17.34						
	Group 5. Carboxylic acids.								
(55)	Acrylic acid	0.67							
(56)	2,2-Dimethyl-3-oxo-propionic acid							-0.76	
(57)	But-3-enoic acid								0.44

Table S11. Nonnext neighbor correction for the specific heat (in cal/mol K) at 600 K.

		NN_{G2}^{I}	NN_{Gauche}	NN_{cis}^{O-H}	NN^{O-H}	NN_{G1}^{I}	NN_{G1}^{II}	NN_{G2}^{II}	NN_{Other}
	Group 1. Ethers and alcohols.								
(3)	1-Vinyloxy-ethenol		0.46						
(4)	1-Methoxy-1-vinyloxy-ethene						-0.68		
(5)	1-(1-Hydroxy-vinyloxy)-ethenol						-1.94		
(6)	1-(1-Methoxy-vinyloxy)-ethenol						-0.63		
(9)	Propene-1,2-diol					-2.50			
(13)	1-(2-Hydroxy-vinyloxy)-ethenol						0.65		
(14)	1,1-Dimethoxy-ethene					-3.00			
(15)	1-Ethoxy-1-methoxy-ethene					-3.53			
	Group 2. Aldehydes and ketones.								
(23)	3-Oxo-butyraldehyde							0.22	
(27)	2-Methyl-3-oxo-pent-4-enal	0.63						-0.33	
(28)	Hexa-1,5-dien-3-one	0.73							
(29)	2-Methyl-penta-1,4-dien-3-one	0.63							
(30)	3-Oxo-hex-5-enal							0.63	
(31)	Pent-1-en-3-one	0.63							
(32)	2,4-Dimethyl-penta-1,4-dien-3-one		-0.87						
(33)	2-Methyl-hexa-1,5-dien-3-one								1.28
	Group 3. Carbonyl (C=O) and hydroxyl and alkoxyl groups.								
(34)	5-Hydroxy-hexa-1,4-dien-3-one			-1.82					
(35)	3-Hydroxy-2-methyl-but-3-enal		-0.97						
(36)	3-Hydroxy-2,2-dimethyl-but-3-enal		-0.42						
(37)	5-Hydroxy-3-oxo-pent-4-enal	0.63		-1.73				0.07	
(38)	3,3-Dihydroxy-propenal				-1.83				
(39)	3-Vinyloxy-propenal								-0.22
(40)	4-Hydroxy-2-methyl-but-3-enal								1.11
(41)	4-Hydroxy-2,2-dimethyl-but-3-enal		2.50						
(42)	3-Hydroxy-but-3-enal		0.22						
(43)	4-Hydroxy-but-3-enal				-1.20				
(44)	2-Hydroxymethyl-2-methyl-							4.24	
(45)	1,1-Dihydroxy-pent-1-en-3-one	0.63			-2.47				
(46)	1-Hydroxy-pent-1-en-3-one	0.63		-2.41					
(47)	4-Hydroxy-but-3-en-2-one			-1.64					
(48)	3-Hydroxy-propenal			-1.91					
(49)	4,4-Dihydroxy-but-3-en-2-one				-1.57				
(50)	1,1-Dihydroxy-penta-1,4-dien-3-one				-1.02				
(51)	3-Hydroxy-butenal			-2.47					
	Group 4. Ester group.								
(53)	3-Oxo-propionic acid vinyl ester		0.16						
(54)	2-Methyl-acrylic acid vinyl ester		-18.61						
	Group 5. Carboxylic acids.								
(55)	Acrylic acid	0.63							
(56)	2,2-Dimethyl-3-oxo-propionic acid							-0.34	
(57)	But-3-enoic acid								0.57

Table S12. Nonnext neighbor correction for the specific heat (in cal/mol K) at 800 K.

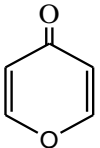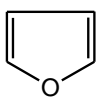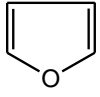|		NN_{G2}^{I}	NN_{Gauche}	NN_{cis}^{O-H}	NN^{O-H}	NN_{G1}^{I}	NN_{G1}^{II}	NN_{G2}^{II}	NN_{Other}
	Group 1. Ethers and alcohols.								
(3)	1-Vinyloxy-ethenol		-0.10						
(4)	1-Methoxy-1-vinyloxy-ethene						-0.76		
(5)	1-(1-Hydroxy-vinyloxy)-ethenol						-2.42		
(6)	1-(1-Methoxy-vinyloxy)-ethenol						-1.30		
(9)	Propene-1,2-diol					-2.03			
(13)	1-(2-Hydroxy-vinyloxy)-ethenol						0.25		
(14)	1,1-Dimethoxy-ethene					-2.76			
(15)	1-Ethoxy-1-methoxy-ethene					-3.17			
	Group 2. Aldehydes and ketones.								
(23)	3-Oxo-butyraldehyde							0.09	
(27)	2-Methyl-3-oxo-pent-4-enal	0.35						0.08	
(28)	Hexa-1,5-dien-3-one	0.57							
(29)	2-Methyl-penta-1,4-dien-3-one	0.35							
(30)	3-Oxo-hex-5-enal							0.51	
(31)	Pent-1-en-3-one	0.35							
(32)	2,4-Dimethyl-penta-1,4-dien-3-one		-1.40						
(33)	2-Methyl-hexa-1,5-dien-3-one								0.77
	Group 3. Carbonyl (C=O) and hydroxyl and alkoxyl groups.								
(34)	5-Hydroxy-hexa-1,4-dien-3-one			-0.71					
(35)	3-Hydroxy-2-methyl-but-3-enal		-0.47						
(36)	3-Hydroxy-2,2-dimethyl-but-3-enal		-0.20						
(37)	5-Hydroxy-3-oxo-pent-4-enal	0.35		-0.59				0.40	
(38)	3,3-Dihydroxy-propenal				-0.48				
(39)	3-Vinyloxy-propenal								0.09
(40)	4-Hydroxy-2-methyl-but-3-enal								0.67
(41)	4-Hydroxy-2,2-dimethyl-but-3-enal		2.97						
(42)	3-Hydroxy-but-3-enal		0.77						
(43)	4-Hydroxy-but-3-enal				-0.66				
(44)	2-Hydroxymethyl-2-methyl-							3.85	
(45)	1,1-Dihydroxy-pent-1-en-3-one	0.35			-0.80				
(46)	1-Hydroxy-pent-1-en-3-one	0.35		-0.83					
(47)	4-Hydroxy-but-3-en-2-one			-0.40					
(48)	3-Hydroxy-propenal			-0.45					
(49)	4,4-Dihydroxy-but-3-en-2-one				-0.24				
(50)	1,1-Dihydroxy-penta-1,4-dien-3-one				0.17				
(51)	3-Hydroxy-butenal			-1.15					
	Group 4. Ester group.								
(53)	3-Oxo-propionic acid vinyl ester		0.13						
(54)	2-Methyl-acrylic acid vinyl ester		-19.00						
	Group 5. Carboxylic acids.								
(55)	Acrylic acid	0.35							
(56)	2,2-Dimethyl-3-oxo-propionic acid							0.42	
(57)	But-3-enoic acid								0.97

Table S13. Nonnext neighbor correction for the specific heat (in cal/mol K) at 1000 K.

		NN_{G2}^{I}	NN_{Gauche}	NN_{cis}^{O-H}	NN^{O-H}	NN_{G1}^{I}	NN_{G1}^{II}	NN_{G2}^{II}	NN_{Other}
				Group 1. Ethers and alcohols.					
(3)	1-Vinyloxy-ethenol		-0.24						
(4)	1-Methoxy-1-vinyloxy-ethene							-0.68	
(5)	1-(1-Hydroxy-vinyloxy)-ethenol							-2.13	
(6)	1-(1-Methoxy-vinyloxy)-ethenol							-1.29	
(9)	Propene-1,2-diol					-1.44			
(13)	1-(2-Hydroxy-vinyloxy)-ethenol							0.15	
(14)	1,1-Dimethoxy-ethene					-2.26			
(15)	1-Ethoxy-1-methoxy-ethene					-2.61			
				Group 2. Aldehydes and ketones.					
(23)	3-Oxo-butyraldehyde							-0.09	
(27)	2-Methyl-3-oxo-pent-4-enal	0.33						0.12	
(28)	Hexa-1,5-dien-3-one	0.45							
(29)	2-Methyl-penta-1,4-dien-3-one	0.33							
(30)	3-Oxo-hex-5-enal							0.28	
(31)	Pent-1-en-3-one	0.33							
(32)	2,4-Dimethyl-penta-1,4-dien-3-one		-1.39						
(33)	2-Methyl-hexa-1,5-dien-3-one								0.50
				Group 3. Carbonyl (C=O) and hydroxyl and alkoxyl groups.					
(34)	5-Hydroxy-hexa-1,4-dien-3-one			0.45					
(35)	3-Hydroxy-2-methyl-but-3-enal		-0.16						
(36)	3-Hydroxy-2,2-dimethyl-but-3-enal		-0.01						
(37)	5-Hydroxy-3-oxo-pent-4-enal	0.33		0.55				0.46	
(38)	3,3-Dihydroxy-propenal				0.71				
(39)	3-Vinyloxy-propenal								0.30
(40)	4-Hydroxy-2-methyl-but-3-enal								0.45
(41)	4-Hydroxy-2,2-dimethyl-but-3-enal		2.77						
(42)	3-Hydroxy-but-3-enal		1.08						
(43)	4-Hydroxy-but-3-enal				-0.28				
(44)	2-Hydroxymethyl-2-methyl-							3.20	
(45)	1,1-Dihydroxy-pent-1-en-3-one	0.33				0.49			
(46)	1-Hydroxy-pent-1-en-3-one	0.33		0.63					
(47)	4-Hydroxy-but-3-en-2-one			0.86					
(48)	3-Hydroxy-propenal			0.97					
(49)	4,4-Dihydroxy-but-3-en-2-one				0.87				
(50)	1,1-Dihydroxy-penta-1,4-dien-3-one				1.21				
(51)	3-Hydroxy-butenal			0.25					
				Group 4. Ester group.					
(53)	3-Oxo-propionic acid vinyl ester		0.31						
(54)	2-Methyl-acrylic acid vinyl ester		-18.71						
				Group 5. Carboxylic acids.					
(55)	Acrylic acid	0.33							
(56)	2,2-Dimethyl-3-oxo-propionic acid							1.04	
(57)	But-3-enoic acid								1.39

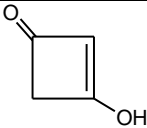**Table S14.** Nonnext neighbor correction for the specific heat (in cal/mol K) at 1500 K.

		NN_{G2}^{I}	NN_{Gauche}	NN_{cis}^{O-H}	NN^{O-H}	NN_{G1}^{I}	NN_{G1}^{II}	NN_{G2}^{II}	NN_{Other}
	Group 1. Ethers and alcohols.								
(3)	1-Vinyloxy-ethenol		-0.21						
(4)	1-Methoxy-1-vinyloxy-ethene						-0.43		
(5)	1-(1-Hydroxy-vinyloxy)-ethenol						-1.24		
(6)	1-(1-Methoxy-vinyloxy)-ethenol						-0.84		
(9)	Propene-1,2-diol					-0.59			
(13)	1-(2-Hydroxy-vinyloxy)-ethenol						0.13		
(14)	1,1-Dimethoxy-ethene					-1.29			
(15)	1-Ethoxy-1-methoxy-ethene					-1.58			
	Group 2. Aldehydes and ketones.								
(23)	3-Oxo-butyraldehyde							0.02	
(24)	2-Methyl-malonaldehyde								
(25)	2,2-Dimethyl-malonaldehyde								
(26)	But-3-en-2-one								
(27)	2-Methyl-3-oxo-pent-4-enal	0.82						-0.42	
(28)	Hexa-1,5-dien-3-one	0.31							
(29)	2-Methyl-penta-1,4-dien-3-one	0.82							
(30)	3-Oxo-hex-5-enal							0.31	
(31)	Pent-1-en-3-one	0.82							
(32)	2,4-Dimethyl-penta-1,4-dien-3-one		-0.91						
(33)	2-Methyl-hexa-1,5-dien-3-one								0.31
	Group 3. Carbonyl (C=O) and hydroxyl and alkoxyl groups.								
(34)	5-Hydroxy-hexa-1,4-dien-3-one			2.81					
(35)	3-Hydroxy-2-methyl-but-3-enal		0.08						
(36)	3-Hydroxy-2,2-dimethyl-but-3-enal		0.13						
(37)	5-Hydroxy-3-oxo-pent-4-enal	0.82		2.57				0.13	
(38)	3,3-Dihydroxy-propenal				2.88				
(39)	3-Vinyloxy-propenal								0.49
(40)	4-Hydroxy-2-methyl-but-3-enal								0.26
(41)	4-Hydroxy-2,2-dimethyl-but-3-enal		1.86						
(42)	3-Hydroxy-but-3-enal		1.10						
(43)	4-Hydroxy-but-3-enal				0.13				
(44)	2-Hydroxymethyl-2-methyl-							1.91	
(45)	1,1-Dihydroxy-pent-1-en-3-one	0.82			2.62				
(46)	1-Hydroxy-pent-1-en-3-one	0.82		3.19					
(47)	4-Hydroxy-but-3-en-2-one			3.30					
(48)	3-Hydroxy-propenal			3.19					
(49)	4,4-Dihydroxy-but-3-en-2-one				2.82				
(50)	1,1-Dihydroxy-penta-1,4-dien-3-one				3.07				
(51)	3-Hydroxy-butenal			2.79					
	Group 4. Ester group.								
(53)	3-Oxo-propionic acid vinyl ester		0.41						
(54)	2-Methyl-acrylic acid vinyl ester		-18.97						
	Group 5. Carboxylic acids.								
(55)	Acrylic acid	0.82							
(56)	2,2-Dimethyl-3-oxo-propionic acid							1.79	
(57)	But-3-enoic acid								1.89

Table S15. Checking of ΔH_f° in kcal/mol for some compounds by the use of isodesmic reactions[*].

	ΔH_{rxn}^{298}	ΔH_f°
Group 2. (22) 2,2-Dimethyl-but-3-enal:		
$HCOC(CH_3)_2CHCH_2$ + $CH_4 \longrightarrow CH_2CHC(CH_3)HCH_3$ + CH_3COH	6.13	-35.60
+ $CH_4 \longrightarrow CH_2CHCH_3$ + $HC(CH_3)_2COH$	7.26	-35.50
+ $C_2H_6 \longrightarrow tBuCHCH_2$ + CH_3COH	-0.23	-34.98
+ $H_2O \longrightarrow HC(CH_3)_2\,CHCH_2$ + CH_3COOH	-5.50	-33.68
Average (-34.44)		-34.94
8c) Pyran-4-one:		
Pyran-4-one + $3CH_4 \longrightarrow$ [tetrahydropyran structure] + $HCOH$ + C_2H_4	26.50	-39.86
+ $4C_2H_6 \longrightarrow CH_3CH_2COCH_2CH_3$ + $CH_3CH_2OCH_2CH_3$ + C_2H_4	24.27	-39.43
+ $H_2 \longrightarrow$ [furan structure] + $HCOH$	6.63	-40.95
+ $C_2H_4 \longrightarrow$ [furan structure] + CH_2CHCOH	3.65	-39.59
Average (-39.19)		-39.96
Group 2. (17) Propenal:		
CH_2CHCOH + $CH_4 \longrightarrow CH_3C(=O)OH$ + CH_2CH_2	6.73	-17.18
+ $C_2H_6 \longrightarrow CH_2CHCH_2CH_3$ + H_2CO	9.43	-15.50
+ $HC(=O)H \longrightarrow CH_2CHCH_3$ + CO_2	-47.78	-15.42
+ $CH_3OH \longrightarrow CH_2CHCH_3$ + $HCOOH$	-21.82	-15.71
Average (-15.08)		-15.95
Group 2. (16) Penta-1,4-dien-3-one:		
$CH_2CHCOCHCH_2$ + $CH_4 \longrightarrow H_2C=C=O$ + $CH_2CHCH_2CH_3$	8.10	-1.82
+ $C_2H_6 \longrightarrow CH_3CH=C=O$ + $2C_2H_4$	31.98	-2.00
+ $C_2H_6 \longrightarrow CH_2CHCH_2CH_3$ + CH_2CHCOH	6.66	-1.81
Average (-0.83)		-1.87
Group 1. (1) Ethene-1,1-diol:		
$CH_2C(OH)_2$ + $CH_4 \longrightarrow CH_2C(OH)H$ + CH_3OH	16.71	-75.85
+ $C_2H_4 \longrightarrow 2CH_2C(OH)H$	4.56	-74.87
+ $HCOH \longrightarrow CH_2C(OH)H$ + $HCOOH$	-17.33	-76.07
Average (-75.62)		-75.60

[*] Results from atomization reaction procedure in parenthesis.

Table S15. Checking of $\Delta H_f\,^\circ$ in kcal/mol for some compounds by the use of isodesmic reactions (continuation)[*].

	$\Delta H_{rxn}\,^{298}$	$\Delta H_f\,^\circ$
12c) Cyclobut-2-enone (CBE):		
CBE + CH$_4$ → [cyclobutene] + H$_2$CO	20.89	8.41
+ 2CH$_4$ → CH$_3$CH$_2$CH$_2$CH$_4$ + H$_2$C=C=O	-16.51	10.71
+ 3CH$_4$ → CH$_3$CH=C=O + 2C$_2$H$_6$	-12.03	10.23
+ HC(=O)H → [cyclobutene] + CO$_2$	-39.11	8.49
	Average (10.32)	9.46
16c) 3-Hydroxy-cyclobut-2-enone (CBEOH):		
CBEOH + 2CH$_4$ → CH$_3$COCH$_2$CH$_3$ + CH$_2$CHOH	-12.28	-37.97
+ 3CH$_4$ → CH$_3$CHC=C=O + CH$_3$CH$_2$OH + C$_2$H$_6$	0.88	-38.77
+ C$_2$H$_6$ → [cyclobutanone] + CH$_2$CHOH	7.33	-40.34
+ 2HC(=O)H → [cyclobutene] + HCOOH + CO$_2$	-54.34	-40.80
	Average (-38.32)	-39.47
Group 1. (7) Vinyloxy-ethene:		
CH$_2$CHOCHCH$_2$ + 2CH$_4$ → 2C$_2$H$_4$ + CH$_3$OCH$_2$CH$_3$	20.18	-3.47
+ C$_2$H$_6$ → CH$_3$CH$_2$OCHCH$_2$ + 2C$_2$H$_4$	1.78	-2.68
+ HCOH → H$_2$C=C=O + CH$_3$OCHCH$_2$	-8.20	-1.95
+ CH$_3$OH → CH$_2$CHOH + CH$_3$OCHCH$_2$	-4.09	-1.46
	Average (-2.09)	-2.39
Group 1. (11) Propen-2-ol:		
CH$_2$C(OH)CH$_3$ + CH$_4$ → C$_2$H$_5$OH + C$_2$H$_5$	8.92	-40.05
+ C$_2$H$_6$ → CH$_2$CHCH$_3$ + C$_2$H$_5$OH	9.68	-40.89
+ C$_2$H$_4$ → C$_2$H$_3$OH + CH$_2$CHCH$_3$	3.43	-39.97
→ CH$_2$CH$_2$ + H$_2$CO	26.61	-40.06
	Average (-40.1)	-40.24

[*] Results from atomization reaction procedure in parenthesis.

Table S15. Checking of ΔH_f° in kcal/mol for some compounds by the use of isodesmic reactions (continuation)[*].

|	$\Delta H_{rxn}{}^{298}$	ΔH_f°
Group 1. (10) Ethenol:		
$CH_2CHOH + CH_4 \longrightarrow CH_3OH + CH_2CH_2$	12.14	-29.87
$+ C_2H_6 \longrightarrow CH_2CH_2 + C_2H_5OH$	6.25	-29.81
$+ (CH_3)_2O \longrightarrow CH_3OH + CH_3OC_2H_4$	0.015	-28.83
$+ H_2 \longrightarrow CH_2CH_2 + H_2O$	-14.01	-31.26
Average (-28.89)		-29.94
Group 1. (2) 1-Methoxy-ethenol:		
$CH_2C(OCH_3)(OH) + CH_4 \longrightarrow CH_3OC_2H_4 + CH_3OH$	16.97	-71.96
$+ 2CH_4 \longrightarrow C_2H_4 + (CH_3)_2O + CH_3OH$	29.10	-73.00
$+ C_2H_6 \longrightarrow CH_3OC_2H_4 + C_2H_5OH$	11.07	-71.90
$+ C_2H_4 \longrightarrow CH_3OC_2H_4 + C_2H_4OH$	4.82	-70.97
Average (-71.84)		-71.95
Group 1. (14) 1,1-Dimethoxy-ethene:		
$CH_2C(OCH_3)_2 + CH_4 \longrightarrow CH_3OC_2H_4 + (CH_3)_2O$	15.13	-66.05
$+ 2CH_4 \longrightarrow C_2H_4 + 2(CH_3)_2O + CH_3OH$	27.26	-67.08
$+ C_2H_4OH \longrightarrow CH_3OC_2H_4 + CH_2C(OCH_3)(OH)$	-1.82	-65.87
Average (-65.72)		-66.33
Group 1. (5) 1-(1-Hydroxy-vinyloxy)-ethenol:		
$CH_2C(OH)OC(OH)CH_2 + CH_4 \longrightarrow CH_2C(OH)CH_3 + CH_2C(OH)_2$	-4.65	-93.24
$+ CH_4 \longrightarrow C_2H_4OH + CH_2C(OCH_3)(OH)$	9.71	-92.62
$+ 2C_2H_4 \longrightarrow 2C_2H_4OH + C_2H_3OC_2H_3$	6.48	-91.40
Average (-91.75)		-92.42
Group 1. (6) 1-(1-Methoxy-vinyloxy)-ethenol:		
$CH_3OC(CH_2)OC(CH_2)(OH) + CH_4 \longrightarrow CH_3OC_2H_4 + CH_2C(OCH_3)(OH)$	9.67	-88.42
$+ CH_4 \longrightarrow C_2H_4OH + CH_2C(OCH_3)_2$	11.49	-88.27
$+ 2C_2H_4 \longrightarrow C_2H_4OH + C_2H_3OC_2H_3 + CH_3OC_2H_4$	6.44	-87.20
Average (-88.05)		-87.96
11c) 2-Hydroxy-pyran-4-one (POH):		
$POH + CH_4 \longrightarrow CH_2C(OH)_2 + CBE$	40.20	-87.68
$+ 3CH_4 \longrightarrow$ $+ CH_3OH + CH_3COCH_3$	39.78	-87.80
$+ 4CH_4 \longrightarrow$ $+ C_2H_4 + H_2CO$	44.36	-87.97
$+ CBE \longrightarrow Pyran\text{-}4\text{-}one + CBEOH$	-0.96	-86.87
Average (-86.87)		-87.58
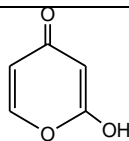
Table S16. Fourier coefficients for hindered potential of internal rotations in molecules of Group 1.

		a0 (b0)	a1 (b1)	a2 (b2)	a3 (b3)	a4 (b4)	a5 (b5)	a6 (b6)	a7 (b7)	a8 (b8)	a9 (b9)	a10 b(10)
(1)	257 (Cd-O)	11.26	-4.17	-8.97	1.42	0.44	-0.04	0.04	0.00	0.00	0.00	
	417 (Cd-O)	14.231	-8.843	-2.744	-4.253	2.416	-1.522	1.594	-1.421	1.191	-1.219	
(2)	131 (Cd-OCH3)	15.985	-10.99	-0.79	-5.09	1.20	-0.77	1.00	-0.75	0.65	-0.70	0.56667
	254 (O-C)	6.321	-0.14	0.24	-6.90	-0.10	-0.02	0.92	0.01	0.02	-0.34	
	298 (Cd-OH)	12.184	-4.66	-9.72	1.66	0.79	-0.30	0.00	-0.10	-0.07	0.11	0
(3)	86 (O-Cd)	7.296	-5.038 (4.216)	-0.162 (0.847)	-1.157 (-1.981)	-0.634 (-0.224)	-0.529 (0.190)	-0.081 (0.119)	0.048 (0.357)	0.097 (0.092)	0.158 (-0.043)	
	116 (O-Cd)	8.713	-6.777 (2.466)	-0.174 (0.145)	-1.221 (2.115)	0.378 (-2.143)	-0.040 (-0.229)	-0.369 (-0.639)	0.006 (0.004)	-0.371 (-0.133)	0.00	-0.158 (0.058)
	301 (Cd-O)	10.697	-4.522 (0.771)	-8.102 (-1.900)	1.698 (0.232)	0.289 (0.006)	-0.074 (0.041)	0.019 (0.037)	-0.027 (-0.173)	-0.039 (-0.034)	0.060	
(4)	45 (O-Cd)	8.490	-5.78	-5.19	2.33	0.00	0.34	-0.39	-0.15	0.08	0.27	
	64 (Cd-O)	2.754	-0.992 (-0.840)	-0.445 (-2.475)	-0.478 (0.845)	-1.264 (0.456)	0.592 (0.211)	-0.200 (-0.336)	-0.050 (0.326)	0.225 (-0.194)	-0.142	
	123 (O-Cd)	7.057	0.070 (0.964)	-3.391 (-1.369)	-3.629 (1.637)	-0.616 (-0.982)	0.502 (0.621)	-0.322 (-0.219)	0.629 (0.215)	-0.497 (-0.155)	0.197	
	266 (O-C)	6.426	-0.015 (-0.026)	0.015 (-0.026)	-6.869 (-0.974)	0.015 (0.026)	-0.015 (0.026)	0.710 (0.153)	-0.015 (-0.026)	0.015 (-0.026)	-0.266	
(5)	65 (O-Cd)*											
	71 (Cd-O)*											
	256 (Cd-O)	6.024	-1.736 (-2.069)	-4.676 (-2.249)	0.393 (2.157)	-0.259 (-0.275)	0.190 (-0.153)	0.152 (0.084)	0.008 (0.107)	-0.067 (0.044)	-0.030	
	257 (Cd-O)	6.024	-1.736 (-2.069)	-4.676 (-2.249)	0.393 (2.157)	-0.259 (-0.275)	0.190 (-0.153)	0.152 (0.084)	0.008 (0.107)	-0.067 (0.044)	-0.030	
(6)	44 (O-Cd)	5.594	-3.504 (-2.656)	-1.129 (-1.472)	-1.367 (2.462)	0.996 (-0.998)	-0.570 (-0.706)	-0.223 (0.715)	0.466 (-0.338)	-0.359 (0.181)	0.132 (0.178)	-0.052 (-0.089)
	70 (Cd-O)	4.489	-0.730 (-2.304)	-1.898 (1.327)	-2.166 (-0.921)	0.295 (-0.054)	0.422 (-0.367)	-0.074 (0.348)	-0.221 (-0.491)	-0.206 (-0.150)	0.032 (-0.216)	0.077 (-0.064)
	105 (O-Cd)	9.047	-2.187 (1.442)	-3.892 (-2.444)	-3.521 (-0.893)	0.625 (0.111)	0.024 (0.496)	-0.078 (0.129)	-0.110 (-0.166)	0.055 (-0.103)	0.037	
	262 (O-C)	5.909	0.000 (-0.029)	0.030 (0.000)	-6.144 (1.067)	-0.030 (0.000)	0.001 (-0.028)	0.181 (-0.414)	-0.003 (0.017)	-0.009 (-0.003)	0.067	
	282 (O-H)	10.266	-4.791 (0.125)	-7.316 (1.310)	1.670 (-0.762)	0.287 (-0.370)	-0.158 (0.083)	0.027 (0.010)	-0.030 (0.050)	0.117 (-0.007)	-0.098 (-0.064)	0.026
(7)	57 (Cd-O)*											
	78 (Cd-O)*											
(8)	237 (O-Cd)	10.973	-0.28	-6.96	-3.60	-0.34	0.03	0.17	0.05	-0.02	-0.03	
	269 (O-C)	7.096	-0.11	0.22	-7.54	-0.18	0.04	0.72	0.06	-0.03	-0.26	
(9)	209 (Cd-C)	5.451	-0.001 (0.002)	-0.001 (-0.002)	-5.705 (-0.583)	-0.001 (0.002)	-0.001 (-0.002)	0.298 (0.045)	-0.001 (0.002)	-0.001 (-0.002)	-0.035	
	321(Cd-O)	5.534	-2.528 (-4.378)	-0.289 (0.500)	-3.764 (0.000)	0.802 (1.388)	0.532 (-0.921)	-0.274 (0.000)	-0.079 (-0.136)	-0.238 (0.411)	0.304	
	555 (Cd-O)	7.893	0.26	-3.44	-4.33	-0.94	-0.19	0.33	0.27	0.13	0.02	
(10)	476 (Cd-O)	13.194	-3.00	-8.59	-2.28	0.43	0.27	0.14	0.07	-0.12	-0.12	
(11)	204 (Cd-C)	4.612	0.08	-0.07	-4.86	0.06	-0.08	0.26	-0.01	0.00		
	463 (O-H)	13.972	-4.51	-7.92	-1.84	0.21	0.01	0.06	0.01	0.02	0.01	
(12)	115 (O-C)	16.755	-15.29	6.70	-8.16	-0.68	-0.23	1.41	-0.52	0.51	-0.50	
	214 (O-Cd)	10.125	0.24	-6.43	-3.68	-0.47	-0.01	0.18	0.09	-0.01	-0.03	
	287 (C-C)	7.212	0.00	0.00	-7.50	0.00	0.00	0.29	0.00	0.00	0.00	
(13)	59 (O-Cd)	7.986	-4.121 (7.135)	-2.385 (-4.129)	-0.335 (0.000)	-1.391 (2.407)	-0.336 (-0.583)	0.848 (0.000)	-0.017 (0.030)	-0.357 (-0.616)	0.107	
	92 (O-Cd)	11.556	-5.324 (1.641)	-3.210 (-2.139)	-1.418 (1.613)	-2.581 (-0.054)	-0.135 (0.021)	1.594 (0.905)	0.081 (-0.114)	-0.534 (-1.418)	-0.029	-0.203
	309 (Cd-O)	9.574	-2.959 (-0.024)	-7.166 (3.932)	0.593 (-1.222)	-0.022 (-0.219)	0.005 (0.032)	-0.016 (-0.031)	0.001 (-0.015)	-0.007 (-0.009)	-0.004	
	461 (Cd-O)	17.505	-7.918 (-0.516)	-7.460 (-0.076)	-2.086 (-0.094)	-0.249 (0.045)	-0.099 (0.017)	0.022 (0.012)	0.078 (0.007)	0.132 (0.002)	0.074	
(14)	100 (Cd-O)	5.754	1.99	-4.24	-3.46	-0.30	0.13	0.12	0.03	-0.01	-0.02	
	141 (Cd-O)	5.754	1.99	-4.24	-3.46	-0.30	0.13	0.12	0.03	-0.01	-0.02	
	265 (O-C)	6.494	-0.23	0.35	-6.96	-0.01	-0.14	0.93	-0.11	0.12	-0.61	0.119
	282 (O-C)	6.494	-0.23	0.35	-6.96	-0.01	-0.14	0.93	-0.11	0.12	-0.61	0.119
(15)	79 (Cd-O)	5.295	1.64	-3.80	-3.21	-0.20	0.16	0.14	0.02	-0.02	-0.02	
	127 (O-C)	8.951	-7.05	2.90	-4.48	0.62	-0.73	-0.08	0.14	0.00	-0.26	
	135 (Cd-O)	5.678	1.79	-4.20	-3.35	-0.24	0.19	0.14	0.01	-0.01	-0.02	
	274 (O-C)	6.899	0.00	0.00	-7.59	0.00	0.00	1.29	0.00	0.00	-0.60	
	276 (C-C)	7.573	0.035 (-0.060)	0.017 (0.028)	-7.693 (-0.003)	-0.025 (0.037)	-0.024 (-0.050)	0.124 (-0.010)	-0.011 (0.010)	0.008 (0.008)	-0.004	

* The Shcrödinger equation was solved by the finite difference boundary value method (See Truhlar, D.B. J. Comp. Phys. 1972, 10, 123; Ercolani, G. J. Chem. Educ. 2000, 77, 1495).

Table S17. Fourier coefficients for hindered potential of internal rotations in molecules of Group 2.

		a0 (b0)	a1 (b1)	a2 (b2)	a3 (b3)	a4 (b4)	a5 (b5)	a6 (b6)	a7 (b7)	a8 (b8)	a9 (b9)
(16)	71, 119 (Cd-CO)	11.109	-1.044	-10.824	-0.725	1.797	-0.304	-0.076	0.061	0.037	-0.035
(17)	173 (Cd-CO)	16.850	-2.635	-14.524	-1.180	1.367	0.305	-0.090	-0.125	0.004	0.029
(18)	158 (Cd-O)	19.187	-5.019	-14.110	-1.417	1.191	0.348	-0.073	-0.132	-0.006	0.031
	189 (Cd-C)	3.715	0.077	-0.052	-3.927	0.035	-0.064	0.169	-0.014	0.013	0.048
(19)	85 (C-CO)	6.511	-3.574 (-4.259)	-0.021 (0.120)	-2.648 (1.528)	-0.390 (-0.141)	0.029 (0.080)	0.044 (-0.075)	0.061 (-0.010)	-0.009 (-0.007)	0.000 (0.001)
	156 (C-Cd)	4.606	0.450 (2.313)	-2.047 (1.025)	-2.851 (-0.160)	-0.220 (-0.166)	-0.037 (-0.051)	0.094 (-0.004)	-0.002 (-0.005)	0.007 (-0.000)	-0.001
(21)	84 (C-CO)	5.571	-2.847 (-0.404)	0.294 (0.409)	-3.018 (-0.424)	0.054 (-0.008)	-0.136 (-0.037)	0.095 (0.016)	-0.015 (0.001)	0.002 (-0.004)	0.000 (0.001)
	96 (C-Cd)	7.506	-1.483 (-0.119)	-3.486 (-0.165)	-3.542 (-0.583)	0.829 (0.203)	0.269 (-0.021)	-0.003 (0.116)	-0.086 (-0.015)	-0.016 (-0.017)	0.012 (-0.024)
	237 (C-C)	6.584	0.002 (-0.000)	-0.002 (0.000)	-6.702 (0.999)	-0.001 (0.000)	0.001 (-0.000)	0.145 (-0.107)	0.001 (-0.000)	-0.001 (0.000)	-0.028 (0.014)
(22)	78 (C-CO)	5.137	-2.669 (-0.250)	0.775 (0.989)	-3.330 (-0.337)	0.153 (-0.028)	-0.018 (-0.089)	-0.051 (-0.003)	0.000 (-0.018)	-0.008 (0.031)	0.023 (-0.009)
	100 (C-Cd)	4.641	0.733 (0.732)	-2.530 (0.300)	-3.319 (0.245)	0.466 (-0.447)	0.068 (-0.098)	-0.030 (-0.182)	-0.047 (-0.024)	0.005 (0.025)	0.000 (0.048)
	254 (C-C)	7.817	-0.002 (0.000)	0.002 (0.000)	-7.945 (-1.500)	0.002 (0.000)	-0.002 (-0.000)	0.134 (0.092)	-0.001 (-0.000)	0.001 (0.000)	-0.006 (-0.012)
	292 (C-C)	9.623	0.000 (-0.000)	0.000 (0.000)	-9.958 (-0.051)	0.000 (0.000)	0.000 (-0.000)	0.310 (0.155)	0.000 (-0.000)	0.000 (0.000)	0.060 (-0.109)
(23)	34 (C-CO)	6.927	-7.181 (-0.417)	0.072 (1.231)	0.687 (0.206)	0.010 (-1.143)	-0.738 (0.062)	-0.148 (0.349)	0.377 (0.184)	0.119 (-0.147)	-0.181 (-0.036)
	69 (C-CO)	3.142	-1.568 (-1.315)	-0.346 (-1.958)	-1.076 (1.864)	-0.595 (0.216)	0.289 (0.106)	0.142 (0.247)	0.070 (-0.404)	0.186 (-0.156)	-0.245
	125 (CO-CH3)	1.491	0.038 (-0.026)	-0.015 (0.042)	-1.456 (0.630)	0.032 (0.024)	-0.035 (-0.001)	-0.005 (-0.214)	-0.006 (0.020)	-0.008 (-0.019)	0.000 (-0.018)
(24)	79 (CO-C)	5.550	-2.936 (2.154)	-1.066 (2.500)	-2.002 (1.364)	0.451 (0.468)	0.002 (0.204)	0.040 (0.032)	-0.026 (0.000)	-0.007 (0.009)	-0.005 (0.002)
	96 (CO-C)	5.113	1.078 (0.254)	-3.063 (1.819)	-4.021 (0.392)	0.249 (0.516)	1.231 (0.183)	0.954 (0.071)	-0.019 (0.188)	-0.798 (0.096)	-0.941 (0.080)
	222 (C-C)	5.954	-0.047	0.112	-6.052	-0.101	-0.007	0.087	0.053	-0.009	0.011
(25)	62 (CO-C)	5.265	-2.718 (2.923)	-0.532 (0.715)	-2.442 (0.972)	0.462 (0.367)	-0.064 (0.216)	0.044 (0.022)	-0.017 (0.017)	0.003 (0.021)	-0.002 (0.009)
	68 (CO-C)	5.292	-2.715 (2.966)	-0.382 (0.776)	-2.562 (0.600)	0.321 (0.498)	0.011 (0.214)	0.028 (0.019)	0.014 (0.049)	0.005	-0.005 (-0.006)
	222, 254 (C-C)	6.847	0.015	-0.094	-6.889	0.111	-0.028	0.040	0.011	-0.018	0.004
(26)	128 (CO-Cd)	11.208	-0.834	-11.449	0.152	0.902	0.094	-0.128	0.053	0.042	-0.041
	160 (CO-C)	2.969	0.091	0.079	-3.012	-0.078	-0.103	0.056	0.002	0.002	-0.006
(27)	53 (CO-C)	5.962	-3.521 (1.093)	1.081 (1.912)	-1.958 (2.211)	-0.928 (1.058)	-0.301 (0.645)	-0.197 (0.204)	0.067 (0.277)	-0.181 (0.021)	0.028 (0.038)
	65 (CO-C)	4.810	-3.571 (1.338)	-0.049 (0.855)	-1.085 (2.262)	-0.045 (0.358)	-0.018 (0.150)	-0.060 (0.040)	0.021 (0.019)	0.010 (0.026)	-0.031 (0.001)
	98 (CO-Cd)	12.511	-1.182 (0.049)	-13.122 (1.030)	0.506 (0.339)	1.586 (0.197)	-0.223 (0.054)	-0.195 (0.186)	0.124 (0.050)	0.044 (0.070)	-0.050
	223 (C-C)	6.204	0.003 (0.045)	-0.044 (0.005)	-6.319 (0.086)	0.035 (0.011)	0.014 (0.029)	0.139 (0.089)	-0.019 (0.015)	0.008 (0.020)	-0.022
(28)	54 (CO-C)	5.931	-2.178 (2.855)	-0.339 (0.435)	-3.160 (0.415)	-0.382 (0.396)	0.077 (0.002)	0.040 (0.017)	0.003 (0.019)	0.009 (0.008)	
	81 (Cd-C)	7.231	-4.190 (4.993)	-0.020 (0.116)	-2.714 (1.566)	-0.446 (0.161)	0.041 (0.110)	0.044 (0.077)	0.065 (0.010)	-0.005 (0.000)	0.001 (0.000)
	119 (CO-Cd)	11.319	-1.313	-10.786	-0.161	0.896	0.128	-0.141	0.062	0.028	-0.030
(29)	55 (CO-Cd)	8.947	-4.076 (1.483)	-5.294 (4.440)	0.364 (0.630)	0.269 (1.526)	-0.092 (0.521)	-0.031 (0.052)	0.085 (0.073)	-0.120 (0.044)	-0.052
	78 (CO-Cd)	7.632	-2.467 (0.447)	-5.502 (1.984)	-1.210 (0.718)	1.706 (1.458)	-0.261 (0.340)	0.166 (0.310)	-0.006 (0.061)	-0.020 (0.265)	0.001 (0.125)
	191 (Cd-C)	4.200	0.000 (0.000)	0.000 (0.000)	-4.202 (0.243)	0.000 (0.000)	0.000 (0.000)	0.015 (0.042)	0.000 (0.000)	0.000 (0.000)	-0.013
(30)	39 (CO-C)	3.759	-1.996 (1.939)	-1.152 (0.369)	-0.724 (1.813)	0.219 (0.215)	0.009 (0.110)	-0.075 (0.296)	-0.002 (0.077)	-0.023 (0.026)	-0.016
	44 (CO-C)	6.506	-3.289 (6.580)	-1.213 (0.182)	-1.084 (0.470)	-1.055 (0.662)	-0.412 (0.813)	-0.012 (0.462)	0.099 (0.608)	0.271 (0.273)	0.189
	68 (CO-C)	3.444	-1.686 (0.875)	-0.624 (2.086)	-0.959 (1.803)	-0.683 (0.280)	0.422 (0.164)	0.147 (0.348)	-0.009 (0.428)	0.214 (0.030)	-0.266
	98 (Cd-C)	7.644	-4.191 (4.942)	-0.562 (0.636)	-2.538 (1.418)	-0.566 (0.140)	0.101 (0.009)	0.017 (0.017)	0.132 (0.026)	-0.001 (0.060)	-0.046 (0.004)
(31)	68 (CO-Cd)	8.226	-4.946	0.160	-2.916	-0.610	0.145	-0.057	-0.006	0.014	-0.010
	113 (CO-C)	11.308	-1.312	-10.752	-0.175	0.869	0.156	-0.151	0.061	0.032	-0.035
	236 (C-C)	5.949	0.000 (0.000)	0.000 (0.000)	-6.003 (0.051)	0.000 (0.000)	0.000 (0.000)	0.073 (0.007)	0.000 (0.000)	0.000 (0.000)	-0.019
(32)	47, 92 (CO-Cd)	7.420	-5.953 (3.436)	0.376 (0.678)	0.000 (0.136)	-1.058 (1.799)	-0.221 (0.128)	-0.609 (0.000)	0.040 (0.022)	-0.078 (0.475)	-0.132 (0.056)
	181, 188 (Cd-C)	4.102	-0.109 (0.039)	0.088 (0.074)	-4.163 (0.458)	0.020 (0.113)	0.020 (0.113)	0.007 (0.058)	0.088 (0.074)	-0.109 (0.039)	0.054
(33)	49 (CO-Cd)	10.778	-3.630 (0.021)	-7.772 (0.350)	0.377 (0.049)	0.710 (0.081)	-0.515 (0.288)	0.033 (0.045)	-0.022 (0.067)	0.006 (0.065)	0.035
	74 (CO-C)	8.490	-6.451 (2.185)	2.704 (0.682)	-4.372 (0.935)	-0.500 (1.030)	-0.071 (0.396)	0.033 (0.367)	0.343 (0.235)	-0.316 (0.129)	0.142
	101 (Cd-C)	8.070	-4.800 (5.720)	-0.119 (0.673)	-2.842 (1.640)	-0.466 (0.169)	0.049 (0.133)	0.047 (0.080)	0.072 (0.012)	-0.005 (0.005)	-0.001 (0.000)
	195 (Cd-C)	4.365	0.000 (0.000)	0.000 (0.000)	-4.327 (0.101)	0.000 (0.000)	0.000 (0.000)	-0.026 (0.026)	0.000 (0.000)	0.000 (0.000)	-0.012

Table S18. Fourier coefficients for hindered potential of internal rotations in molecules of Group 3.

		a0 (b0)	a1 (b1)	a2 (b2)	a3 (b3)	a4 (b4)	a5 (b5)	a6 (b6)	a7 (b7)	a8 (b8)	a9 (b9)
(34)	71 (CO-Cd)	12.723	-1.714	-11.054	-1.261	1.346	-0.029	0.052	-0.100	0.039	-0.002
	159 (Cd-C)	3.257	0.000 (-0.063)	-0.059 (-0.001)	-3.421 (-0.099)	0.049 (0.002)	0.002 (-0.040)	0.180 (-0.035)	-0.003 (0.021)	0.011 (0.002)	-0.015
	210 (CO-Cd)	44.362	-26.520	-18.890	-2.999	5.517	-1.819	0.833	-1.293	1.373	-0.564
	649 (CO-H)	52.430	-30.977	-19.663	-1.816	-0.418	0.073	0.130	0.041	0.144	0.057
(35)	67 (Cd-C)	7.999	0.961 (1.896)	-5.728 (0.260)	-4.609 (-0.405)	1.175 (0.332)	0.246 (0.117)	0.037 (0.069)	-0.145 (-0.057)	0.030 (-0.034)	0.034
	94 (CO-C)	6.884	-2.354 (4.689)	-2.892 (0.728)	-1.630 (-2.480)	0.188 (-0.118)	-0.167 (0.071)	-0.033 (-0.030)	0.000 (-0.033)	0.005 (-0.001)	0.000
	245 (C-C)	6.380	-0.023	0.218	-6.488	-0.188	0.051	0.113	-0.031	-0.031	0.000
	463 (Cd-OH)	12.191	-2.216 (-1.056)	-7.865 (3.213)	-3.396 (-2.214)	1.879 (-0.083)	-0.363 (1.118)	-0.787 (-0.468)	0.675 (-0.616)	0.307 (0.827)	-0.425
(36)	70 (Cd-C)	6.367	0.651 (1.589)	-2.556 (0.832)	-4.756 (-1.130)	0.340 (1.039)	0.034 (0.076)	-0.064 (0.153)	-0.060 (-0.122)	-0.021 (-0.003)	0.065
	89 (CO-C)	6.682	-2.365 (5.889)	-3.119 (-0.228)	-1.121 (-2.856)	0.140 (0.098)	-0.254 (0.049)	0.032 (-0.016)	-0.019 (-0.080)	0.019 (-0.009)	0.004
	261 (C-C)	7.119	0.004 (0.005)	-0.003 (0.007)	-7.310 (1.207)	-0.001 (-0.013)	0.015 (-0.002)	0.181 (-0.114)	-0.017 (0.002)	-0.002 (-0.016)	0.013
	321 (C-C)	10.998	-0.221	1.509	-10.803	-1.340	-0.184	-0.210	0.316	-0.130	0.066
	455 (Cd-OH)	11.112	-2.092 (-2.617)	-5.990 (3.618)	-4.157 (-0.820)	0.666 (-1.294)	0.925 (0.275)	-0.081 (0.850)	-0.770 (-0.080)	0.037 (-0.695)	0.348
(37)	36 (CO-C)	4.509	-5.400 (-0.060)	1.438 (0.089)	-1.163 (-0.136)	0.875 (0.083)	-0.277 (-0.053)	0.057 (0.035)	-0.117 (-0.011)	0.175 (-0.005)	-0.098
	57 (CO-C)	4.207	-2.926 (2.455)	-0.235 (1.331)	-1.002 (-1.736)	-0.431 (-0.156)	0.205 (-0.074)	0.204 (-0.353)	0.069 (0.389)	0.140 (0.117)	-0.231
	116 (CO-Cd)	40.742	-23.939	-20.053	1.220	2.447	-0.189	-0.185	-0.134	-0.111	0.202
	802 (Cd-OH)	44.540	-24.443	-18.440	-1.505	-0.317	0.063	0.148	-0.075	0.050	-0.021
(38)	313 (CO-Cd)	55.968	-26.973	-32.436	0.662	3.223	-0.450	-0.361	0.417	0.081	-0.131
	506 (Cd-OH)	21.557	-6.060	-15.939	0.523	-0.028	-0.244	-0.081	0.038	0.149	0.085
	901 (Cd-OH)	59.944	-39.228	-15.380	-5.668	0.920	-1.012	1.067	-0.833	0.559	-0.368
(39)	47 (Cd-O)	4.312	-0.795	-3.456	-0.772	1.104	-0.671	0.510	-0.381	0.344	-0.196
	92 (Cd-O)	8.619	-0.398 (0.144)	-6.739 (5.655)	0.139 (-0.239)	0.186 (-1.055)	-0.171 (-0.970)	-0.386 (-0.668)	-0.420 (-0.352)	-0.532 (-0.193)	-0.298
	168 (Cd-CO)	18.846	-1.685	-20.097	1.399	1.942	-0.379	-0.151	0.205	-0.006	-0.072
(40)	74 (CO-C)	6.282	-3.270 (0.088)	0.048 (0.372)	-3.124 (0.329)	0.053 (-0.066)	-0.023 (0.057)	0.004 (-0.027)	0.028 (0.018)	-0.009 (-0.000)	0.012
	203 (Cd-C)	9.455	-1.935 (0.505)	-5.350 (-0.588)	-3.109 (-1.318)	0.760 (0.640)	0.277 (0.078)	-0.063 (0.053)	-0.074 (-0.098)	0.010 (-0.001)	0.029
	228 (C-C)	6.908	0.027 (-0.024)	-0.004 (0.028)	-7.076 (0.035)	0.006 (0.011)	-0.010 (-0.014)	0.164 (-0.014)	-0.018 (0.010)	-0.001 (-0.016)	0.005
	497 (Cd-OH)	12.007	-2.963	-6.764	-2.197	-0.121	0.132	-0.084	0.009	0.014	-0.035
(41)	104 (CO-C)	14.110	-4.551 (-1.093)	-6.944 (-3.307)	-2.774 (-0.094)	-0.208 (0.636)	0.216 (0.027)	0.139 (-0.118)	0.012 (-0.060)	-0.032 (0.078)	0.033
	112 (Cd-C)	9.561	-0.068	0.808	-9.598	-0.675	-0.026	0.056	0.083	-0.134	-0.008
	253 (C-C)	7.600	0.125	-0.366	-7.793	0.277	-0.064	0.240	-0.058	0.077	-0.039
	291 (C-C)	16.291	-7.842 (4.333)	-2.617 (4.531)	2.788 (2.618)	-0.803 (-0.938)	-3.123 (0.983)	-2.048 (2.581)	0.433 (0.574)	-1.331 (-1.244)	-1.748
	623 (C-C)	13.292	-11.932 (-6.429)	-0.203 (-0.206)	-0.464 (5.153)	-1.683 (-3.246)	2.397 (1.469)	-2.095 (0.540)	0.638 (-1.379)	0.890 (1.316)	-0.840
(42)	87 (CO-C)	12.236	-7.649 (5.564)	-4.536 (-0.011)	-0.712 (-2.434)	0.673 (-0.165)	0.090 (-0.069)	-0.132 (-0.052)	0.035 (-0.020)	0.020 (0.062)	-0.024
	143 (Cd-C)	15.467	-8.989 (-11.04)	-0.682 (2.309)	-6.743 (3.478)	0.298 (0.091)	0.368 (0.040)	0.507 (-0.926)	-0.041 (-0.094)	-0.254 (0.010)	0.000 (0.283)
	522 (Cd-OH)	10.717	-6.328 (7.194)	-3.187 (-6.449)	-0.550 (2.085)	-0.206 (0.966)	-0.740 (-0.096)	0.052 (-0.688)	0.642 (0.068)	-0.061 (0.647)	-0.340
(43)	52 (Cd-C)	3.730	-2.575 (-4.460)	-2.056 (3.561)	1.867 (1.013)	-0.843 (-1.459)	-0.192 (0.332)	-0.373 (-5.132)	0.490 (0.848)	0.576 (-0.998)	-0.623
	159 (CO-C)	5.424	-5.938	2.691	-1.141	-0.812	-0.172	0.189	-0.292	0.170	-0.119
	762 (Cd-OH)	12.489	-10.247	-1.281	-3.304	5.115	-5.294	5.156	-4.817	4.203	-2.019
(44)	73 (CO-C)	10.850	-7.681 (8.367)	-4.551 (-1.979)	0.866 (-2.831)	0.690 (0.572)	-0.252 (0.038)	0.026 (-0.190)	0.074 (-0.030)	-0.001 (0.040)	-0.022
	102 (CO-C)	10.332	-2.989 (0.663)	-4.203 (0.008)	-0.876 (-0.839)	-1.445 (2.147)	0.750 (0.020)	-1.415 (-0.734)	0.773 (1.000)	-1.953 (-0.856)	1.026
	152 (C-C)	20.232	-6.672 (3.386)	-1.772 (-2.165)	-11.725 (-0.132)	-0.336 (0.544)	-0.675 (-0.519)	1.594 (-0.595)	-0.007 (0.532)	-0.512 (0.620)	-0.568 (-0.331)
	230 (C-C)	7.940	0.025 (-0.038)	-0.036 (0.004)	-8.508 (0.303)	0.028 (0.044)	-0.032 (-0.056)	0.115 (0.585)	-0.009 (0.003)	-0.014 (0.018)	0.492
	549 (C-OH)	11.959	4.141 (0.576)	-5.105 (2.804)	-5.445 (-4.290)	-0.964 (-1.296)	-0.906 (-0.080)	-1.040 (0.208)	-1.045 (0.251)	-0.815 (0.224)	-0.646 (0.155)
(45)	45 (CO-C)	2.643	-1.102 (1.908)	-0.599 (-1.038)	-0.722 (-1.098)	-0.208 (0.359)	-0.039 (-0.067)	0.138 (4.622)	-0.023 (0.039)	-0.112 (-0.194)	0.024
	118 (CO-Cd)	58.918	-33.462 (6.344)	-27.435 (2.589)	-0.220 (1.749)	2.020 (-3.159)	0.565 (5.266)	-0.042 (-3.300)	-0.092 (1.961)	-0.066 (-4.011)	-0.186
	243 (C-C)	6.126	0.037 (7.363)	0.000 (-1.447)	-6.141 (4.923)	-0.006 (7.307)	-0.030 (1.490)	0.073 (-1.461)	-0.010 (1.650)	-0.006 (1.118)	-0.043
	491 (Cd-OH)	20.868	-6.495 (-2.061)	-15.400 (4.699)	1.037 (-5.879)	0.111 (3.229)	-0.215 (5.688)	0.145 (-2.034)	-0.071 (2.170)	0.028 (-4.747)	-0.006
	782 (Cd-OH)	59.279	-41.584 (5.397)	-14.387 (-4.754)	-4.403 (4.618)	1.281 (1.331)	-0.785 (4.145)	0.979 (1.789)	-0.912 (5.443)	1.132 (-2.485)	-0.600

262

Table S18. Fourier coefficients for hindered potential of internal rotations in molecules of Group 3 (continuation).

		a0 (b0)	a1 (b1)	a2 (b2)	a3 (b3)	a4 (b4)	a5 (b5)	a6 (b6)	a7 (b7)	a8 (b8)	a9 (b9)
(46)	62 (CO-C)	2.626	-2.253 (1.067)	-1.313 (-4.333)	1.211 (-1.081)	-0.185 (3.544)	0.291 (2.050)	-0.329 (2.520)	0.146 (1.704)	-0.239 (-3.950)	0.043
	106 (CO-Cd)	42.600	-23.084 (-5.353)	-20.348 (-1.439)	-0.461 (-1.269)	0.569 (6.791)	0.827 (-1.303)	0.041 (1.591)	-0.112 (4.837)	0.196 (-9.562)	-0.227
	238 (C-C)	6.065	-0.029 (-4.470)	-0.063 (-4.549)	-6.030 (7.172)	-0.038 (-4.282)	-0.052 (-5.047)	0.138 (-2.620)	-0.011 (7.512)	0.001 (6.527)	0.019
	822 (Cd-OH)	46.088	-26.314 (-3.251)	-17.951 (-2.823)	-1.670 (-2.831)	-0.372 (3.805)	0.148 (2.167)	0.058 (3.214)	0.035 (-2.303)	-0.057 (-3.268)	0.035
(47)	101 (CO-C)	1.698	-0.235 (0.407)	-0.009 (-0.016)	-1.471 (1.087)	0.008 (-0.013)	0.021 (0.037)	-0.015 (-2.308)	-0.003 (0.005)	0.002 (0.002)	0.005
	122, 834 (CO-Cd)	46.352	-26.299 (-9.141)	-18.323 (-4.920)	-1.489 (-7.618)	-0.569 (5.128)	0.342 (-1.345)	-0.133 (1.967)	0.237 (7.028)	-0.256 (-4.560)	0.138
(48)	251 (CO-Cd)	39.185	-17.143 (-5.049)	-23.647 (1.120)	0.122 (-6.969)	1.683 (3.805)	-0.219 (1.185)	-0.079 (3.566)	0.156 (-1.841)	-0.008 (-6.519)	-0.051
	819 (Cd-OH)	42.932	-23.835 (-6.339)	-17.854 (-1.905)	-1.382 (-9.922)	0.068 (1.904)	0.089 (-3.137)	0.162 (-4.051)	-0.055 (5.007)	-0.096 (-9.061)	-0.030
(49)	69 (CO-C)	0.681	0.000 (-0.000)	0.000 (-0.000)	-0.693 (0.008)	0.000 (0.000)	0.000 (0.000)	0.016 (0.009)	0.000 (-0.000)	0.000 (-0.000)	-0.005
	137 (CO-Cd)	59.303	-33.750	-28.270	0.089	2.610	0.286	-0.045	-0.101	-0.077	-0.044
	494 (Cd-OH)	21.099	-6.406	-15.493	0.703	0.165	-0.061	0.019	0.001	-0.010	-0.018
	908 (Cd-OH)	61.280	-40.203	-15.855	-5.554	1.008	-1.232	1.258	-1.150	1.072	-0.623
(50)	77 (CO-Cd)	12.801	-1.335	-11.216	-1.829	1.710	-0.059	-0.096	0.004	0.041	-0.020
	150 (CO-Cd)	57.994	-30.471	-29.301	-2.178	4.409	0.276	-1.469	1.204	-0.576	0.112
	502 (Cd-OH)	21.411	-6.315	-15.806	0.638	0.139	-0.086	0.010	0.004	0.011	-0.005
	939 (Cd-OH)	63.236	-41.530	-16.531	-5.603	0.849	-1.127	1.225	-1.063	1.143	-0.598
(51)	155 (Cd-C)	3.372	0.094 (-2.454)	-0.046 (5.529)	-3.400 (1.048)	0.043 (9.393)	-0.096 (-2.900)	0.034 (-4.345)	-0.005 (5.791)	0.003 (5.660)	0.000
	186 (CO-Cd)	42.975	-19.436 (1.793)	-25.782 (-5.700)	0.203 (-2.802)	2.147 (1.233)	-0.161 (3.729)	-0.047 (3.482)	0.270 (2.798)	-0.056 (-5.778)	-0.114
	828 (Cd-OH)	48.889	-27.776 (-1.070)	-19.379 (-1.724)	-1.743 (-9.177)	-0.150 (3.953)	0.026 (1.028)	0.153 (8.163)	0.000 (4.744)	-0.016 (-5.948)	-0.004

Table S19. Fourier coefficients for hindered potential of internal rotations in molecules of Group 4 and 5.

		a0	a1 (b1)	a2 (b2)	a3 (b3)	a4 (b4)	a5 (b5)	a6 (b6)	a7 (b7)	a8 (b8)	a9 (b9)
(52)	69 (CO-O)	9.927	-6.658	-4.194	0.802	0.261	-0.125	-0.025	0.012	-0.002	0.003
	304 (O-Cd)	28.846	-10.125 (-0.027)	-19.227 (0.026)	-0.028 (-0.001)	0.436 (-0.024)	-0.049 (0.026)	0.193 (0.000)	-0.047 (-0.025)	-0.068 (0.025)	0.068
(53)	33 (CO-C)	4.439	-2.618 (0.429)	-1.905 (0.286)	-0.528 (-0.121)	1.074 (-0.288)	0.205 (0.584)	-0.419 (0.401)	-0.345 (-0.139)	0.004 (-0.242)	0.092
	52 (CO-C)	5.037	-3.608 (-2.805)	-0.191 (-2.655)	-1.818 (2.611)	0.547 (-0.020)	0.117 (0.021)	-0.015 (-0.233)	-0.163 (0.053)	0.014 (0.124)	0.078
	71 (O-Cd)	10.298	-7.192 (0.004)	-3.868 (-0.026)	0.697 (-0.027)	0.249 (0.001)	-0.152 (0.002)	-0.035 (-0.000)	0.015 (0.000)	-0.010 (0.001)	-0.002
	152 (CO-O)	32.968	-18.091 (-0.445)	-14.469 (-0.232)	-1.060 (0.359)	0.543 (-0.403)	0.071 (0.402)	-0.022 (-0.312)	0.185 (0.221)	-0.280 (-0.115)	0.155
(54)	70 (CO-Cd)	26.585	-11.647 (-2.622)	-11.252 (0.916)	-4.121 (1.161)	-0.140 (-0.641)	0.196 (-0.557)	0.510 (-0.238)	0.267 (0.382)	-0.190 (0.433)	-0.207
	72 (O-Cd)	4.737	0.361 (0.992)	-2.417 (2.014)	-2.538 (-1.466)	0.068 (-0.467)	-0.197 (0.034)	0.052 (0.118)	-0.093 (0.110)	-0.026 (-0.003)	0.053
	144 (CO-O)	13.834	-0.919 (-0.032)	-14.196 (-0.048)	0.094 (-0.012)	1.499 (-0.003)	-0.232 (-0.001)	-0.190 (0.001)	0.118 (0.000)	0.027 (-0.000)	-0.034
	205 (Cd-C)	4.327	0.012 (-0.004)	-1.286 (0.007)	-4.608 (-0.008)	1.051 (0.008)	0.101 (-0.006)	0.339 (0.003)	-0.118 (-0.002)	0.233 (0.000)	-0.052
(55)	124 (CO-Cd)	13.813	-0.799	-14.238	0.061	1.424	-0.194	-0.173	0.094	0.055	-0.044
	706 (CO-OH)	36.861	-14.505	-20.502	-1.884	0.396	-0.052	-0.065	-0.098	-0.097	-0.053
(56)	44 (CO-C)	3.590	0.509 (-1.634)	-1.384 (0.151)	-1.999 (1.439)	-0.156 (0.962)	-0.139 (-0.124)	-0.021 (-0.059)	-0.156 (0.163)	-0.264 (-0.085)	0.021
	68 (CO-C)	3.977	0.366 (2.016)	-1.838 (0.787)	-2.390 (-1.083)	0.433 (0.012)	-0.208 (-0.079)	-0.114 (0.209)	-0.262 (-0.066)	0.005 (0.002)	-0.066 (-0.184)
	235 (C-C)	7.744	-0.057 (0.019)	-0.024 (0.030)	-7.843 (-0.005)	0.025 (0.026)	0.059 (0.017)	0.096 (-0.035)	-0.002 (-0.000)	-0.001 (-0.003)	0.004
	280 (C-C)	7.470	-0.048 (0.045)	0.005 (0.084)	-7.662 (-0.566)	-0.011 (0.081)	0.048 (0.037)	0.198 (0.051)	-0.001 (-0.015)	-0.006 (-0.002)	0.006
	655 (CO-OH)	36.248	-18.532 (-5.917)	-12.888 (2.599)	-5.321 (4.555)	-1.480 (-3.473)	2.437 (-0.075)	-1.069 (0.738)	0.979 (-1.369)	0.913 (2.224)	-1.288
(57)	54 (CO-C)	4.717	-1.542 (0.102)	-1.810 (1.735)	-1.472 (-0.922)	0.023 (-0.270)	0.054 (0.001)	0.038 (0.092)	-0.004 (-0.004)	-0.008 (0.005)	0.015 (0.000)
	95 (Cd-C)	6.727	-3.715 (-4.427)	0.029 (-0.166)	-2.821 (1.628)	-0.458 (-0.166)	0.029 (0.079)	0.045 (-0.078)	0.099 (-0.013)	0.027 (0.023)	0.000 (-0.008)
	560 (CO-OH)	36.384	-14.923	-20.088	-0.912	-0.063	-0.063	-0.090	-0.103	-0.088	-0.056

263

Table S20. Thermochemical properties for acyclic base compounds from the GAVs calculated in this work.

		ΔH_f^o, Kcal/mol	S_{intr}, cal/mol K	Cp, cal/mol k						
				300 K	400 K	500 K	600 K	800 K	1000 K	1500 K
				Group 1. Ethers and alcohols.						
(1)	Ethene-1,1-diol	-75.66	67.55	18.87	23.25	26.56	28.88	31.75	33.57	36.56
(2)	1-Methoxy-ethenol	-71.93	77.76	23.83	29.55	34.02	37.51	42.40	45.77	50.87
(3)	1-Vinyloxy-ethenol	-48.26	83.58	27.67	33.42	37.84	41.25	46.28	49.94	55.82
(4)	1-Methoxy-1-vinyloxy-ethene	-42.76	94.49	30.10	37.58	43.73	48.74	56.28	61.70	69.91
(5)	1-(1-Hydroxy-vinyloxy)-ethenol	-91.60	93.98	27.33	33.57	38.67	43.12	50.30	55.70	63.90
(6)	1-(1-Methoxy-vinyloxy)-ethenol	-88.01	101.33	36.90	44.39	50.25	54.90	61.88	66.94	74.84
(7)	Vinyloxy-ethene	-2.05	77.83	21.48	26.67	31.06	34.68	40.24	44.32	50.67
(8)	Methoxy-ethene	-25.23	71.95	19.76	24.54	28.27	31.39	36.27	39.91	45.52
(9)	Propene-1,2-diol	-78.84	80.60	25.11	29.10	32.56	35.53	40.28	43.88	49.71
(10)	Ethenol	-28.95	61.75	14.80	18.24	20.81	22.77	25.61	27.71	31.21
(11)	Propen-2-ol	-40.10	71.24	19.98	25.01	29.11	32.27	36.84	40.15	45.46
(12)	Ethoxy-ethene	-33.33	79.75	26.21	32.44	37.32	41.42	47.86	52.69	60.15
(13)	1-(2-Hydroxy-vinyloxy)-ethenol	-88.66	88.49	31.15	38.71	44.43	48.54	53.75	56.95	61.78
(14)	1,1-Dimethoxy-ethene	-65.98	91.72	27.33	33.57	38.67	43.12	50.30	55.70	63.90
(15)	1-Ethoxy-1-methoxy-ethene	-74.21	100.80	33.95	41.05	47.17	52.63	61.48	68.13	78.23
				Group 2. Aldehydes and ketones.						
(16)	Penta-1,4-dien-3-one	-0.77	81.18	25.54	31.01	35.79	39.76	45.87	50.20	56.65
(17)	Propenal	-15.05	66.56	16.82	20.37	23.45	26.05	30.08	32.97	37.24
(18)	2-Methyl-propenal	-24.99	78.18	21.48	26.67	31.06	34.68	40.24	44.32	50.67
(19)	But-3-enal	-17.70	79.56	21.39	26.13	30.45	34.13	39.91	44.18	50.73
(20)	Malonaldehyde	-60.61	76.81	18.60	22.36	25.74	28.63	33.17	36.46	41.37
(21)	2-Methyl-but-3-enal	-25.94	87.15	29.02	34.38	39.41	43.84	51.03	56.45	64.90
(22)	2,2-Dimethyl-but-3-enal	-34.46	95.88	33.12	40.67	47.51	53.34	62.44	69.13	79.39
(23)	3-Oxo-butyraldehyde	-74.54	88.65	23.96	29.13	33.77	37.75	43.98	48.54	55.44
(24)	2-Methyl-malonaldehyde	-67.98	87.41	25.40	30.14	34.45	38.21	44.24	48.71	55.53
(25)	2,2-Dimethyl-malonaldehyde	-77.20	95.26	31.62	38.17	43.58	48.25	55.73	61.33	69.81
(26)	But-3-en-2-one	-26.43	78.76	21.60	26.38	30.75	34.48	40.30	44.53	50.93
(27)	2-Methyl-3-oxo-pent-4-enal	-57.74	100.62	34.20	41.03	47.21	52.50	60.75	66.72	75.65
(28)	Hexa-1,5-dien-3-one	-5.79	91.43	31.89	38.13	43.90	48.84	56.57	62.20	70.77
(29)	2-Methyl-penta-1,4-dien-3-one	-10.72	90.93	31.83	38.50	44.59	49.74	57.37	62.94	71.69
(30)	3-Oxo-hex-5-enal	-53.76	102.02	32.89	40.07	46.42	51.79	60.09	66.12	75.26
(31)	Pent-1-en-3-one	-32.59	86.48	29.06	34.90	40.12	44.61	51.75	57.06	65.25
(32)	2,4-Dimethyl-penta-1,4-dien-3-one	-19.05	102.26	36.61	44.94	51.83	57.59	66.77	73.62	84.19
(33)	2-Methyl-hexa-1,5-dien-3-one	-15.68	100.24	37.44	45.71	52.83	58.74	67.92	74.65	84.99
				Group 3. Carbonyl (C=O) and hydroxyl and alkoxyl groups.						
(34)	5-Hydroxy-hexa-1,4-dien-3-one	-71.09	93.32	33.32	41.01	47.66	53.21	61.86	68.27	78.54
(35)	3-Hydroxy-2-methyl-but-3-enal	-72.03	93.29	32.23	38.77	44.56	49.35	56.66	61.95	70.05
(36)	3-Hydroxy-2,2-dimethyl-but-3-enal	-83.35	101.29	37.78	46.22	53.47	59.40	68.35	74.78	84.59
(37)	5-Hydroxy-3-oxo-pent-4-enal	-101.89	93.19	30.11	36.81	42.54	47.36	54.88	60.54	69.45
(38)	3,3-Dihydroxy-propenal	-119.13	75.29	22.54	28.00	32.53	36.10	41.21	44.72	50.30
(39)	3-Vinyloxy-propenal	-31.65	88.69	27.68	33.74	39.07	43.52	50.27	55.05	62.02
(40)	4-Hydroxy-2-methyl-but-3-enal	-67.42	93.78	35.16	41.59	46.62	50.72	57.16	62.08	69.99
(41)	4-Hydroxy-2,2-dimethyl-but-3-enal	-77.76	99.13	37.35	46.82	55.03	61.60	70.89	77.08	86.08
(42)	3-Hydroxy-but-3-enal	-63.43	83.88	26.22	31.90	36.81	40.82	46.79	50.92	56.90
(43)	4-Hydroxy-but-3-enal	-61.11	86.95	24.43	30.02	34.75	38.69	44.72	49.08	55.69
(44)	2-Hydroxymethyl-2-methyl-malonal	-114.04	97.37	37.54	45.75	51.97	56.93	64.15	69.14	76.36
(45)	1,1-Dihydroxy-pent-1-en-3-one	-140.55	94.34	33.00	41.23	48.28	54.03	62.56	68.59	78.05
(46)	1-Hydroxy-pent-1-en-3-one	-85.66	90.01	29.46	36.48	42.67	47.96	56.40	62.86	73.27
(47)	4-Hydroxy-but-3-en-2-one	-78.94	80.87	23.62	29.31	34.33	38.61	45.37	50.56	59.06
(48)	3-Hydroxy-propenal	-65.33	71.02	18.64	22.93	26.68	29.91	35.10	39.11	45.26
(49)	4,4-Dihydroxy-but-3-en-2-one	-133.14	85.49	27.31	34.23	40.09	44.80	51.67	56.43	63.93
(50)	1,1-Dihydroxy-penta-1,4-dien-3-one	-110.10	86.71	31.84	39.57	45.76	50.62	57.64	62.44	69.90
(51)	3-Hydroxy-butenal	-78.94	80.27	24.26	29.67	34.61	38.85	45.64	50.83	59.11
				Group 4. Ester group.						
(52)	Formic acid vinyl ester	-61.83	73.09	19.54	23.93	27.86	31.04	35.77	38.94	43.09
(53)	3-Oxo-propionic acid vinyl ester	-96.82	94.95	31.70	38.17	43.81	48.43	55.56	60.71	68.02
(54)	2-Methyl-acrylic acid vinyl ester	-58.21	97.58	33.71	41.42	48.11	53.92	62.92	69.24	77.91
				Group 5. Carboxylic acids.						
(55)	Acrylic acid	-77.01	72.67	30.89	39.01	44.56	48.62	53.67	56.92	62.12
(56)	2,2-Dimethyl-3-oxo-propionic acid	-140.10	100.61	33.24	40.80	47.11	52.51	61.05	67.37	76.52
(57)	But-3-enoic acid	-81.50	83.50	24.85	30.33	35.19	39.30	45.78	50.57	57.54

Table S21. Correction for ring formation and substituent position Cp 400 – 600 K.

		Cp 400 K		Cp 500 K		Cp 600 K	
		RC	SC	RC	SC	RC	SC
	Diketenes						
1c)	Diketene	-2.91		-3.30		-3.56	
2c)	Me_diketene	-2.91	-1.27	-3.30	-0.76	-3.56	-0.45
3c)	MeMe_diketene	-2.91	0.12	-3.30	-0.01	-3.56	-0.12
	Cyclobutanediones						
4c)	Ciclobutanodiona	0.30		0.27		0.20	
5c)	Me_ciclobutanodiona	0.30	-1.00	0.27	-0.79	0.20	-0.61
6c)	2,2 dimetil ciclobutanodiona	0.30	-1.43	0.27	-1.14	0.20	-0.89
7c)	T 2,4 dimetil ciclobutanodiona	0.30	-1.89	0.27	-1.45	0.20	-1.10
	Trimer						
8c)	Ring Trimero de cetena	-4.32		-3.62		-3.01	
9c)	(32) 2 me Trimer	-4.32	0.30	-3.62	-0.18	-3.01	-0.40
10c)	(33) 3 me Trimer	-4.32	0.31	-3.62	-0.17	-3.01	-0.40
11c)	Trimer OH	-4.32	0.37	-3.62	-0.17	-3.01	-0.49
	Enolized form						
12c)	Enolized Form	-2.47		-2.15		-1.91	
13c)	(38) 4 me enolized form	-2.47	-1.03	-2.15	-0.59	-1.91	-0.33
14c)	(39) 2 me enolized form	-2.47	-0.26	-2.15	-0.63	-1.91	-0.78
15c)	(40) 4,4 dime enolized form	-2.47	0.39	-2.15	0.17	-1.91	-0.01
16c)	Enolized form OH	-2.47	-0.38	-2.15	-0.78	-1.91	-0.75
17c)	(34) 2 me Enolized form OH	-2.47	-1.03	-2.15	-1.75	-1.91	-1.84
18c)	(35) 4 me Enolized form OH	-2.47	-1.36	-2.15	-1.28	-1.91	-1.00
19c)	(36) 2,4 dime Enolized form OH	-2.47	-1.97	-2.15	-2.29	-1.91	-2.14
20c)	(37) 4,4 dime Enolized form OH	-2.47	-0.07	-2.15	-0.62	-1.91	-0.75

Table S22. Correction for ring formation and substituent position Cp 800 – 1500 K.

|		Cp 800 K		Cp 1000 K		Cp 1500 K	
		RC	SC	RC	SC	RC	SC
1c)	Diketene	-3.38		-3.02		-3.37	
2c)	Me_diketene	-3.38	-0.14	-3.02	-0.03	-3.37	0.04
3c)	MeMe_diketene	-3.38	-0.20	-3.02	-0.20	-3.37	-0.12
4c)	Ciclobutanodiona	0.22		-0.05		0.25	
5c)	Me_ciclobutanodiona	0.22	-0.37	-0.05	-0.24	0.25	-0.08
6c)	2,2 dimetil ciclobutanodiona	0.22	-0.57	-0.05	-0.39	0.25	-0.05
7c)	T 2,4 dimetil ciclobutanodiona	0.22	-0.66	-0.05	-0.41	0.25	-0.12
8c)	Ring Trimero de cetena	-2.20		-1.61		-0.71	
9c)	(32) 2 me Trimer	-2.20	-0.46	-1.61	-0.36	-0.71	-0.14
10c)	(33) 3 me Trimer	-2.20	-0.50	-1.61	-0.42	-0.71	-0.15
11c)	Trimer OH	-2.20	-0.63	-1.61	-0.53	-0.71	-0.30
12c)	Enolized Form	-1.62		-1.45		-1.17	
13c)	(38) 4 me enolized form	-1.62	-0.10	-1.45	-0.01	-1.17	0.04
14c)	(39) 2 me enolized form	-1.62	-0.76	-1.45	-0.59	-1.17	-0.23
15c)	(40) 4,4 dime enolized form	-1.62	-0.18	-1.45	-0.20	-1.17	-0.14
16c)	Enolized form OH	-1.62	-0.34	-1.45	0.00	-1.17	0.30
17c)	(34) 2 me Enolized form OH	-1.62	-1.37	-1.45	-0.84	-1.17	-0.12
18c)	(35) 4 me Enolized form OH	-1.62	-0.36	-1.45	0.06	-1.17	0.38
19c)	(36) 2,4 dime Enolized form OH	-1.62	-1.47	-1.45	-0.86	-1.17	-0.10
20c)	(37) 4,4 dime Enolized form OH	-1.62	-0.49	-1.45	-0.17	-1.17	0.18
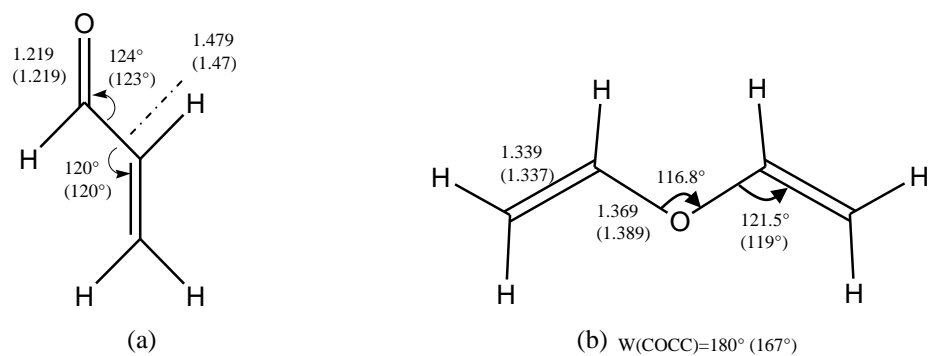
Figure S1. Some calculated geometrical parameters for (a) Acrolein (b) Ethoxy-ethene (longitudes in Å). Experimental data in parenthesis (Ref. 33).
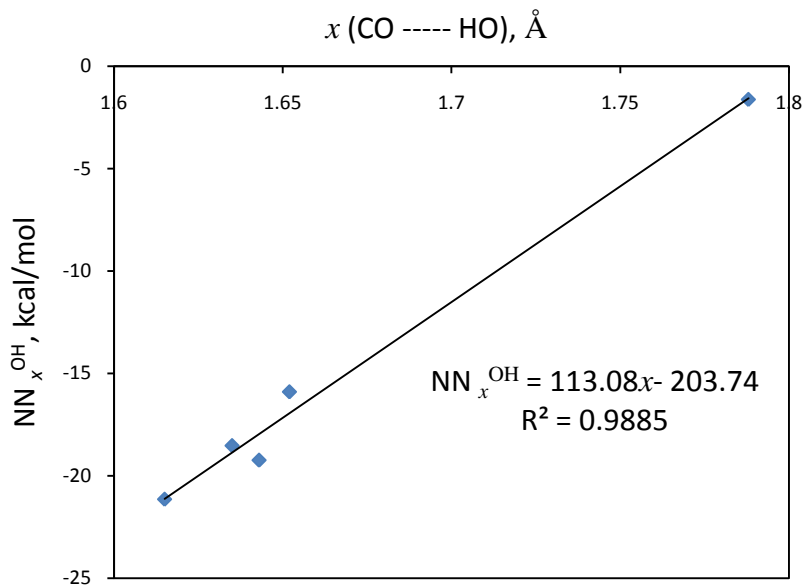

Figure S2. Corrections for ΔH_f in molecules with NN_x^{OH} interactions. Distances based on the MP2/6-31† level.
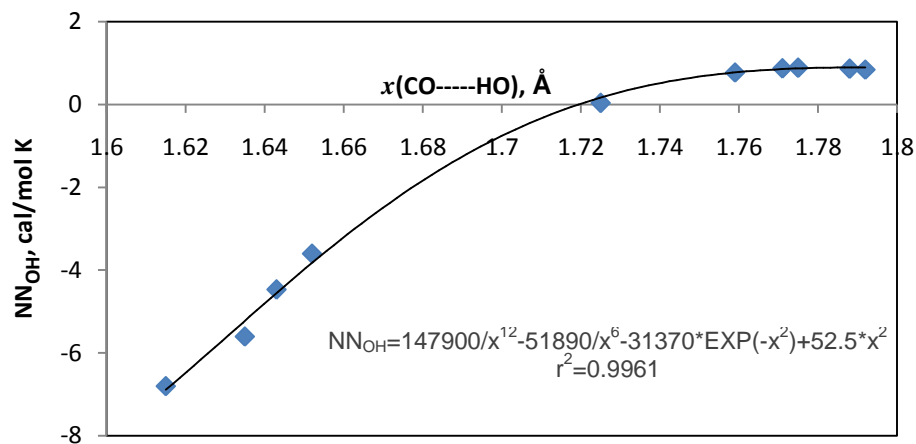
Figure S3. Variation of the nonnext neighbor interactions for the intrinsic entropy of molecules with H-bridge and NNcis interactions. Distances based on MP2/6-31G(d') calculations.
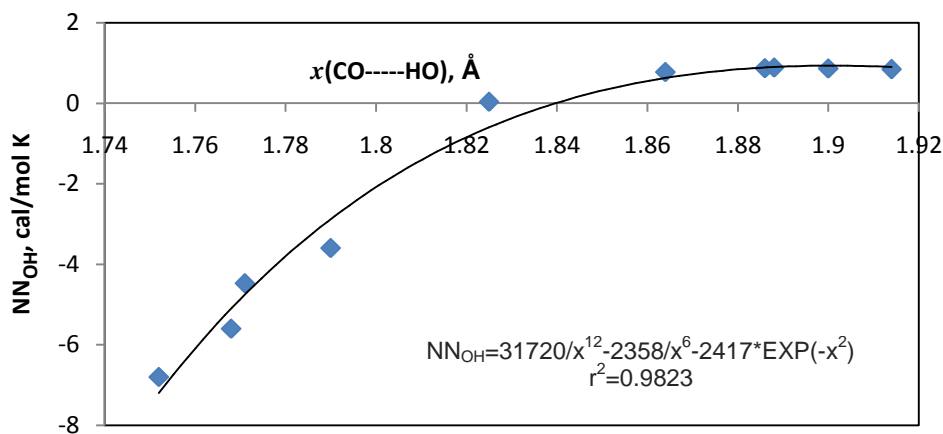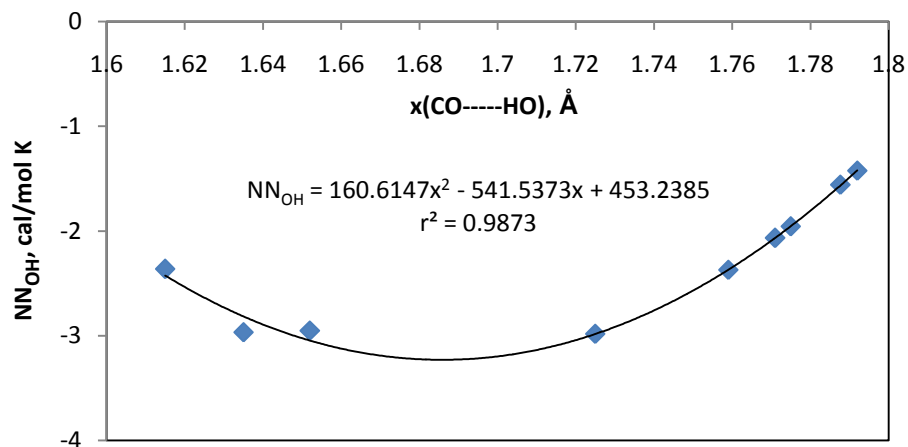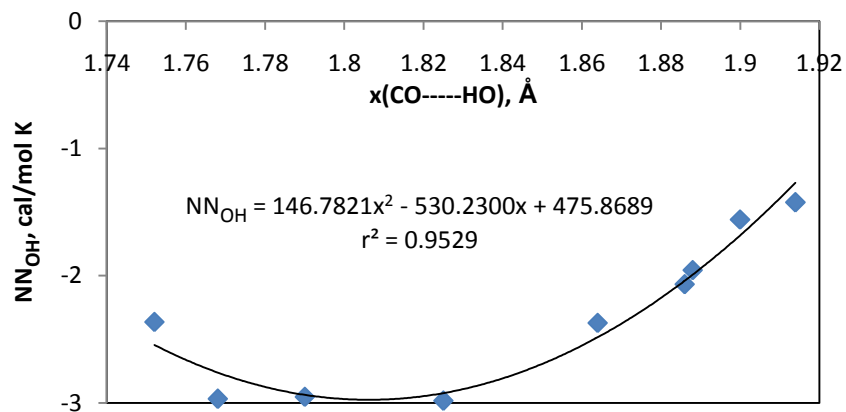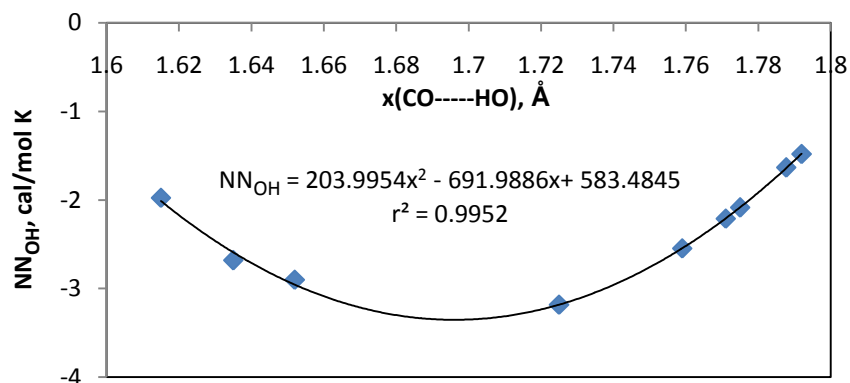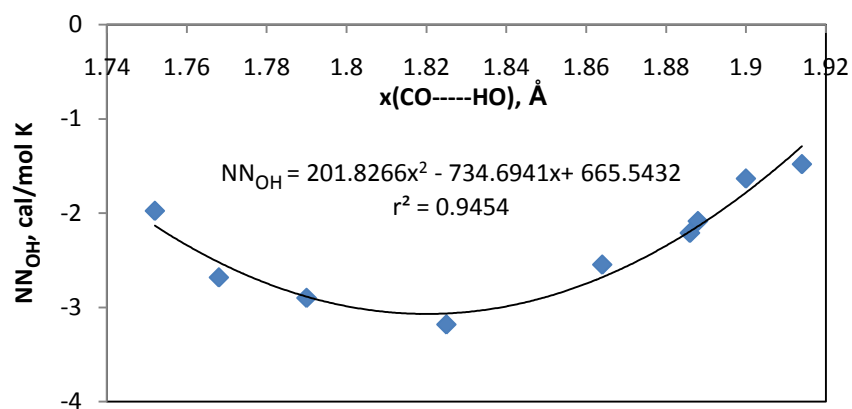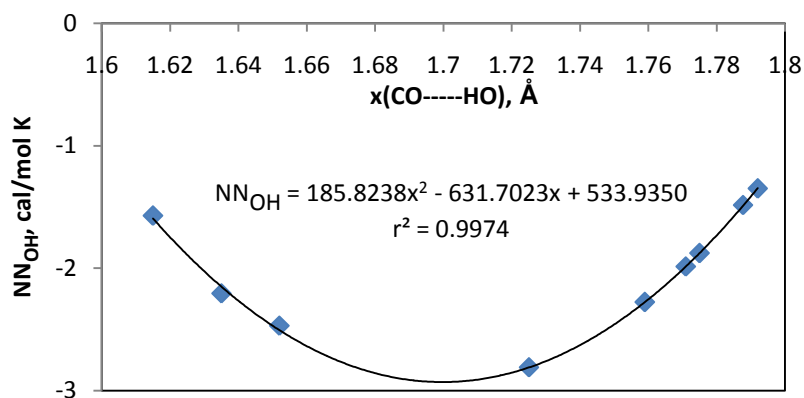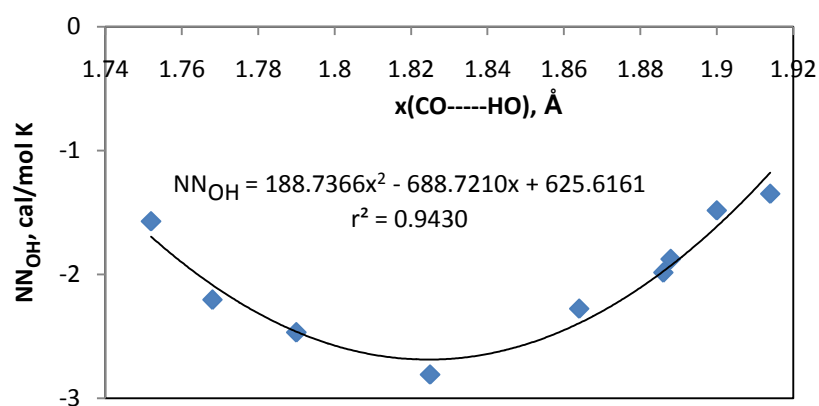

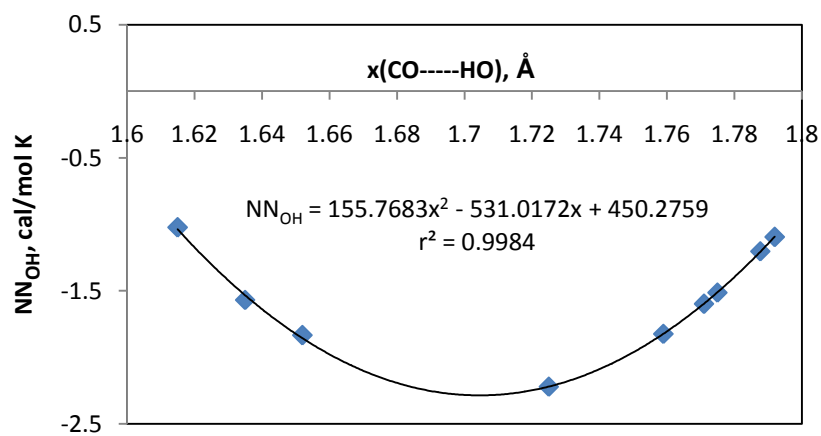**Figure S4**. Variation of the nonnext neighbor interactions for the intrinsic entropy of molecules with H-bridge and NNcis interactions. Distances based on HF/6-31G(d') calculations.

Figure S5. Variation of the nonnext neighbor interactions for the specific heat at 300 K of molecules with H-bridge and NNcis interactions. Distances based on MP2/6-31G(d') calculations.
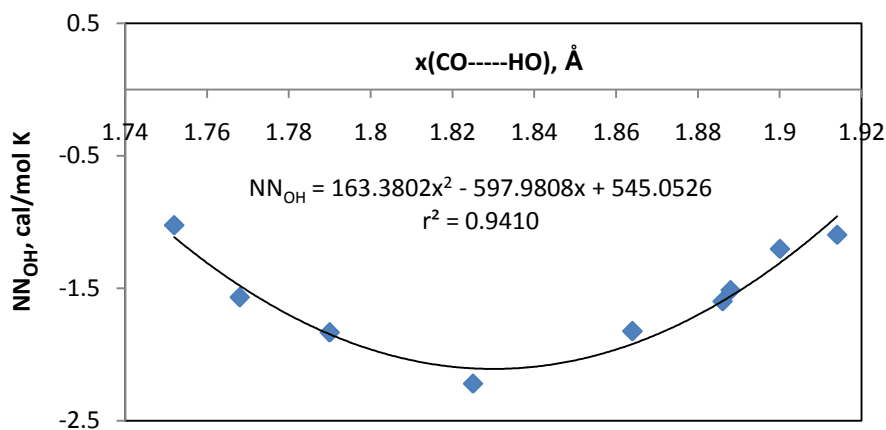
Figure S6. Variation of the nonnext neighbor interactions for the specific heat at 300 K of molecules with H-bridge and NNcis interactions. Distances based on HF/6-31G(d') calculations.
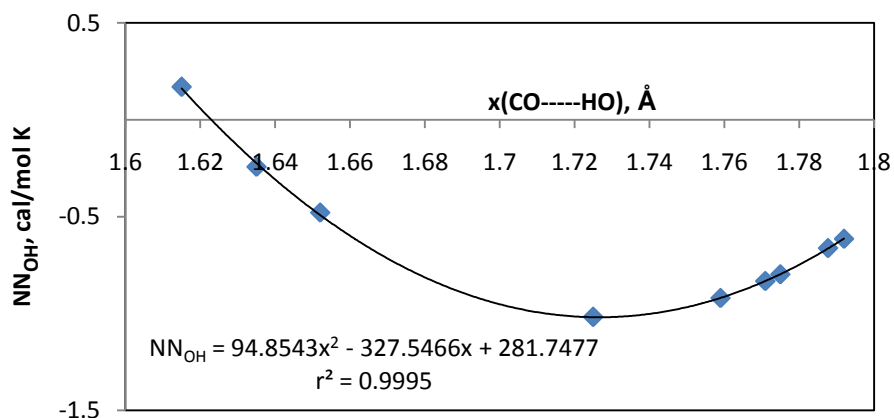

Figure S7. Variation of the nonnext neighbor interactions for the specific heat at 400 K for molecules with H-bridge and NNcis interactions. Distances based on MP2/6-31G(d') calculations.
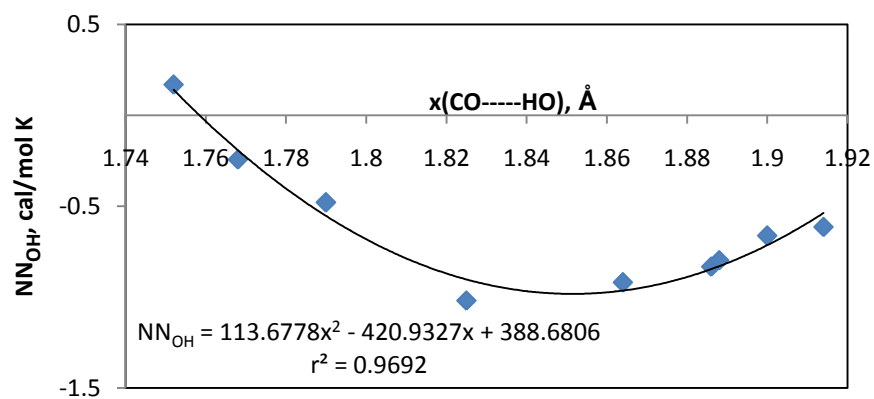

Figure S8. Variation of the nonnext neighbor interactions for the specific heat at 400 K for molecules with H-bridge and NNcis interactions. Distances based on HF/6-31G(d') calculations.
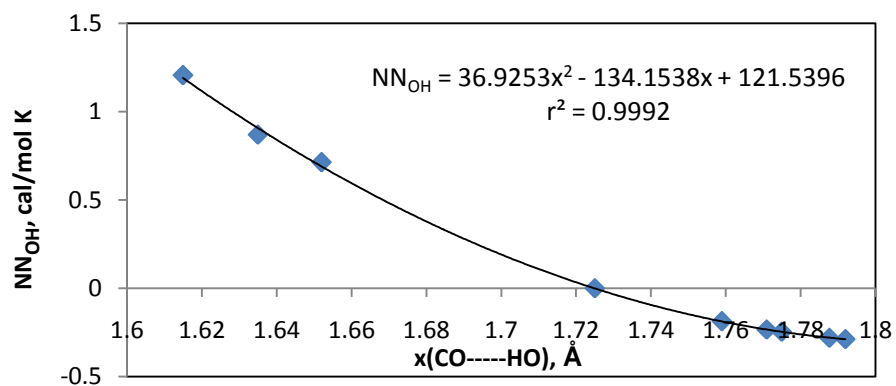
Figure S9. Variation of the nonnext neighbor interactions for the specific heat at 500 K for molecules with H-bridge and NNcis interactions. Distances based on MP2/6-31G(d') calculations.

Figure S10. Variation of the nonnext neighbor interactions for the specific heat at 500 K for molecules with H-bridge and NNcis interactions. Distances based on HF/6-31G(d') calculations.

Figure S11. Variation of the nonnext neighbor interactions for the specific heat at 600 K for molecules with H-bridge and NNcis interactions. Distances based on MP2/6-31G(d') calculations.
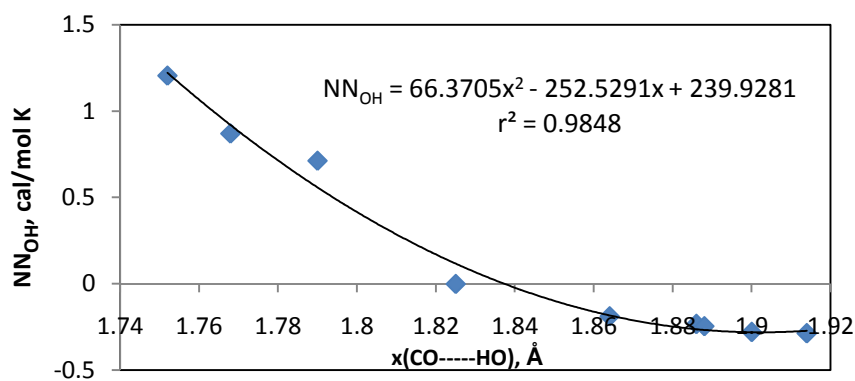
Figure S12. Variation of the nonnext neighbor interactions for the specific heat at 600 K for molecules with H-bridge and NNcis interactions. Distances based on HF/6-31G(d') calculations.
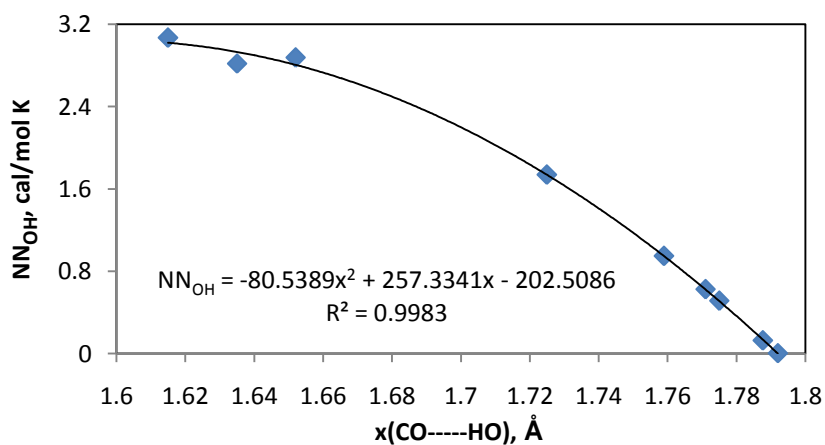

Figure S13. Variation of the nonnext neighbor interactions for the specific heat at 800 K for molecules with H-bridge and NNcis interactions. Distances based on MP2/6-31G(d') calculations.
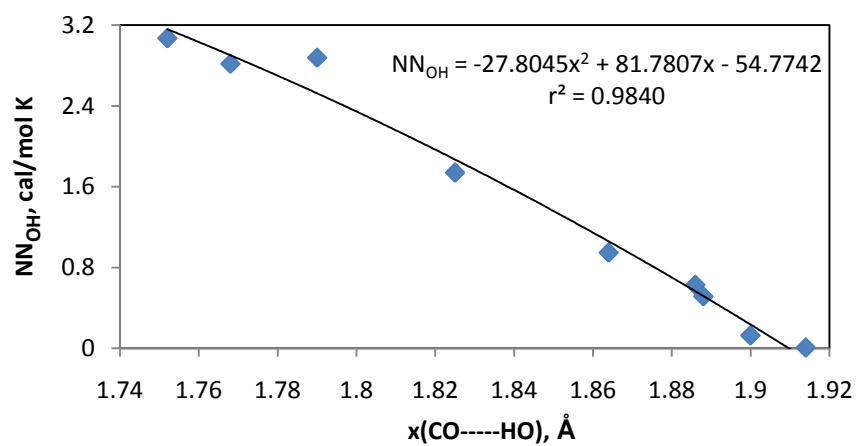

Figure S14. Variation of the nonnext neighbor interactions for the specific heat at 800 K for molecules with H-bridge and NNcis interactions. Distances based on HF/6-31G(d') calculations.

Figure S15. Variation of the nonnext neighbor interactions for the specific heat at 1000 K for molecules with H-bridge and NNcis interactions. Distances based on MP2/6-31G(d') calculations.

Figure S16. Variation of the nonnext neighbor interactions for the specific heat at 1000 K for molecules with H-bridge and NNcis interactions. Distances based on HF/6-31G(d') calculations.


Figure S17. Variation of the nonnext neighbor interactions for the specific heat at 1500 K for molecules with H-bridge and NNcis interactions. Distances based on MP2/6-31G(d') calculations.

Figure S18. Variation of the nonnext neighbor interactions for the specific heat at 1500 K for molecules with H-bridge and NNcis interactions. Distances based on HF/6-31G(d') calculations.
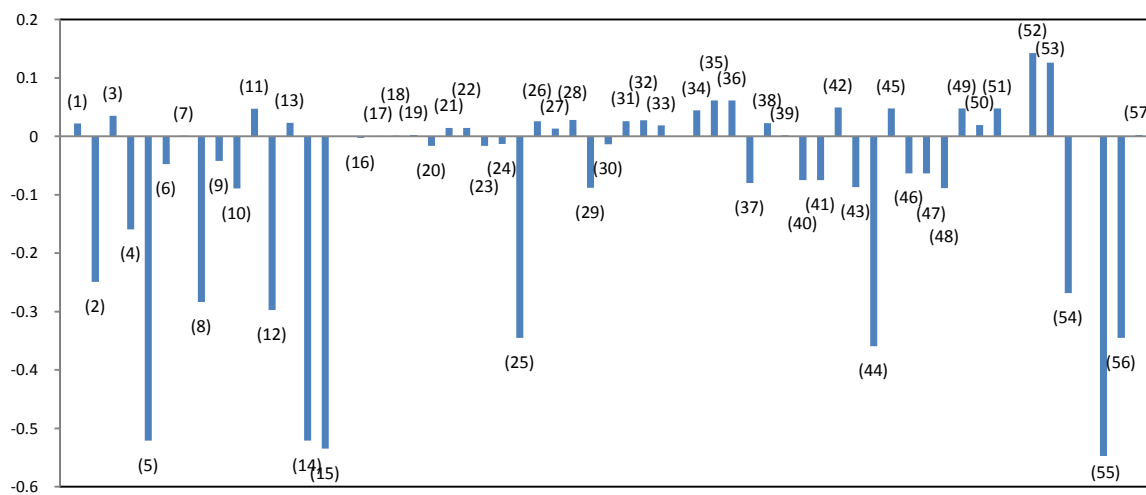
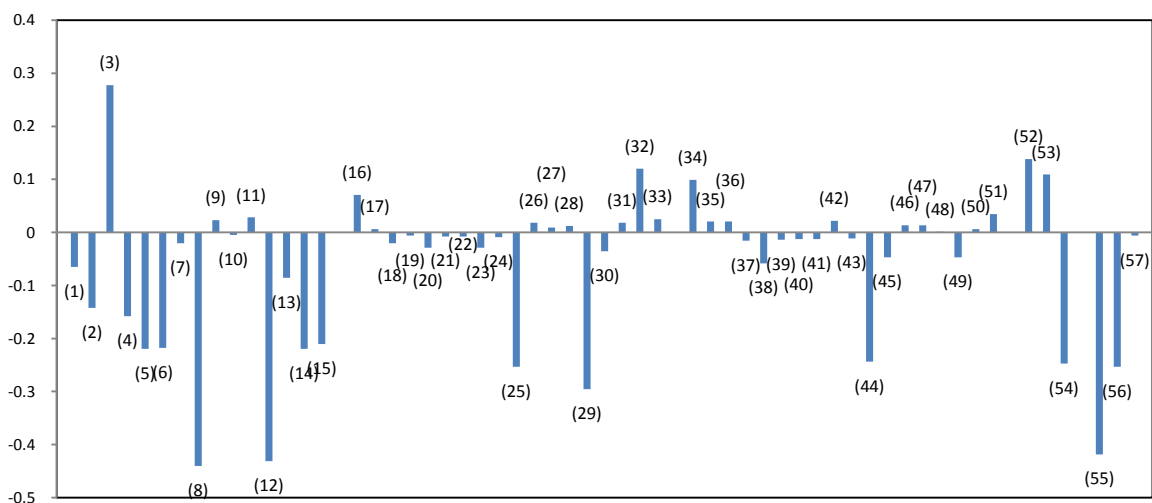**Figure S19.** Deviations (in cal/ mol K) for the predictions from GAVS for the specific heat at 400 K.

272

Figure S20. Deviations (in cal/ mol K) for the predictions from GAVS for the specific heat at 500 K.
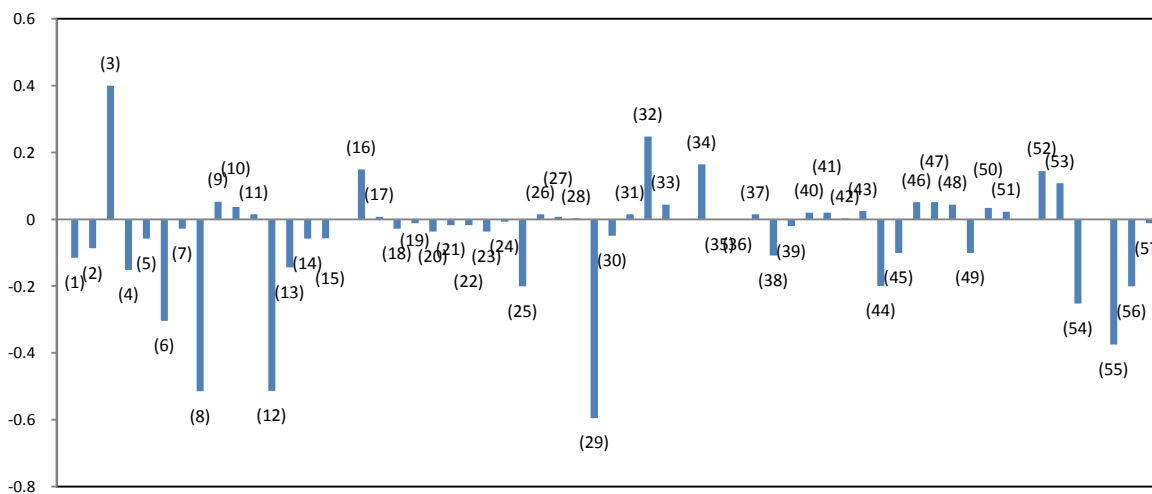

Figure S21. Deviations (in cal/ mol K) for the predictions from GAVS for the specific heat at 600 K.
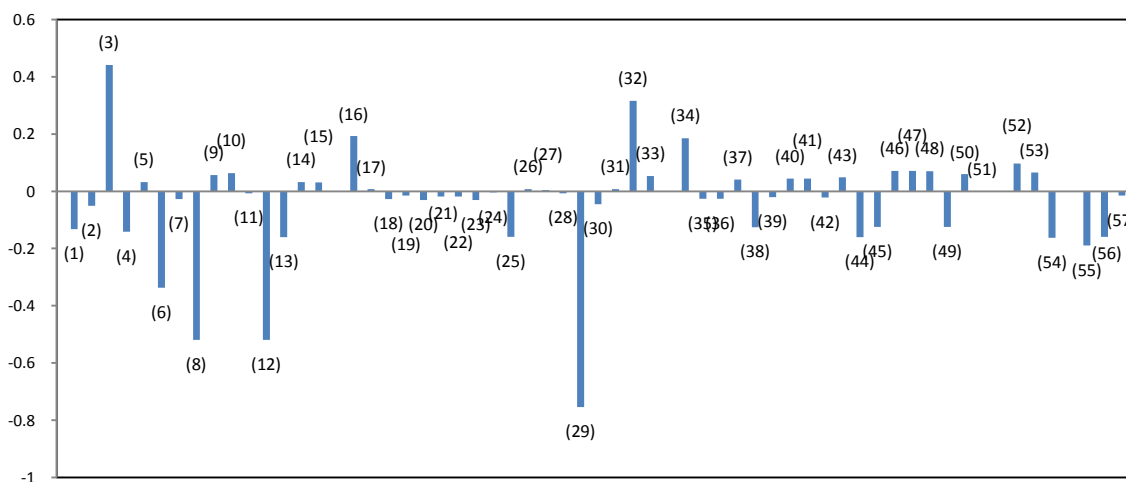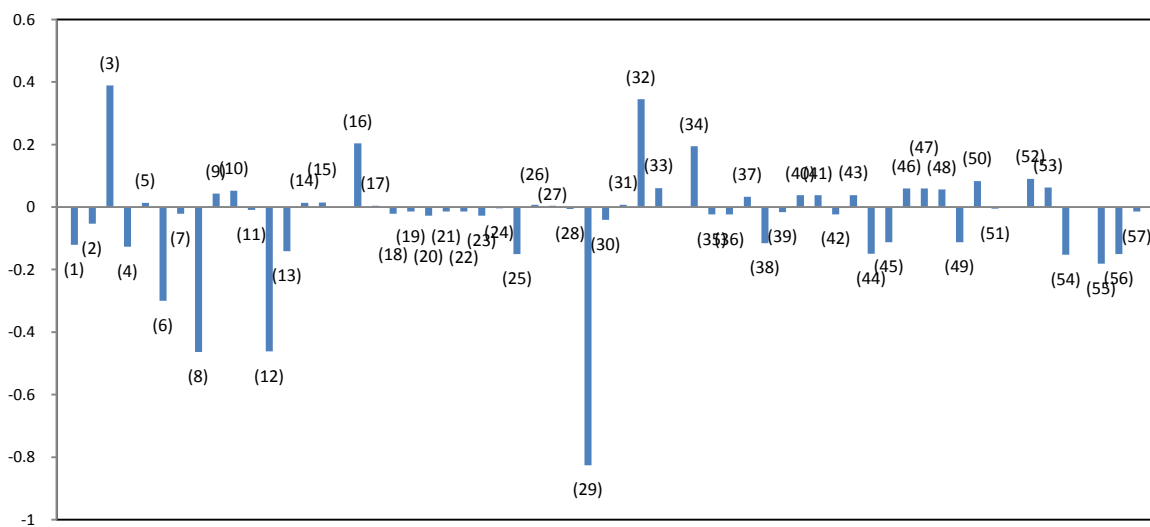
273

Figure S22. Deviations (in cal/ mol K) for the predictions from GAVS for the specific heat at 800 K.

Figure S23. Deviations (in cal/ mol K) for the predictions from GAVS for the specific heat at 1000 K.
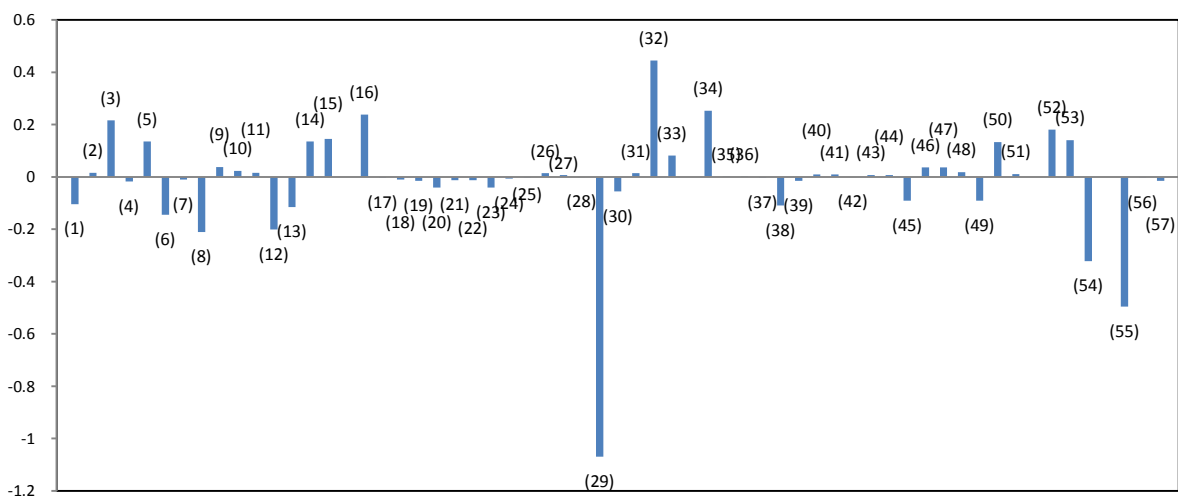
274

Figure S24. Deviations (in cal/ mol K) for the predictions from GAVS for the specific heat at 1500 K.